UNIVERSIDADE FEDERAL DE GOIÁS

PROGRAMA DE PÓS-GRADUAÇÃO EM MEDICINA TROPICAL E SAÚDE PÚBLICA

Amanda Alves de Oliveira

REPOSICIONAMENTO *IN SILICO* DE FÁRMACOS PARA TRATAMENTO DA PARACOCCIDIOIDOMICOSE

Goiânia
2018

sistema de bibliotecas ufg

PRPG
PRÓ REITORIA DE PÓS-GRADUAÇÃO

UFG

TERMO DE CIÊNCIA E DE AUTORIZAÇÃO PARA DISPONIBILIZAR VERSÕES ELETRÔNICAS DE TESES E DISSERTAÇÕES NA BIBLIOTECA DIGITAL DA UFG

Na qualidade de titular dos direitos de autor, autorizo a Universidade Federal de Goiás (UFG) a disponibilizar, gratuitamente, por meio da Biblioteca Digital de Teses e Dissertações (BDTD/UFG), regulamentada pela Resolução CEPEC nº 832/2007, sem ressarcimento dos direitos autorais, de acordo com a Lei nº 9610/98, o documento conforme permissões assinaladas abaixo, para fins de leitura, impressão e/ou *download*, a título de divulgação da produção científica brasileira, a partir desta data.

1. Identificação do material bibliográfico: **[X] Dissertação** **[ ] Tese**

2. Identificação da Tese ou Dissertação:

Nome completo do autor: Amanda Alves de Oliveira

Título do trabalho: Reposicionamento *in silico* de fármacos para tratamento da Paracoccidioidomicose

3. Informações de acesso ao documento:
Concorda com a liberação total do documento [X] SIM [ ] NÃO[1]

Havendo concordância com a disponibilização eletrônica, torna-se imprescindível o envio do(s) arquivo(s) em formato digital PDF da tese ou dissertação.

Amanda Alves de Oliveira
Assinatura do(a) autor(a)[2]

Ciente e de acordo:

Assinatura do(a) orientador(a)[2] Data: 19 / 06 / 19

[1] Neste caso o documento será embargado por até um ano a partir da data de defesa. A extensão deste prazo suscita justificativa junto à coordenação do curso. Os dados do documento não serão disponibilizados durante o período de embargo.
Casos de embargo:
- Solicitação de registro de patente;
- Submissão de artigo em revista científica;
- Publicação como capítulo de livro;
- Publicação da dissertação/tese em livro.

[2] A assinatura deve ser escaneada.

Amanda Alves de Oliveira

REPOSICIONAMENTO *IN SILICO* DE FÁRMACOS PARA TRATAMENTO DA PARACOCCIDIOIDOMICOSE

Dissertação de Mestrado apresentada ao Programa de Pós-Graduação em Medicina Tropical e Saúde Pública da Universidade Federal de Goiás, para obtenção do título de mestre.

Orientador: prof.ª Dra. Maristela Pereira
Co-orientador: prof.ª Dra. Carolina Horta Andrade

Goiânia
2018

Ficha de identificação da obra elaborada pelo autor, através do
Programa de Geração Automática do Sistema de Bibliotecas da UFG.

Alves de Oliveira, Amanda
REPOSICIONAMENTO IN SILICO DE FÁRMACOS PARA TRATAMENTO DA PARACOCCIDIOIDOMICOSE [manuscrito] / Amanda Alves de Oliveira. - 2018.
CXVIII, 118 f.: il.

Orientador: Profa. Dra. Maristela Pereira ; co-orientadora Dra. Carolina Andrade.
Dissertação (Mestrado) - Universidade Federal de Goiás, Instituto de Patologia Tropical e Saúde Pública (IPTSP), Programa de Pós Graduação em Medicina Tropical e Saúde Pública, Goiânia, 2018.
Bibliografia. Anexos.
Inclui siglas, abreviaturas, tabelas, lista de figuras, lista de tabelas.

1. Paracoccidioides spp. 2. Paracoccidioidomicose. 3. Reposicionamento de fármacos. 4. Homologia. 5. Ancoragem molecular. I. Pereira , Maristela , orient. II. Título.

CDU 582.28

MINISTÉRIO DA EDUCAÇÃO
UNIVERSIDADE FEDERAL DE GOIÁS
INSTITUTO DE PATOLOGIA TROPICAL E SAÚDE PÚBLICA
PROGRAMA DE PÓS-GRADUAÇÃO EM MEDICINA TROPICAL E SAÚDE PÚBLICA
Rua 235, s/n – Setor Universitário - Goiânia/GO – CEP: 74.605-050
Fones: (62) 3209.6362 - 3209.6102 – Fax: (62) 3209.6363 – **e-mail : ppgmtsp.ufg@gmail.com**

ATA DA REUNIÃO DA BANCA EXAMINADORA DA DEFESA DE DISSERTAÇÃO DE AMANDA ALVES DE OLIVEIRA – Aos sete dias do mês de março do ano de 2018 (07/03/2018), às 14:00 horas, reuniram-se os componentes da Banca Examinadora: Profas. Dras. MARISTELA PEREIRA, MELINA MOTTIN e NILCE MARIA MARTINEZ ROSSI, para, sob a presidência da primeira, e em sessão pública realizada no CENTRO DE RECURSOS COMPUTACIONAIS (CERCOMP/UFG), procederem à avaliação da defesa de dissertação intitulada: **"REPOSICIONAMENTO *IN SILICO* DE FÁRMACOS PARA TRATAMENTO DA PARACOCCIDIOIDOMICOSE"**, em nível de **MESTRADO**, área de concentração em **MICROBIOLOGIA**, de autoria de **AMANDA ALVES DE OLIVEIRA,** discente do PROGRAMA DE PÓS-GRADUAÇÃO EM MEDICINA TROPICAL E SAÚDE PÚBLICA, da Universidade Federal de Goiás. A sessão foi aberta pela Orientadora, Profa. Dra. **MARISTELA PEREIRA**, que fez a apresentação formal dos membros da Banca e orientou a Candidata sobre como utilizar o tempo durante a apresentação de seu trabalho. A palavra a seguir, foi concedida ao autor da dissertação que, em 30 minutos procedeu à apresentação de seu trabalho. Terminada a apresentação, cada membro da Banca argüiu a Candidata, tendo-se adotado o sistema de diálogo seqüencial. Terminada a fase de argüição, procedeu-se à avaliação da defesa. Tendo-se em vista o que consta na Resolução nº. 1034/2014 do Conselho de Ensino, Pesquisa, Extensão e Cultura (CEPEC), que regulamenta o Programa de Pós-Graduação em Medicina Tropical e Saúde Pública a Banca, em sessão secreta, expressou seu Julgamento, considerando a candidata **Aprovada** ou **Reprovada**:

Banca Examinadora	**Aprovada / Reprovada**
Profa. Dra. Maristela Pereira	Aprovada
Profa. Dra. Melina Mottin	Aprovada
Profa. Dra. Nilce Maria Martinez Rossi	Aprovada

Em face do resultado obtido, a Banca Examinadora considerou a candidata Amanda Alves, (**Habilitada ou não Habilitada**), cumprindo todos os requisitos para fins de obtenção do título de **MESTRE EM MEDICINA TROPICAL E SAÚDE PÚBLICA**, na área de concentração em **MICROBIOLOGIA**, pela Universidade Federal de Goiás. Cumpridas as formalidades de pauta, às 16 h 30 min, a presidência da mesa encerrou esta sessão de defesa de tese e para constar eu, KARINY VIEIRA SOARES E SILVA, secretária do Programa de Pós-Graduação em Medicina Tropical e Saúde Pública lavrei a presente Ata que depois de lida e aprovada, será assinada pelos membros da Banca Examinadora e por mim em duas vias de igual teor.

A Banca Examinadora aprovou a seguinte alteração no título da Dissertação:

_____

_____

_____

	Assinatura
Profa. Dra. Maristela Pereira (ICB/UFG)	Maristela Pereira
Profa. Dra. Melina Mottin (FF/UFG)	Melina Mottin
Profa. Dra. Nilce Maria Martinez Rossi (USP/ SP)	Nilce Maria Martinez Rossi
Secretário da Pós-Graduação:	

MINISTÉRIO DA EDUCAÇÃO
UNIVERSIDADE FEDERAL DE GOIÁS
INSTITUTO DE PATOLOGIA TROPICAL E SAÚDE PÚBLICA
PROGRAMA DE PÓS-GRADUAÇÃO EM MEDICINA TROPICAL E SAÚDE PÚBLICA
Rua 235, s/n – Setor Universitário - Goiânia/GO – CEP: 74.605-050
Fones: (62) 3209.6362 - 3209.6102 – Fax: (62) 3209.6363 – e-mail: **ppgmtsp.ufg@gmail.com**

UFG

FOLHA DE MODIFICAÇÃO DE DISSERTAÇÃO/TESE

Modificações exigidas na Ata da reunião da banca examinadora da defesa de dissertação **AMANDA ALVES DE OLIVEIRA**, realizada em 07/03/2018. Declaro que a dissertação segue a Norma 04/2009 do CPGMTSP (Modelo de elaboração de Teses/Dissertação):

O prazo para a entrega da versão final corrigida é de **40 (quarenta) dias após a defesa**, sendo responsável pelo recebimento, a orientadora da aluna Profa. Dra. **Maristela Pereira**, Presidente da Banca.

Candidata: Amanda Alves de Oliveira
Amanda Alves de Oliveira

Atesto que as alterações exigidas foram cumpridas, dentro do prazo estipulado.

Maristela Pereira
Profa. Dra. **Maristela Pereira**

SENHOR PROFESSOR ORIENTADOR
Este documento deverá ser entregue à Secretaria do PPGMTSP pelo aluno, devidamente assinado, juntamente com 1 CD-Rom gravado com a versão corrigida da dissertação.

Dedico esse trabalho primeiramente aos meus pais que sempre me incentivaram a estudar, posteriormente a todos meus familiares e amigos que de alguma forma me apoiaram nessa etapa da minha vida.

AGRADECIMENTOS

Agradeço primeiramente a Deus por todas as bênçãos recebidas na minha vida, principalmente durante meu mestrado, agradeço por me dar força e me fazer persistente.

Agradeço ao Instituto de Patologia Tropical e Saúde Pública (IPTSP), ao seu corpo docente, direção e administração pelo ensino gratuito de qualidade. Ao Conselho Nacional de Desenvolvimento Científico e Tecnológico (CNPq) pelo financiamento do meu projeto que possibilitou seu desenvolvimento e a OpenEye pela licença acadêmica gratuita dos programas utilizados nesse trabalho.

Agradeço minha orientadora prof.ª Dra. Maristela Pereira pela oportunidade, por investir no meu desenvolvimento acadêmico, por acreditar no meu potencial e dividir parte do seu conhecimento comigo. A minha co-orientadora prof.ª Dra. Carolina Andrade pela ajuda, opiniões, sugestões e dedicação que possibilitaram o desenvolvimento do nosso projeto.

Agradeço ao prof. Dr. Bruno pela paciência, dedicação, ensinamentos, por sempre estar disposto a tirar minhas dúvidas e pela imensa ajuda. Esse projeto só foi possível por causa de seu auxílio e esforço.

Agradeço por toda assistência técnica dada pelo Daniel, você já salvou meus notebooks várias vezes, muito obrigada, e ao Arthur pela assistência quando os programas não queriam funcionar.

A todos meus amigos do laboratório, vocês fizeram meus dias mais felizes, principalmente a Laura pelos longos momentos de risadas. Aos amigos do grupo Maristela pelo companheirismo, pelas ajudas, pela amizade, principalmente a Lívia por sempre estar disposta a ajudar e por me aguentar fazendo inúmeras perguntas. Sou muito feliz por fazer parte desse grupo, admiro muito vocês. Agradeço a todos do LabMol por me acolher no laboratório de vocês, por sempre me tratarem bem e me ajudar sempre que precisei, obrigada.

Agradeço aos meus amigos, mesmos os mais distantes, que de alguma forma colaboraram para que eu me tornasse a pessoa que sou hoje.

Agradeço minha família por estar do meu lado, me apoiando e possibilitando que essa conquista fosse possível, principalmente meus pais, José e Santina, por me ensinarem os valores da vida, me educarem e me incentivarem sempre a investir na minha educação, sem eles eu não estaria aqui. A minha segunda família que me acolheu como membro, me

fizeram sentir parte dela, sempre me apoiando e incentivando, principalmente a vó Nice por me acolher como neta, obrigada a todos por me deixarem fazer parte da vida de vocês.

Por fim, agradeço meu namorado Matheus pelas ajudas nas formatações, pela paciência, apoio e compreensão, você tem sido fonte de inspiração, seja por ser essa pessoa maravilhosa, seja pela sua dedicação de sempre correr atrás de seus objetivos e sonhos. Obrigada por todo carinho.

SUMÁRIO

TABELAS, FIGURAS E ANEXOS

SÍMBOLOS, SIGLAS E ABREVIATURAS

DEG: *Data base of Essentials Genes*;

D-AMB: Desoxicolato anfotericina B

ECM: Componentes da matriz celular;

FDA: *Food and Drug Administration*;

GAPDH: Gliceraldeido-3-fosfato desidrogenase;

GMQE: *Global Model Quality Estimation;*

HPPD-4: 4-hidroxifenilpiruvato dioxigenase;

MLS: Malato sintase;

NCCN: *National Comprehensive Cancer Network*;

P. brasiliensis: *Paracoccidioides brasiliensis;*

P. Lutzii: *Paracoccidioides Lutzii;*

PCM: Paracoccidioidomicose;

S. cerevisiae: *Saccharomyces cerevisiae;*

TFI: Triose fosfato isomerase;

TTD: *Therapeutic Target Database*;

RESUMO

Reposicionamento *in silico* de fármacos para tratamento da paracoccidioidomicose

A paracoccidioidomicose (PCM) é uma micose sistêmica, causada por fungos termos dimórficos *Paracoccidioides* spp., comum na América Latina. O tratamento da PCM é de longa duração feito por quimioterápicos que causam vários efeitos adversos. O objetivo deste trabalho foi reposicionar fármacos mais seguros e com maior eficácia para o tratamento da PCM. Foram utilizados dados de diferentes linhagens de *Paracoccidioides* spp. *Pb*01, *Pb*03 e *Pb*18. As proteínas ortólogas foram selecionadas a partir da comparação das proteínas dos três isolados, posteriormente, essas proteínas foram comparadas com as proteínas dos bancos de dados *DrugBank* e *Therapeutic Target Database* (TTD), visando a identificação de fármacos que tivessem essas proteínas como alvo. Os critérios de inclusão e exclusão foram: seleção de medicamentos a partir da fase II; identidade das sequências ≥ 30% das proteínas de *Paracoccidioides* spp. com as proteínas dos bancos de fármacos; e remoção de nutracêuticos, de peptídeos e de anticorpos. Como resultado, foram identificadas 145 proteínas como potenciais alvos de fármaco, com um total de 811 compostos sugeridos. Em seguida, a essencialidade dos alvos previstos foi investigada usando como modelo *Saccharomyces cerevisiae*. Após essa etapa, 46 proteínas de *Paracoccidioides* spp. foram identificadas como ortólogas às proteínas essenciais de *S. cerevisiae*. Essas proteínas foram submetidas à modelagem por homologia e ancoragem molecular para predição de estrutura tridimensional do complexo proteína-fármaco e avaliação de energia de ligação dos complexos formados. Os resultados obtidos foram analisados para a escolha dos 17 fármacos que serão testados *in vitro* como forma de confirmação dos resultados obtidos *in silico*.

Palavras-chave: *Paracoccidioides* spp, Paracoccidioidomicose, Reposicionamento de fármacos, Homologia, Ancoragem molecular;

ABSTRACT

Drug repositioning in silico for Paracoccidioidomycosis treatment

Paracoccidioidomycosis (PCM) is a systemic mycosis, caused by thermally dimorphic fungus *Paracoccidioides* spp., common in Latin America. PCM treatment is long-term chemotherapeutic approach and causes adverse effects. The goal of this work is repositioning of the drugs safer and more effective for PCM treatment. It was used data from different lineages of Paracoccidioides spp., *Pb*01, *Pb*03 and *Pb*18. The orthologous proteins were selected from the protein comparison of three isolates, posteriorly, those proteins were compared with proteins of two drugs databases, DrugBank and Therapeutic Target Database (TTD) aiming to identify drugs that had those proteins as target. Inclusion and exclusion criteria, such as consideration drugs starting the phase II of the clinical trials, sequence identity ≥ 30% in between *Paracoccidioides* spp. proteins and database drugs proteins, and removal of nutraceuticals, peptides, and antibodies. As a result, 145 *Paracoccidioides* spp. proteins were orthologous to drug targets of the drug banks and a total of 811 drugs were suggested. After, the essentiality of predicted targets was investigated by using the model microorganism *Saccharomyces cerevisiae*. As a result, 46 *Paracoccidioides* spp. were orthologous to the essential *S. cerevisiae* proteins. These proteins were submitted to homology modeling and molecular docking to the prediction of the three-dimensional structure of the protein-compound complex and power evaluation of complexes formed. The obtained results were analyzed for selection of the 17 compounds which will be tested *in vitro* for confirmation of results *in silico.*

Keyword: *Paracoccidioides* spp., Paracoccidioidomycosis, Drug repositioning, Homology, Molecular docking;

1. INTRODUÇÃO

1.1. Paracoccidiodomicose

Considerada endêmica nos países da América Latina, a paracoccidioidomicose (PCM) é uma micose sistêmica que possui ocorrência na Venezuela, Colômbia, Argentina e no Brasil, onde cerca de 80% dos casos são registrados (RESTREPO et al, 2001; MARTINEZ, 2015). No Brasil, a doença possui maior endemicidade no Sudeste, Centro-oeste e Sul (principalmente no Paraná e no norte do Rio Grande do Sul), com casos registrados nos estados do Pará, Maranhão, Tocantins, Rondônia e na região da Amazônia Ocidental (MARTINEZ, 2015; VIEIRA et al., 2014; MATOS et al., 2012), como apresentado na Figura 1.

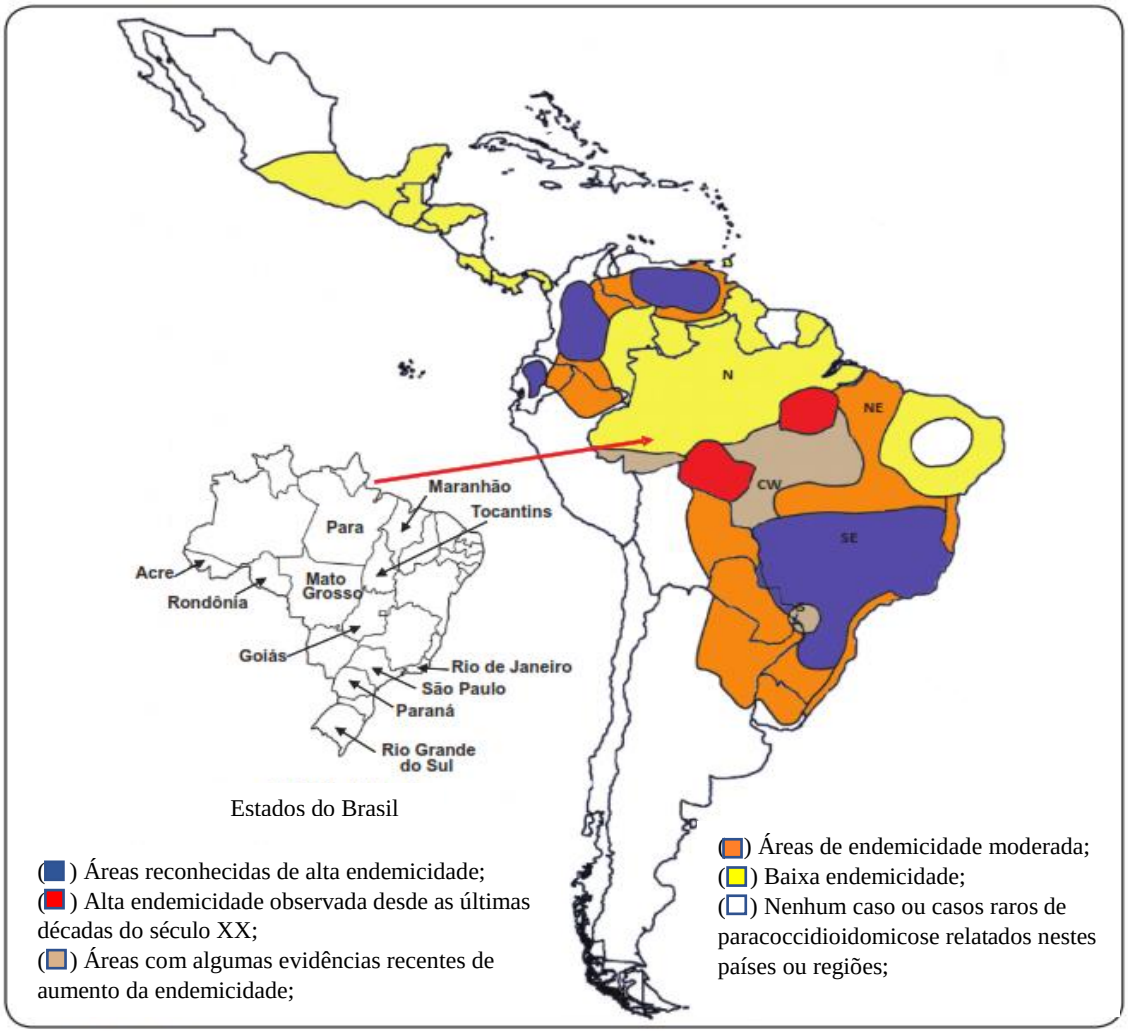

Figura 1: Distribuição geográfica das áreas endêmicas da PCM na América Latina. **Fontes:** Martinez, 2017; Shikanai-Yasuda et al., 2017.

A PCM foi inicialmente descrita por Adolfo Lutz em 1908 e posteriormente por Splendore em 1912, que isolaram o fungo *Paracoccidioides* spp. de pacientes da Santa Casa de Misericórdia no estado de São Paulo (COUTINHO et al., 2002). A micose é comumente adquirida nos primeiros 20 anos de vida com apresentações de sintomas na fase adulta entre os 30 e 50 anos (SHIKANAI-YASUDA et al., 2006).

Quando manifestada na infância, o número de casos de PCM é igual para os ambos sexos. Na juventude os casos registrados para o sexo masculino são ligeiramente maiores. Já na fase adulta, varia entre 10 a 15 homens para uma mulher (SHIKANAI-YASUDA et al., 2017). O hormônio estrogênio é considerado a causa da maior imunidade das mulheres contra a PCM, porque diminui o potencial do fungo em se diferenciar de micélio para levedura, condição essencial para o estabelecimento do processo infeccioso (RESTREPO et al., 1984; ARISTIZABAL et al., 1998; SHANKAR et al., 2011; MENDES et al., 2017).

A via mais comum de infecção é por meio da inalação de conídios ou de fragmentos de micélios (BRUMMER; CASTANEDA; RESTREPO, 1993), que ao chegarem nos pulmões, frequentemente são controlados pelo sistema imune ficando latente na forma de levedura (MARTINEZ, 2017), Figura 2.

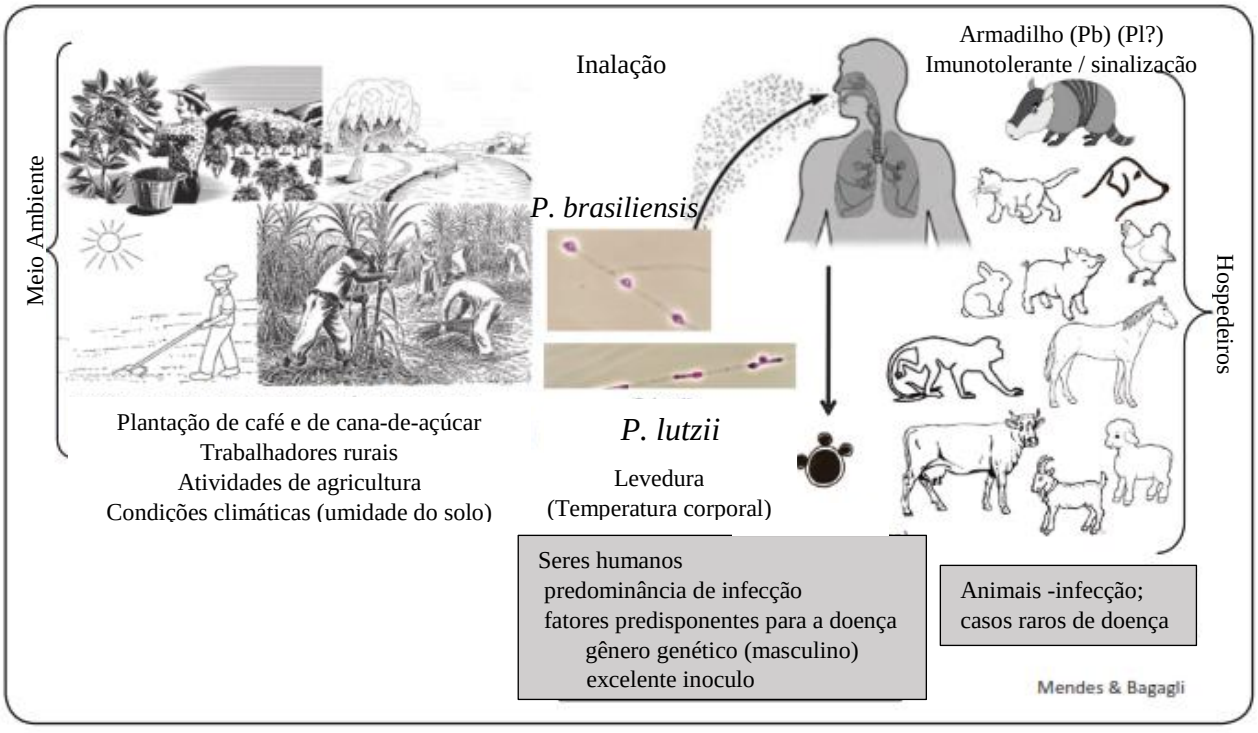

Figura 2: Epidemiologia de *Paracoccidioides brasiliensis* e *Paracoccidioides lutzii*. *Pb*: *Paracoccidioides brasiliensis*; *Pl*: *Paracoccidioides lutzii*. **Fonte:** Shikanai-Yasuda et al., 2017.

Os serem humanos não são os únicos hospedeiros de *Paracoccidioides* spp. esses fungos já foram identificados em várias especiais de animais domésticos e selvagens (MARTINEZ, 2015). O armadilho (Tatu) é um reservatório de *P. brasiliensis* que cresce a partir dos seus órgãos internos: baço, fígado e linfonodos (SHIKANAI-YASUDA et al., 2017). Até o momento não há registro de identificação do *P. lutzii* em armadilho (SHIKANAI-YASUDA et al., 2017).

As formas clínicas da PCM podem ser classificadas em: paracoccidioidomicose infeção, paracoccidioidomicose doença, e forma residual ou sequela (FRANCO et al., 1987; SHIKANAI-YASUDA et al., 2017). Durante o período de infecção, a PCM é raramente diagnosticada, os poucos registros de pacientes nessa fase apresentaram lesões no pulmão e linfonodomegalia hilar (MARTINEZ, 2015).

Após as manifestações clínicas, a PCM pode ser classificada em aguda/subaguda e crônica (MARQUES, 2013). Com desenvolvimento mais rápido, a PCM nas formas aguda e subaguda são mais comuns em crianças e adolescentes (SHIKANAI-YASUDA et al., 2006). Alguns sintomas dessas fases são: lesões cutâneas, linfonodomegalia, hepatoesplenomegalia, problemas ósteo-articulares (SHIKANAI-YASUDA et al., 2006), comprometimento do fígado e baço (MARQUES, 2013). A fase crônica é mais frequente entre os trabalhadores rurais, fumantes, com higiene, alimentação e condição econômica precárias (PALMEIRO; CHERUBINI; YURGEL, 2005; BOCCA et al., 2013). De desenvolvimento lento e silencioso, a PCM na fase crônica pode atingir um ou vários órgãos ao mesmo tempo, sendo os pulmões, mucosas e pele os mais afetados (SHIKANAI-YASUDA et al., 2006).

As formas residuais são alterações anatômicas manifestadas após o tratamento. Diversos órgãos podem ficar com sequelas, porém, pulmões, pele, laringe, traqueia, suprarrenais, mucosa do trato aero digestivo superior, sistema nervoso central e sistema linfático são os mais frequentes (VALLE et al., 1995; TOBÓN et al., 2003; SHIKANAI-YASUDA et al., 2017). As principais sequelas pulmonares são fibrose e enfisema, no trato gastrointestinal pode ocorrer obstrução ou sub-obstrução, na laríngeas o comprometimento das cordas vocais podem ser irreversível, e dependendo do local das sequelas no sistema nervoso central o paciente pode ficar com suas atividades limitadas (MENDES et al., 2017).

Exames clínicos, laboratoriais e de imagem podem ser usados para o diagnóstico da PCM. A anamnese e o exame físico são usados nas distintas fases da doença com diferentes focos: na fase aguda para observação de alterações dos linfonodos, e na fase

crônica, na análise do comprometimento dos pulmões e laringe (SHIKANAI-YASUDA et al., 2006). Em adição, são indicados exames de raios X, ultrassonografia abdominal, hemograma completo, velocidade de hemossedimentação, avaliação renal e metabólica (SHIKANAI-YASUDA et al., 2006). A sorologia por meio da pesquisa do substrato antigênico, uma glicoproteína de 43 kDa, é indicada para o diagnóstico final (COUTINHO et al., 2002).

Como as manifestações clínicas de várias doenças são similares às da PCM, é necessário, principalmente na fase crônica, o diagnóstico diferencial entre doenças que envolvem as mucosas, tais como câncer, leishmaniose, sífilis secundária ou terciária, sarcoidose, histoplasmose e tuberculose (PATO; GIUSIANO; MANGIATERRA, 2007). A tuberculose pulmonar apresenta resultados do exame radiológico muito parecido com os da PCM, diferenciando pela presença do bacilo ao invés do fungo (Wanke; Aidê, 2009). Assim, pesquisas têm sido realizadas para sugerir novas ferramentas, como o *Western blot*, para a realização do diagnóstico diferencial (BERTONI et al., 2012).

Estudo realizado utilizando dados entre 1980 e 1995 classificou a PCM como a oitava causadora de mortes nesse período, na frente até que a Leishmaniose, baseando nos 3.181 casos de óbitos causados pela PCM documentados pelo Ministério da Saúde (COUTINHO et al., 2002; SHIKANAI-YASUDA et al., 2017). A prevalência da PCM na América Latina ainda é alta, com mais de 15.000 casos registrados entre 1930 e 2012, sendo o Brasil o país com maior registro (MARTINEZ, 2015), apresentando casos raros como o de um trabalhador rural do estado do Mato Grosso do Sul que tinha uma lesão óssea na tíbia causada por leveduras de *P. brasiliensis* (CORREA-DE-CASTRO et al., 2012).

1.2. Agente etiológico da PCM

Paracoccidioides spp. são fungos termo dimórficos que à 25ºC, e no meio ambiente, são encontrados na forma de micélio, e à 37ºC, e em células dos hospedeiros, na forma de levedura (TEIXEIRA et al., 2014). Teixeira e colaboradores (2009) utilizaram o método de concordância genealógica do reconhecimento de espécies filogenéticas, para classificar o gênero *Paracoccidioides* em dois grupos filogênicos distintos, *Paracoccidioides brasiliensis* e *Paracoccidioides lutzii* (TEIXEIRA et al., 2009, 2013a).

P. brasiliensis é um grupo monofilético composto por diferentes linhagens, S1, PS2, PS3 e PS4 (MATUTE et al., 2005; TEIXEIRA et al., 2009, 2014; MUÑOZ et al.,

2016). Amplamente distribuída na América do Sul, a linhagem S1 é relacionada à maioria dos casos de PCM (MATUTE et al., 2005; TEIXEIRA et al., 2009, 2014; MUÑOZ et al., 2016). Em 2016, MUÑOZ e colaboradores propuseram a divisão da linhagem S1 em dois clados, S1a e S1b apresentando evidências de recombinação e por S1b ter maior diversidade. S1b seria a linhagem mais antiga de *P. brasiliensis* que passou por recombinações com as outras linhagens (MUÑOZ et al., 2016). Com distribuições mais restrita, PS2 foi identificada apenas no Brasil e Venezuela, PS3 principalmente em regiões endêmicas na Colombia (TEIXEIRA et al., 2009, 2014; MUÑOZ et al., 2016) e PS4 somente numa região da Venezuela (MATUTE et al., 2005; MUÑOZ et al., 2016).

Pertencente ao grupo filogenético *P. lutzii*, o isolado *Pb*01 é o mais distinto fisiologicamente em relação aos outros isolados, (TEIXEIRA et al., 2009; DESJARDINS et al., 2011). Morfologicamente, além dos conídios com aspectos de barris e chapéus produzidos por *P. lutzii* e *P. brasiliensis*, *Pb*01 apresenta conídios maiores, alongados e em formato de hastes (TEIXEIRA et al., 2013a). Provenientes do grupo filogenético *P. brasiliensis*, os isolados *Pb*03 e *Pb*18 pertencem às espécies PS2 (DESJARDINS et al., 2011) e S1 (DESJARDINS et al., 2011; MATUTE et al., 2005), respectivamente. Apesar de apresentarem semelhanças como tamanho do genoma e a alta identidade na comparação do genoma mitocondrial (DESJARDINS et al., 2011), desencadeiam diferentes processos de infecções; *Pb*03 provoca uma infecção mais leve com maior resposta do sistema imune do hospedeiro que *Pb*18 (CARVALHO et al., 2005).

Pesquisas com foco no genoma do fungo têm apontado a possibilidade de que a reprodução sexuada possa estar presente no seu ciclo de vida. Proteínas envolvidas no acasalamento (MAT-1 e MAT-2) foram identificadas no transcriptoma de *P. brasiliensis* (FERNANDES et al., 2005). Teixeira *et al.* (2013) analisaram a presença desses locus de acasalamento em 98 isolados de *Paracoccidioides* spp., desses, 55 tiveram os locus MAT1-1, 30 os locus MAT1-2 e 13 isolados, inclusive *Pb*01, *Pb*03 e *Pb*18, apresentaram os dois locus.

Características morfológicas relacionadas à reprodução sexuada também foram observadas, como a formação de jovens ascocarpos, hifas estreitas enroladas e do tipo botão, além da presença de vários núcleos nas hifas enroladas apontando possível migração dos núcleos durante o acasalamento. Contudo, o processo de sua reprodução ainda não é bem compreendido (TEIXEIRA et al., 2014).

As espécies de *Paracoccidioides* spp. também diferem no processo de infecção. Para que a infecção se manifeste e ocorra a disseminação das células fúngicas, alguns

fatores de virulência foram sugeridos, como a capacidade de reconhecimento e adesão nas células hospedeiras pelo fungo, a rápida resposta à alterações no ambiente e a secreção de enzimas que auxiliam na infecção (SOARES et al., 2010). Considerando a capacidade de adesão das espécies de *Paracoccidioides* spp., foi observado que *P. brasiliensis* aderem melhor aos pneumócitos e é mais virulento que *P. lutzii* (DE OLIVEIRA et al., 2015).

1.3. Quimioterapia da PCM

Antes de iniciar o tratamento da PCM é necessário considerar a gravidade da doença, o local da lesão e as contraindicações para o uso de determinada medicação (SHIKANAI-YASUDA et al., 2006). Os fármacos mais usados são o itraconazol e a combinação sulfametoxazol-trimetoprima para o tratamento das formas leves e moderada, e a anfotericina B é indicada para as formas mais graves (MARQUES, 2013; SHIKANAI-YASUDA et al., 2006). Contudo, é necessária uma avaliação detalhada do paciente para verificar alguma condição especial que deve ser considerada. Para gestantes, o fármaco indicado é a anfotericina B; para crianças, a combinação sulfametoxazol-trimetoprima é a mais indicada, porém o itraconazol também é usado; em casos de insuficiência renal, é recomendado antifúngicos da classe dos azóis, como o itraconazol (MARQUES, 2013; SHIKANAI-YASUDA et al., 2006).

Outros fármacos também são usados no tratamento da PCM: cetoconazol, que apesar de ter sua eficiência comprovada (M et al., 1983), é pouco usado por ser menos eficiente que o itraconazol (SHIKANAI-YASUDA, 2015); fluconazol, recomendado em casos de neuro-PCM, quando há o aumento das enzimas hepáticas e reações imunes excessivas à administração de sulfas ou anfotericina B (SHIKANAI-YASUDA, 2015); e voriconazol, antifúngico considerado tão eficiente no tratamento da PCM quanto o Itraconazol (TELLES et al., 2007);

Pertencente ao grupo dos triazóis, o itraconazol é um composto sintético multi-anelado que contem três átomos de nitrogênio no anel azol (NETO et al., 2014). Os triazóis causam modificações na membrana das células fúngicas, inibindo a síntese do ergosterol, levando à morte celular (BURGESS; HASTINGS, 2000; NETO et al., 2014). A via de biossíntese do ergosterol é bloqueada por intermédio da inibição da enzima lanosterol 14-α desmetilase (Erg11) pelo itraconazol (LAMB et al., 1999; NETO et al., 2014).

A atuação do itraconazol nas células de *Paracoccidioides* spp. foi identificada por Neto e colaboradores (2014) através da investigação do transcritoma do fungo na presença

do fármaco. Eles observaram as alterações dos níveis de transcritos relacionados ao transporte celular, metabolismo e energia, transcrição, resgaste celular, defesa e virulência. Foi identificado um aumento nos níveis dos transcritos de lanosterol 14-α-desmetilase (ERG11), C5,6-desaturase (ERG3), C-metiltransferase delta-24-esterol (ERG6), esterol desaturase C-22 (ERG5) e esterol metano C-4 oxidase (ERG25), os quais foram maiores após 6 h de contado com o fármaco (NETO et al., 2014).

Usados no tratamento de diversas infecções causadas por bactérias nas vias respiratórias, urinária e gastrointestinais, a combinação sulfametoxazol-trimetoprima age em estágios sucessivos da via de biossíntese de folato, que é sintetizado por plantas, fungos e bactérias (VILCHÈZE; JACOBS, 2012). A dihidropteroato sintase, responsável por estimular a adição da di-hidropterina difosfato ao ácido *p*-aminobenzóico, é inibida pelo sulfametoxazol. A trimetoprima inibe a dihidrofolato redutase que reduz o dihidrofolato à tetrahidrofolato. O dihidrofolato é o resultado da interação do 7,8-dihidropteroato, produto da dihidropteroato sintase, com o glutamato (VILCHÈZE; JACOBS, 2012). No tratamento da PCM, Zambuzzi-Carvalho colaboradores (2015) sugeriram que o mecanismo de ação do sulfametoxazol é atuando como competidor de aminoácidos, ácidos nucleicos e biossíntese de cofatores de folato, suspendendo as funções mitocondriais em *P. lutzii* (ZAMBUZZI-CARVALHO et al., 2015)

A anfotericina B tem potencial de ação contra leveduras e protozoário como *Leishmania* spp (JOHANSEN; GØTZSCHE, 2000). Na membrana celular fúngica, anfotericina B se associa ao ergosterol formando orifícios e causando fuga de íons, levando à morte celular (JOHANSEN; GØTZSCHE, 2000). Para diminuir a taxa de toxicidade da anfotericina B, foi desenvolvida sua formulação na forma lipídica (KLEINBERG, 2006; MISTRO et al., 2012).

A parte lipídica da anfotericina B lipossomal é constituída principalmente por três componentes: fosfadilcolina de soja hidrogenada, responsável pela formação da maior parte da bicamada lipídica, é dificilmente hidrolisada à temperatura corporal por apresentar ponto de transição de gel para cristais líquido superior que 37ºC (JOHANSEN; GØTZSCHE, 2000; PAPAHADJOPOULOS et al., 1973); diestearoil fosfatidil glicerol, possui carga líquida negativa que interage com o grupo amino da anfotericina B, de carga positiva, para retenção da anfotericina B dentro da bicamada lipossomal (FUJII et al., 1997; JOHANSEN; GØTZSCHE, 2000; ADLER-MOORE; PROFFITT, 2002); e o colesterol, que facilita a retenção da anfotericina B dentro da bicamada lipossomal ao se ligar na mesma (STONE et al., 2016).

Outra estratégia de otimização terapêutica e redução da toxidade da anfotericina B, é a formulação em nanopartículas (SOUZA et al., 2015) . Amaral e colaboradores (2009) desenvolveram nano-D-AMB (desoxicolato anfotericina B) para liberarem o medicamento de forma prolongada e gradualmente. Eles analisaram a eficiência da nano-D-AMB no tratamento da PCM. Como resultado a nano-D-AMB demostrou efeitos antifúngicos, causou menos efeitos adversos e possibilitou a redução da frequência de dosagem de desoxicolato anfotericina B em três vezes (AMARAL et al., 2009).

Apesar da eficiência desses fármacos no tratamento da PCM, são descritos efeitos adversos provenientes dos mesmos. A anfotericina B pode causar febre, calafrios, hipotensão, distúrbios metabólicos, cardiotoxicidade e nefrotoxicidade (JOHANSEN; GØTZSCHE, 2000; MISTRO et al., 2012). O itraconazol pode causar náuseas, vômitos, aumento das aminotransferases séricas, erupção cutânea, hipocalemia, hipotrigliceridemia, hiperuricemia e tem efeito hepatotóxico (SHIKANAI-YASUDA, 2015). Entre os fármacos mais frequentemente receitados, o tratamento com a combinação sulfametoxazol-trimetoprima é o mais longo, com duração de mais de um ano, que pode causar reações de hipersensibilidade, leucopenia, anemia megaloblástica e trombocitopenia ao paciente (SHIKANAI-YASUDA, 2015).

O tempo de tratamento depende do tipo de medicamento e da gravidade da doença, contudo, o tratamento geralmente é longo para garantir que todos os sintomas da PCM tenham sido tratados e que não ocorram recaídas (SHIKANAI-YASUDA et al., 2006, 2017). Para o paciente ser considerado clinicamente curado, o médico deve considerar os critérios clínicos, além de analisar exames radiológicos e sorológicos. Todavia, existe a possibilidade de acontecer uma reativação tardia, pois o *Paracoccidioides* spp. não é completamente eliminado do organismo. Assim, o objetivo do tratamento é a redução da carga fúngica para que a imunidade celular consiga controlar o parasita de modo que não cause mais danos à saúde do hospedeiro (SHIKANAI-YASUDA et al., 2006, 2017).

1.4. Reposicionamento de fármacos

O desenvolvimento de novos fármacos é um processo longo, complexo, arriscado, que exige muita pesquisa e dedicação, assim, poucas indústrias farmacêuticas estão dispostas a realizar esse investimento financeiro (LOMBARDINO; LOWE, 2004). Uma alternativa mais acessível é o reposicionamento de fármacos, a utilização de fármacos já existentes e comercializados para tratamentos diferentes dos quais foram inicialmente

desenvolvidos (ASHBURN; THOR, 2004). Devido aos fármacos comercializados possuírem dados de toxidade, farmacocinética e farmacodinâmica estabelecidos, o processo de reposicionamento torna-se vantajoso, já que obter estas informações é geralmente demorado e oneroso (ASHBURN; THOR, 2004).

Em 2013 Hurle e colaboradores compararam o processo de descoberta e desenvolvimento de novos fármacos com o reposicionamento, abordando as diferenças das duas estratégias (Figura 3). Além da indicação de novas atribuições para medicamentos que ainda são usados ou que perderam a eficiência no tratamento para o qual foram desenvolvidos (GELIJNS; ROSENBERG; MOSKOWITZ, 1998; HURLE et al., 2013), o reposicionamento diminui, consideravelmente, o tempo para a disponibilização dos fármacos aos pacientes (ASHBURN; THOR, 2004; HURLE et al., 2013).

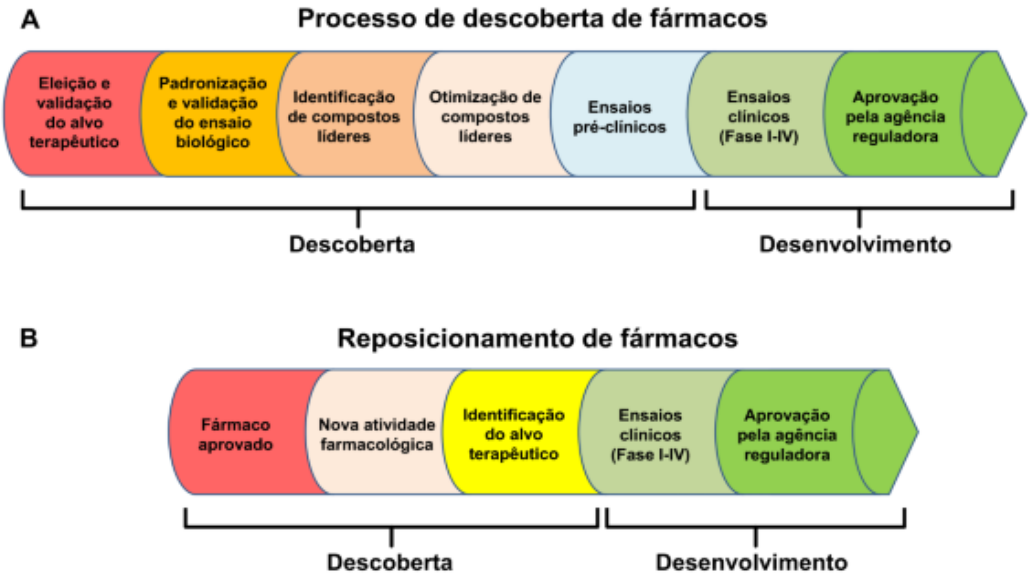

Figura 3: Comparação dos processos de descoberta e reposicionamento de fármacos. **(A)** Etapas envolvidas no planejamento de novos fármacos; e **(B)** Etapas envolvidas no reposicionamento de fármacos (Adaptado de: HURLE et al., 2013).

No reposicionamento de fármacos, duas estratégias são usadas: (i) Partindo de um fármaco, com objetivo de analisar seu potencial de ação no tratamento de doenças diferentes das quais é usualmente prescrito. (ii) Partindo da doença, com objetivo de identificar novos quimioterápicos para o seu tratamento. Essas abordagens proporcionam rapidez no processo de obtenção de fármacos que sejam mais eficientes e menos tóxicos para um determinado tratamento (DUDLEY; DESHPANDE; BUTTE, 2011).

Comumente, o processo de reposicionamento se baseia nos mecanismos de ações dos fármacos. Entretanto, Yang & Agarwal (2011) propuseram a utilização de informações clínicas dos efeitos adversos, que são frequentemente considerados indesejáveis, para redirecionar as aplicações terapêuticas dos fármacos estudados. Para os autores, um medicamento que cause hipotensão pode ser usado como anti-hipertensivo, controlando a dosagem, melhorando a formulação e direcionando-a para uma determinada população, com a justificativa de que os efeitos adversos e as indicações são mudanças comportamentais e fisiológicas do paciente e se um fármaco possui o mesmo efeito adversos de uma doença, pode existir um mecanismo de ação comum entre eles (YANG; AGARWAL, 2011).

Vários fármacos já passaram pelo processo de reposicionamento (Tabela 1). O sildenafil, fármaco desenvolvido nos anos 80 para tratar angina, dor no peito causada pela diminuição do fluxo de sangue para o coração, foi inicialmente reposicionado para tratar disfunção erétil (NOVAC, 2013) e, mais recentemente, para o tratamento de hipertensão arterial pulmonar (TAMBUYZER, 2010; LI; JONES, 2012). Milnaciprano, um antidepressivo atualmente prescrito para o tratamento de fibromialgia (ASHBURN; THOR, 2004). O antifúngico acrisorcina, redirecionado como antimalárico (SHAHINAS et al., 2010). O antipsicótico acetofenazina, o qual foi redirecionado como antagonista de receptor de androgênio humano (EKINS et al., 2011).

O itraconazol, um antifúngico triazol criado na década de 1980 que possui grande eficiência no combate de infecções fúngicas sistêmicas (EDWARDS; BETTS, 1853; SHIM; LIU, 2014), teve em 2007 a atividade anticancerígena descrita (CHONG et al., 2007). Estudos realizados para comprovar sua eficiência contra o câncer, utilizando-o isoladamente ou em combinação com outros anticancerígenos, mostraram forte atividade contra câncer de pulmão de células não pequenas (AFTAB et al., 2011; SHIM; LIU, 2014), contra meduloblastoma (KIM et al., 2010; SHIM; LIU, 2014), entre outros tipos de cânceres. Assim como o itraconazol, um glicosídeo cardíaco utilizado em vários tratamentos de doenças cardíacas, a digoxina, tem sido estudada como anticancerígeno (SHIM; LIU, 2014; YANG; AGARWAL, 2011).

Tabela 1: Lista de fármacos reposicionados entre os anos de 1943 a 2012. Ano referente a aprovação da comercialização para a nova indicação. (Adaptado de Novac 2013).

Fármaco	Indicação original	Nova indicação	Ano
Anfetamina	Estimulante	Hipercinesia em crianças (transtorno de déficit de atenção e hiperatividade, TDAH)	1943
Alopurinol	Síndrome de lise tumoral	Gota	1967
Zidovudina	Câncer	HIV / AIDS	1985
Minoxidil	Hipertensão	Alopecia	1988
Bupropiona	Depressão	Parar de fumar	1997
Sibutramina	Depressão	Obesidade	1997
Finasteride	Hiperplasia benigna da próstata	Alopecia	1997
Metotrexato	Câncer	Artrite reumatoide	1999
Fluoxetina	Depressão	Transtorno disfórico pré-menstrual	2000
Atomoxetina	Mal de Parkinson	Transtorno do déficit de atenção com hiperatividade	2002
Talidomida	Enjoo matinal	Mieloma múltiplo	2003
Cymbalta	Depressão	Neuropatia periférica diabética	2004
Topiramato	Epilepsia	Enxaqueca	2004
Paclitaxel	Câncer	Restenosis	2004
Sildenafil	Angina	Disfunção erétil	2005
Requip	Mal de Parkinson	Pernas inquietas	2005
Lumigan	Glaucoma	Hipotricose simples	2009
Dapoxetina	Analgesia e depressão	Ejaculação precoce	2009
Milnaciprano	Depressão	Síndrome da Fibromialgia	2009
Phentolamine	Hipertensão	Agente de reversão da anestesia dental	2009
Lidocaína	Anestesia local	Arritmia	2010
Mifepristona (RU486)	Término de gravidez	Síndrome de Cushing	2012

As ferramentas computacionais são extremamente importantes para guiar a síntese de novos compostos e para o reposicionamento de fármacos, facilitando e simplificando o processo, possibilitam análise de grandes conjuntos de dados racionalizando o número de compostos que serão avaliados e diminuindo o número de animais utilizados (EKINS; MESTRES; TESTA, 2007; EKINS et al., 2011).

Na farmacologia, *softwares* que usam diferentes fontes de informações biológicas e médicas vêm sendo utilizados para criação de modelos computacionais, sugerindo hipóteses e proporcionando descobertas de potenciais fármacos (EKINS; MESTRES; TESTA, 2007). Além disso, para facilitar o acesso de informações sobre alvos terapêuticos, bases de dados públicas acessíveis, como *DrugBank* (WISHART et al., 2006) e *Therapeutic Target Database* (TTD) (CHEN; JI; CHEN, 2002), as quais possuem várias informações de compostos e seus alvos, têm sido desenvolvidas.

Plataformas online que realizam comparações das sequências de genes ou proteínas, como o OrthoVenn, possibilitam comparar várias sequências ao mesmo tempo e identificar a presença de ortólogos em diferentes espécies (WANG et al., 2015). Partindo da sequência FASTA de uma proteína, é possível construir sua estrutura 3D pelo método de modelagem por homologia. O SWISS-MODEL é um dos bancos de dados usados para gerar modelos 3D de proteínas partindo das sequências de aminoácido. A plataforma desenvolve modelos por análise de homologia com os modelos de sua biblioteca (KIEFER et al., 2009).

Após a construção dos modelos é possível analisar as interações entre proteínas e fármacos por intermédio da ancoragem molecular, que estuda a energia de interação do ligante à proteína e analisa quais as interações são mais prováveis de ocorrerem. Por intermédio da ancoragem molecular é possível realizar triagens virtuais úteis no processo de descoberta, desenvolvimento e reposicionamento de fármacos, proporcionando estudos mais abrangentes e auxiliando na seleção de compostos mais promissores para os testes *in vitro* (CROSS et al., 2009; MCGANN, 2012).

Dessa forma, a implementação de estratégias de reposicionamento, usando ferramentas computacionais mostra-se como uma oportunidade para explorar o potencial de vários fármacos existentes, gerando tratamentos alternativos para diversas doenças.

2. JUSTIFICATIVA

Tendo em vista a relevância e a prevalência da PCM nos países da América Latina, o longo tempo de tratamento e as sequelas causadas, o reposicionamento de fármacos para PCM é uma alternativa viável na busca de fármacos com maior eficácia e mais seguros para o tratamento da PCM.

Os avanços obtidos com o sequenciamento dos genomas de *Paracoccidioides* spp. proporcionaram um recurso inestimável para a priorização, identificação e estudo da funcionalidade de novos candidatos a alvos terapêuticos de fármacos e ao mesmo tempo permitiram o desenvolvimento e aplicação de ferramentas computacionais de quimiogenômica aplicadas a estudos de reposicionamento de fármacos.

Levando em consideração o conceito de que proteínas que compartilham algum tipo de semelhança estrutural também podem compartilhar os mesmos ligantes, o processo de reposicionamento de fármacos para PCM pode ser desenvolvido em um intervalo menor de tempo e a custos mais baixos. Além de fornecer informações valiosas sobre a toxicidade e perfil farmacocinético dos fármacos a serem estudados.

Como as diversas bases de dados armazenam informações de alvos biológicos, além de informações químicas e farmacológicas de fármacos e candidatos a fármacos, o reposicionamento *in silico* de fármacos para PCM pode ser conduzido através da busca por proteínas do fungo que tenham homologia com alvos terapêuticos de fármacos disponíveis nas bases de dados *DrugBank* e TTD.

Os estudos computacionais podem ser úteis para reduzir o custo operacional e tempo necessários para realização dos ensaios biológicos, *in vitro* e *in vivo*, importantes para investigação da atividade contra PCM. Os candidatos a fármacos para o tratamento da PCM identificados também poderão servir como *scaffolds* para o planejamento e síntese de análogos estruturais com maior potência e seletividade.

3. OBJETIVOS

3.1. OBJETIVO GERAL

Identificar fármacos alternativos para o tratamento da PCM pela estratégia de reposicionamento de fármacos.

3.2. OBJETIVOS ESPECÍFICOS

- Por estratégias *in silico*, compilar, integrar e preparar um conjunto de proteínas de *Paracoccidioides* spp. e proteínas dos bancos de compostos, *DrugBank* e TTD;
- Determinar a presença de proteínas ortólogas comuns entre os três isolados de *Paracoccidioides* spp.;
- Realizar uma busca baseada em homologia nas bases de dados *DrugBank* e TTD, visando identificar fármacos com potencial atividade contra PCM;
- Selecionar proteínas alvos por comparação aos genes essenciais de *S. cerevisiae*;
- Priorizar fármacos para a avaliação biológica, utilizando estudos de ancoragem molecular;
- Determinar a atividade contra PCM, dos fármacos priorizados, nos estudos *in vitro*.

4. MATERIAL E MÉTODOS

4.1. Compilação da lista de genes de *Paracoccidioides* spp.

Com o intuito de prospectar potenciais alvos terapêuticos, as sequências FASTA de proteínas dos isolados de *Paracoccidioides* spp., *Pb*01, *Pb*03 e *Pb*18, foram obtidas a partir do *Broad Institute – Paracoccidioides brasilienses Database*, acessado no dia 15 de julho de 2016 (https://www.broadinstitute.org/fungal-genome-initiative/). As proteínas dos isolados foram submetidas à plataforma online OrthoVenn (WANG et al., 2015) para seleção de proteínas ortólogas aos três isolados (*E-value* $\leq 10^{-20}$). Esses isolados foram escolhidos para representar as diferentes linhagens de *Paracoccidioides* spp. e por serem isolados estudados em nosso laboratório.

4.2. Pesquisa em bases de dados

Para a identificação de fármacos com potenciais terapêuticos contra a PCM, as proteínas previamente selecionadas foram comparadas com alvos terapêuticos de fármacos aprovados para uso em humanos ou candidatos a fármacos em estudos clínicos. Estruturas superpostas permitem comparar características funcionalmente relevantes e identificar resíduos conservados necessários para catálise ou ligação de fármacos. Portanto, todos os alvos terapêuticos presentes nas bases de dados *DrugBank* (KNOX et al., 2011; WISHART et al., 2006) e TTD (CHEN; JI; CHEN, 2002; ZHU et al., 2010, 2012) foram considerados para a comparação, utilizando a plataforma OrthoVenn (*E-value* $\leq 10^{-20}$). Em seguida, a similaridade entre proteínas do *Paracoccidioides* spp. e proteínas alvos terapêuticos de fármacos foi investigada utilizando o servidor BLASTP de alinhamento par-a-par; somente proteínas homólogas com identidade sequencial $\geq 30\%$ foram consideradas nas análises seguintes.

4.3. Comparação com os genes essenciais de *Saccharomyces cerevisiae*

Com a finalidade de selecionar potenciais proteínas essenciais para *Paracoccidioides* spp., os alvos selecionados anteriormente foram comparados com as proteínas essências de *S. cerevisiae* utilizando a plataforma online OrthoVenn. As

sequências das proteínas essenciais foram obtidas da plataforma online *Database of Essential Genes* – DEG acessada no dia 15 de julho de 2016 (http://tubic.tju.edu.cn/deg/).

4.4. Modelagem por homologia

Com o intuito de explorar as bases estruturais das potenciais interações entre fármaco e a proteína, as estruturas tridimensionais (3D) dos alvos de *Paracoccidioides* spp. foram preditas utilizando a estratégia de modelagem por homologia. Inicialmente, as sequências FASTA de aminoácidos das proteínas foram submetidas ao servidor automatizado SWISS-MODEL (BIASINI et al., 2014; BORDOLI et al., 2009). Esse servidor é constituído basicamente de quatro etapas: (i) identificação e seleção de proteínas-molde disponíveis na base de dados *Protein Data Bank* (BERMAN et al., 2000), (ii) alinhamento das sequências, (iii) construção das coordenadas 3D e (iv) validação e seleção do melhor modelo utilizando parâmetros de seleção iniciais como a estimativa global de qualidade do modelo (GMQE do inglês *Global Model Quality Estimation*) e função de pontuação Análise de energia de modelo qualitativo (QMEAN do inglês *Qualitative Model Energy Analysis*) (BENKERT; KUNZLI; SCHWEDE, 2009). O GMQE representa uma estimativa de qualidade que combina propriedades do alinhamento proteína-molde. A função de pontuação QMEAN4 estima a qualidade global do modelo baseando-se na combinação linear de quatro descritores estruturais: geometria local, dois potenciais de interação dependentes de distância (baseados em todos os átomos ou *Cβ*,), e potencial de solvatação (BENKERT; KUNZLI; SCHWEDE, 2009).

4.5. Otimização dos modelos iniciais

Após construção dos modelos iniciais, suas estruturas foram submetidas separadamente ao processo de otimização estrutural no servidor KoBaMIN (CHOPRA; KALISMAN; LEVITT, 2010; CHOPRA; SUMMA; LEVITT, 2008; RODRIGUES; LEVITT; CHOPRA, 2012a). O protocolo de refinamento é composto de duas etapas: (i) minimização de energia usando o potencial de força média baseado em conhecimento e (ii) correção estereoquímica.

4.6. Definição dos estados de protonação dos cofatores e aminoácidos

Após o processo de refinamento, os modelos refinados foram submetidos separadamente ao módulo *Protein Preparation Wizard*, disponível no pacote de programas MAESTRO versão 9.3 (Schrödinger, LLC, New York, NY, 2014). Nesta etapa, foi realizada a correção das ordens de ligação e adição de hidrogênio, bem como a definição dos estados de protonação em pH 7,0 ± 1,0 (para ambos: aminoácidos, substrato e cofator) utilizando o programa Epik versão 2.7 (SHELLEY et al., 2007). Ao final deste processo, as estruturas foram novamente submetidas a uma nova minimização de energia utilizando o campo de força OPLS-2005 (BANKS et al., 2005)**.**

4.7. Validação do modelo 3D

Com o objetivo de avaliar a qualidade dos ângulos *phi* (ϕ) e *psi* (ψ) da cadeia principal (análise de Ramachandran) e dos ângulos *chi* (χ) dos rotâmeros de cadeia lateral, as estruturas 3D foram submetidas a uma análise estatística de qualidade utilizando o servidor MolProbity (CHEN et al., 2010). O programa gráfico PyMOL versão 1.3 (Schrödinger, LLC, New York, NY, 2010) foi utilizado para a visualização.

4.8. Ancoragem molecular

O *input* das estruturas dos compostos foi feito no *software Maestro workspace* versão 9.3 e preparadas usando LigPrep 2.5 (Schrödinger, LCC, New York, 2012) a um pH de 7,0 ± 1. Posteriormente, 2000 conformações foram geradas usando o OMEGA v.2.5.1 (OMEGA versão 2.5.1: *OpenEye Scientific Software*, Santa Fe, NM; http://www.eyesopen.com., no date; Hawkins et al., 2010), enquanto as cargas AM1-BCC (Jakalian, Jack, Bayly, 2002) foram adicionadas usando o QUACPAC versão 1.6.3 (QUACPAC v.1.6.3: OpenEye Scientific Software, Santa Fe, NM. http://www.eyesopen.com.'). Antes dos estudos de ancoragem, *grids* (caixa 3D construídas ao redor do sito ativo das proteínas) foram gerados por intermédio de uma sonda molecular para detecção de *pockets* ao redor das proteínas, os quais poderiam potencialmente ser locais de ligações catalíticas e sítios alostéricos, usando o programa Make Receptor 3.2.0.2. Por último, para a ancoragem molecular foi utilizado o protocolo de alta resolução

do programa FRED e o *score* ChemGauss4, ambos disponíveis no OEDocking *suite* v.3.2.0 (OEDocking v.3.2.0: *OpenEye Scientific Software*, Santa Fe, NM. http://www.eyesopen.com., no date; McGann, 2011, 2012).

5. RESULTADOS E DISCUSSÃO

Este estudo teve como objetivo identificar fármacos para combater a PCM, micose sistêmica negligenciada e endêmica na América Latina (MUÑOZ et al., 2014), sendo o Brasil o país com maior número de casos (BRUMMER; CASTANEDA; RESTREPO, 1993; MUÑOZ et al., 2014). Com alta taxa de incidência e longo tratamento (BELLISSIMO-RODRIGUES; MACHADO; MARTINEZ, 2011; SHIKANAI-YASUDA et al., 2006), o paciente com PCM pode ficar com sequelas em vários órgãos como pulmão, pele e sistema nervoso central (TOBÓN et al., 2003; SHIKANAI-YASUDA et al., 2006, 2017).

Para a triagem quimiogenômica, realizou-se a comparação das proteínas do *Pb*01, *Pb*03 e *Pb*18 com objetivo de prosseguir os estudos apenas com proteínas ortólogas aos três isolados (Figura 4). *Pb*03 e *Pb*18 possuem genoma de tamanho semelhantes, 29,01 Mb e 30,0 Mb, respectivamente, e são mais semelhantes entre si, compartilhando 96% de similaridade (DESJARDINS et al., 2011), enquanto o genoma *Pb*01 é maior com 32,9 Mb (DESJARDINS et al., 2011).

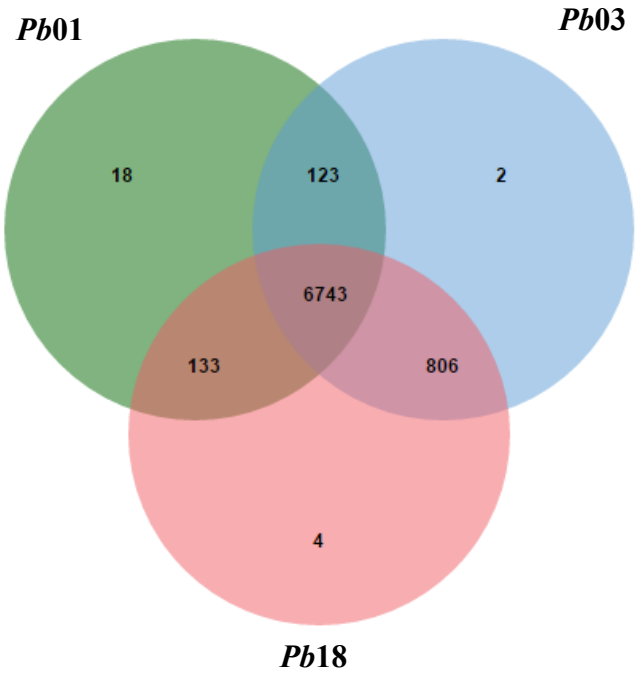

Figura 4: Comparação das sequências dos três isolados. Diagrama de Venn mostrando a quantidade de clusters gerados após a comparação. No total, identificou-se 6782 proteínas ortólogas aos três isolados.

Ao comparar as proteínas dos três isolados, obteve-se 6743 clusters contendo 6782 proteínas ortólogas aos três isolados. Clusters são grupos gerados, pela plataforma usada para comparar os isolados, que agrupam as proteínas que são ortólogas. Os isolados usados pertencem a diferentes linhagens e têm diferentes distribuições geográficas, porém os três isolados estão presentes no Brasil (MUÑOZ et al., 2016; TEIXEIRA et al., 2009). Embora o Pb01 seja mais distinto, possui 90% das sequências semelhantes com as do Pb03 e Pb18 (DESJARDINS et al., 2011), por isso foi obtido muitas proteínas ortológas entre os três isolados.

Na predição dos compostos para o combate à PCM, as proteínas do *Paracoccidioides* spp., selecionadas na etapa anterior, foram comparadas com as proteínas dos bancos de compostos *Drugbank* e TTD. Para ter maior precisão, a comparação foi realizada separadamente, como mostrado na Figura 5. No total, 1012 compostos, em diferentes fases de desenvolvimento e indicações clínicas, foram sugeridos para 265 proteínas do *Pb*01, ortólogas aos outros isolados. Desse valor, 46% foi sugerido pelo *DrugBank*, 39% pelo TTD e apenas 15% foram sugeridos pelos dois, mostrando a importância da utilização dos dois bancos de dados.

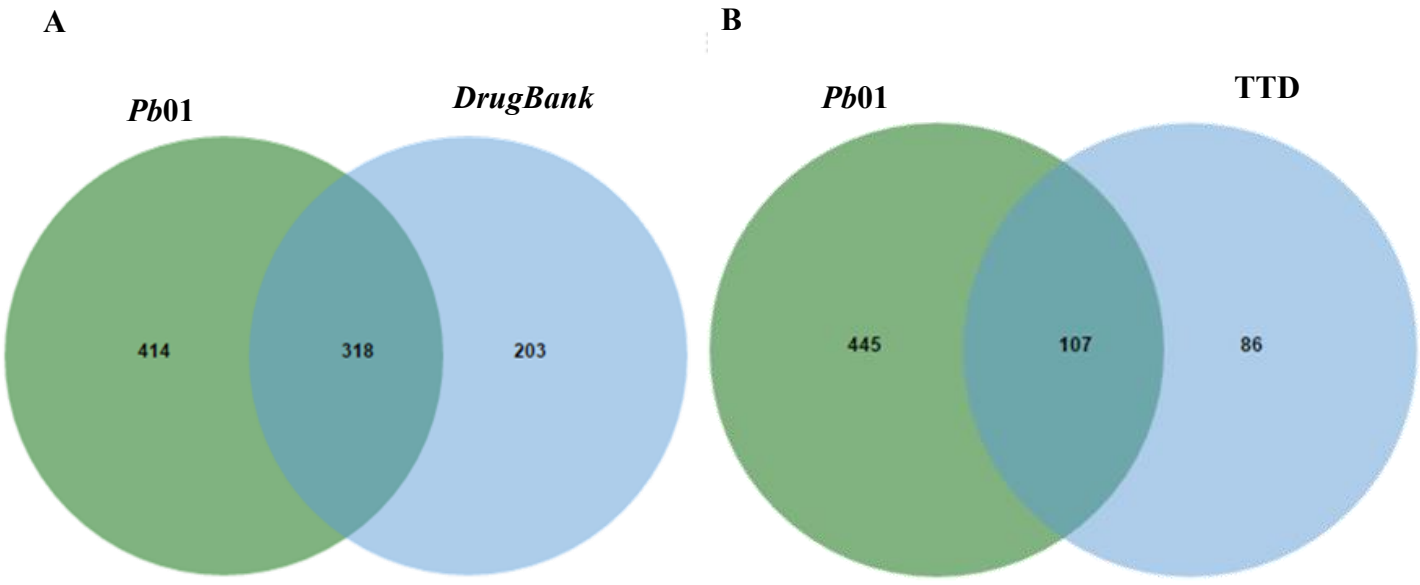

Figura 5: Comparação das proteínas do *Pb*01 com as proteínas dos bancos de fármacos. (A): Comparação das proteínas do *Pb*01 com as proteínas do DrugBank. Foram gerados 318 clusters contendo 228 proteínas ortólogas. (B): Comparação das proteínas do *Pb*01 com as proteínas do TTD. Foram gerados 107 clusters contendo 120 proteínas ortólogas.

O Blast P foi realizado para analisar a porcentagem de caracteres similares existente entre as proteínas do fungo com as proteínas dos bancos de fármacos. Das 265 proteínas do fungo que tiveram sugestão de fármacos, 145 apresentaram identidade ≥ 30%, as quais possuem 809 fármacos sugeridos.

Visando a acurácia dos resultados, essas proteínas foram comparadas com as proteínas essenciais de *S. cerevisiae,* proteínas considerados importantes para a sobrevivência do fungo (SERINGHAUS et al., 2006). Das 145 proteínas de *Paracoccidioides* spp., apenas 46 foram homologas as proteínas essenciais de *S. cerevisiae* (Figura 6).

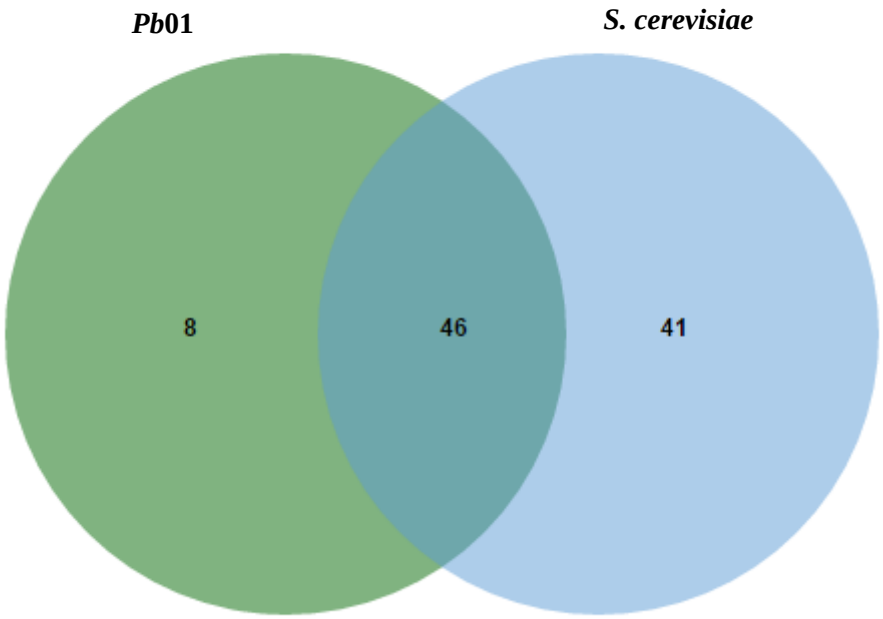

Figura 6: Comparação das proteínas de *Pb*01 com as proteínas essenciais de S. cerevisiae, 46 cluster foram gerados contendo 46 proteínas ortólogas as proteínas do *Pb*01.

Estudos usando *S. cerevisiae* para descrever funções de genes e de proteínas em *Paracoccidioides* spp. são comuns. Fernandes et al. (2005) realizaram análises transcricionais comparativas de *P. brasiliensis* com outros fungos, entre eles, *S. cerevisiae*, para identificação de componentes das vias de sinalização em *P. brasiliensis* relacionadas à regulação celular, morfogêneses e virulência (FERNANDES et al., 2005). A comparação dos genomas de *Paracoccidioides* spp. com *S. cerevisiae* possibilitou a identificação de genes envolvidos na reprodução sexual em *Paracoccidioides* spp., espécies consideradas assexuadas (TEIXEIRA et al., 2013).

As vantagens e limitações do uso de *S. cerevisiae* como organismo modelo foram estudados por comparações proteômicas completa com 704 organismos de diferentes filos, com representantes de quase todos os reinos, e por categorização funcional das proteínas em diferentes processos. Como conclusão do trabalho, os autores apoiaram o uso *S. cerevisiae* como organismo modelo nos diversos estudos de processos e caminhos biológicos em outros organismo (KARATHIA et al., 2011).

Para a construção das estruturas 3D, as sequências das 46 proteínas foram submetidas no servidor *SWISS-MODEL* (BIENERT et al., 2017), o qual prediz modelos para as proteínas através de homologia, comparando as sequências submetidas com o banco de dados PDB. Das 46 proteínas submetidas, 43 proteínas tiveram modelos sugeridos.

Os modelos gerados foram otimizados pelo KoBaMIN (RODRIGUES; LEVITT; CHOPRA, 2012), onde as estruturas passam por verificações, analisando se há ausência de átomos, resíduos perdidos e erros no formato salvo, sendo refinados posteriormente. Para validação, os modelos foram submetidos ao *MolProbity* (CHEN et al., 2010); Das 43 proteínas submetidas, a plataforma não gerou resultados para os modelos de duas proteínas, as quais foram usadas nas etapas posteriores mesmo sem a validação. Os dados de qualidade dos modelos gerados para as proteínas que tiveram compostos selecionados para os testes *in vitro*, são mostrados na tabela 2.

Tabela 2: Análise de geometria das proteínas para os modelos construídos.

PAAG	**Proteínas alvos do *Pb*01**	***Template***	***MolProbity score***	**Resolução *MolProbity score***
PAAG_03031	Beta tubulina beta	***4I50***	1.60	92º percentis
PAAG_07279	Farnesil pirofosfato sintetase	***4QPF***	1.68	90º percentis
PAAG_04243	Na+/K+ cadeia alfa ATPase	***3A3Y***	2.05	73º percentis
PAAG_01410	Fosfatidilinositol 3-quinase tor2	***4JSN***	1.86	83º percentis
PAAG_00827	Lanosterol 14-α desmetilase	***4UYM***	1.75	87º percentis
PAAG_02441	Proteína quinase C	***3TXO***	1.83	84º percentis
PAAG_08991	Serina Treonina-proteína quinase	***3D2k***	1.73	88º percentis
PAAG_08597	Timidilato sintase	***2AAZ***	1.95	78º percentis

O *MolProbity score* é um parâmetro que avalia a estatística de qualidade geral do modelo. Ele combina alguns parâmetros, tais como, pontuação do *clashscore*, porcentagem de *Ramachandran* e porcentagem de rotâmeros. *Clashscore* é o número de colisões sérios por 1000 átomos. (CHEN et al., 2010). O valor de percentil está relacionado com a resolução de raios-X dos modelos; quanto mais próximo do 100º melhor a qualidade deles. Todos os modelos validados apresentaram resolução do *MolProbity score* superior à 50º percentil (Anexo 1). As oito proteínas, selecionadas após a ancoragem molecular, que tiveram os fármacos sugeridos selecionados para os testes *in vitro* (Tabela 2), apresentaram resolução igual ou superior a 73 percentis.

Após a preparação dos modelos, *grids* foram construídos para cada proteína e os confôrmeros dos fármacos foram gerados para a realização da ancoragem molecular. Dentre os 292 fármacos sugeridos para as proteínas modeladas, o programa não conseguiu analisar as interações de 11 fármacos com seus respectivos alvos, por serem íons metálicos, peptídeos ou por terem estruturas muito grandes. Todos os dados das etapas realizadas estão no Anexo 2.

Para a realização da ancoragem molecular foi usado o programa FRED do pacote da OpenEye. Esse programa usa logaritmo de busca exaustiva que analisa rotações de cada conformero gerado dos fármacos (ligante) dentro do sítio ativo marcado da proteína. Filtragens são realizadas, durante a busca exaustiva, para desconsideração das posições irregulares dos confôrmeros e pontuação das melhores posições. Durante a ancoragem molecular a proteína é considerada rígida e o ligante flexível, por ter várias conformações avaliadas na interação com a proteína (MCGANN, 2011).

O FRED *score* gerado é um conjunto de várias funções de pontuações, entre elas, *chemgauss*, *chemscore*, *shapegauss* (MCGANN, 2011). A pontuação *chemgauss* mede a interação do ligante no sítio ativo da proteína, analisando as interações relacionadas à forma, ligação de hidrogênio entre ligante e proteína, interações de hidrogênio com solvente implícito e interações metal-quelato (OpenEye 2017).

Chemscore é a soma das interações lipofílica (ligações que ocorrem entre dois átomos não polares, do ligante com da proteína), ligação de hidrogênio, quelato de metais (interação de átomos do ligante com átomo de metal da proteína), choque (penalidade que ocorre quando átomos do ligante colidem com a proteína), e ligação rotativa (termo de penalidade relacionada às ligações do ligantes que ao ser encaixado no sítio ativo da proteína não é mais livre para girar) (OpenEye 2017).

Shapegauss, pontuação baseada na pose mais favorável do ligante para se encaixar no sítio ativo da proteína, sem levar em consideração qualquer interação química existente. Essa pontuação é calculada somando o potencial de emparelhamento entre os átomos da proteína com os átomos do ligante, sendo mais favorável quando os átomos se aproximam sem ocorrer sobreposições (OpenEye 2017).

Após analisar e calcular todas as pontuações geradas durante a ancoragem molecular, o FRED score é gerado, quanto mais negativo for seu valor mais favoráveis serão as interações dos fármacos-proteínas. Para a seleção dos fármacos que serão testados *in vitro*, além dos resultados da ancoragem molecular, foram considerados o tipo de alvo (proteína estudada), tipo de fármaco, e se já foram usados no tratamento da PCM. Foram realizadas pesquisas no PubMed (HAROON, 1998) e PubChem Bioassay (PUBCHEM, 2017) visando a exclusão de compostos que já são, ou foram usados contra a PCM.

Os resultados da ancoragem molecular para os compostos selecionados são apresentados na tabela 3. As Figuras 7 a 12 ilustram as interações desses compostos com seus respectivos alvos.

Tabela 3: Compostos selecionados para os testes *in vitro.*

Alvos do *Pb*01	**Compostos**	**Classe terapêutica**	**Fase de desenvolvimento**	**Score *Docking***
PAAG_03031 Beta Tubulina	ABT-751	Antitumoral	Fase 2	-8.318.228
PAAG_03031 Beta Tubulina	Mebendazol	Antinematódeos	Aprovado	-9.034.729
PAAG_12506 Beta Tubulina	Albendazol	Antiprotozoários	Aprovado	-8.118.922
PAAG_07279 Farnesil pirofosfato sintetase	Pamidronato	Bisfosfonato	Aprovado	-19.165.264
PAAG_07279 Farnesil pirofosfato sintetase	Minodronato	Tratamento de osteoporose	Aprovado	-18.478.310
PAAG_00827 Lanosterol 14-α desmetilase	Luliconazol	Antifúngico	Aprovado	-12.363.360
PAAG_00827 Lanosterol 14-α desmetilase	Butoconazol	Antifúngico	Aprovado	-15.730.254
PAAG_00827 Lanosterol 14-α desmetilase	Bifonazol	Antifúngico	Aprovado	-18.365.929
PAAG_00827 Lanosterol 14-α desmetilase	Sertaconazol	Antifúngico	Aprovado	-14.937.805

Alvos do *Pb*01	Compostos	Classe terapêutica	Fase de desenvolvimento	Score *Docking*
PAAG_04243 Na+/K+ cadeia alfa ATPase	Dexlansoprazol	Refluxo gastroesofágico	Aprovado	-10.104.547
PAAG_01410 Fosfatidilinositol 3-quinase tor2	Dactolisib	Antineoplásico	Fase 2	-14.269.496
PAAG_01410 Fosfatidilinositol 3-quinase tor2	AZD2014	Antineoplásico	Fase 2	-13.222.617
PAAG_01410 Fosfatidilinositol 3-quinase tor2	BGT226	Antitumoral	Fase 1/2	-13.027.889
PAAG_02441 Proteína quinase C	Midostaurin	Antineoplásico	Fase 2	-14.511.683
PAAG_08991 Serina Treonina-proteína quinase	ENMD-2076	Leucemia mielóide aguda	Fase 2	-14.994.042
PAAG_08991 Serina Treonina-proteína quinase	Tozasertib	Anticancerígena	Fase 2	-15.114.143
PAAG_08597 Timidilato sintase	Raltitrexed	Anticancerígena	Aprovado	-13.317.190

A Figura 7 ilustra modo de ligação do fármaco dexlansoprazol na cadeia α da (Na^+, K^+)-ATPase. De forma geral, os grupamentos tionila, imidazol e piridina do fármaco dexlansoprazol fazem ligações de hidrogênio com os resíduos Gln854, Ser858 e Ser376, respectivamente. Interações hidrofóbicas são observadas entre os anéis aromáticos e trifluorometil e Leu174, Ile379, Leu178, Val172, Trp353, Trp364 e Val848.

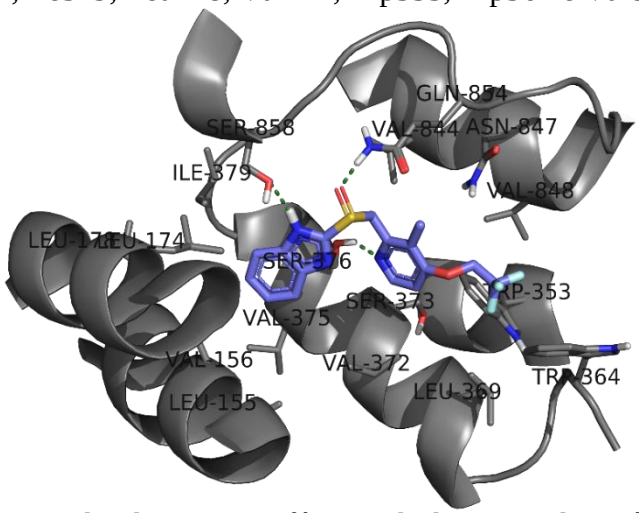

Figura 7: Interações intermoleculares entre o fármaco dexlansoprazol e resíduos de aminoácido da cadeia α da (Na+, K+) ATPase de *Paracoccidioides* spp.

Os estudos de ancoragem molecular também demonstraram que alguns antifúngicos ainda não utilizados na quimioterapia da PCM possuem elevada afinidade pela enzima lanosterol 14-α desmetilase de *Paracoccidioides* spp. De acordo com a Figura 9, o nitrogênio do anel imidazol dos fármacos bifonazol e sertaconazol se coordenam diretamente com o Fe^{2+} heme enquanto os demais resíduos de aminoácidos do sítio ativo (por exemplo, Tyr122, Phe130, Tyr136, Phe130, etc.) realizam interações hidrofóbicas com os anéis aromáticos de ambos os ligantes. O mesmo perfil de interação foi observado para os outros inibidores (Luliconazol e Butoconazol) de lanosterol 14-α desmetilase preditos nesta abordagem.

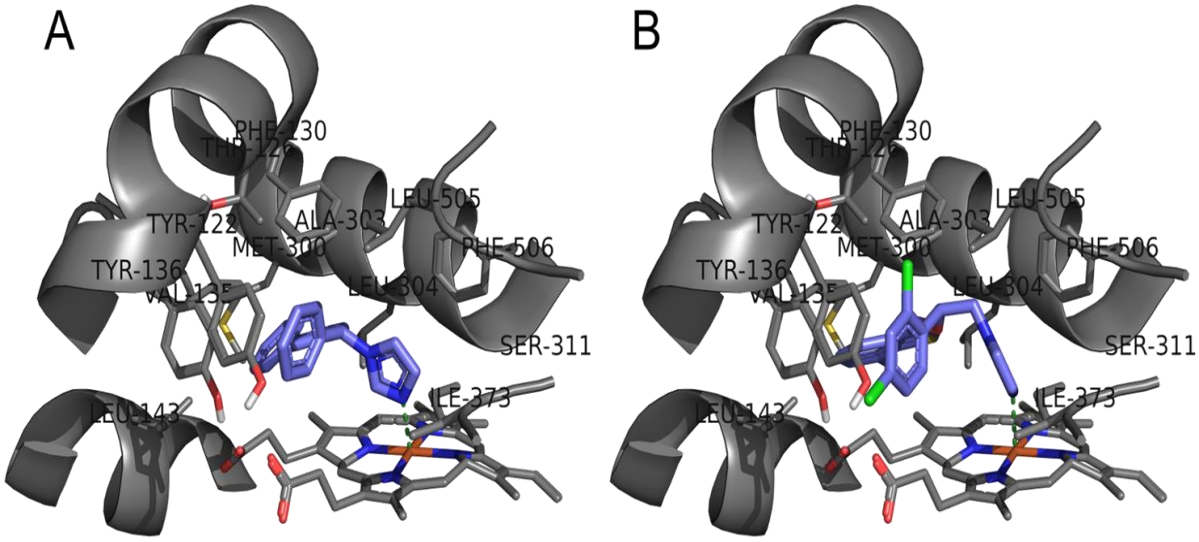

Figura 8: Interações intermoleculares dos fármacos **(A)** bifonazol e **(B)** sertaconazol com o sítio ativo da enzima lanosterol 14-α desmetilase de *Paracoccidioides* spp.

A Figura 9 representa o modo de ligação da midostaurina no sítio de ligação do ATP da proteína quinase C. Como pode ser observado, os átomos de nitrogênio e oxigênio do anel pirrolidona formam ligações de hidrogênio com a cadeia principal dos resíduos Ile86 e Glu84, ao passo que a carbonila do grupo benzamida forma uma ligação de hidrogênio com a Lys130. Os demais grupamentos químicos da midostaurina formam interações hidrofóbicas com os resíduos Phe55, Met86, Phe14, Phe296, Phe292, Leu9, Phe14, Val17 e Met83.

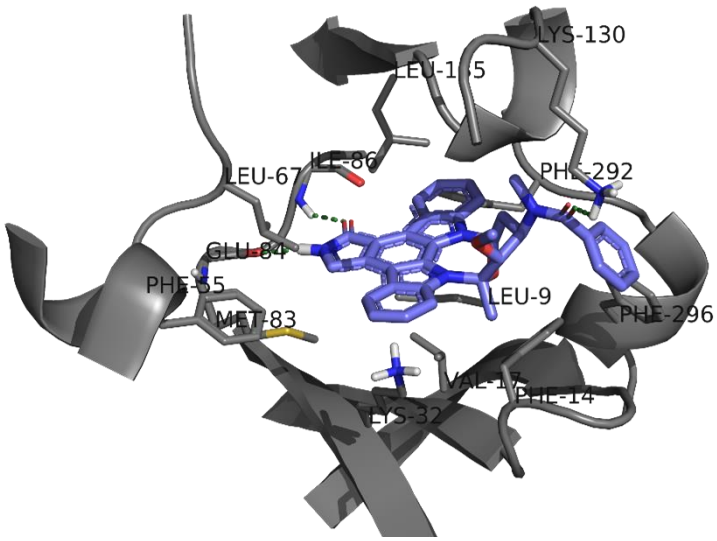

Figura 9: Interações intermoleculares entre a midostaurina e resíduos de aminoácido do sítio de ligação do ATP da proteína quinase C de *Paracoccidioides* spp.

A Figura 10 representa o modo de ligação dos fármacos minodronato (A) e pamidronato (B) com o sítio ativo da enzima farnesil pirofosfato sintase. O perfil de interação de ambos os fármacos é bastante semelhante. De forma geral, o grupamento pirofosfato de isopentenilo se coordena com os átomos de Mg^{2+} (esferas verdes) facilitando a formação de ligações de hidrogênio com os resíduos Arg103, Gln231 e Asp234. Entretanto, o anel imidazopiridina do minodronato forma uma ligação de hidrogênio com a Arg53 e interações hidrofóbicas com os resíduos Tyr195, Phe230 e Leu91, ao passo que a amina alifática do pamidronato forma ligações de hidrogênio com a Tyr195 e Thr192.

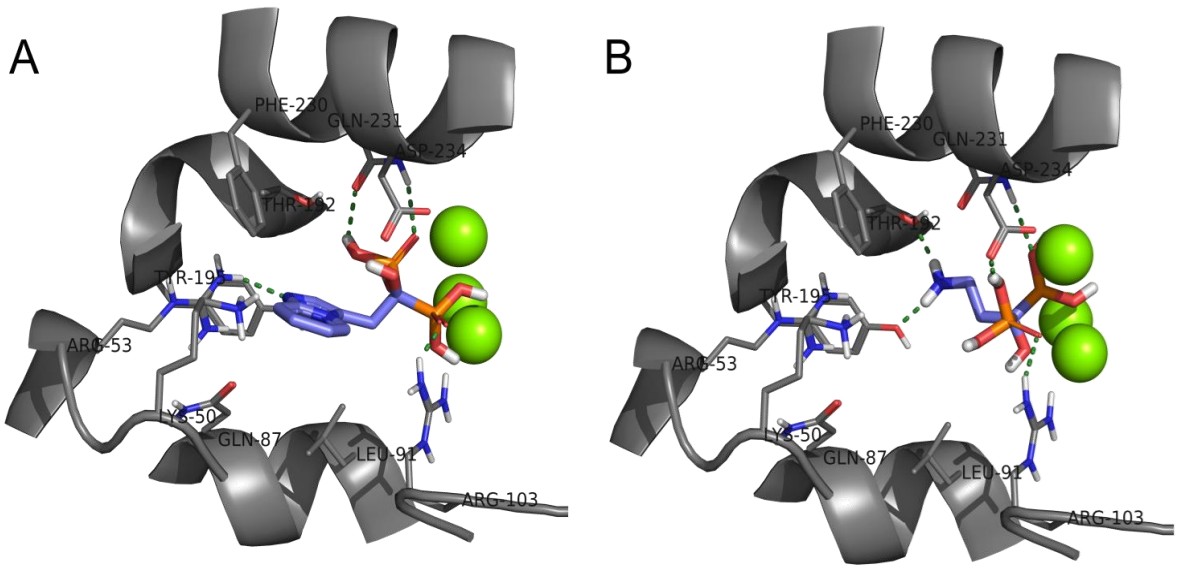

Figura 10: Interações intermoleculares dos fármacos **(A)** minodronato e **(B)** pamidronato com o sítio ativo da enzima farnesil pirofosfato sintase de *Paracoccidioides* spp.

As interações intermoleculares entre o fármaco raltitrexede e resíduos de aminoácido do sítio ativo da timidilato sintase estão representadas na Figura 11. Como

pode ser observado, os ácidos carboxílicos da cadeia alifática formam ligações de hidrogênio com Asn141, Ile360 e His300, ao passo que o nitrogênio do anel 1,4-diidroquinazolina-4-ona forma uma ligação de hidrogênio com a Asn270. Interações hidrofóbicas também são observadas entre o anel tiofeno e resíduos Leu265 e Met358 e entre o anel 1,4-diidroquinazolina-4-ona e resíduos Trp138 e Tyr164.

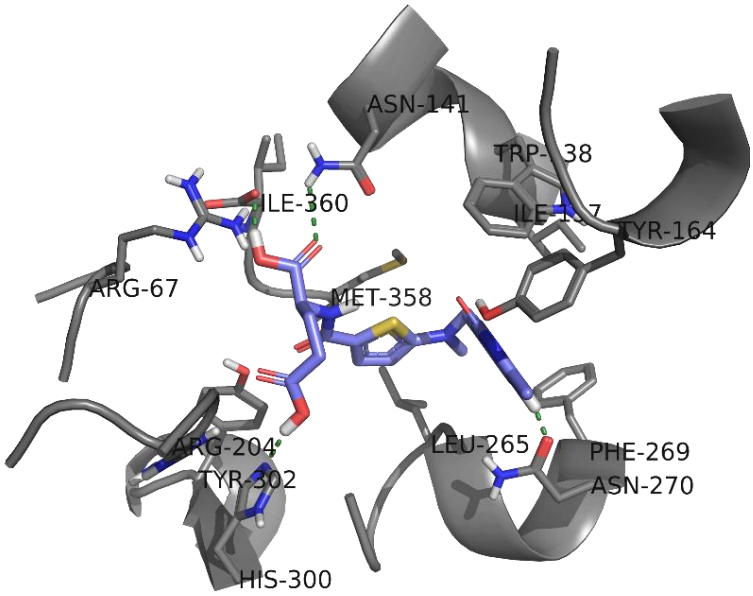

Figura 11: Interações intermoleculares entre o fármaco raltitrexede e resíduos de aminoácido do sítio ativo da timidilato sintase de *Paracoccidioides* spp.

As interações intermoleculares entre o fármaco mebendazol (A) e do candidato a fármaco ABT-751 (B) com os resíduos de aminoácido beta tubulina estão representadas na Figura 12. Ao analisar o modo de ligação do fármaco mebendazol, observa-se a formação de ligações de hidrogênio entre o anel benzimidazol e os resíduos Gln21 e Arg358, enquanto que o grupamento acetofenona forma interações hidrofóbicas com os resíduos His226, Pro357, Leu360 e Phe269. O fármaco albendazol apresenta interações intermoleculares semelhantes. Por outro lado, o nitrogênio do grupamento sulfonamida presente na estrutura do candidato a fármaco ABT-751 forma uma ligação de hidrogênio com o Trp22, ao passo que seu grupamento acetofenona também forma interações hidrofóbicas com os resíduos His226, Pro357, Leu360 e Phe269.

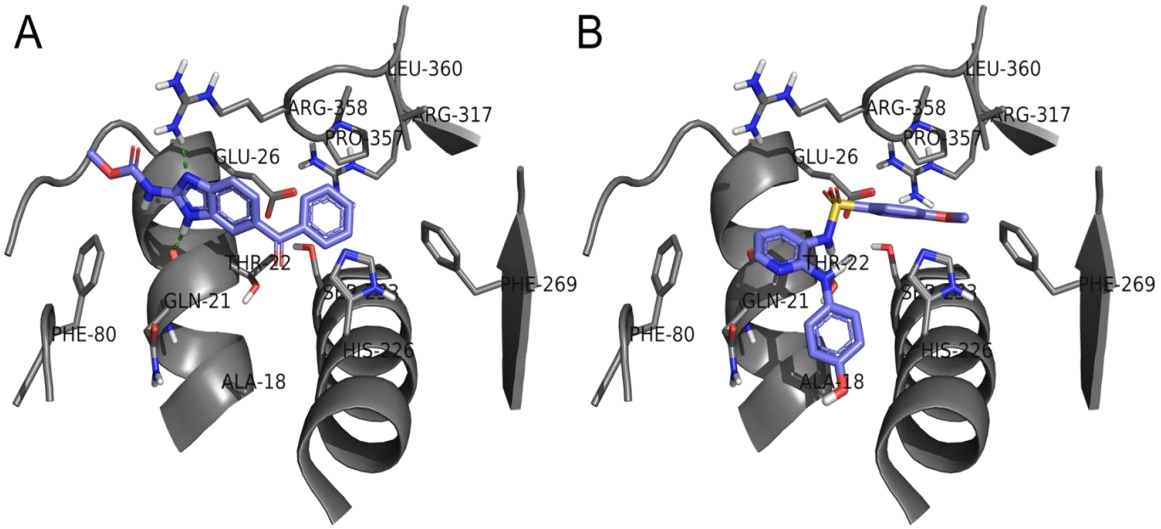

Figura 12: Interações **intermoleculares** do fármaco **(A)** mebendazol e do candidato a fármaco **(B)** ABT-751 com os resíduos de aminoácido da cadeia β da tubulina de *Paracoccidioides* spp.

A figura 13 resume os resultados alcançados, através dos métodos utilizados.

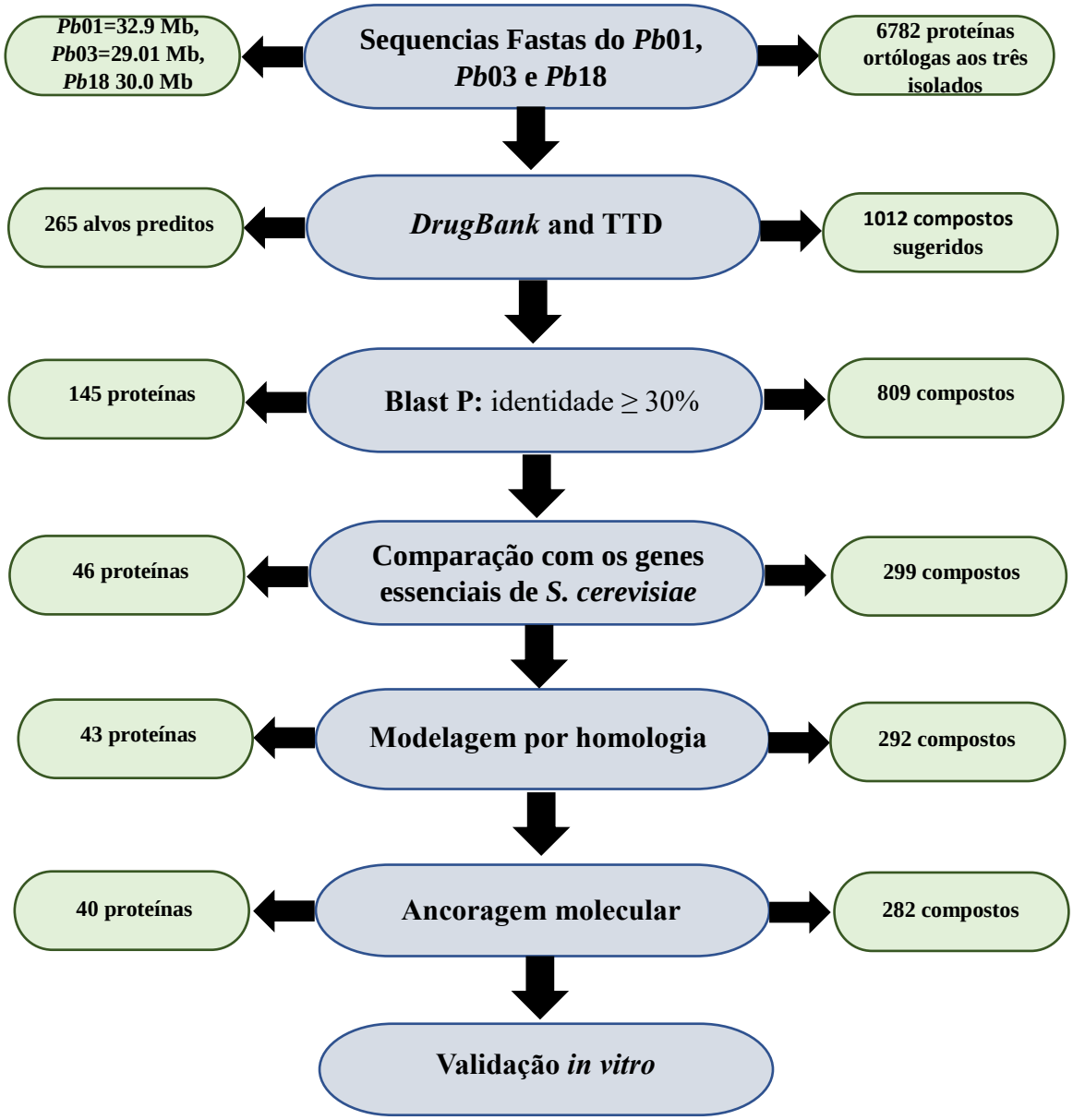

Figura 13: Fluxograma com os métodos utilizados e resultados obtidos em cada etapa.

Entre os fármacos sugeridos para o reposicionamento, foram identificados fármacos usados para o combate à PCM, como itraconazol, cetoconazol, fluconazol e Voriconazol. Apesar de não serem comumente usados no tratamento da PCM, miconazol e econazol foram usados para evitar a reativação da PCM (NEGRONI et al., 1977), e no tratamento de caso de PCM disseminada (CARMEN MARCANO, 1990), respectivamente.

Para a proteína lanosterol 14-α desmetilase, quatro compostos foram selecionados: luliconazol, um antifúngico eficiente no combate a várias micoses como as causadas por *Candida albicans* e *Trichophyton* spp. (KHANNA; BHARTI, 2014); butoconazol, bifonazol e sertaconazol usados principalmente para o tratamento de candidíase (BORELLI et al., 2007; HENG; CHEN; TAN, 2012; WÄCHTLER; WILSON; HUBE, 2011).

Usada como alvo de fármacos, a farnesil pirofosfato sintetase desempenha funções cruciais na regulação do metabolismo de isoprenóide (DHAR; KOUL; KAUL, 2013) e, ao se ligar aos receptores dos fatores de crescimentos, participa da transdução de sinal mediada pelo fator de crescimento dos fibroblastos (REILLY et al., 2002). Dois bifosfonatos nitrogenados foram reposicionados para ela: o minodronato, indicado para o tratamento de osteoporose (OKAZAKI et al., 2012), para o qual possuem estudos sugerindo seu uso como uma alternativa no tratamento de melanoma (YAMAGISHI et al., 2004), e o pamidronato usado no tratamento da metástase de câncer relacionado aos ossos (STEFANIK et al., 2008).

A subunidade transportadora de sódio/potássio alfa ATPase, uma proteína transmembranar responsável pelo transporte de sódio e potássio contra seus gradientes de concentração (TEJRAL et al., 2017), o dexlansoprazol, um R-enantiômero de lansoprazol usado no tratamento de pacientes com refluxo gastroesofágico (WU et al., 2016), foi sugerido para o reposicionamento e selecionado para os testes *in vitro.*

Os compostos selecionados para a fosfatidilinositol 3-quinase tor2, proteína relacionada ao controle da divisão celular (KRASILNIKOV, 2000), estão em fase de investigação. O dactolisib um antineoplásico (NETLAND et al., 2016), AZD2014 um inibidor de mTOR (alvo mamífero da rapamicina) estudado para o combate de carcinoma de células escamosas orais (YU et al., 2016) e BGT226 estudado como antitumoral contra células de câncer de cabeça e pescoço (CHANG et al., 2011).

A proteína quinase C tem sido relacionada com várias alterações vasculares associadas a diversas doenças: diabetes, onde a ativação da proteína quinase C por indução de hiperglicemia seria a responsável pela disfunção endotelial observada em

pacientes diabéticos (FERREIRA; BRUM; MOCHLY-ROSEN, 2011); nos pacientes com determinados tipos de cânceres, como de cólon (FERREIRA; BRUM; MOCHLY-ROSEN, 2011), de estômago (SONG et al., 2001) e de próstata (WU et al., 2002) foi identificada a alta expressão da proteína quinase C; doenças cardíacas, quando a proteína quinase C não desempenha a resposta adequada causando hipertrofia cardiomiócitos, fibrose miocárdica e inflamação (FERREIRA; BRUM; MOCHLY-ROSEN, 2011). Dessa forma, a proteína quinase C tem sido considerada um bom alvo para desenvolvimento de fármacos (MOCHLY-ROSEN; DAS; GRIMES, 2012). O fármaco selecionado com potencial de ação na quinase C foi a midostaurina, um inibidor de tirosina quinase que está em fase de investigação para o tratamento de leucemia mielóide aguda e mastocitose sistêmica avançada (PETER et al., 2016).

A proteína serina/treonina quinase é relacionada com a virulência de bactérias, responsável por identificar o meio, percebendo vários sinais e coordenando respostas de processos celulares, e por interferir nas respostas do sistema imune dos hospedeiros (CANOVA; MOLLE, 2014). Dois compostos em fase de desenvolvimento foram sugeridos para elas, ENMD-2076 um inibidor de pequenas moléculas de quinases com ação em vias que envolvam o crescimento e sobrevivência de tumor, está sendo avaliado em pacientes com câncer de ovário resistente à platina (FLETCHER et al., 2011) e tozasertib um inibidor de quinase com atividade anticancerígena (MICHAELIS et al., 2015).

A timidilato sintase participa da formação de timidilato, percussor essencial para a biossíntese de DNA (CARRERAS; SANTI, 1995) considerada bom alvo para fármacos (CHERNYSHEV; FLEISCHMANN; KOHEN, 2007), o Raltitrexed, um anticancerígeno usado em tratamento de tumores como o colorretal (CUNNINGHAM et al., 1996), foi sugerido para o reposicionamento no combate à PCM.

A beta tubulina é uma proteína importante para a formação de microtúbulos, elementos essenciais do citoesqueleto das células eucariotas (JANKE, 2014). Para ela, foram selecionados os seguintes compostos: ABT-751, um agente antimitótico e agente de interrupção vascular com atividades anticancerígena, que está em fase de desenvolvimento (RUDIN et al., 2011); Mebendazol e o Albendazol, derivados do benzimidazol usados no tratamento de equinococoses císticas e outros parasitas encontrados no sistema nervoso central (PRESS, 2010; PANTZIARKA et al., 2014).

Todos os fármacos selecionados são candidatos promissores para o tratamento da PCM. Como perspectiva, os testes *in vitro* de concentração inibitória mínima,

determinação da concentração fungicida mínima e citotoxidade serão realizados para validação dos resultados obtidos *in silico*.

6. CONCLUSÕES

Utilizando estratégias computacionais, foi possível a identificação de fármacos alternativos para o tratamento da Paracoccidioidomicoses, micose sistêmica, endêmica na América Latina que tem alta taxa de morbidade e mortalidade todo ano.

Através de comparações das sequências das proteínas selecionou-se proteínas ortológas aos isolados *Pb*01, *Pb*03, *Pb*18 e foram preditos fármacos com potenciais de ação nas mesmas. Na comparação com *S. cerevisiae* selecionou-se potenciais proteínas essenciais para *Paracoccidioides* spp.

Após várias etapas de filtragem, 43 proteínas e 292 fármacos foram submetidos à ancoragem molecular analisando o quanto é favorável para que as interações entre fármaco e proteína ocorram. Com os resultados obtidos, foi possível concluir que o método aplicado foi eficiente no reposicionamento de fármacos para a PCM, sendo listados 17 fármacos mais promissores.

7. REFERÊNCIAS

ADLER-MOORE, J.; PROFFITT, R. T. AmBisome: liposomal formulation, structure, mechanism of action and pre-clinical experience. **Journal of Antimicrobial …**, n. March 2002, p. 21–30, 2002.

AFTAB, B. T. et al. Itraconazole inhibits angiogenesis and tumor growth in non-small cell lung cancer. **Cancer Res.**, v. 71, n. 21, p. 6764–6772, 2011.

AMARAL, A. C. et al. Amphotericin B in poly(lactic-co-glycolic acid) (PLGA) and dimercaptosuccinic acid (DMSA) nanoparticles against paracoccidioidomycosis. **Journal of Antimicrobial Chemotherapy**, v. 63, n. 3, p. 526–533, 2009.

ARISTIZABAL, B. H. et al. Morphological transition of Paracoccidioides brasiliensis conidia to yeast cells: In vivo inhibition in females. **Infection and Immunity**, v. 66, n. 11, p. 5587–5591, 1998.

ASHBURN, T. T.; THOR, K. B. Drug repositioning: identifying and developing new uses for existing drugs. **Nature reviews. Drug discovery**, v. 3, n. 8, p. 673–683, 2004.

BANKS, J. L. et al. Integrated Modeling Program, Applied Chemical Theory (IMPACT). **Journal of Computational Chemistry**, v. 26, n. 16, p. 1752–1780, 2005.

BELLISSIMO-RODRIGUES, F.; MACHADO, A. A.; MARTINEZ, R. Paracoccidioidomycosis epidemiological features of a 1,000-cases series from a hyperendemic area on the southeast of Brazil. **American Journal of Tropical Medicine and Hygiene**, v. 85, n. 3, p. 546–550, 2011.

BENKERT, P.; KUNZLI, M.; SCHWEDE, T. QMEAN server for protein model quality estimation. **Nucleic Acids Research**, v. 37, n. Web Server, p. W510–W514, jul. 2009.

BERMAN, H. M. et al. The Protein Data Bank. **Nucleic acids research**, v. 28, n. 1, p. 235–242, 2000.

BERTONI, T. A. et al. Western blotting is an efficient tool for differential diagnosis of paracoccidioidomycosis and pulmonary tuberculosis. **Clinical and Vaccine Immunology**, v. 19, n. 11, p. 1887–1888, 2012.

BIASINI, M. et al. SWISS-MODEL: Modelling protein tertiary and quaternary structure using evolutionary information. **Nucleic Acids Research**, v. 42, n. W1, p. 252–258, 2014.

BIENERT, S. et al. The SWISS-MODEL Repository-new features and functionality. **Nucleic Acids Research**, v. 45, n. D1, p. D313–D319, 2017.

BOCCA, A. L. et al. Paracoccidioidomycosis: eco-epidemiology, taxonomy and clinical

and therapeutic issues. **Future Microbiology**, v. 8, n. 9, p. 1177–1191, 2013.

BORDOLI, L. et al. Protein structure homology modeling using SWISS-MODEL workspace. **Nature Protocols**, v. 4, n. 1, p. 1–13, 2009.

BORELLI, C. et al. Comparative study of 2% sertaconazole solution and cream formulations in patients with tinea corporis, tinea pedis interdigitalis, or a corresponding candidosis. **American journal of clinical dermatology**, v. 8, n. 6, p. 371–8, 2007.

BRUMMER, E.; CASTANEDA, E.; RESTREPO, A. Paracoccidioidomycosis: An update. **Clinical Microbiology Reviews**, v. 6, n. 2, p. 89–117, 1993.

BURGESS, D. S.; HASTINGS, R. W. A comparison of dynamic characteristics of fluconazole, itraconazole, and amphotericin B against Cryptococcus neoformans using time-kill methodology. **Diagnostic Microbiology and Infectious Disease**, v. 38, n. 2, p. 87–93, 2000.

CANOVA, M. J.; MOLLE, V. Bacterial serine/threonine protein kinases in host-pathogen interactions. **Journal of Biological Chemistry**, v. 289, n. 14, p. 9473–9479, 2014.

CARMEN MARCANO. Iv encuentro internacional sobre paracoccidioidomicosis. v. 28, p. 37–39, 1990.

CARRERAS, C. W.; SANTI, D. V. The Catalytic Mechanism and Structure of Thymidylate Synthase. **Annual Review of Biochemistry**, v. 64, n. 1, p. 721–762, jun. 1995.

CARVALHO, K. C. et al. Virulence of Paracoccidioides brasiliensis and gp43 expression in isolates bearing known PbGP43 genotype. v. 7, p. 55–65, 2005.

CHANG, K. Y. et al. Novel phosphoinositide 3-kinase/mTOR dual inhibitor, NVP-BGT226, displays potent growth-inhibitory activity against human head and neck cancer cells in vitro and in vivo. **Clinical Cancer Research**, v. 17, n. 22, p. 7116–7126, 2011.

CHEN, V. B. et al. MolProbity : all-atom structure validation for macromolecular crystallography. **Acta Crystallographica Section D Biological Crystallography**, v. 66, n. 1, p. 12–21, jan. 2010.

CHEN, X.; JI, Z. L.; CHEN, Y. Z. TTD: Therapeutic Target Database. **Nucleic acids research**, v. 30, n. 1, p. 412–415, jan. 2002.

CHERNYSHEV, A.; FLEISCHMANN, T.; KOHEN, A. Thymidyl biosynthesis enzymes as antibiotic targets. **Applied Microbiology and Biotechnology**, v. 74, n. 2, p. 282–289, 2007.

CHONG, C. R. et al. Inhibition of Angiogenesis by the Antifungal Drug Itraconazole. **ACS Chemical Biology**, v. 2, n. 4, p. 263–270, abr. 2007.

CHOPRA, G.; KALISMAN, N.; LEVITT, M. Consistent refinement of submitted models at CASP using a knowledge-based potential. **Proteins**, v. 78, n. 12, p. 2668–2678, set. 2010.

CHOPRA, G.; SUMMA, C. M.; LEVITT, M. Solvent dramatically affects protein structure refinement. **Proceedings of the National Academy of Sciences**, v. 105, n. 51, p. 20239–20244, 23 dez. 2008.

CORREA-DE-CASTRO, B. et al. Case report: Unifocal bone paracoccidioidomycosis, Brazil. **American Journal of Tropical Medicine and Hygiene**, v. 86, n. 3, p. 470–473, 2012.

COUTINHO, Z. F. et al. Paracoccidioidomycosis mortality in Brazil (1980-1995). **Cadernos de Saúde Pública**, v. 18, n. 5, p. 1441–1454, out. 2002.

CROSS, J. B. et al. Comparison of several molecular docking programs: Pose prediction and virtual screening accuracy. **Journal of Chemical Information and Modeling**, v. 49, n. 6, p. 1455–1474, 2009.

CUNNINGHAM, D. et al. Final results of a randomised trial comparing Tomudex'® (raltitrexed) with 5-fluorouracil plus leucovorin in advanced colorectal cancer. **Annals of Oncology**, v. 7, p. 961–965, 1996.

DE OLIVEIRA, H. C. et al. Importance of adhesins in virulence of Paracoccidioides spp. **Frontiers in Microbiology**, v. 6, n. MAR, p. 1–14, 2015.

DESJARDINS, C. A. et al. Comparative genomic analysis of human fungal pathogens causing paracoccidioidomycosis. **PLoS Genetics**, v. 7, n. 10, 2011.

DHAR, M. K.; KOUL, A.; KAUL, S. Farnesyl pyrophosphate synthase: A key enzyme in isoprenoid biosynthetic pathway and potential molecular target for drug development. **New Biotechnology**, v. 30, n. 2, p. 114–123, 2013.

DUDLEY, J. T.; DESHPANDE, T.; BUTTE, A. J. Exploiting drug-disease relationships for computational drug repositioning. **Briefings in Bioinformatics**, v. 12, n. 4, p. 303–311, 2011.

EDWARDS, J. R.; BETTS, M. J. Itracooazole and fiocooazok: new drags for deep fungal infection It. **BMJ**, v. s3-1, n. 23, p. 497–499, 10 jun. 1853.

EKINS, S. et al. In silico repositioning of approved drugs for rare and neglected diseases. **Drug Discovery Today**, v. 16, n. 7–8, p. 298–310, abr. 2011.

EKINS, S.; MESTRES, J.; TESTA, B. In silico pharmacology for drug discovery: methods for virtual ligand screening and profiling. **British Journal of Pharmacology**, v. 152, n. December 2006, p. 9–20, 2007.

FERNANDES, L. et al. Cell signaling pathways in Paracoccidioides brasiliensis--inferred from comparisons with other fungi. **Genetics and molecular research : GMR**, v. 4, n. 2, p. 216–231, 2005.

FERREIRA, J. C. B.; BRUM, P. C.; MOCHLY-ROSEN, D. βIIPKC and εPKC isozymes as potential pharmacological targets in cardiac hypertrophy and heart failure. **Journal of Molecular and Cellular Cardiology**, v. 51, n. 4, p. 479–484, out. 2011.

FLETCHER, G. C. et al. **ENMD-2076 is an orally active kinase inhibitor with antiangiogenic and antiproliferative mechanisms of action.** [s.l: s.n.]. v. 10

FRANCO, M. et al. Paracoccidioidomycosis: A Recently Proposed Classification of Its Clinical Forms. **Revista da Sociedade Brasileira de Medicina Tropical**, v. 20, n. 2, p. 129–132, 1987.

FUJII, G. et al. The formation of amphotericin B ion channels in lipid bilayers. **Biochemistry**, v. 36, n. 16, p. 4959–4968, 1997.

GELIJNS, A. C.; ROSENBERG, N.; MOSKOWITZ, A. J. Capturing the Unexpected Benefits of Medical Research. **New England Journal of Medicine**, v. 339, n. 10, p. 693–698, 1998.

HENG, L. Z.; CHEN, Y.; TAN, T. C. Treatment of recurrent vulvo-vaginal candidiasis with sustained-release butoconazole pessary. **Singapore Medical Journal**, v. 53, n. 12, p. 269–271, 2012.

HURLE, M. R. et al. Computational drug repositioning: from data to therapeutics. **Clinical pharmacology and therapeutics**, v. 93, n. 4, p. 335–41, 2013.

JANKE, C. The tubulin code: Molecular components, readout mechanisms, functions. **Journal of Cell Biology**, v. 206, n. 4, p. 461–472, 2014.

JOHANSEN, H. K.; GØTZSCHE, P. C. Amphotericin B lipid soluble formulations versus amphotericin B in cancer patients with neutropenia. In: JOHANSEN, H. K. (Ed.). . **Cochrane Database of Systematic Reviews**. Chichester, UK: John Wiley & Sons, Ltd, 2000. v. 76p. 1–16.

KARATHIA, H. et al. Saccharomyces cerevisiae as a Model Organism: A Comparative Study. **PLoS ONE**, v. 6, n. 2, p. e16015, 2 fev. 2011.

KHANNA, D.; BHARTI, S. Luliconazole for the treatment of fungal infections: an evidence-based review. **Core Evidence**, v. 9, p. 113, set. 2014.

KIEFER, F. et al. The SWISS-MODEL Repository and associated resources. **Nucleic Acids Research**, v. 37, n. Database, p. D387–D392, 1 jan. 2009.

KIM, J. et al. Itraconazole, a Commonly Used Antifungal that Inhibits Hedgehog Pathway

Activity and Cancer Growth. **Cancer Cell**, v. 17, n. 4, p. 388–399, abr. 2010.

KLEINBERG, M. What is the current and future status of conventional amphotericin B? **International Journal of Antimicrobial Agents**, v. 27, n. SUPPL. 1, p. 12–16, 2006.

KNOX, C. et al. DrugBank 3.0: a comprehensive resource for “omics” research on drugs. **Nucleic Acids Research**, v. 39, p. D1035-41, jan. 2011.

KRASILNIKOV, M. A. Phosphatidylinositol-3 kinase dependent pathways: the role in control of cell growth, survival, and malignant transformation. **Biochemistry. Biokhimiiầ**, v. 65, n. 1, p. 59–67, 2000.

LAMB, D. C. et al. Purification, reconstitution, and inhibition of cytochrome P-450 sterol delta22-desaturase from the pathogenic fungus Candida glabrata. **Antimicrobial agents and chemotherapy**, v. 43, n. 7, p. 1725–1728, 1999.

LI, Y. Y.; JONES, S. J. M. Drug repositioning for personalized medicine. **Genome Medicine**, v. 4, n. 3, 2012.

LOMBARDINO, J. G.; LOWE, J. A. The role of the medicinal chemist in drug discovery-then and now. **Nat Rev Drug Discov**, v. 3, n. 10, p. 853–862, 2004.

M, A. R. et al. Treatment of paracoccidioidomycosis with ketoconazole: A three-year experience. **The American Journal of Medicine**, v. 74, n. 1, p. 48–52, jan. 1983.

MARQUES, S. A. Paracoccidioidomycosis: epidemiological, clinical, diagnostic and treatment up-dating. **Anais brasileiros de dermatologia**, v. 88, n. 5, p. 700–11, 2013.

MARTINEZ, R. Epidemiology of Paracoccidioidomycosis. **Revista do Instituto de Medicina Tropical de São Paulo**, v. 57 Suppl 1, p. 11–20, 2015.

MARTINEZ, R. New Trends in Paracoccidioidomycosis Epidemiology. **Journal of Fungi**, v. 3, n. 1, p. 1, 2017.

MATUTE, D. R. et al. Cryptic Speciation and Recombination in the Fungus Paracoccidioides brasiliensis as Revealed by Gene Genealogies. **Molecular Biology and Evolution**, v. 23, n. 1, p. 65–73, 1 jan. 2005.

MCGANN, M. FRED Pose Prediction and Virtual Screening Accuracy. **Journal of Chemical Information and Modeling**, v. 51, n. 3, p. 578–596, mar. 2011.

MCGANN, M. FRED and HYBRID docking performance on standardized datasets. **Journal of computer-aided molecular design**, v. 26, n. 8, p. 897–906, ago. 2012.

MENDES, R. P. et al. **Paracoccidioidomycosis: Current Perspectives from Brazil**. [s.l: s.n.]. v. 11

MICHAELIS, M. et al. ABCG2 impairs the activity of the aurora kinase inhibitor tozasertib but not of alisertib. **BMC Research Notes**, v. 8, n. 1, p. 484, 2015.

MISTRO, S. et al. Does lipid emulsion reduce amphotericin B nephrotoxicity? A systematic review and meta-analysis. **Clinical Infectious Diseases**, v. 54, n. 12, p. 1774–1777, 2012.

MOCHLY-ROSEN, D.; DAS, K.; GRIMES, K. K. V. Protein kinase C, an elusive therapeutic target? **Nature Reviews Drug Discovery**, v. 11, n. 12, p. 937–957, 2012.

MUÑOZ, J. F. et al. Genome Update of the Dimorphic Human Pathogenic Fungi Causing Paracoccidioidomycosis. **PLoS Neglected Tropical Diseases**, v. 8, n. 12, 2014.

MUÑOZ, J. F. et al. Genome Diversity, Recombination, and Virulence across the Major Lineages of Paracoccidioides. **mSphere**, v. 1, n. 5, p. e00213-16, 26 out. 2016.

NEGRONI, R. et al. Results of miconazole therapy in twenty-eight patients with paracoccidioidomycosis (South American blastomycosis). **Proceedings of the Royal Society of Medicine**, v. 70, p. 24, 1977.

NETLAND, I. A. et al. Dactolisib (NVP-BEZ235) toxicity in murine brain tumour models. **BMC Cancer**, p. 1–12, 2016.

NETO, B. R. DA S. et al. Transcriptional profile of Paracoccidioides spp. in response to itraconazole. **BMC Genomics**, v. 15, n. 1, 2014.

NOVAC, N. Challenges and opportunities of drug repositioning. **Trends in Pharmacological Sciences**, v. 34, n. 5, p. 267–272, 2013.

OKAZAKI, R. et al. Efficacy and safety of monthly oral minodronate in patients with involutional osteoporosis. **Osteoporosis International**, v. 23, n. 6, p. 1737–1745, 2012.

PANTZIARKA, P. et al. Repurposing Drugs in Oncology (ReDO)-mebendazole as an anti-cancer agent. **Ecancermedicalscience**, v. 8, p. 443, 2014.

PAPAHADJOPOULOS, D. et al. Phase transitions in phospholipid vesicles Fluorescence polarization and permeability measurements concerning the effect of temperature and cholesterol. **BBA - Biomembranes**, v. 311, n. 3, p. 330–348, 1973.

PATO, A. M.; GIUSIANO, G.; MANGIATERRA, M. Paracoccidioidomicosis asociada a otras patolog??as respiratorias en un hospital de Corrientes, Argentina. **Revista Argentina de Microbiologia**, v. 39, n. 3, p. 161–165, 2007.

PETER, B. et al. Target interaction profiling of midostaurin and its metabolites in neoplastic mast cells predicts distinct effects on activation and growth. **Leukemia**, v. 30, n. 2, p. 464–72, 2016.

PRESS, D. Study of Albendazole-Encapsulated Nanosize Liposomes. **International Journal**, v. 5, p. 101–108, 2010.

REILLY, J. F. et al. A novel role for farnesyl pyrophosphate synthase in fibroblast growth

factor-mediated signal transduction. **Biochemical Journal**, v. 366, n. 2, p. 501–510, 1 set. 2002.

RESTREPO, A. et al. Estrogens inhibit mycelium-to-yeast transformation in the fungus Paracoccidioides brasiliensis: Implications for resistance of females to Paracoccidioidomycosis. **Infection and Immunity**, v. 46, n. 2, p. 346–353, 1984.

RESTREPO, A; MCEWEN, J. G.; CASTAÑEDA, E. The habitat of Paracoccidioides brasiliensis: how far from solving the riddle? **Medical mycology : official publication of the International Society for Human and Animal Mycology**, v. 39, n. 3, p. 233–241, 2001.

RODRIGUES, J. P. G. L. M.; LEVITT, M.; CHOPRA, G. KoBaMIN: a knowledge-based minimization web server for protein structure refinement. **Nucleic Acids Research**, v. 40, n. W1, p. W323–W328, 1 jul. 2012a.

RODRIGUES, J. P. G. L. M.; LEVITT, M.; CHOPRA, G. KoBaMIN: a knowledge-based minimization web server for protein structure refinement. **Nucleic Acids Research**, v. 40, n. W1, p. W323–W328, 1 jul. 2012b.

RUDIN, C. M. et al. Phase I/II study of pemetrexed with or without ABT-751 in advanced or metastatic non-small-cell lung cancer. **Journal of Clinical Oncology**, v. 29, n. 8, p. 1075–1082, 2011.

SERINGHAUS, M. et al. Predicting essential genes in fungal genomes. **Genome Research**, v. 16, n. 9, p. 1126–1135, 2006.

SHAHINAS, D. et al. A repurposing strategy identifies novel synergistic inhibitors of plasmodium falciparum heat shock protein 90. **Journal of Medicinal Chemistry**, v. 53, n. 9, p. 3552–3557, 2010.

SHANKAR, J. et al. Hormones and the resistance of women to paracoccidioidomycosis. **Clinical Microbiology Reviews**, v. 24, n. 2, p. 296–313, 2011.

SHELLEY, J. C. et al. Epik: A software program for pKa prediction and protonation state generation for drug-like molecules. **Journal of Computer-Aided Molecular Design**, v. 21, n. 12, p. 681–691, 2007.

SHIKANAI-YASUDA, M. A. et al. Consenso em paracoccidioidomicose. **Revista da Sociedade Brasileira de Medicina Tropical**, v. 39, n. 3, p. 297–310, 2006.

SHIKANAI-YASUDA, M. A. Paracoccidioidomycosis Treatment. **Revista do Instituto de Medicina Tropical de Sao Paulo**, v. 57 Suppl 1, n. 1, p. 31–37, 2015.

SHIKANAI-YASUDA, M. A. et al. Brazilian guidelines for the clinical management of paracoccidioidomycosis. **Revista da Sociedade Brasileira de Medicina Tropical**, n. 0,

2017.

SHIM, J. S.; LIU, J. O. Recent advances in drug repositioning for the discovery of new anticancer drugs. **International Journal of Biological Sciences**, v. 10, n. 7, p. 654–663, 2014.

SOARES, D. A. et al. Extracellular Paracoccidioides brasiliensis phospholipase B involvement in alveolar macrophage interaction. **BMC microbiology**, v. 10, p. 241, 2010.

SONG, M. S. et al. Induction of glucose-regulated protein 78 by chronic hypoxia in human gastric tumor cells through a protein kinase C-epsilon/ERK/AP-1 signaling cascade. **Cancer research**, v. 61, n. 22, p. 8322–8330, 2001.

SOUZA, A. C. O. et al. Activity and in vivo tracking of Amphotericin B loaded PLGA nanoparticles. **European journal of medicinal chemistry**, v. 95, p. 267–276, 2015.

STEFANIK, D. et al. Disparate osteogenic response of mandible and iliac crest bone marrow stromal cells to pamidronate. **Oral Diseases**, v. 14, n. 5, p. 465–471, jul. 2008.

TAMBUYZER, E. Rare diseases, orphan drugs and their regulation: Questions and misconceptions. **Nature Reviews Drug Discovery**, v. 9, n. 12, p. 921–929, 2010.

TEIXEIRA, M. D. M. et al. Paracoccidioides lutzii sp. nov.: biological and clinical implications. **Medical Mycology**, v. 52, n. 1, p. 1–10, 14 jun. 2013a.

TEIXEIRA, M. DE M. et al. Molecular and morphological data support the existence of a sexual cycle in species of the genus Paracoccidioides. **Eukaryotic Cell**, v. 12, n. 3, p. 380–389, 2013b.

TEIXEIRA, M. M. et al. Phylogenetic analysis reveals a high level of speciation in the Paracoccidioides genus. **Molecular Phylogenetics and Evolution**, v. 52, n. 2, p. 273–283, 2009.

TEIXEIRA, M. M. et al. Paracoccidioides Species Complex: Ecology, Phylogeny, Sexual Reproduction, and Virulence. **PLoS Pathogens**, v. 10, n. 10, p. 4–7, 2014.

TEJRAL, G. et al. Computer modelling reveals new conformers of the ATP binding loop of Na^{+}/K^{+}-ATPase involved in the transphosphorylation process of the sodium pump. **PeerJ**, v. 5, p. e3087, 2017.

TELLES, F. Q. et al. An Open-Label Comparative Pilot Study of Oral Voriconazole and Itraconazole for Long-Term Treatment of Paracoccidioidomycosis. **Clinical Infectious Diseases**, v. 45, n. 11, p. 1462–1469, 2007.

TOBÓN, A M. et al. Residual pulmonary abnormalities in adult patients with chronic paracoccidioidomycosis: prolonged follow-up after itraconazole therapy. **Clinical infectious diseases : an official publication of the Infectious Diseases Society of**

America, v. 37, n. 7, p. 898–904, 2003.

VALLE, A. C. F. DO et al. Clinical and endoscopic findings in the mucosae of the upper respiratory and digestive tracts in post-treatment follow-up of paracoccidioidomycosis patients. **Revista do Instituto de Medicina Tropical de São Paulo**, v. 37, n. 5, p. 407–413, out. 1995.

VIEIRA, G. DE D. et al. Paracoccidioidomycosis in a western Brazilian Amazon State: Clinical-epidemiologic profile and spatial distribution of the disease. **Revista da Sociedade Brasileira de Medicina Tropical**, v. 47, n. 1, p. 63–68, 2014.

VILCHÈZE, C.; JACOBS, W. R. The combination of sulfamethoxazole, trimethoprim, and isoniazid or rifampin is bactericidal and prevents the emergence of drug resistance in Mycobacterium tuberculosis. **Antimicrobial Agents and Chemotherapy**, v. 56, n. 10, p. 5142–5148, 2012.

WÄCHTLER, B.; WILSON, D.; HUBE, B. Candida albicans adhesion to and invasion and damage of vaginal epithelial cells: Stage-specific inhibition by clotrimazole and bifonazole. **Antimicrobial Agents and Chemotherapy**, v. 55, n. 9, p. 4436–4439, 2011.

WANG, Y. et al. OrthoVenn: A web server for genome wide comparison and annotation of orthologous clusters across multiple species. **Nucleic Acids Research**, v. 43, n. W1, p. W78–W84, 2015.

WANKE, B.; AIDÊ, M. A. Capítulo 6 - Paracoccidioidomicose. **Jornal Brasileiro de Pneumologia**, v. 35, n. 12, p. 1245–1249, dez. 2009.

WISHART, D. S. et al. DrugBank: a comprehensive resource for in silico drug discovery and exploration. **Nucleic Acids Research**, v. 34, n. Database issue, p. D668-72, jan. 2006.

WU, D. et al. Protein kinase cepsilon has the potential to advance the recurrence of human prostate cancer. **Cancer Res**, v. 62, n. 8, p. 2423–2429, 2002.

WU, D.-C. et al. A Pilot Randomized Controlled Study of Dexlansoprazole MR-Based Triple Therapy for Helicobacter Pylori Infection. **Medicine**, v. 95, n. 11, p. e2698, 2016.

YAMAGISHI, S. et al. Minodronate, a newly developed nitrogen-containing bisphosphonate, suppresses melanoma growth and improves survival in nude mice by blocking vascular endothelial growth factor signaling. **The American journal of pathology**, v. 165, n. 6, p. 1865–74, 2004.

YANG, L.; AGARWAL, P. Systematic Drug Repositioning Based on Clinical Side-Effects. **PLoS ONE**, v. 6, n. 12, p. e28025, 21 dez. 2011.

YU, C. C. et al. AZD2014 Radiosensitizes Oral Squamous Cell Carcinoma by Inhibiting AKT/mTOR Axis and Inducing G1/G2/M Cell Cycle Arrest. **PloS one**, v. 11, n. 3, p.

e0151942, 2016.

ZAMBUZZI-CARVALHO, P. F. et al. Transcriptional profile of the human pathogenic fungus Paracoccidioides lutzii in response to sulfamethoxazole. **Medical Mycology**, v. 53, n. 5, p. 477–492, 2015.

ZHU, F. et al. Update of TTD: Therapeutic Target Database. **Nucleic Acids Research**, v. 38, n. Database issue, p. D787–D791, jan. 2010.

ZHU, F. et al. Therapeutic target database update 2012: A resource for facilitating target-oriented drug discovery. **Nucleic Acids Research**, v. 40, n. D1, p. 1128–1136, 2012.

9. ANEXO

Anexo 1: Validação dos modelos construídos pelo *MolProbity* das proteínas de *Paracoccidioides* spp.

PAAG	Proteínas alvos do *Pb*01	*MolProbity score*	Resolução *MolProbity score*
PAAG_04259	2Fe-2S proteína com domínio de ferro-enxofre	1,93	79° percentis
PAAG_01387	3-acetil-CoA tiolase B	1,70	89° percentis
PAAG_02414	26S proteassoma subunidade reguladora RPN1	2,15	68º percentis
PAAG_03447	Acetil-CoA acetil transferase	Não otimizada	
PAAG_08731	Acetil-CoA carboxilase	1,93	79° percentis
PAAG_08620	ADP, ATP proteína transportadora	1,65	91° percentis
PAAG_12506	Alfa tubulina	1,73	88° percentis
PAAG_03031	Beta tubulina	1,60	92° percentis
PAAG_00826	cálcio/calmodulina proteína quinase tipo IV	2,02	75° percentis
PAAG_08247	Calmodulina	1,38	97° percentis
PAAG_01186	Proteína de controle de divisão celular 1	1,91	80° percentis
PAAG_05894	Proteína de controle de divisão celular 2	1,77	87° percentis
PAAG_00827	Citocromo P450 51	1,75	87° percentis
PAAG_04743	Caseína quinase 2 - subunidade alfa	1,60	92° percentis
PAAG_00299	Delta-aminolevulinico desidratada ácido	1,74	88° percentis
PAAG_07676	Dihidrofolato sintetase	2,20	65° percentis
PAAG_07212	DNA ligase	2,21	64° percentis
PAAG_06486	DNA polimerase 1	1,87	82° percentis
PAAG_06601	DNA polimerase 2	1,88	82° percentis
PAAG_03486	DNA topoisomerase 2	1,79	86° percentis
PAAG_07279	Farnesil pirofosfato sintetase	1,68	90° percentis
PAAG_01524	Fat ácido sinthase subunitade beta dehidratase	Não otimizada	

PAAG	Proteínas alvos do *Pb*01	*MolProbity score*	Resolução *MolProbity score*
PAAG_08770	Ferrochelatase	1,92	80° percentis
PAAG_05758	Glutamate carboxipeptidase	2,23	62° percentis
PAAG_07003	Glutamina sintetase	1,78	86° percentis
PAAG_08003	Proteína 2 de choque e calor 70 kDa	1,57	93° percentis
PAAG_12584	Isoleucina-tRNA ligase	2,35	56° percentis
PAAG_05015	Leucil-tRNA sintetase	2,27	60° percentis
PAAG_00557	Manose-6-fosfato isomerase	1,99	76° percentis
PAAG_04243	Na+/K+ cadeia alfa ATPase	2,05	73° percentis
PAAG_11783	NADPH-citocrome P450 redutase	2,01	75° percentis
PAAG_01410	Fosfatidilinositol 3-quinase tor2	1,86	83° percentis
PAAG_04060	Fosfatidilinositol 3-quinase vps34	1,64	91° percentis
PAAG_01150	Proteasome subunidade beta	1,87	82° percentis
PAAG_02441	Proteína quinase C	1,83	84° percentis
PAAG_05449	RAC-alfa Serina/Treonina-proteína quinase	2,09	71° percentis
PAAG_02499	Ribonucleótido redutase subunidade R2	2,15	67° percentis
PAAG_08991	Serina/Treonina-proteina quinase	1,73	88° percentis
PAAG_07148	Serina/Treonina-proteina quinase ksg1	2,28	60° percentis
PAAG_03141	Serina/Treonina-proteina quinase SAPK2	1,79	86° percentis
PAAG_12360	STE/STE11/BCK1 proteína quinase	1,92	80° percentis
PAAG_07020	Tioredoxina redutase	1,90	81° percentis
PAAG_08597	Timidilato sintase	1,95	78° percentis

Anexo 2: Tabela geral com todos os resultados obtidos em cada

GeneDB informations				Results																	
Gene information				Identified targets	E-value or Score		Identified drugs			BLAST alignment			SWISS-MODEL						Docking	
Pb01 targets	PAAG	Cluster	*S.cerevisiae*	Name (*organism*)	TTD	DrugBank	Name	Status	Therapeutic class	Overlap	E-Value	Sequential identity	GMQE	QMEAN	TEMPLATE	RESOLUTION	SEQ Identif	COVERAGE	RECEPTOR	FRED SCORE
2Fe-2S iron-sulfur cluster binding domain-containing protein	PAAG_04259	cluster763	DEG20011060	Adrenodoxin, mitochondrial (Human)		C	Mitotane	approved	unknown	95%	0.0	67%	-	-	-	-	-	-	-	-
3-ketoacyl-CoA thiolase B	PAAG_01387	cluster927	DEG20011020	3-ketoacyl-CoA thiolase, peroxisomal (Human)		C	Trimetazidine	approved	Inhibitor	97%	0.0	60%	-	-	-	-	-	-	-	-
Fatty acid synthase subunit beta dehydratase	PAAG_01524	cluster632	DEG20010641	Fatty acid synthase subunit beta	C		Pyrazinamide	Approved	Tuberculosis	64%	2E-91	31%	-	-	-	-	-	-	-	-
Leucyl-tRNA synthetase	PAAG_05015	cluster928	DEG20011041	Cytosolic leucyl-tRNA synthetase (Yeast)		C	Tavaborole	approved	inhibitor	29%	3E-32	33%	-	-	-	-	-	-	-	-
Serine/threonine-protein kinase ksg1	PAAG_07148	cluster822	DEG20011045	3-phosphoinositide-dependent protein kinase 1 (Human)		C	Celecoxib	approved, investigational	inhibitor	98%	0.0	47%	-	-	-	-	-	-	-	-
STE/STE11/BCK1 protein kinase	PAAG_12360	cluster21	DEG20010012	MEKK-1 kinase	C		E6201	Phase 2		97%	0.0	58%	-	-	-	-	-	-	-	-
Uncharacterized protein	PAAG_02835	cluster71	Without similarity	Complement C1q subcomponent subunit C (Human)		C	Cetuximab	approved		98%	3E-136	56%	0.77	-0.10	1GJP	X-ray, 1.8Å	65.86%	88%	Receptor2	-4.561.302
1,3-beta-glucan synthase component bgs3	PAAG_05071	cluster736	Without similarity	1,3-beta-glucan synthase component FKS1 Aspergillus niger (strain CBS 513.88 / FGSC A1513)	C	C	Anidulafungin	approved, investigational	inhibitor	87%	5E-126	42%	-	-	-	-	-	-	-	-
1,3-beta-glucan synthase component bgs3	PAAG_05071	cluster736	Without similarity	1,3-beta-glucan synthase component FKS1 (Aspergillus niger (strain CBS 513.88 / FGSC A1513))	C	C	Caspofungin	approved	inhibitor	97%	3E-160	40%	-	-	-	-	-	-	-	-
1,3-beta-glucan synthase component bgs3	PAAG_05071	cluster736	Without similarity	1,3-beta-glucan synthase component FKS1 (Aspergillus niger (strain CBS 513.88 / FGSC A1513))	C	C	Micafungin	approved, investigational	inhibitor	96%	2E-92	45%	-	-	-	-	-	-	-	-
26S proteasome regulatory subunit RPN1	PAAG_02414	cluster766	DEG20010506	26S proteasome non-ATPase regulatory subunit 2 (Human)		C	Bortezomib	approved, investigational	inhibitor	98%	3E-136	56%	0.77	-0.10	1GJP	X-ray, 1.8Å	65.86%	88%	Receptor2	-7.286.346
37S ribosomal protein S12, mitochondrial	PAAG_02289	cluster933	Without similarity	30S ribosomal protein S12 (Escherichia coli (strain K12))		C	Amikacin	approved, vet_approved	inhibitor	97%	0.0	41%	-	-	-	-	-	-	-	-
37S ribosomal protein S12, mitochondrial	PAAG_02289	cluster933	Without similarity	30S ribosomal protein S12 (Escherichia coli (strain K12))		C	Arbekacin	approved	inhibitor	98%	9E-129	48%	0.74	-1.68	1PMI	X-ray, 1.70 Å	47.43%	93%	Receptor3	-6.754.422
37S ribosomal protein S12, mitochondrial	PAAG_02289	cluster933	Without similarity	30S ribosomal protein S12 (Escherichia coli (strain K12))		C	Framycetin	approved	inhibitor	31%	4E-36	31%	-	-	-	-	-	-	-	-
37S ribosomal protein S12, mitochondrial	PAAG_02289	cluster933	Without similarity	30S ribosomal protein S12 (Escherichia coli (strain K12))		C	Gentamicin	approved, vet_approved	adduct	98%	9E-129	48%	0.74	-1.68	1PMI	X-ray, 1.70 Å	47.43%	93%	Receptor3	-6.472.907
37S ribosomal protein S12, mitochondrial	PAAG_02289	cluster933	Without similarity	30S ribosomal protein S12 (Escherichia coli (strain K12))		C	Kanamycin	approved, vet_approved	inhibitor	78%	2E-32	56%	-	-	-	-	-	-	-	-
37S ribosomal protein S12, mitochondrial	PAAG_02289	cluster933	Without similarity	30S ribosomal protein S12 (Escherichia coli (strain K12))		C	Neomycin	approved, vet_approved	inhibitor	98%	9E-129	48%	0.74	-1.68	1PMI	X-ray, 1.70 Å	47.43%	93%	Receptor2	-9.312.977

37S ribosomal protein S12, mitochondrial	PAAG_02289	cluster933	Without similarity	30S ribosomal protein S12 (Escherichia coli (strain K12))		C	Netilmicin	approved	inhibitor	82%	7E-58	31%	-	-	-	-	-	-	-	-
37S ribosomal protein S12, mitochondrial	PAAG_02289	cluster933	Without similarity	30S ribosomal protein S12 (Escherichia coli (strain K12))		C	Ribostamycin	approved		73%	1E-84	39%	0.23	-2.09	4FG8	X-ray, 2.20 Å	42.38%	41%	Receptor1	-10.073.805
37S ribosomal protein S12, mitochondrial	PAAG_02289	cluster933	Without similarity	30S ribosomal protein S12 (Escherichia coli (strain K12))		C	Spectinomycin	approved, vet_approved	inhibitor	97%	8E-158	47%	-	-	-	-	-	-	-	-
37S ribosomal protein S12, mitochondrial	PAAG_02289	cluster933	Without similarity	30S ribosomal protein S12 (Escherichia coli (strain K12))		C	Streptomycin	approved, vet_approved	inhibitor	99%	0.0	72%	0.78	-1.57	4UYM	X-ray, 2.55Å	74.73%	89%	Receptor1	-12.373.743
37S ribosomal protein S12, mitochondrial	PAAG_02289	cluster933	Without similarity	30S ribosomal protein S12 (Escherichia coli (strain K12))		C	Tigecycline	approved	adduct	99%	0.0	72%	0.78	-1.57	4UYM	X-ray, 2.55Å	74.73%	89%	Receptor1	-18.365.929
37S ribosomal protein S12, mitochondrial	PAAG_02289	cluster933	Without similarity	30S ribosomal protein S12 (Escherichia coli (strain K12))		C	Tobramycin	approved, investigational	inhibitor	99%	0.0	72%	0.78	-1.57	4UYM	X-ray, 2.55Å	74.73%	89%	Receptor1	-15.730.254
3-hydroxy-3-methylglutaryl-coenzyme A reductase	PAAG_05791	cluster781	Without similarity	3-hydroxy-3-methylglutaryl-coenzyme A reductase (Human)	C	C	Atorvastatin	approved	inhibitor	94%	3E-168	48%	0.78	-1.57	4UYM	X-ray, 2.55Å	74.73%	89%	Receptor1	-13.522.453
3-hydroxy-3-methylglutaryl-coenzyme A reductase	PAAG_05791	cluster628	Without similarity	3-hydroxy-3-methylglutaryl-coenzyme A reductase	C		Bervastatin	Discontinued in Phase 2	Thrombosis	99%	0.0	72%	0.78	-1.57	4UYM	X-ray, 2.55Å	74.73%	89%	Receptor1	-6.861.999
3-hydroxy-3-methylglutaryl-coenzyme A reductase	PAAG_05791	cluster628	Without similarity	3-hydroxy-3-methylglutaryl-coenzyme A reductase	C		BMS-180431	Discontinued in Phase 2	Hyperlipidemia	70%	3E-151	49%	-	-	-	-	-	-	-	-
3-hydroxy-3-methylglutaryl-coenzyme A reductase	PAAG_05791	cluster628	Without similarity	3-hydroxy-3-methylglutaryl-coenzyme A reductase	C		BMY-21950	Discontinued in Phase 2	Hyperlipidemia	67%	2E-52	31%	-	-	-	-	-	-	-	-
3-hydroxy-3-methylglutaryl-coenzyme A reductase	PAAG_05791	cluster781	Without similarity	3-hydroxy-3-methylglutaryl-coenzyme A reductase (Human)		C	Cerivastatin	withdrawn	inhibitor	99%	0.0	72%	0.78	-1.57	4UYM	X-ray, 2.55Å	74.73%	89%	Receptor1	-15.234.054
3-hydroxy-3-methylglutaryl-coenzyme A reductase	PAAG_05791	cluster628	Without similarity	3-hydroxy-3-methylglutaryl-coenzyme A reductase	C		Crestor/TriLipix	Approved	Dyslipidaemia	92%	5E-121	35%	-	-	-	-	-	-	-	-
3-hydroxy-3-methylglutaryl-coenzyme A reductase	PAAG_05791	cluster628	Without similarity	3-hydroxy-3-methylglutaryl-coenzyme A reductase	C		CRILVASTATIN	Phase 2	Hyperlipidemia	99%	0.0	72%	0.78	-1.57	4UYM	X-ray, 2.55Å	74.73%	89%	Receptor1	-12.708.447
3-hydroxy-3-methylglutaryl-coenzyme A reductase	PAAG_05791	cluster628	Without similarity	3-hydroxy-3-methylglutaryl-coenzyme A reductase	C		Dalvastatin	Discontinued in Phase 3	Hyperlipidemia	99%	0.0	72%	0.78	-1.57	4UYM	X-ray, 2.55Å	74.73%	89%	Receptor1	-12.677.217
3-hydroxy-3-methylglutaryl-coenzyme A reductase	PAAG_05791	cluster781	Without similarity	3-hydroxy-3-methylglutaryl-coenzyme A reductase (Human)	C	C	Fluvastatin	approved	inhibitor	46%	3E-84	36%	-	-	-	-	-	-	-	-
3-hydroxy-3-methylglutaryl-coenzyme A reductase	PAAG_05791	cluster628	Without similarity	3-hydroxy-3-methylglutaryl-coenzyme A reductase	C		GLENVASTATIN	Discontinued in Phase 2	Hyperlipidemia	99%	0.0	72%	0.78	-1.57	4UYM	X-ray, 2.55Å	74.73%	89%	Receptor1	-14.026.605
3-hydroxy-3-methylglutaryl-coenzyme A reductase	PAAG_05791	cluster628	Without similarity	3-hydroxy-3-methylglutaryl-coenzyme A reductase	C		MK-0524B	Discontinued in Phase 3	Atherosclerosis	97%	0.0	60%	-	-	-	-	-	-	-	-
3-hydroxy-3-methylglutaryl-coenzyme A reductase	PAAG_05791	cluster628	Without similarity	3-hydroxy-3-methylglutaryl-coenzyme A reductase	C		NK-104	Phase 4	Discovery agent	89%	3E-59	30%	-	-	-	-	-	-	-	-

3-hydroxy-3-methylglutaryl-coenzyme A reductase	PAAG_05791	cluster628	Without similarity	3-hydroxy-3-methylglutaryl-coenzyme A reductase	C		PF-3052334	Discontinued in Phase 1	Atherosclerosis	99%	0.0	72%	0.78	-1.57	4UYM	X-ray, 2.55Å	74.73%	89%	Receptor1	-13.921.816
3-hydroxy-3-methylglutaryl-coenzyme A reductase	PAAG_05791	cluster781	Without similarity	3-hydroxy-3-methylglutaryl-coenzyme A reductase (Human)		C	Pitavastatin	approved	inhibitor	99%	0.0	72%	0.78	-1.57	4UYM	X-ray, 2.55Å	74.73%	89%	Receptor1	-12.363.360
3-hydroxy-3-methylglutaryl-coenzyme A reductase	PAAG_05791	cluster628	Without similarity	3-hydroxy-3-methylglutaryl-coenzyme A reductase	C		PITAVASTATIN CALCIUM	Approved	Dyslipidaemias	70%	2E-97	41%	-	-	-	-	-	-	-	-
3-hydroxy-3-methylglutaryl-coenzyme A reductase	PAAG_05791	cluster628	Without similarity	3-hydroxy-3-methylglutaryl-coenzyme A reductase	C		PPD-10558	Phase 2	Lipid metabolism disorder	67%	2E-52	31%	-	-	-	-	-	-	-	-
3-hydroxy-3-methylglutaryl-coenzyme A reductase	PAAG_05791	cluster781	Without similarity	3-hydroxy-3-methylglutaryl-coenzyme A reductase (Human)	C	C	Pravastatin	approved	inhibitor	99%	0.0	72%	0.78	-1.57	4UYM	X-ray, 2.55Å	74.73%	89%	Receptor1	-14.313.613
3-hydroxy-3-methylglutaryl-coenzyme A reductase	PAAG_05791	cluster628	Without similarity	3-hydroxy-3-methylglutaryl-coenzyme A reductase	C		Pravigard	Approved	Myocardial infarction, cerebrovascular ischaemia	88%	2E-25	35%	-	-	-	-	-	-	-	-
3-hydroxy-3-methylglutaryl-coenzyme A reductase	PAAG_05791	cluster628	Without similarity	3-hydroxy-3-methylglutaryl-coenzyme A reductase	C		Premarin/Pravacho	Phase 3	Hyperlipidemia	99%	0.0	72%	0.78	-1.57	4UYM	X-ray, 2.55Å	74.73%	89%	Receptor1	-13.258.447
3-hydroxy-3-methylglutaryl-coenzyme A reductase	PAAG_05791	cluster628	Without similarity	3-hydroxy-3-methylglutaryl-coenzyme A reductase	C		RBx10558	Discontinued in Phase 2	Hyperlipidemia	46%	3E-84	36%	-	-	-	-	-	-	-	-
3-hydroxy-3-methylglutaryl-coenzyme A reductase	PAAG_05791	cluster781	Without similarity	3-hydroxy-3-methylglutaryl-coenzyme A reductase (Human)	C	C	Rosuvastatin	approved	inhibitor	99%	0.0	72%	0.78	-1.57	4UYM	X-ray, 2.55Å	74.73%	89%	Receptor1	-10.478.906
3-hydroxy-3-methylglutaryl-coenzyme A reductase	PAAG_05791	cluster781	Without similarity	3-hydroxy-3-methylglutaryl-coenzyme A reductase (Human)	C	C	Simvastatin	approved	inhibitor	99%	0.0	72%	0.78	-1.57	4UYM	X-ray, 2.55Å	74.73%	89%	Receptor1	-12.103.181
3-hydroxy-3-methylglutaryl-coenzyme A reductase	PAAG_05791	cluster781	Without similarity	3-hydroxy-3-methylglutaryl-coenzyme A reductase (Human)		C	SP-01A	investigational		99%	0.0	72%	0.78	-1.57	4UYM	X-ray, 2.55Å	74.73%	89%	Receptor1	-14.937.805
3-hydroxy-3-methylglutaryl-coenzyme A reductase	PAAG_05791	cluster628	Without similarity	3-hydroxy-3-methylglutaryl-coenzyme A reductase	C		Statins	Phase 1/2	Multiple myeloma	99%	0.0	72%	0.78	-1.57	4UYM	X-ray, 2.55Å	74.73%	89%	Receptor1	-13.576.427
3-hydroxy-3-methylglutaryl-coenzyme A reductase	PAAG_05791	cluster781	Without similarity	3-hydroxy-3-methylglutaryl-coenzyme A reductase (Human)		C	TAK-475	investigational		67%	2E-52	31%	-	-	-	-	-	-	-	-
3-hydroxy-3-methylglutaryl-coenzyme A reductase	PAAG_05791	cluster628	Without similarity	3-hydroxy-3-methylglutaryl-coenzyme A reductase	C		TOCOTRIENOL	Approved	Hyperlipidemia	67%	2E-52	31%	-	-	-	-	-	-	-	-
3-hydroxy-3-methylglutaryl-coenzyme A reductase	PAAG_05791	cluster628	Without similarity	3-hydroxy-3-methylglutaryl-coenzyme A reductase	C		XZK-monascus	Phase 2	Hyperlipidemia	98%	0.0	64%	-	-	-	-	-	-	-	-
3-oxoacyl-[acyl-carrier-protein] synthase homolog	PAAG_11454	cluster851	Without similarity	3-oxoacyl-[acyl-carrier-protein] synthase 2 (Escherichia coli (strain K12))	C	C	Cerulenin	approved	inhibitor	99%	0.0	72%	0.78	-1.57	4UYM	X-ray, 2.55Å	74.73%	89%	Receptor1	-13.170.559
40S ribosomal protein S0-A	PAAG_02111	cluster745	Without similarity	40S ribosomal protein SA (Human)		C	PCK3145	investigational		98%	0.0	47%	-	-	-	-	-	-	-	-
4-aminobutyrate aminotransferase	PAAG_00468	cluster612	Without similarity	4-aminobutyrate aminotransferase, mitochondrial	C		CPP -15	Approved	Infantile spasms	99%	0.0	72%	0.78	-1.57	4UYM	X-ray, 2.55Å	74.73%	89%	Receptor1	-12.198.807
4-aminobutyrate aminotransferase	PAAG_00468	cluster612	Without similarity	4-aminobutyrate aminotransferase, mitochondrial	C		CPP-115	Approved	Substance dependence	92%	5E-121	35%	-	-	-	-	-	-	-	-

4-aminobutyrate aminotransferase	PAAG_00468	cluster612	Without similarity	4-aminobutyrate aminotransferase, mitochondrial	C		Divalproex sodium	Approved	Seizures	92%	5E-121	35%	-	-	-	-	-	-	-	-
4-aminobutyrate aminotransferase	PAAG_00468	cluster612	Without similarity	4-aminobutyrate aminotransferase, mitochondrial	C		K-828-AB	Approved	Dementia	86%	1E-90	54%	0.67	-0.59	3NZJ	X-ray, 2.40 Å	64.16%	99%	Receptor1	4.764.316
4-aminobutyrate aminotransferase	PAAG_00468	cluster612	Without similarity	4-aminobutyrate aminotransferase, mitochondrial	C		Pyridoxal Phosphate	Approved	Dietary shortage	96%	1E-146	65%	0,74	-1,53	1VYW	X-ray, 2.3Å	65,77%	89%	Receptor1	-10.285.525
54S ribosomal protein L9, mitochondrial	PAAG_07484	cluster885	Without similarity	50S ribosomal protein L3 (Streptococcus pyogenes serotype M1)		C	Retapamulin	approved	inhibitor	89%	3E-59	30%	-	-	-	-	-	-	-	-
60S ribosomal protein L3	PAAG_00088	cluster750	DEG20010949	60S ribosomal protein L3 (Human)		C	Homoharringtonine	approved	antagonist	95%	6E-69	32%	-	-	-	-	-	-	-	-
6-phosphogluconate dehydrogenase, decarboxylating	PAAG_01178	cluster847	Without similarity	6-phosphogluconate dehydrogenase, decarboxylating (Human)		C	Dacarbazine	approved, investigational	inhibitor	96%	1E-146	65%	0,74	-1,53	1VYW	X-ray, 2.3Å	65,77%	89%	Receptor1	-10.386.665
6-phosphogluconate dehydrogenase, decarboxylating	PAAG_01178	cluster847	Without similarity	6-phosphogluconate dehydrogenase, decarboxylating (Human)	C	C	Furosemide	approved, vet_approved	inhibitor	99%	5E-49	60%	-	-	-	-	-	-	-	-
6-phosphogluconate dehydrogenase, decarboxylating	PAAG_01178	cluster847	Without similarity	6-phosphogluconate dehydrogenase, decarboxylating		C	Gadopentetate dimeglumine	approved	inhibitor	54%	6E-48	32%	-	-	-	-	-	-	-	-
6-phosphogluconate dehydrogenase, decarboxylating	PAAG_01178	cluster847	Without similarity	6-phosphogluconate dehydrogenase, decarboxylating (Human)		C	Ketotifen	approved	inhibitor	96%	1E-146	65%	0,74	-1,53	1VYW	X-ray, 2.3Å	65,77%	89%	Receptor1	-7.744.120
6-phosphogluconate dehydrogenase, decarboxylating	PAAG_01178	cluster847	Without similarity	6-phosphogluconate dehydrogenase, decarboxylating (Human)		C	Meloxicam	approved, vet_approved	inhibitor	96%	1E-146	65%	0,74	-1,53	1VYW	X-ray, 2.3Å	65,77%	89%	Receptor1	-6.963.912
6-phosphogluconate dehydrogenase, decarboxylating	PAAG_01178	cluster847	Without similarity	6-phosphogluconate dehydrogenase, decarboxylating (Human)		C	Methotrexate	approved	inhibitor	96%	1E-146	65%	0,74	-1,53	1VYW	X-ray, 2.3Å	65,77%	89%	Receptor1	-13.168.548
6-phosphogluconate dehydrogenase, decarboxylating	PAAG_01178	cluster847	Without similarity	6-phosphogluconate dehydrogenase, decarboxylating (Human)		C	Ritodrine	approved	inhibitor	96%	5E-135	59%	0,74	-1,53	1VYW	X-ray, 2.3Å	65,77%	89%	Receptor1	-14.196.286
Acetamidase	PAAG_03626	cluster23	Without similarity	Fatty-acid amide hydrolase	C		IW-6118	Phase 2	Inflammatory diseases	96%	1E-146	65%	0,74	-1,53	1VYW	X-ray, 2.3Å	65,77%	89%	Receptor1	-9.499.157
Acetamidase	PAAG_03626	cluster23	Without similarity	Fatty-acid amide hydrolase	C		PF-04457845	Phase 2	Liver disease	41%	2E-36	31%	-	-	-	-	-	-	-	-
Acetamidase	PAAG_03626	cluster23	Without similarity	Fatty-acid amide hydrolase	C		SSR411298	Phase 2	Major Depressive Disorder,Depression	41%	2E-36	31%	-	-	-	-	-	-	-	-
Acetyl-CoA acetyltransferase	PAAG_03447	cluster845	DEG20011020	Acetyl-CoA acetyltransferase, mitochondrial (Human)		C	Sulfasalazine	approved	inhibitor	82%	0.0	65%	-	-	-	-	-	-	-	-
Acetyl-CoA carboxylase	PAAG_08731	cluster623	DEG20010908	Acetyl-CoA carboxylase 2	C		Metformin	Approved	Diabetes mellitus	92%	5E-121	35%	-	-	-	-	-	-	-	-
Acetyl-CoA carboxylase	PAAG_08731	cluster623	DEG20010908	Acetyl-CoA carboxylase 2	C		Hydroxychloroquine	Discontinued in Phase 3	Obesity	88%	2E-25	35%	-	-	-	-	-	-	-	-
ADP,ATP carrier protein	PAAG_08620	cluster151	DEG20010020	ADP/ATP translocase 2 (Human)	C	C	Clodronate	approved, investigational, vet_approved	inhibitor	99%	0.0	79%	-	-	-	-	-	-	-	-
A-factor-processing enzyme	PAAG_04661	cluster567	Without similarity	Insulin-degrading Enzyme	C		PRO-001	Phase 2	Retinitis pigmentosa	96%	1E-146	65%	0,74	-1,53	1VYW	X-ray, 2.3Å	65,77%	89%	Receptor1	-12.962.872
Alcohol dehydrogenase 4, mitochondrial	PAAG_02382	cluster757	Without similarity	Quinone oxidoreductase (Human)		C	Dicoumarol	approved	inhibitor	96%	1E-146	65%	0,74	-1,53	1VYW	X-ray, 2.3Å	65,77%	89%	Receptor1	-11.608.564
Alpha-galactosidase mel1	PAAG_05254	cluster594	Without similarity	Alpha-galactosidase A	C		AT1001	Phase 3	Autoimmune diseases	96%	1E-146	65%	0,74	-1,53	1VYW	X-ray, 2.3Å	65,77%	89%	Receptor1	-11.608.564
Alpha-galactosidase mel1	PAAG_05254	cluster594	Without similarity	Alpha-galactosidase A	C		PRX-102	Phase 1/2	Fabry's disease	41%	2E-36	31%	-	-	-	-	-	-	-	-
Beta-mannosyltransferase 4	PAAG_06742	cluster256	Without similarity	Histone deacetylase 1 (Human)		C	CRA-024781	investigational		96%	1E-146	65%	0,74	-1,53	1VYW	X-ray, 2.3Å	65,77%	89%	Receptor1	-12.009.933
Beta-mannosyltransferase 4	PAAG_06742	cluster256	Without similarity	Histone deacetylase 2 (Human)	C	C	Lovastatin	approved, investigational	other	70%	3E-151	49%	-	-	-	-	-	-	-	-

Beta-mannosyltransferase 4	PAAG_06742	cluster256	Without similarity	Histone deacetylase 1 (Human)	C	C	MGCD-0103	investigational		99%	5E-49	60%	-	-	-	-	-	-	-	-
Beta-mannosyltransferase 4	PAAG_06742	cluster256	Without similarity	Histone deacetylase 1 (Human)		C	Panobinostat	approved, investigational	inhibitor	96%	1E-146	65%	0,74	-1,53	1VYW	X-ray, 2.3Å	65,77%	89%	Receptor1	-11.608.564
Beta-mannosyltransferase 4	PAAG_06742	cluster256	Without similarity	Histone deacetylase 1 (Human)	C	C	Romidepsin	approved, investigational	antagonistinhibitor	98%	2E-61	57%	-	-	-	-	-	-	-	-
Beta-mannosyltransferase 4	PAAG_06742	cluster256	Without similarity	Histone deacetylase 1 (Human)		C	SB939	investigational		41%	2E-36	31%	-	-	-	-	-	-	-	-
Biotin synthase, mitochondrial	PAAG_08157	cluster870	Without similarity	Biotin synthase (Escherichia coli (strain K12))		C	Tris	approved		61%	3E-136	48%	-	-	-	-	-	-	-	-
C-8 sterol isomerase	PAAG_05857	cluster569	Without similarity	Sigma(1)-type opioid receptor	C		ADX N05	Phase 3	Mood disorder	97%	6E-129	47%	-	-	-	-	-	-	-	-
C-8 sterol isomerase	PAAG_05857	cluster569	Without similarity	Sigma(1)-type opioid receptor	C		ANAVEX 1007	Phase 2	Breast cancer	96%	5E-135	59%	0,74	-1,53	1VYW	X-ray, 2.3Å	65,77%	89%	Receptor1	-11.768.664
C-8 sterol isomerase	PAAG_05857	cluster569	Without similarity	Sigma(1)-type opioid receptor	C		BMS-181100	Discontinued in Phase 3	Psychotic disorders	70%	1E-60	37%	-	-	-	-	-	-	-	-
C-8 sterol isomerase	PAAG_05857	cluster289	Without similarity	Sigma non-opioid intracellular receptor 1 (Human)		C	Captodiame	approved, investigational	agonist	91%	2E-140	55%	0.75	-1.28	2IIK	X-ray, 2.55 Å	54.78%	94%	Receptor1	-5.757.028
C-8 sterol isomerase	PAAG_05857	cluster569	Without similarity	Sigma(1)-type opioid receptor	C		CM-2395	Phase 3	Schizophrenia	94%	0.0	46%	0.34	-2.38	4JSN	X-ray, 3.20 Å	52.46%	46%	No docking	No docking
C-8 sterol isomerase	PAAG_05857	cluster569	Without similarity	Sigma(1)-type opioid receptor	C		DUP-734	Discontinued in Phase 1	Psychotic disorders	94%	0.0	46%	0.34	-2.38	4JSN	X-ray, 3.20 Å	52.46%	46%	Receptor1	-0.449890
C-8 sterol isomerase	PAAG_05857	cluster569	Without similarity	Sigma(1)-type opioid receptor	C		Igmesine	Phase 2	Igmesine	91%	5E-93	31%	-	-	-	-	-	-	-	-
C-8 sterol isomerase	PAAG_05857	cluster569	Without similarity	Sigma(1)-type opioid receptor	C		KB-5492	Discontinued in Phase 2	Peptic ulcer	71%	3E-173	57%	-	-	-	-	-	-	-	-
C-8 sterol isomerase	PAAG_05857	cluster569	Without similarity	Sigma(1)-type opioid receptor	C		OPC-14523	Phase 2	Bulimia nervosa OCD MDD, Severe Mood Disorders	94%	1E-59	34%	-	-	-	-	-	-	-	-
C-8 sterol isomerase	PAAG_05857	cluster569	Without similarity	Sigma(1)-type opioid receptor	C		OxycoDex	Discontinued in Phase 2	Pain	87%	5E-126	42%	-	-	-	-	-	-	-	-
C-8 sterol isomerase	PAAG_05857	cluster569	Without similarity	Sigma(1)-type opioid receptor	C		Panamesine	Discontinued in Phase 2	Psychotic disorders	41%	2E-36	31%	-	-	-	-	-	-	-	-
C-8 sterol isomerase	PAAG_05857	cluster289	Without similarity	Sigma non-opioid intracellular receptor 1 (Human)		C	Pentazocine	approved, vet_approved	agonist	94%	0.0	46%	0.34	-2.38	4JSN	X-ray, 3.20 Å	52.46%	46%	Receptor1	-13.222.617
C-8 sterol isomerase	PAAG_05857	cluster289	Without similarity	Sigma non-opioid intracellular receptor 1 (Human)		C	Phencyclidine	illicit		94%	0.0	46%	0.34	-2.38	4JSN	X-ray, 3.20 Å	52.46%	46%	Receptor1	-12.455.471
C-8 sterol isomerase	PAAG_05857	cluster569	Without similarity	Sigma(1)-type opioid receptor	C		PRX-00023	Discontinued in Phase 2	Severe Mood Disorders	94%	0.0	46%	0.34	-2.38	4JSN	X-ray, 3.20 Å	52.46%	46%	Receptor1	-14.269.496
C-8 sterol isomerase	PAAG_05857	cluster289	Without similarity	Sigma non-opioid intracellular receptor 1 (Human)		C	Remoxipride	approved, withdrawn	antagonist	95%	6E-69	32%	-	-	-	-	-	-	-	-
Calcium/calmodulin-dependent protein kinase type IV	PAAG_00826	cluster866	DEG20011040	Serine/threonine-protein kinase Chk2 (Human)		C	XL844	investigational		94%	0.0	46%	0.34	-2.38	4JSN	X-ray, 3.20 Å	52.46%	46%	Receptor1	-13.027.889
Calcium-binding protein NCS-1	PAAG_03551	cluster237	Without similarity	Calcineurin subunit B type 2 (Human)		C	Cyclosporine	approved, investigational, vet_approved	inhibitor	46%	3E-84	36%	-	-	-	-	-	-	-	-
Calcium-binding protein NCS-1	PAAG_03551	cluster237	Without similarity	Calcineurin subunit B type 2 (Human)		C	ISA247	investigational		72%	4E-80	44%	-	-	-	-	-	-	-	-
Calmodulin	PAAG_08247	cluster896	DEG20010051	Calmodulin (Human)		C	Aprindine	approved	inhibitor	61%	3E-136	48%	-	-	-	-	-	-	-	-
Calmodulin	PAAG_08247	cluster896	DEG20010051	Calmodulin (Human)		C	Bepridil	approved, withdrawn	binder	95%	6E-69	32%	-	-	-	-	-	-	-	-
Calmodulin	PAAG_08247	cluster896	DEG20010051	Calmodulin (Human)		C	Chlorpromazine	approved, vet_approved		95%	6E-69	32%	-	-	-	-	-	-	-	-
Calmodulin	PAAG_08247	cluster896	DEG20010051	Calmodulin (Human)		C	Cinchocaine	approved, vet_approved	inhibitor	94%	0.0	46%	0.34	-2.38	4JSN	X-ray, 3.20 Å	52.46%	46%	Receptor2	-12.022.519
Calmodulin	PAAG_08247	cluster603	DEG20010051	Troponin C	C		Dihydroxyaluminium	Approved	Skin irritations	69%	1E-46	31%	-	-	-	-	-	-	-	-
Calmodulin	PAAG_08247	cluster896	DEG20010051	Calmodulin (Human)		C	Felodipine	approved, investigational	other	94%	0.0	46%	0.34	-2.38	4JSN	X-ray, 3.20 Å	52.46%	46%	Receptor1	-1.007.891
Calmodulin	PAAG_08247	cluster896	DEG20010051	Calmodulin (Human)		C	Flunarizine	approved		93%	0.0	38%	-	-	-	-	-	-	-	-
Calmodulin	PAAG_08247	cluster896	DEG20010051	Calmodulin (Human)		C	Fluphenazine	approved	inhibitor	94%	0.0	46%	0.34	-2.38	4JSN	X-ray, 3.20 Å	52.46%	46%	Receptor1	-10.137.499
Calmodulin	PAAG_08247	cluster603	DEG20010051	Troponin C	C		Levosimendan	Approved	Congestive heart failure	82%	7E-58	31%	-	-	-	-	-	-	-	-
Calmodulin	PAAG_08247	cluster896	DEG20010051	Calmodulin (Human)		C	Loperamide	approved	inhibitor	94%	0.0	46%	0.34	-2.38	4JSN	X-ray, 3.20 Å	52.46%	46%	Receptor2	-11.774.111

Calmodulin	PAAG_08247	cluster896	DEG20010051	Calmodulin (Human)		C	Nicardipine	approved	other/ unknown	67%	2E-52	31%	-	-	-	-	-	-	-	-
Calmodulin	PAAG_08247	cluster896	DEG20010051	Calmodulin (Human)		C	Nifedipine	approved	inhibitor	94%	0.0	46%	0.34	-2.38	4JSN	X-ray, 3.20 Å	52.46%	46%	Receptor1	-11.911.247
Calmodulin	PAAG_08247	cluster896	DEG20010051	Calmodulin (Human)		C	Perphenazine	approved	inhibitor	94%	0.0	46%	0.34	-2.38	4JSN	X-ray, 3.20 Å	52.46%	46%	Receptor2	-7.476.795
Calmodulin	PAAG_08247	cluster896	DEG20010051	Calmodulin (Human)		C	Phenoxybenzamine	approved	inhibitor	94%	0.0	46%	0.34	-2.38	4JSN	X-ray, 3.20 Å	52.46%	46%	Receptor1	-11.162.820
Calmodulin	PAAG_08247	cluster896	DEG20010051	Calmodulin (Human)		C	Pimozide	approved	inhibitor	70%	3E-151	49%	-	-	-	-	-	-	-	-
Calmodulin	PAAG_08247	cluster896	DEG20010051	Calmodulin (Human)		C	Prenylamine	withdrawn		70%	3E-151	49%	-	-	-	-	-	-	-	-
Calmodulin	PAAG_08247	cluster896	DEG20010051	Calmodulin (Human)		C	Promethazine	approved	inhibitor	62%	2E-81	30%	-	-	-	-	-	-	-	-
Calmodulin	PAAG_08247	cluster896	DEG20010051	Calmodulin (Human)		C	Trifluoperazine	approved	inhibitor	87%	5E-126	42%	-	-	-	-	-	-	-	-
cAMP-dependent protein kinase regulatory subunit	PAAG_07887	cluster230	Without similarity	cAMP-dependent protein kinase type II-alpha regulatory subunit (Human)		C	GEM-231	investigational		94%	0.0	46%	0.34	-2.38	4JSN	X-ray, 3.20 Å	52.46%	46%	Receptor2	-11.335.812
Carboxylic ester hydrolase	PAAG_00885	cluster157	Without similarity	Acetylcholinesterase (Human)		C	Zanapezil	investigational		94%	0.0	46%	0.34	-2.38	4JSN	X-ray, 3.20 Å	52.46%	46%	Receptor1	-8.367.253
Carnitine O-acetyltransferase YAT2	PAAG_06224	cluster228	Without similarity	Choline O-acetyltransferase (Human)		C	Nicotine	approved		94%	0.0	46%	0.34	-2.38	4JSN	X-ray, 3.20 Å	52.46%	46%	Receptor1	-3.468.243
Carnitine O-acetyltransferase, mitochondrial	PAAG_03062	cluster827	Without similarity	Carnitine O-palmitoyltransferase 2, mitochondrial (Human)	C	C	Perhexiline	approved	inhibitor	94%	0.0	46%	0.34	-2.38	4JSN	X-ray, 3.20 Å	52.46%	46%	Receptor1	-10.137.499
Carnitine O-acetyltransferase, mitochondrial	PAAG_06224	cluster620	Without similarity	Carnitine O-palmitoyltransferase I	C		SDZ-CPI-975	Discontinued in Phase 1	Diabetes	71%	3E-173	57%	-	-	-	-	-	-	-	-
Catalase	PAAG_01454	cluster891	Without similarity	Catalase (Human)		C	Fomepizole	approved, vet_approved	inhibitor	94%	0.0	46%	0.34	-2.38	4JSN	X-ray, 3.20 Å	52.46%	46%	Receptor1	-0.657237
Cell division control protein 1	PAAG_01186	cluster270	DEG20010065	Cyclin-dependent kinase 2 (Human)	C	C	AT7519	investigational		97%	3E-160	40%	-	-	-	-	-	-	-	-
Cell division control protein 1	PAAG_01186	cluster149	DEG20010065	Cell division protein kinase 2	C		BAY 10-00394	Phase 2	Small-cell lung cancer	70%	3E-151	49%	-	-	-	-	-	-	-	-
Cell division control protein 1	PAAG_01186	cluster270	DEG20010065	Cyclin-dependent kinase 2 (Human)		C	Bosutinib	approved	inhibitor	67%	2E-52	31%	-	-	-	-	-	-	-	-
Cell division control protein 1	PAAG_01186	cluster149	DEG20010065	Cell division protein kinase 2	C		Capridine-beta	Approved	Psoriasis	94%	0.0	46%	0.34	-2.38	4JSN	X-ray, 3.20 Å	52.46%	46%	Receptor1	-10.437.837
Cell division control protein 1	PAAG_01186	cluster149	DEG20010065	Cell division protein kinase 2	C	C	Flavopiridol	Phase 3	Graft-versus-host disease	94%	0.0	46%	0.34	-2.38	4JSN	X-ray, 3.20 Å	52.46%	46%	Receptor1	-5.017.303
Cell division control protein 1	PAAG_01186	cluster149	DEG20010065	Cell division control protein 2 homolog	C		Riviciclib	Phase 2	Mantle cell lymphoma	94%	0.0	46%	0.34	-2.38	4JSN	X-ray, 3.20 Å	52.46%	46%	Receptor1	-3.270.941
Cell division control protein 1	PAAG_01186	cluster149	DEG20010065	Cell division protein kinase 2	C		PHA848125	Phase 2	Solid tumours	92%	5E-121	35%	-	-	-	-	-	-	-	-
Cell division control protein 1	PAAG_01186	cluster149	DEG20010065	Cell division protein kinase 2	C		Ro 31-7453	Phase 2	Solid tumours	94%	0.0	46%	0.34	-2.38	4JSN	X-ray, 3.20 Å	52.46%	46%	Receptor1	0.893575
Cell division control protein 1	PAAG_01186	cluster149	DEG20010065	Cell division protein kinase 2	C		Roscovitine	Phase 2	Discovery agent	92%	1E-52	36%	-	-	-	-	-	-	-	-
Cell division control protein 1	PAAG_01186	cluster149	DEG20010065	Cell division protein kinase 2	C		R-roscovitine	Phase 2	Cancer	94%	0.0	46%	0.34	-2.38	4JSN	X-ray, 3.20 Å	52.46%	46%	Receptor1	-10.437.837
Cell division control protein 1	PAAG_01186	cluster149	DEG20010065	Cell division protein kinase 2	C		SCH 727965	Phase 3	Acute lymphoblastic leukemia	97%	6E-129	47%	-	-	-	-	-	-	-	-
Cell division control protein 1	PAAG_01186	cluster149	DEG20010065	Cell division protein kinase 2	C		Seliciclib	Phase 2	Non-small cell lung cancer	94%	0.0	46%	0.34	-2.38	4JSN	X-ray, 3.20 Å	52.46%	46%	Receptor1	-1.886.353
Cell division control protein 1	PAAG_01186	cluster149	DEG20010065	Cell division control protein 2 homolog	C		Terameprocol	Phase 2	Solid tumours	99%	0.0	57%	0.93	-1.14	4V59	X-ray, 3.10 Å	81.83%	99%	Receptor3	-8.734.272
Cell division control protein 2	PAAG_05894	cluster265	DEG20010727	NADPH oxidase (Human)	C	C	Dextromethorphan	approved		94%	0.0	52%	0.70	-4.74	4CR2	EM, 7.70 Å	52.07%	94%	Receptor2	-8.851904
Chromatin modification-related protein EAF1	PAAG_02610	cluster626	Without similarity	CBP	C		PRI-724	Phase 1/2	Cancer	46%	3E-84	36%	-	-	-	-	-	-	-	-
Cytidine deaminase	PAAG_01751	cluster865	Without similarity	Cytidine deaminase (Human)		C	DN-101	investigational		71%	3E-173	57%	-	-	-	-	-	-	-	-
Cytochrome c	PAAG_06268	cluster913	Without similarity	Cytochrome c (Human)		C	Minocycline	approved, investigational	negative modulator	88%	2E-25	35%	-	-	-	-	-	-	-	-
Damage response protein 1	PAAG_01861	cluster761	Without similarity	Sigma receptor (Human)		C	Nortriptyline	approved	binder	71%	3E-173	57%	-	-	-	-	-	-	-	-

Decaprenyl-diphosphate synthase subunit 1	PAAG_00510	cluster917	Without similarity	Geranylgeranyl pyrophosphate synthase (Human)	C	C	Zoledronic acid	approved	inhibitor	70%	3E-151	49%	-	-	-	-	-	-	-	-
Delta-aminolevulinic acid dehydratase	PAAG_00299	cluster610	DEG20010350	Delta-aminolevulinic acid dehydratase	C		Aminolevulinic acid	Approved	Photodynamic therapy	98%	0.0	47%	-	-	-	-	-	-	-	-
Delta-aminolevulinic acid dehydratase	PAAG_00299	cluster610	DEG20010350	Delta-aminolevulinic acid dehydratase	C		Porphobilinogen	Phase 2	Discovery agent	84%	3E-102	50%	0.17	-1.49	3TXO	X-ray, 2.05 Å	54.57%	29%	Receptor1	-13.717.440
Dihydrofolate synthetase	PAAG_07676	cluster810	DEG20010803	Bifunctional protein FolC (Escherichia coli (strain K12))		C	Sulfamethoxazole	approved	inhibitor	87%	3E-114	52%	0.17	-1.49	3TXO	X-ray, 2.05 Å	54.57%	29%	Receptor1	-11.811.606
Dihydroorotate dehydrogenase (quinone), mitochondrial	PAAG_06458	cluster218	Without similarity	Dihydroorotate dehydrogenase (quinone), mitochondrial (Human)		C	Atovaquone	approved	inhibitor	79%	9E-107	50%	0.17	-1.49	3TXO	X-ray, 2.05 Å	54.57%	29%	Receptor1	16.858.719
Dihydroorotate dehydrogenase (quinone), mitochondrial	PAAG_06458	cluster218	Without similarity	Dihydroorotate dehydrogenase (quinone), mitochondrial (Human)		C	Leflunomide	approved, investigational	inhibitor	81%	5E-119	52%	0.17	-1.49	3TXO	X-ray, 2.05 Å	54.57%	29%	Receptor1	-12.762.236
Dihydroorotate dehydrogenase (quinone), mitochondrial	PAAG_06458	cluster218	Without similarity	Dihydroorotate dehydrogenase (quinone), mitochondrial (Human)		C	SC12267	investigational		62%	3E-115	51%	0.17	-1.49	3TXO	X-ray, 2.05 Å	54.57%	29%	Receptor1	-11.834.323
Dihydroorotate dehydrogenase (quinone), mitochondrial	PAAG_06458	cluster218	Without similarity	Dihydroorotate dehydrogenase (quinone), mitochondrial (Human)		C	Teriflunomide	approved	inhibitor	50%	2E-119	52%	0.17	-1.49	3TXO	X-ray, 2.05 Å	54.57%	29%	Receptor1	-11.157.833
Dipeptidyl peptidase 4	PAAG_06844	cluster89	Without similarity	Dipeptidyl peptidase IV	C		ABT-279	Discontinued in Phase 1	Type 2 Diabetes	84%	3E-102	50%	0.17	-1.49	3TXO	X-ray, 2.05 Å	54.57%	29%	-	-
Dipeptidyl peptidase 4	PAAG_06844	cluster89	Without similarity	Dipeptidyl peptidase IV	C		ALS 2-0426	Discontinued in Phase 2	Diabetes mellitus type 2	46%	3E-84	36%	-	-	-	-	-	-	-	-
Dipeptidyl peptidase 4	PAAG_06844	cluster89	Without similarity	Dipeptidyl peptidase IV	C		Anagliptin	Approved	Diabetes mellitus type 2	64%	2E-91	31%	-	-	-	-	-	-	-	-
Dipeptidyl peptidase 4	PAAG_06844	cluster89	Without similarity	Dipeptidyl peptidase IV	C		BI-1356	Approved	Type 2 diabetes	68%	1E-115	52%	0.17	-1.49	3TXO	X-ray, 2.05 Å	54.57%	29%	Receptor1	-11.811.606
Dipeptidyl peptidase 4	PAAG_06844	cluster89	Without similarity	Dipeptidyl peptidase IV	C		Denagliptin	Phase 2/3	Diabetes mellitus type 2	79%	9E-107	50%	0.17	-1.49	3TXO	X-ray, 2.05 Å	54.57%	29%	Receptor1	-14.511.683
Dipeptidyl peptidase 4	PAAG_01724	cluster89	Without similarity	Dipeptidyl peptidase IV	C		Dutogliptin	Phase 3	Diabetes mellitus type 2	87%	3E-114	52%	0.17	-1.49	3TXO	X-ray, 2.05 Å	54.57%	29%	Receptor1	-11.702.345
Dipeptidyl peptidase 4	PAAG_01724	cluster89	Without similarity	Dipeptidyl peptidase IV	C		Gemigliptin	Phase 3	Diabetes mellitus	96%	0.0	40%	-	-	-	-	-	-		
Dipeptidyl peptidase 4	PAAG_06844	cluster89	Without similarity	Dipeptidyl peptidase IV	C		IDDBCP161883	Phase 3	Diabetes mellitus type 2	94%	0.0	68%	0.63	-1.23	3OLJ	X-ray, 2.10 Å	77.03%	69%	Receptor1	-7.957.572
Dipeptidyl peptidase 4	PAAG_06844	cluster89	Without similarity	Dipeptidyl peptidase IV	C		IP 10.C8-1	Phase 2	Psoriasis	97%	0.0	82%	0.87	-1.11	4I50	X-ray, 2.30 Å	82.64%	99%	Receptor1	-6.342.248
Dipeptidyl peptidase 4	PAAG_06844	cluster89	Without similarity	Dipeptidyl peptidase IV	C		Isoleucine thiazolidide DPP IV	Discontinued at Phase 2	Type 2 Diabetes	97%	0.0	82%	0.87	-1.11	4I50	X-ray, 2.30 Å	82.64%	99%	Receptor1	-8.318.228
Dipeptidyl peptidase 4	PAAG_06844	cluster89	Without similarity	Dipeptidyl peptidase IV	C		Kombiglyze XR/Komboglyze FDC	Approved	Diabetes mellitus	97%	0.0	84%	0.87	-1.11	4I50	X-ray, 2.30 Å	82.64%	99%	Receptor1	-8.118.922
Dipeptidyl peptidase 4	PAAG_06844	cluster89	Without similarity	Dipeptidyl peptidase IV	C		LC-150444	Phase 3	Diabetes mellitus type 2	70%	3E-151	49%	-	-	-	-	-	-	-	-
Dipeptidyl peptidase 4	PAAG_06844	cluster89	Without similarity	Dipeptidyl peptidase IV	C		LEZ763	Phase 1/2	Peripheral arterial disease	97%	0.0	82%	0.87	-1.11	4I50	X-ray, 2.30 Å	82.64%	99%	Receptor1	-5.048.985
Dipeptidyl peptidase 4	PAAG_06844	cluster89	Without similarity	Dipeptidyl peptidase IV	C	C	Linagliptin	Phase 3	Diabetes mellitus type II	97%	0.0	82%	0.87	-1.11	4I50	X-ray, 2.30 Å	82.64%	99%	Receptor1	-7.340.505
Dipeptidyl peptidase 4	PAAG_06844	cluster89	**Without similarity**	Dipeptidyl peptidase IV	C		Melogliptin	Phase 2	Type 2 Diabetes	98%	0.0	82%	0.87	-1.11	4I50	X-ray, 2.30 Å	82.64%	99%	Receptor1	-7.476.926
Dipeptidyl peptidase 4	PAAG_06844	cluster89	Without similarity	Dipeptidyl peptidase IV	C		MK-3102	Phase 3	Diabetes mellitus type 2	97%	0.0	82%	0.87	-1.11	4I50	X-ray, 2.30 Å	82.64%	99%	Receptor1	0.319388
Dipeptidyl peptidase 4	PAAG_06844	cluster89	Without similarity	Dipeptidyl peptidase IV	C		NVP DPP728	Discontinued at Phase 2	Diabetes mellitus type 2	91%	5E-93	31%	-	-	-	-	-	-	-	-
Dipeptidyl peptidase 4	PAAG_06844	cluster89	Without similarity	Dipeptidyl peptidase IV	C		P32/98	Phase 2	Autism	98%	0.0	82%	0.87	-1.11	4I50	X-ray, 2.30 Å	82.64%	99%	Receptor1	-5.775.519
Dipeptidyl peptidase 4	PAAG_06844	cluster89	Without similarity	Dipeptidyl peptidase IV	C		PF-00734200	Phase 2	Diabetes mellitus type 2	88%	2E-25	35%	-	-	-	-	-	-	-	-
Dipeptidyl peptidase 4	PAAG_06844	cluster89	Without similarity	Dipeptidyl peptidase IV	C		R-1438	Discontinued at Phase 2	Type 2 Diabetes	97%	0.0	82%	0.87	-1.11	4I50	X-ray, 2.30 Å	82.64%	99%	Receptor1	-4.433.053
Dipeptidyl peptidase 4	PAAG_06844	cluster89	Without similarity	Dipeptidyl peptidase IV	C		SAND-26	Phase 3	Autoimmune diseases	87%	5E-126	42%	-	-	-	-	-	-	-	-

Dipeptidyl peptidase 4	PAAG_06844	cluster89	Without similarity	Dipeptidyl peptidase IV	C		SaxaDapa FDC	Phase 3	Diabetes mellitus	98%	2E-61	57%	-	-	-	-	-	-	-	-
Dipeptidyl peptidase 4	PAAG_06844	cluster89	Without similarity	Dipeptidyl peptidase IV	C	C	Saxagliptin	Approved	Type 2 diabetes	97%	0.0	84%	0.87	-1.11	4I50	X-ray, 2.30 Å	82.64%	99%	Receptor1	-6.408.911
Dipeptidyl peptidase 4	PAAG_06844	cluster89	Without similarity	Dipeptidyl peptidase IV	C	C	Sitagliptin	Approved	Diabetes mellitus	98%	0.0	47%	-	-	-	-	-	-	-	-
Dipeptidyl peptidase 4	PAAG_06844	cluster89	Without similarity	Dipeptidyl peptidase IV	C		SSR-162369	Discontinued in Phase 1	Type 2 Diabetes	99%	0.0	79%	-	-	-	-	-	-	-	-
Dipeptidyl peptidase 4	PAAG_06844	cluster89	Without similarity	Dipeptidyl peptidase IV	C		SYR-472	Phase 3	Metabolic disorders	97%	0.0	84%	0.87	-1.11	4I50	X-ray, 2.30 Å	82.64%	99%	Receptor1	-5.350.420
Dipeptidyl peptidase 4	PAAG_06844	cluster89	Without similarity	Dipeptidyl peptidase IV	C		TA-6666	Discontinued at Phase 2	Diabetes mellitus type 2	41%	2E-36	31%	-	-	-	-	-	-	-	-
Dipeptidyl peptidase 4	PAAG_06844	cluster89	Without similarity	Dipeptidyl peptidase IV	C		TAK-100	Discontinued in Phase 1	Diabetes mellitus	98%	0.0	81%	0.87	-1.11	4I50	X-ray, 2.30 Å	82.64%	99%	Receptor1	-6.026.620
Dipeptidyl peptidase 4	PAAG_06844	cluster89	Without similarity	Dipeptidyl peptidase IV	C		TAK-472	Phase 2	Type 2 Diabetes	41%	2E-36	31%	-	-	-	-	-	-	-	-
Dipeptidyl peptidase 4	PAAG_06844	cluster89	Without similarity	Dipeptidyl peptidase IV	C	C	Vildagliptin	Approved	Type 2 Diabetes	97%	0.0	82%	0.87	-1.11	4I50	X-ray, 2.30 Å	82.64%	99%	Receptor1	-7.183.609
Dipeptidyl peptidase 4	PAAG_06844	cluster89	Without similarity	Dipeptidyl peptidase IV	C		YSCMA	Phase 1/2	Hematological malignancies	97%	0.0	84%	0.87	-1.11	4I50	X-ray, 2.30 Å	82.64%	99%	Receptor1	-9.034.729
DNA ligase	PAAG_07212	cluster792	DEG20010144	DNA ligase 1 (Human)		C	Bleomycin	approved	inhibitor	97%	0.0	84%	0.87	-1.11	4I50	X-ray, 2.30 Å	82.64%	99%	Receptor1	-7.364.854
DNA polymerase 1	PAAG_06486	cluster867	DEG20010854	DNA polymerase alpha catalytic subunit (Human)		C	Nelarabine	approved, investigational	inhibitor	46%	3E-84	36%	-	-	-	-	-	-	-	-
DNA polymerase 2	PAAG_06601	cluster104	DEG20010126	DNA polymerase catalytic subunit (HHV-5)		C	Cidofovir	approved	inhibitor	71%	3E-173	57%	-	-	-	-	-	-	-	-
DNA polymerase 2	PAAG_06601	cluster104	DEG20010126	DNA polymerase catalytic subunit (HHV-5)		C	Foscarnet	approved	inhibitor	99%	1E-127	48%	-	-	-	-	-	-	-	-
DNA topoisomerase 1	PAAG_05577	cluster85	Without similarity	DNA topoisomerase I	C		9-Nitrocamptothecin (9-NC)	Phase 2	Discovery agent	67%	2E-52	31%	-	-	-	-	-	-	-	-
DNA topoisomerase 1	PAAG_05577	cluster85	Without similarity	Non-camptothecin topo1	C		AR-67	Phase 2	Glioblastoma	87%	5E-126	42%	-	-	-	-	-	-	-	-
DNA topoisomerase 1	PAAG_05577	cluster85	Without similarity	DNA topoisomerase I	C		BECATECARIN	Discontinued in Phase 3	Solid tumours	89%	0.0	53%	-	-	-	-	-	-	-	-
DNA topoisomerase 1	PAAG_05577	cluster85	Without similarity	DNA topoisomerase I	C		Belotecan hydrocholoride	Approved	Small-cell lung cancer	97%	0.0	82%	0.87	-1.11	4I50	X-ray, 2.30 Å	82.64%	99%	Receptor1	-1.180.448
DNA topoisomerase 1	PAAG_05577	cluster85	Without similarity	DNA topoisomerase I	C		Beta-Lapachone	Phase 2	Solid tumours	98%	0.0	82%	0.87	-1.11	4I50	X-ray, 2.30 Å	82.64%	99%	Receptor1	-6.460.081
DNA topoisomerase 1	PAAG_05577	cluster272	Without similarity	DNA topoisomerase 1 (Human)		C	BNP 1350	investigational		98%	0.0	47%	-	-	-	-	-	-	-	-
DNA topoisomerase 1	PAAG_05577	cluster85	Without similarity	DNA topoisomerase I	C		Camptothecin	Phase 3	Solid Tumors	97%	0.0	82%	0.87	-1.11	4I50	X-ray, 2.30 Å	82.64%	99%	Receptor1	-6.432.246
DNA topoisomerase 1	PAAG_05577	cluster85	Without similarity	DNA topoisomerase I	C		CKD602	Phase 2	Cancer	62%	2E-81	30%	-	-	-	-	-	-	-	-
DNA topoisomerase 1	PAAG_05577	cluster85	Without similarity	Non-camptothecin topo1	C		CRLX101	Phase 2	Late-stage solid tumors	93%	0.0	38%	-	-	-	-	-	-	-	-
DNA topoisomerase 1	PAAG_05577	cluster272	Without similarity	DNA topoisomerase 1 (Human)		C	Edotecarin	investigational		97%	0.0	82%	0.87	-1.11	4I50	X-ray, 2.30 Å	82.64%	99%	Receptor1	3.106.042
DNA topoisomerase 1	PAAG_05577	cluster85	Without similarity	Non-camptothecin topo1	C		Etirinotecan pegol	Phase 3	Metastatic breast cancer	41%	2E-36	31%	-	-	-	-	-	-	-	-
DNA topoisomerase 1	PAAG_05577	cluster272	Without similarity	DNA topoisomerase 1 (Human)	C	C	Irinotecan	approved, investigational	inhibitor	86%	3E-180	65%	-	-	-	-	-	-	-	-
DNA topoisomerase 1	PAAG_05577	cluster85	Without similarity	Non-camptothecin topo1	C		Karenitecin	Phase 3	Advanced ovarian cancer	82%	0.0	65%	-	-	-	-	-	-	-	-
DNA topoisomerase 1	PAAG_05577	cluster272	Without similarity	DNA topoisomerase 1 (Human)		C	LE-SN38	investigational		97%	0.0	82%	0.87	-1.11	4I50	X-ray, 2.30 Å	82.64%	99%	Receptor1	-6.293.358
DNA topoisomerase 1	PAAG_05577	cluster85	Without similarity	DNA topoisomerase I	C		Liposomal lurtotecan	Discontinued in Phase 1	Lung cancer	98%	0.0	82%	0.87	-1.11	4I50	X-ray, 2.30 Å	82.64%	99%	Receptor1	1.928.719
DNA topoisomerase 1	PAAG_05577	cluster85	Without similarity	DNA topoisomerase I	C		NC-190	Discontinued in Phase 2	Solid tumours	97%	0.0	82%	0.87	-1.11	4I50	X-ray, 2.30 Å	82.64%	99%	Receptor1	-1.800.987
DNA topoisomerase 1	PAAG_05577	cluster85	Without similarity	DNA topoisomerase I	C		NK-611	Discontinued in Phase 2	Solid tumours	85%	7E-101	43%	-	-	-	-	-	-	-	-
DNA topoisomerase 1	PAAG_05577	cluster85	Without similarity	Non-camptothecin topo1	C		PEG-SN38	Phase 2	Metastatic breast cancer	98%	0.0	82%	0.87	-1.11	4I50	X-ray, 2.30 Å	82.64%	99%	Receptor1	-0.755413
DNA topoisomerase 1	PAAG_05577	cluster85	Without similarity	DNA topoisomerase I	C		PYRAZOLOACRIDINE	Phase 2	Colorectal cancer	41%	2E-36	31%	-	-	-	-	-	-	-	-
DNA topoisomerase 1	PAAG_05577	cluster85	Without similarity	DNA topoisomerase I	C		S-16020-2	Discontinued in Phase 2	Solid tumours	97%	0.0	82%	0.87	-1.11	4I50	X-ray, 2.30 Å	82.64%	99%	Receptor1	-7.066.279
DNA topoisomerase 1	PAAG_05577	cluster85	Without similarity	DNA topoisomerase I	C		SN-38	Phase 2	Cancer	67%	2E-67	42%	0,14	-1,41	3THB	X-ray, 2.50 Å	42,00%	22%	Receptor1	-12.357.041

DNA topoisomerase 1	PAAG_05577	cluster272	Without similarity	DNA topoisomerase 1 (Human)		C	Sodium stibogluconate	approved, investigational	inhibitor	67%	2E-67	42%	0,14	-1,41	3THB	X-ray, 2.50 Å	42,00%	22%	Receptor1	-6.890.459
DNA topoisomerase 1	PAAG_05577	cluster85	Without similarity	DNA topoisomerase I	C		Sphingosomal topotecan	Approved	Cancer	82%	7E-58	31%	-	-	-	-	-	-	-	-
DNA topoisomerase 1	PAAG_05577	cluster85	Without similarity	DNA topoisomerase I	C		Teloxantrone	Discontinued in Phase 1	Cancer	70%	3E-151	49%	-	-	-	-	-	-	-	-
DNA topoisomerase 1	PAAG_05577	cluster85	Without similarity	Non-camptothecin topo1	C		TLC-388	Phase 2	Solid tumours	99%	0.0	73%	-	-	-	-	-	-	-	-
DNA topoisomerase 1	PAAG_05577	cluster85	Without similarity	DNA topoisomerase I	C		Topetecan	Approved	Small cell lung cancer	67%	2E-67	42%	0,14	-1,41	3THB	X-ray, 2.50 Å	42,00%	22%	Receptor1	-9.462.092
DNA topoisomerase 1	PAAG_05577	cluster272	Without similarity	DNA topoisomerase 1 (Human)	C	C	Topotecan	approved, investigational	inhibitor	67%	2E-67	42%	0,14	-1,41	3THB	X-ray, 2.50 Å	42,00%	22%	Receptor1	-6.764.010
DNA topoisomerase 1	PAAG_05577	cluster272	Without similarity	DNA topoisomerase 1 (Human)		C	XMT-1001	investigational		99%	0.0	73%	-	-	-	-	-	-	-	-
DNA topoisomerase 2	PAAG_03486	cluster255	DEG20010853	DNA topoisomerase 2-beta (Human)		C	99mTc-ciprofloxacin	investigational		95%	9E-137	49%	0.70	-1.41	2F2S	X-ray, 2.00 Å	50.78%	88%	Receptor1	-7.171.270
DNA topoisomerase 2	PAAG_03486	cluster568	DEG20010853	DNA topoisomerase II	C		Aclarubicin	Approved	Cancer	71%	0.0	51%	0,24	-1,75	1BJT	X-ray, 2.50 Å	46,00%	41%	Receptor1	-10.621.546
DNA topoisomerase 2	PAAG_03486	cluster568	DEG20010853	DNA topoisomerase II	C		Amifloxacin	Discontinued in Phase 2	Discovery agent	81%	0.0	50%	0,24	-1,75	1BJT	X-ray, 2.50 Å	46,00%	41%	Receptor1	-6.570.233
DNA topoisomerase 2	PAAG_03486	cluster255	DEG20010853	DNA topoisomerase 2-alpha (Human)		C	Amonafide	investigational		88%	2E-25	35%	-	-	-	-	-	-	-	-
DNA topoisomerase 2	PAAG_03486	cluster255	DEG20010853	DNA topoisomerase 2-alpha (Human)	C	C	Amsacrine	approved	inhibitor	94%	0.0	65%	-	-	-	-	-	-	-	-
DNA topoisomerase 2	PAAG_03486	cluster568	DEG20010853	DNA topoisomerase II	C		Anthracycline	Phase 2	Solid tumours	94%	3E-137	51%	-	-	-	-	-	-	-	-
DNA topoisomerase 2	PAAG_03486	cluster255	DEG20010853	DNA topoisomerase 2-alpha (Human)	C	C	Banoxantrone	investigational		81%	0.0	50%	0,24	-1,75	1BJT	X-ray, 2.50 Å	46,00%	41%	Receptor1	-11.328.490
DNA topoisomerase 2	PAAG_03486	cluster568	DEG20010853	DNA topoisomerase II	C		Berubicin	Phase 2	Cancer	81%	0.0	50%	0,24	-1,75	1BJT	X-ray, 2.50 Å	46,00%	41%	Receptor1	-10.957.759
DNA topoisomerase 2	PAAG_03486	cluster568	DEG20010853	DNA topoisomerase II	C		Besifloxacin	Approved	Ocular inflammation	83%	5E-98	45%	-	-	-	-	-	-	-	-
DNA topoisomerase 2	PAAG_03486	cluster568	DEG20010853	DNA topoisomerase II	C		BW-773U82	Discontinued in Phase 2	Solid tumours	81%	0.0	50%	0,24	-1,75	1BJT	X-ray, 2.50 Å	46,00%	41%	Receptor1	-10.616.997
DNA topoisomerase 2	PAAG_03486	cluster568	DEG20010853	DNA topoisomerase II	C		Cinoxacin	Approved	Urinary tract infections	81%	0.0	50%	0,24	-1,75	1BJT	X-ray, 2.50 Å	46,00%	41%	Receptor1	-10.653.918
DNA topoisomerase 2	PAAG_03486	cluster255	DEG20010853	DNA topoisomerase 2-alpha (Human)	C	C	Ciprofloxacin	approved, investigational	inhibitor	94%	1E-124	40%	-	-	-	-	-	-	-	-
DNA topoisomerase 2	PAAG_03486	cluster255	DEG20010853	DNA topoisomerase 2 (Homo sapiens)		C	Dactinomycin	approved		94%	1E-124	40%	-	-	-	-	-	-	-	-
DNA topoisomerase 2	PAAG_03486	cluster255	DEG20010853	DNA topoisomerase 2-alpha (Human)		C	Daunorubicin	approved	inhibitor	82%	0.0	65%	-	-	-	-	-	-	-	-
DNA topoisomerase 2	PAAG_03486	cluster255	DEG20010853	DNA topoisomerase 2-alpha (Human)	C	C	Dexrazoxane	approved, withdrawn	inhibitor	71%	3E-173	57%	-	-	-	-	-	-	-	-
DNA topoisomerase 2	PAAG_03486	cluster568	DEG20010853	DNA topoisomerase II	C		Dhaq diacetate	Approved	Cancer	71%	3E-173	57%	-	-	-	-	-	-	-	-
DNA topoisomerase 2	PAAG_03486	cluster255	DEG20010853	DNA topoisomerase 2-alpha (Human)		C	Doxorubicin	approved, investigational	inhibitor	81%	0.0	50%	0,24	-1,75	1BJT	X-ray, 2.50 Å	46,00%	41%	Receptor1	-10.669.003
DNA topoisomerase 2	PAAG_03486	cluster568	DEG20010853	DNA topoisomerase II	C		ELINAFIDE MESILATE	Discontinued in Phase 2	Solid tumours	70%	3E-151	49%	-	-	-	-	-	-	-	-
DNA topoisomerase 2	PAAG_03486	cluster255	DEG20010853	DNA topoisomerase 2-alpha (Human)		C	Elsamitrucin	investigational		81%	0.0	50%	0,24	-1,75	1BJT	X-ray, 2.50 Å	46,00%	41%	Receptor1	-10.880.312
DNA topoisomerase 2	PAAG_03486	cluster255	DEG20010853	DNA topoisomerase 2-alpha (Human)	C	C	Enoxacin	approved	inhibitor	81%	0.0	50%	0,24	-1,75	1BJT	X-ray, 2.50 Å	46,00%	41%	Receptor1	-10.799.807
DNA topoisomerase 2	PAAG_03486	cluster568	DEG20010853	DNA topoisomerase II	C	C	Epirubicin	Approved	Cancers	98%	3E-54	30%	-	-	-	-	-	-	-	-
DNA topoisomerase 2	PAAG_03486	cluster255	DEG20010853	DNA topoisomerase 2-alpha	C	C	Etoposide	approved	inhibitor	98%	0.0	47%	-	-	-	-	-	-	-	-
DNA topoisomerase 2	PAAG_03486	cluster568	DEG20010853	DNA topoisomerase II	C		F-14512	Phase 1/2	Cancer	87%	5E-126	42%	-	-	-	-	-	-	-	-
DNA topoisomerase 2	PAAG_03486	cluster568	DEG20010853	DNA topoisomerase II	C		FANDOFLOXACIN HYDROCHLORIDE	Discontinued in Phase 2	Bacterial infection	92%	1E-70	60%	-	-	-	-	-	-	-	-
DNA topoisomerase 2	PAAG_03486	cluster255	DEG20010853	DNA topoisomerase 2-alpha (Human)	C	C	Finafloxacin	approved	inhibitor	81%	0.0	50%	0,24	-1,75	1BJT	X-ray, 2.50 Å	46,00%	41%	Receptor1	-12.460.532
DNA topoisomerase 2	PAAG_03486	cluster255	DEG20010853	DNA topoisomerase 2-alpha (Human)	C	C	Fleroxacin	approved	inhibitor	41%	2E-36	31%	-	-	-	-	-	-	-	-
DNA topoisomerase 2	PAAG_03486	cluster568	DEG20010853	DNA topoisomerase II	C		Gatifloxacin	Approved	Respiratory tract infections	92%	5E-84	30%	-	-	-	-	-	-	-	-
DNA topoisomerase 2	PAAG_03486	cluster568	DEG20010853	DNA topoisomerase II	C		Gemifloxacin	Approved	Bacterial infections	99%	0.0	66%	-	-	-	-	-	-	-	-
DNA topoisomerase 2	PAAG_03486	cluster255	DEG20010853	DNA topoisomerase 2-alpha (Human)		C	Genistein	investigational		81%	0.0	50%	0,24	-1,75	1BJT	X-ray, 2.50 Å	46,00%	41%	Receptor1	-10.099.338

DNA topoisomerase 2	PAAG_03486	cluster568	DEG20010853	DNA topoisomerase II	C		GL-331	Discontinued in Phase 2	Colorectal cancer	67%	2E-52	31%	-	-	-	-	-	-	-	-
DNA topoisomerase 2	PAAG_03486	cluster568	DEG20010853	DNA topoisomerase II	C		GPX-150D	Phase 2	Breast cancer	81%	0.0	50%	0,24	-1,75	1BJT	X-ray, 2.50 Å	46,00%	41%	Receptor1	-10.621.546
DNA topoisomerase 2	PAAG_03486	cluster568	DEG20010853	DNA topoisomerase II	C		Gepotidacin	Phase 2	Bacterial infection	71%	3E-173	57%	-	-	-	-	-	-	-	-
DNA topoisomerase 2	PAAG_03486	cluster255	DEG20010853	DNA topoisomerase 2-alpha (Human)	C	C	Idarubicin	approved	inhibitor	81%	0.0	50%	0,24	-1,75	1BJT	X-ray, 2.50 Å	46,00%	41%	Receptor1	7.441.094
DNA topoisomerase 2	PAAG_03486	cluster568	DEG20010853	DNA topoisomerase II	C		INNO-206	Phase 2	Solid tumours	41%	2E-36	31%	-	-	-	-	-	-	-	-
DNA topoisomerase 2	PAAG_03486	cluster568	DEG20010853	DNA topoisomerase II	C		KW-2170	Discontinued in Phase 2	Breast cancer	81%	0.0	50%	0,24	-1,75	1BJT	X-ray, 2.50 Å	46,00%	41%	Receptor1	-10.653.918
DNA topoisomerase 2	PAAG_03486	cluster568	DEG20010853	DNA topoisomerase II	C	C	Levofloxacin	approved, investigational	inhibitor	89%	3E-59	30%	-	-	-	-	-	-	-	-
DNA topoisomerase 2	PAAG_03486	cluster568	DEG20010853	DNA topoisomerase II	C	C	Lomefloxacin	Approved	Bacterial infections	98%	0.0	47%	-	-	-	-	-	-	-	-
DNA topoisomerase 2	PAAG_03486	cluster568	DEG20010853	DNA topoisomerase II	C		LOSOXANTRONE	Discontinued in Phase 2	Breast cancer	81%	0.0	50%	0,24	-1,75	1BJT	X-ray, 2.50 Å	46,00%	41%	Receptor1	-8.910.618
DNA topoisomerase 2	PAAG_03486	cluster255	DEG20010853	DNA topoisomerase 2-alpha (Human)	C	C	Lucanthone	approved, investigational	inhibitor	89%	3E-59	30%	-	-	-	-	-	-	-	-
DNA topoisomerase 2	PAAG_03486	cluster568	DEG20010853	DNA topoisomerase II	C		Merbarone	Discontinued in Phase 2	Pancreatic cancer	92%	5E-121	35%	-	-	-	-	-	-	-	-
DNA topoisomerase 2	PAAG_03486	cluster568	DEG20010853	DNA topoisomerase II	C		Mitonafide	Discontinued in Phase 2	Solid tumours	41%	2E-36	31%	-	-	-	-	-	-	-	-
DNA topoisomerase 2	PAAG_03486	cluster255	DEG20010853	DNA topoisomerase 2-alpha (Human)	C	C	Mitoxantrone	approved, investigational	inhibitor	81%	0.0	50%	0,24	-1,75	1BJT	X-ray, 2.50 Å	46,00%	41%	Receptor1	-12.133.675
DNA topoisomerase 2	PAAG_03486	cluster568	DEG20010853	DNA topoisomerase II	C	C	Moxifloxacin	Approved	Bacterial infections	81%	0.0	50%	0,24	-1,75	1BJT	X-ray, 2.50 Å	46,00%	41%	Receptor1	-8.868.177
DNA topoisomerase 2	PAAG_03486	cluster568	DEG20010853	DNA topoisomerase II	C		Nalidixic Acid	Approved	Fungal urinary tract infection	81%	0.0	50%	0,24	-1,75	1BJT	X-ray, 2.50 Å	46,00%	41%	Receptor1	-12.327.397
DNA topoisomerase 2	PAAG_03486	cluster255	DEG20010853	DNA topoisomerase 2-alpha (Human)	C	C	Norfloxacin	approved	inhibitor	81%	0.0	50%	0,24	-1,75	1BJT	X-ray, 2.50 Å	46,00%	41%	Receptor1	-9.614.682
DNA topoisomerase 2	PAAG_03486	cluster568	DEG20010853	DNA topoisomerase II	C	C	Novobiocin	Approved	Bacterial infections	81%	0.0	50%	0,24	-1,75	1BJT	X-ray, 2.50 Å	46,00%	41%	Receptor1	-9.621.758
DNA topoisomerase 2	PAAG_03486	cluster255	DEG20010853	DNA topoisomerase 2-alpha (Human)	C	C	Ofloxacin	approved	inhibitor	81%	0.0	50%	0,24	-1,75	1BJT	X-ray, 2.50 Å	46,00%	41%	Receptor1	-10.008.938
DNA topoisomerase 2	PAAG_03486	cluster568	DEG20010853	DNA topoisomerase II	C		OLAMUFLOXACIN MESILATE	Discontinued in Phase 3	Bacterial infection	81%	0.0	50%	0,24	-1,75	1BJT	X-ray, 2.50 Å	46,00%	41%	Receptor1	-8.548.300
DNA topoisomerase 2	PAAG_03486	cluster568	DEG20010853	DNA topoisomerase II	C		Pafuramidine	Phase 3	Malaria	81%	0.0	50%	0,24	-1,75	1BJT	X-ray, 2.50 Å	46,00%	41%	Receptor1	-11.587.096
DNA topoisomerase 2	PAAG_03486	cluster568	DEG20010853	DNA topoisomerase II	C	C	Pefloxacin	Approved	Gonococcal urethritis	81%	0.0	50%	0,24	-1,75	1BJT	X-ray, 2.50 Å	46,00%	41%	Receptor1	-9.911.546
DNA topoisomerase 2	PAAG_03486	cluster568	DEG20010853	DNA topoisomerase II	C		Pixantrone	Phase 3	Multiple sclerosis	81%	0.0	50%	0,24	-1,75	1BJT	X-ray, 2.50 Å	46,00%	41%	Receptor1	-10.934.879
DNA topoisomerase 2	PAAG_03486	cluster568	DEG20010853	DNA topoisomerase II	C		Podophyllotoxin	Approved	Condyloma	97%	3E-160	40%	-	-	-	-	-	-	-	-
DNA topoisomerase 2	PAAG_03486	cluster568	DEG20010853	DNA topoisomerase II	C		Quinolones	Approved	Tuberculosis	81%	0.0	50%	0,24	-1,75	1BJT	X-ray, 2.50 Å	46,00%	41%	Receptor1	-10.968.245
DNA topoisomerase 2	PAAG_03486	cluster568	DEG20010853	DNA topoisomerase II	C		Ro-23-9424	Discontinued in Phase 2	Bacterial infection	81%	0.0	50%	0,24	-1,75	1BJT	X-ray, 2.50 Å	46,00%	41%	Receptor1	-10.074.821
DNA topoisomerase 2	PAAG_03486	cluster568	DEG20010853	DNA topoisomerase II	C		Rosoxacin	Approved	Bacterial infections	99%	5E-46	33%	-	-	-	-	-	-	-	-
DNA topoisomerase 2	PAAG_03486	cluster568	DEG20010853	DNA topoisomerase II	C		Sabarubicin	Phase 2	Solid tumours	89%	2E-100	50%	-	-	-	-	-	-	-	-
DNA topoisomerase 2	PAAG_03486	cluster568	DEG20010853	DNA topoisomerase II	C		Salvicine	Phase 2	Cancer	56%	5E-84	31%	-	-	-	-	-	-	-	-
DNA topoisomerase 2	PAAG_03486	cluster568	DEG20010853	DNA topoisomerase II	C		SNS-595	Phase 2	Ovarian cancer	82%	7E-58	31%	-	-	-	-	-	-	-	-
DNA topoisomerase 2	PAAG_03486	cluster255	DEG20010853	DNA topoisomerase 2-alpha (Human)	C	C	Sparfloxacin	approved	inhibitor	92%	5E-84	30%	-	-	-	-	-	-	-	-
DNA topoisomerase 2	PAAG_03486	cluster568	DEG20010853	DNA topoisomerase II	C	C	Teniposide	Approved	Acute lymphocytic leukemia	81%	0.0	50%	0,24	-1,75	1BJT	X-ray, 2.50 Å	46,00%	41%	Receptor1	-10.715.301
DNA topoisomerase 2	PAAG_03486	cluster568	DEG20010853	DNA topoisomerase II	C		TH-302	Phase 2	Solid tumours	81%	0.0	50%	0,24	-1,75	1BJT	X-ray, 2.50 Å	46,00%	41%	Receptor1	-11.062.142
DNA topoisomerase 2	PAAG_03486	cluster568	DEG20010853	DNA topoisomerase II	C		Tirapazamine	Phase 3	Mild alzheimer's disease	81%	0.0	50%	0,24	-1,75	1BJT	X-ray, 2.50 Å	46,00%	41%	Receptor1	-9.206.473
DNA topoisomerase 2	PAAG_03486	cluster255	DEG20010853	DNA topoisomerase 2-alpha (Human)	C	C	Trovafloxacin	approved, withdrawn	inhibitor	81%	0.0	50%	0,24	-1,75	1BJT	X-ray, 2.50 Å	46,00%	41%	Receptor1	-10.219.459
DNA topoisomerase 2	PAAG_03486	cluster255	DEG20010853	DNA topoisomerase 2-alpha (Human)	C	C	Valrubicin	approved	inhibitor	94%	3E-137	51%	-	-	-	-	-	-	-	-
DNA topoisomerase 2	PAAG_03486	cluster568	DEG20010853	DNA topoisomerase II	C		XR-5000	Phase 2	Colorectal cancer	89%	3E-59	30%	-	-	-	-	-	-	-	-

Dual specificity protein kinase FUZ7	PAAG_06020	cluster144	Without similarity	MEK2	C		RDEA-436	Discontinued in Phase 1	Cancer	89%	3E-59	30%	-	-	-	-	-	-	-	-
D-xylulose reductase	PAAG_03774	cluster163	Without similarity	Alcohol dehydrogenase 1C (Human)		C	Ethanol	approved		81%	0.0	50%	0,24	-1,75	1BJT	X-ray, 2.50 Å	46,00%	41%	Receptor1	-11.834.139
Elongation factor 2	PAAG_02582	cluster832	DEG20010872	Elongation factor Tu GTP-binding domain-containing protein 1 (Human)		C	Deoxycholic Acid	approved		96%	0.0	58%	-	-	-	-	-	-	-	-
Elongation factor G, mitochondrial	PAAG_03167	cluster930	Without similarity	Elongation factor G (Thermus thermophilus)	C	C	Fusidic Acid	approved	inhibitor	94%	1E-124	40%	-	-	-	-	-	-	-	-
Endosomal/prevacuolar sodium/hydrogen exchanger	PAAG_00404	cluster908	Without similarity	Sodium/hydrogen exchanger 1 (Human)		C	Amiloride	approved	inhibitor	78%	5E-177	62%	-	-	-	-	-	-	-	-
Farnesyl pyrophosphate synthetase	PAAG_07279	cluster584	DEG20010568	Farnesyl pyrophosphate synthetase	C		Alendronate	Approved	Osteoporosis and Paget's disease	87%	2E-40	53%	-	-	-	-	-	-	-	-
Farnesyl pyrophosphate synthetase	PAAG_07279	cluster861	DEG20010568	Farnesyl pyrophosphate synthase (Human)	C	C	Ibandronate	approved, investigational	inhibitor	81%	0.0	50%	0,24	-1,75	1BJT	X-ray, 2.50 Å	46,00%	41%	Receptor1	-10.513.047
Farnesyl pyrophosphate synthetase	PAAG_07279	cluster584	DEG20010568	Farnesyl pyrophosphate synthetase	C		Incadronate	Approved	Hypercalcemia	81%	0.0	50%	0,24	-1,75	1BJT	X-ray, 2.50 Å	46,00%	41%	Receptor1	-10.460.375
Farnesyl pyrophosphate synthetase	PAAG_07279	cluster584	DEG20010568	Farnesyl pyrophosphate synthetase	C		Minodronate	Approved	Osteoporosis	89%	3E-59	30%	-	-	-	-	-	-	-	-
Farnesyl pyrophosphate synthetase	PAAG_07279	cluster584	DEG20010568	Farnesyl pyrophosphate synthetase	C		NERIDRONIC ACID	Approved	Bone disease	81%	0.0	50%	0,24	-1,75	1BJT	X-ray, 2.50 Å	46,00%	41%	Receptor1	-11.958.847
Farnesyl pyrophosphate synthetase	PAAG_07279	cluster861	DEG20010568	Farnesyl pyrophosphate synthase		C	Pamidronate	approved	inhibitor	81%	0.0	50%	0,24	-1,75	1BJT	X-ray, 2.50 Å	46,00%	41%	Receptor1	-10.815.450
Farnesyl pyrophosphate synthetase	PAAG_07279	cluster861	DEG20010568	Farnesyl pyrophosphate synthase (Human)	C	C	Risedronate	approved, investigational	inhibitor	81%	0.0	50%	0,24	-1,75	1BJT	X-ray, 2.50 Å	46,00%	41%	Receptor1	-10.694.554
Farnesyl pyrophosphate synthetase	PAAG_07279	cluster584	DEG20010568	Farnesyl pyrophosphate synthetase	C		YM-175	Approved	Malignant hypercalcaemia	30%	8E-35	31%	-	-	-	-	-	-	-	-
Farnesyl pyrophosphate synthetase	PAAG_07279	cluster584	DEG20010568	Farnesyl pyrophosphate synthetase	C		Zoledronate	Approved	Hypercalcemia	93%	3E-65	32%	-	-	-	-	-	-	-	-
Fatty aldehyde dehydrogenase HFD1	PAAG_08718	cluster840	Without similarity	Succinate-semialdehyde dehydrogenase, mitochondrial (Human)	C	C	Chlormerodrin	approved, withdrawn	inhibitor	88%	2E-25	35%	-	-	-	-	-	-	-	-
Ferric/cupric reductase transmembrane component 2	PAAG_05966	cluster257	Without similarity	NADH oxidase	C		GKT-137831	Phase 2	Fibrosis	88%	2E-100	30%	-	-	-	-	-	-	-	-
Ferrochelatase	PAAG_08770	cluster616	DEG20010971	Ferrochelatase	C		Methyl aminolevulinate	Approved	Acne vulgaris	41%	2E-36	31%	-	-	-	-	-	-	-	-
Fructose-1,6-bisphosphatase	PAAG_02682	cluster625	Without similarity	Fructose-1,6-bisphosphatase	C		Managlinat dialanetil	Phase 2	Diabetes Mellitus Type 2	81%	0.0	50%	0,24	-1,75	1BJT	X-ray, 2.50 Å	46,00%	41%	Receptor1	-11.073.790
Fructose-1,6-bisphosphatase	PAAG_02682	cluster923	Without similarity	Fructose-1,6-bisphosphatase 1 (Human)	C	C	MB07803	investigational		41%	2E-36	31%	-	-	-	-	-	-	-	-
Geranylgeranyl transferase type-1 subunit beta	PAAG_07086	cluster842	Without similarity	Protein farnesyltransferase subunit beta (Human)		C	AZD3409	investigational		81%	0.0	50%	0,24	-1,75	1BJT	X-ray, 2.50 Å	46,00%	41%	Receptor1	-11.081.927
Geranylgeranyl transferase type-1 subunit beta	PAAG_07086	cluster842	Without similarity	Protein farnesyltransferase subunit beta (Human)		C	Tipifarnib	investigational		46%	3E-84	36%	-	-	-	-	-	-	-	-
Glucan synthesis regulatory protein	PAAG_07373	cluster591	Without similarity	1,3-Beta-Glucan synthase	C		Eraxis/Vfend	Phase 3	Fungal infections	97%	0.0	60%	-	-	-	-	-	-	-	-
Glucoamylase 1	PAAG_04290	cluster281	Without similarity	Neutral alpha-glucosidase AB (Human)		C	Miglitol	approved	antagonist	82%	7E-58	31%	-	-	-	-	-	-	-	-
Glutamate carboxypeptidase	PAAG_05758	cluster96	DEG20010988	Glutamate carboxypeptidase II	C		G-202	Phase 2	Solid tumours	82%	7E-58	31%	-	-	-	-	-	-	-	-

Glutamine synthetase	PAAG_07003	cluster836	DEG20011069	Glutamine synthetase (Human)		C	Capsaicin	approved	inducer	81%	0.0	50%	0,24	-1,75	1BJT	X-ray, 2.50 Å	46,00%	41%	Receptor1	-8.760.773
Glutamine synthetase	PAAG_07003	cluster836	DEG20011069	Glutamine synthetase (Human)		C	Ceftriaxone	approved	inducer	81%	0.0	50%	0,24	-1,75	1BJT	X-ray, 2.50 Å	46,00%	41%	Receptor1	-10.142.296
Glutamine synthetase	PAAG_07003	cluster836	DEG20011069	Glutamine synthetase (Human)		C	Diazoxide	approved	inhibitor	70%	3E-151	49%	-	-	-	-	-	-	-	-
Glutamine synthetase	PAAG_07003	cluster836	DEG20011069	Glutamine synthetase (Human)		C	Ethyl biscoumacetate	withdrawn	inhibitor	89%	3E-59	30%	-	-	-	-	-	-	-	-
Glycogen phosphorylase	PAAG_00545	cluster293	Without similarity	Glycogen phosphorylase, liver form (Human)		C	PSN357	investigational		67%	2E-52	31%	-	-	-	-	-	-	-	-
Heat shock 70 kDa protein 2	PAAG_08003	cluster578	DEG20010542	73-kDa molecular chaperone HSP73	C		Gentamicin	Approved	Bacterial Infection	81%	0.0	50%	0,24	-1,75	1BJT	X-ray, 2.50 Å	46,00%	41%	Receptor1	-11.565.552
Heat shock protein 90	PAAG_05679	cluster147	Without similarity	Heat shock protein HSP 90	C		IPI-504	Discontinued in Phase 2	Prostate cancer	86%	3E-135	51%	-	-	-	-	-	-	-	-
Heat shock protein 90	PAAG_05679	cluster147	Without similarity	Heat shock protein HSP 90	C		STA-9090	Phase 3	Leukemia	92%	5E-84	30%	-	-	-	-	-	-	-	-
Heat shock protein 90	PAAG_05679	cluster147	Without similarity	Heat shock protein HSP 90	C		Tanespimycin	Phase 2	Breast Cancer, Melanoma	81%	0.0	50%	0,24	-1,75	1BJT	X-ray, 2.50 Å	46,00%	41%	Receptor1	-11.072.549
Hexokinase	PAAG_06172	cluster197	Without similarity	Hexokinase D	C		AMG 151	Phase 2	Type 2 diabetes	81%	0.0	50%	0,24	-1,75	1BJT	X-ray, 2.50 Å	46,00%	41%	Receptor1	-9.579.049
Hexokinase	PAAG_06172	cluster197	Without similarity	Hexokinase D	C		AZD1656	Phase 2	Diabetes Mellitus	81%	0.0	50%	0,24	-1,75	1BJT	X-ray, 2.50 Å	46,00%	41%	Receptor1	-11.034.164
Hexokinase	PAAG_06172	cluster197	Without similarity	Hexokinase D	C		AZD6370	Discontinued in Phase 2	Diabetes mellitus type 2	98%	0.0	47%	-	-	-	-	-	-	-	-
Hexokinase	PAAG_06172	cluster197	Without similarity	Hexokinase D	C		AZD-6714	Discontinued in Phase 1	Diabetes mellitus type 2	81%	0.0	50%	0,24	-1,75	1BJT	X-ray, 2.50 Å	46,00%	41%	Receptor1	-11.111.344
Hexokinase	PAAG_06172	cluster197	Without similarity	Hexokinase D	C		GK1-399	Phase 2	Diabetes Mellitus	41%	2E-36	31%	-	-	-	-	-	-	-	-
Hexokinase	PAAG_06172	cluster197	Without similarity	Hexokinase D	C		LY-2599506	Phase 2	Diabetes Mellitus	81%	0.0	50%	0,24	-1,75	1BJT	X-ray, 2.50 Å	46,00%	41%	Receptor1	-11.063.239
Hexokinase	PAAG_06172	cluster197	Without similarity	Hexokinase D	C		LY-2608204	Phase 2	Diabetes mellitus type 2	86%	3E-180	65%	-	-	-	-	-	-	-	-
Hexokinase	PAAG_06172	cluster197	Without similarity	Hexokinase D	C		PF-04937319	Phase 2	Diabetes mellitus type 2	89%	3E-59	30%	-	-	-	-	-	-	-	-
Hexokinase	PAAG_06172	cluster197	Without similarity	Hexokinase D	C		PF-04991532	Phase 2	Diabetes Mellitus	81%	0.0	50%	0,24	-1,75	1BJT	X-ray, 2.50 Å	46,00%	41%	Receptor1	-11.646.488
Hexokinase	PAAG_06172	cluster197	Without similarity	Hexokinase D	C		TTP355	Discontinued in Phase 2	Diabetes mellitus	81%	0.0	50%	0,24	-1,75	1BJT	X-ray, 2.50 Å	46,00%	41%	Receptor1	-11.470.780
Histone deacetylase HDA1	PAAG_08467	cluster634	Without similarity	HDAC6	C		ACY-1215	Phase 1/2	Autoimmune diseases	86%	4E-165	54%	-	-	-	-	-	-	-	-
Histone deacetylase RPD3	PAAG_06742	cluster607	Without similarity	Histone deacetylase 1	C		AN-9	Discontinued in Phase 2	Melanoma	81%	0.0	50%	0,24	-1,75	1BJT	X-ray, 2.50 Å	46,00%	41%	Receptor1	-11.397.192
Histone deacetylase RPD3	PAAG_06742	cluster607	Without similarity	Histone deacetylase 1	C		CI-994	Phase 3	Cancer	81%	0.0	50%	0,24	-1,75	1BJT	X-ray, 2.50 Å	46,00%	41%	Receptor1	-10.524.154
Histone deacetylase RPD3	PAAG_06742	cluster607	Without similarity	Histone deacetylase 1	C		HDAC-42	Phase 1/2	Cancers	92%	5E-84	30%	-	-	-	-	-	-	-	-
Histone deacetylase RPD3	PAAG_06742	cluster607	Without similarity	Histone deacetylase 1	C		ITF2357	Phase 2	Myelofibrosis; Essential thrombocythemia; Polycythemia vera	81%	0.0	50%	0,24	-1,75	1BJT	X-ray, 2.50 Å	46,00%	41%	Receptor1	-8.064.808
Histone deacetylase RPD3	PAAG_06742	cluster607	Without similarity	Histone deacetylase 1	C		MS-275	Phase 3	Breast cancer	81%	0.0	50%	0,24	-1,75	1BJT	X-ray, 2.50 Å	46,00%	41%	Receptor1	-10.726.885
Histone deacetylase RPD3	PAAG_06742	cluster607	Without similarity	Histone deacetylase 1	C		NVP-LAQ824	Phase 3	Severe Mood Disorders	81%	0.0	50%	0,24	-1,75	1BJT	X-ray, 2.50 Å	46,00%	41%	Receptor1	-11.431.017
Histone deacetylase RPD3	PAAG_06742	cluster607	Without similarity	Histone deacetylase 1	C		PDX-101	Approved	Non-small cell lung cancer	92%	5E-84	30%	-	-	-	-	-	-	-	-
Histone deacetylase RPD3	PAAG_06742	cluster607	Without similarity	Histone deacetylase 1	C		Phenylbutyrate	Phase 2	Urea cycle disorders	81%	0.0	50%	0,24	-1,75	1BJT	X-ray, 2.50 Å	46,00%	41%	Receptor1	-11.970.498
Histone deacetylase RPD3	PAAG_06742	cluster607	Without similarity	Histone deacetylase 1	C		PXD101	Phase 1/2	Myeloid leukemia; Liver cancer; Sarcoma	92%	5E-84	30%	-	-	-	-	-	-	-	-
Histone deacetylase RPD3	PAAG_06742	cluster607	Without similarity	Histone deacetylase 1	C		Pyroxamide	Discontinued in Phase 1	Cancers	67%	2E-52	31%	-	-	-	-	-	-	-	-
Histone deacetylase RPD3	PAAG_06742	cluster607	Without similarity	Histone deacetylase 1	C		Resminostat	Phase 2	Hepatocellular carcinoma	62%	2E-81	30%	-	-	-	-	-	-	-	-
Histone deacetylase RPD3	PAAG_06742	cluster607	Without similarity	Histone deacetylase 1	C		SB-623	Phase 2	Cerebrovascular ischaemia	97%	1E-126	48%	-	-	-	-	-	-	-	-
Histone deacetylase RPD3	PAAG_06742	cluster607	Without similarity	Histone deacetylase 1	C		SNDX-275	Phase 2	Hodgkin's Lymphoma, Multiple myeloma	81%	0.0	50%	0,24	-1,75	1BJT	X-ray, 2.50 Å	46,00%	41%	Receptor1	-10.992.228
Histone deacetylase RPD3	PAAG_06742	cluster607	Without similarity	Histone deacetylase 1	C		Sodium butyrate	Phase 2	Refractory sickle cell ulcers	82%	7E-58	31%	-	-	-	-	-	-	-	-
Histone deacetylase RPD3	PAAG_06742	cluster607	Without similarity	Histone deacetylase 1	C		Tacedinaline	Discontinued in Phase 2	Cancers	81%	0.0	50%	0,24	-1,75	1BJT	X-ray, 2.50 Å	46,00%	41%	Receptor1	-10.169.464

Histone deacetylase RPD3	PAAG_06742	cluster607	Without similarity	Histone deacetylase 1	C	C	Vorinostat	Approved	Cutaneous T-cell lymphoma	29%	3E-32	33%	-	-	-	-	-	-	-	-
Inosine-5'-monophosphate dehydrogenase 4	PAAG_05803	cluster148	Without similarity	Inosine-5'-monophosphate dehydrogenase 1	C		Azathioprine	Approved	Organ Transplant rejection	70%	3E-151	49%	-	-	-	-	-	-	-	-
Iron-sulfur clusters transporter ATM1, mitochondrial	PAAG_07938	cluster878	Without similarity	ATP-binding cassette sub-family G member 2 (Human)		C	Dabrafenib	approved	substrate, inhibitor	81%	0.0	50%	0,24	-1,75	1BJT	X-ray, 2.50 Å	46,00%	41%	Receptor1	-9.721.782
Iron-sulfur clusters transporter ATM1, mitochondrial	PAAG_07938	cluster878	Without similarity	ATP-binding cassette sub-family G member 2 (Human)		C	Diethylstilbestrol	approved	inhibitor	94%	0.0	31%	-	-	-	-	-	-	-	-
Iron-sulfur clusters transporter ATM1, mitochondrial	PAAG_07938	cluster878	Without similarity	ATP-binding cassette sub-family G member 2 (Human)		C	Elacridar	investigational	inhibitor	81%	0.0	50%	0,24	-1,75	1BJT	X-ray, 2.50 Å	46,00%	41%	Receptor1	-10.673.590
Iron-sulfur clusters transporter ATM1, mitochondrial	PAAG_07938	cluster878	Without similarity	ATP-binding cassette sub-family G member 2 (Human)		C	Erlotinib	approved, investigational	inhibitor	81%	0.0	50%	0,24	-1,75	1BJT	X-ray, 2.50 Å	46,00%	41%	Receptor1	-10.783.855
Iron-sulfur clusters transporter ATM1, mitochondrial	PAAG_07938	cluster878	Without similarity	ATP-binding cassette sub-family G member 2		C	Estradiol	approved, investigational, vet_approved	inhibitor	98%	0.0	47%	-	-	-	-	-	-	-	-
Iron-sulfur clusters transporter ATM1, mitochondrial	PAAG_07938	cluster878	Without similarity	ATP-binding cassette sub-family G member 2		C	Estrone	approved	inhibitor	81%	0.0	50%	0,24	-1,75	1BJT	X-ray, 2.50 Å	46,00%	41%	Receptor1	-8.731.954
Iron-sulfur clusters transporter ATM1, mitochondrial	PAAG_07938	cluster878	Without similarity	ATP-binding cassette sub-family G member 2 (Human)		C	Vismodegib	approved	inhibitor	81%	0.0	50%	0,24	-1,75	1BJT	X-ray, 2.50 Å	46,00%	41%	Receptor1	-9.192.296
Iron-sulfur clusters transporter ATM1, mitochondrial	PAAG_07938	cluster878	Without similarity	ATP-binding cassette sub-family G member 2 (Human)		C	Zafirlukast	approved, investigational	Antagonist	81%	0.0	50%	0,24	-1,75	1BJT	X-ray, 2.50 Å	46,00%	41%	Receptor1	-10.130.178
Isoleucine-tRNA ligase	PAAG_12584	cluster601	DEG20010027	Isoleucyl-tRNA synthetase (bacterial)	C		Icofungipen	Phase 2	Fungal infections	81%	0.0	50%	0,24	-1,75	1BJT	X-ray, 2.50 Å	46,00%	41%	Receptor1	-9.644.725
Isoleucine-tRNA ligase	PAAG_12584	cluster601	DEG20010027	Isoleucyl-tRNA synthetase (bacterial)	C		Mupirocin	Approved	Bacterial infections	93%	2E-65	35%	-	-	-	-	-	-	-	-
Kinesin-like protein bimC	PAAG_09051	cluster86	Without similarity	Kinesin-like protein KIF11	C		ARRY-520	Phase 2	Cancer	81%	0.0	50%	0,24	-1,75	1BJT	X-ray, 2.50 Å	46,00%	41%	Receptor1	-10.756.557
Kinesin-like protein bimC	PAAG_09051	cluster86	Without similarity	Kinesin-like protein KIF11	C		AZD-4877	Phase 2	Acute myeloid leukemia	56%	1E-57	30%	0.49	-0.54	3LS8	X-ray, 2.25 Å	51.44%	61%	Receptor2	-8.420.500
Kinesin-like protein bimC	PAAG_09051	cluster86	Without similarity	Kinesin-like protein KIF11	C		Ispinesib	Phase 2	Solid Tumors	56%	1E-57	30%	0.49	-0.54	3LS8	X-ray, 2.25 Å	51.44%	61%	Receptor2	-9.534.708
Kinesin-like protein bimC	PAAG_09051	cluster86	Without similarity	Kinesin-like protein KIF11	C		LY2523355	Phase 2	Cancers	56%	1E-57	30%	0.49	-0.54	3LS8	X-ray, 2.25 Å	51.44%	61%	Receptor3	-8.876.210
Kinesin-like protein bimC	PAAG_09051	cluster86	Without similarity	Kinesin-like protein KIF11	C		SB-743921	Phase 2	Cancers	56%	1E-57	30%	0.49	-0.54	3LS8	X-ray, 2.25 Å	51.44%	61%	Receptor3	-8.847.961
Kinesin-like protein CIN8	PAAG_05191	cluster889	Without similarity	Centromere-associated protein E (Human)		C	GSK-923295	investigational		99%	0.0	73%	-	-	-	-	-	-	-	-
Lanosterol 14-α desmetilase	PAAG_00827	cluster637	DEG20010452	Cytochrome P450 51	C			Discontinued in Phase 3	Fungal infection	56%	1E-57	30%	0.49	-0.54	3LS8	X-ray, 2.25 Å	51.44%	61%	Receptor2	-9.866.395
Lanosterol 14-α desmetilase	PAAG_00827	cluster637	DEG20010452	Cytochrome P450 51	C	C	Bifonazole	Approved	Fungal infections	56%	1E-57	30%	0.49	-0.54	3LS8	X-ray, 2.25 Å	51.44%	61%	Receptor3	-9.698.295
Lanosterol 14-α desmetilase	PAAG_00827	cluster637	DEG20010452	Cytochrome P450 51	C		Butoconazole	Approved	Candida infection	56%	1E-57	30%	0.49	-0.54	3LS8	X-ray, 2.25 Å	51.44%	61%	Receptor2	-10.206.883
Lanosterol 14-α desmetilase	PAAG_00827	cluster239	DEG20010452	Lanosterol 14-alpha demethylase (Human)		C	Clotrimazole	approved, vet_approved	antagonist, inhibitor	56%	1E-57	30%	0.49	-0.54	3LS8	X-ray, 2.25 Å	51.44%	61%	Receptor2	-7.719.545
Lanosterol 14-α desmetilase	PAAG_00827	cluster637	DEG20010452	Cytochrome P450 51	C		E-1224	Phase 2	Fungal infection	71%	3E-173	57%	-	-	-	-	-	-	-	-
Lanosterol 14-α desmetilase	PAAG_00827	cluster637	DEG20010452	Cytochrome P450 51	C	C	Econazole	Approved	Fungal infections	56%	1E-57	30%	0.49	-0.54	3LS8	X-ray, 2.25 Å	51.44%	61%	Receptor2	-11.685.825
Lanosterol 14-α desmetilase	PAAG_00827	cluster637	DEG20010452	Cytochrome P450 51	C	C	Efinaconazole	Approved	Fungal infection	56%	1E-57	30%	0.49	-0.54	3LS8	X-ray, 2.25 Å	51.44%	61%	Receptor1	-9.759.847
Lanosterol 14-α desmetilase	PAAG_00827	cluster637	DEG20010452	Cytochrome P450 51	C	C	Fluconazole	Approved	Fungal infections	91%	1E-168	50%	-	-	-	-	-	-	-	-
Lanosterol 14-α desmetilase	PAAG_00827	cluster637	DEG20010452	Cytochrome P450 51	C	C	Itraconazole	Approved	Fungal infections	96%	6E-172	35%	0.65	-3.53	3A3Y	X-ray, 2.80 Å	33.99%	90%	Receptor1	2.696.817
Lanosterol 14-α desmetilase	PAAG_00827	cluster637	DEG20010452	Cytochrome P450 51	C	C	Ketoconazole	Approved	Fungal infections	95%	1E-162	35%	0.65	-3.53	3A3Y	X-ray, 2.80 Å	33.99%	90%	Receptor1	-8.015.848
Lanosterol 14-α desmetilase	PAAG_00827	cluster637	DEG20010452	Cytochrome P450 51	C	C	Luliconazole	Approved	Tinea pedis	95%	1E-162	35%	0.65	-3.53	3A3Y	X-ray, 2.80 Å	33.99%	90%	Receptor1	-6.637.439
Lanosterol 14-α desmetilase	PAAG_00827	cluster637	DEG20010452	Cytochrome P450 51	C	C	Miconazole	Approved	Fungal infections	99%	5E-49	60%	-	-	-	-	-	-	-	-

Lanosterol 14-α desmetilase	PAAG_00827	cluster637	DEG20010452	Cytochrome P450 51	C	C	Oxiconazole	Approved	Fungal infections	99%	0.0	66%	-	-	-	-	-	-	-	-
Lanosterol 14-α desmetilase	PAAG_00827	cluster637	DEG20010452	Cytochrome P450 51	C	C	Posaconazole	Approved	Aspergillosis	98%	0.0	46%	-	-	-	-	-	-	-	-
Lanosterol 14-α desmetilase	PAAG_00827	cluster637	DEG20010452	Cytochrome P450 51	C		Pramiconazole	Phase 2	Dermatological disease	96%	6E-172	35%	0.65	-3.53	3A3Y	X-ray, 2.80 Å	33.99%	90%	Receptor1	-6.072.025
Lanosterol 14-α desmetilase	PAAG_00827	cluster637	DEG20010452	Cytochrome P450 51	C	C	Sertaconazole	Approved	Fungal infections	56%	5E-84	31%	-	-	-	-	-	-	-	-
Lanosterol 14-α desmetilase	PAAG_00827	cluster637	DEG20010452	Cytochrome P450 51	C	C	Terconazole	Approved	Fungal infections	84%	3E-101	47%	-	-	-	-	-	-	-	-
Lanosterol 14-α desmetilase	PAAG_00827	cluster637	DEG20010452	Cytochrome P450 51	C	C	Tioconazole	Approved	Fungal infections	99%	0.0	66%	-	-	-	-	-	-	-	-
Lanosterol 14-α desmetilase	PAAG_00827	cluster637	DEG20010452	Cytochrome P450 51	C	C	Voriconazole	Approved	Invasive aspergillosis	89%	3E-59	30%	-	-	-	-	-	-	-	-
Leukotriene A-4 hydrolase homolog	PAAG_08994	cluster586	Without similarity	Leukotriene A-4 hydrolase	C		DG051	Discontinued in Phase 2	Myocardial infarction	89%	3E-59	30%	-	-	-	-	-	-	-	-
Leukotriene A-4 hydrolase homolog	PAAG_08994	cluster586	Without similarity	Leukotriene A-4 hydrolase	C		Bestatin	Approved	Acute myeloid leukemia	99%	0.0	73%	-	-	-	-	-	-	-	-
Leukotriene A-4 hydrolase homolog	PAAG_09004	cluster339	Without similarity	Puromycin-sensitive aminopeptidase (Human)	C	C	CHR-2797	investigational		91%	0.0	79%	-	-	-	-	-	-	-	-
Leukotriene A-4 hydrolase homolog	PAAG_08994	cluster790	Without similarity	Leukotriene A-4 hydrolase (Human)		C	DG051	investigational		96%	6E-172	35%	0.65	-3.53	3A3Y	X-ray, 2.80 Å	33.99%	90%	No docking	No docking
Lipase 1	PAAG_00885	cluster157	Without similarity	Acetylcholinesterase (Human)		C	Acetylcholine	approved		96%	6E-172	35%	0.65	-3.53	3A3Y	X-ray, 2.80 Å	33.99%	90%	Receptor1	-5.901.298
Lipase 1	PAAG_00885	cluster157	Without similarity	Acetylcholinesterase (Human)		C	Ambenonium	approved	inhibitor	95%	1E-162	35%	0.65	-3.53	3A3Y	X-ray, 2.80 Å	33.99%	90%	Receptor1	-9.682.371
Lipase 1	PAAG_00885	cluster157	Without similarity	Cholinesterase (Human)		C	Bambuterol	approved	substrate / inhibitor	96%	6E-172	35%	0.65	-3.53	3A3Y	X-ray, 2.80 Å	33.99%	90%	Receptor1	-6.792.297
Lipase 1	PAAG_00885	cluster157	Without similarity	Cholinesterase (Human)		C	Cisplatin	approved	inhibitor	96%	6E-172	35%	0.65	-3.53	3A3Y	X-ray, 2.80 Å	33.99%	90%	Receptor1	-7.932.648
Lipase 1	PAAG_00885	cluster157	Without similarity	Liver carboxylesterase 1		C	Cyclandelate	approved		78%	3E-74	42%	-	-	-	-	-	-	-	-
Lipase 1	PAAG_00885	cluster157	Without similarity	Acetylcholinesterase (Human)		C	Decamethonium	approved	inhibitor	99%	0.0	73%	-	-	-	-	-	-	-	-
Lipase 1	PAAG_00885	cluster157	Without similarity	Acetylcholinesterase (Human)		C	Demecarium	approved	inhibitor	96%	6E-172	35%	0.65	-3.53	3A3Y	X-ray, 2.80 Å	33.99%	90%	Receptor1	-6.183.628
Lipase 1	PAAG_00885	cluster157	Without similarity	Cholinesterase (Human)		C	Diethylcarbamazine	approved, vet_approved	inhibitor	88%	2E-100	30%	-	-	-	-	-	-	-	-
Lipase 1	PAAG_00885	cluster157	Without similarity	Acetylcholinesterase (Human)		C	Dimetacrine	approved, withdrawn	antagonist	67%	2E-52	31%	-	-	-	-	-	-	-	-
Lipase 1	PAAG_00885	cluster157	Without similarity	Acetylcholinesterase (Human)		C	Dipivefrin	approved		99%	5E-49	60%	-	-	-	-	-	-	-	-
Lipase 1	PAAG_00885	cluster157	Without similarity	Acetylcholinesterase (Human)		C	Donepezil	approved	inhibitor	95%	6E-69	32%	-	-	-	-	-	-	-	-
Lipase 1	PAAG_00885	cluster157	Without similarity	Cholinesterase (Human)		C	Echothiophate	approved	inhibitor	99%	1E-115	36%	-	-	-	-	-	-	-	-
Lipase 1	PAAG_00885	cluster157	Without similarity	Acetylcholinesterase (Human)		C	Edrophonium	approved	inhibitor	96%	6E-172	35%	0.65	-3.53	3A3Y	X-ray, 2.80 Å	33.99%	90%	No docking	No docking
Lipase 1	PAAG_00885	cluster157	Without similarity	Acetylcholinesterase (Human)		C	Ephedrine	approved		71%	3E-173	57%	-	-	-	-	-	-	-	-
Lipase 1	PAAG_00885	cluster157	Without similarity	Cholinesterase (Human)		C	Ethopropazine	approved	inhibitor	95%	1E-162	35%	0.65	-3.53	3A3Y	X-ray, 2.80 Å	33.99%	90%	Receptor1	-10.104.547
Lipase 1	PAAG_00885	cluster157	Without similarity	Acetylcholinesterase (Human)		C	Galantamine	approved	inhibitor	82%	7E-58	31%	-	-	-	-	-	-	-	-
Lipase 1	PAAG_00885	cluster157	Without similarity	Acetylcholinesterase (Human)		C	Gallamine Triethiodide	approved	inhibitor	41%	2E-36	31%	-	-	-	-	-	-	-	-
Lipase 1	PAAG_00885	cluster157	Without similarity	Cholinesterase (Human)		C	Glycine betaine	approved, nutraceutical	inhibitor	91%	5E-93	31%	-	-	-	-	-	-	-	-
Lipase 1	PAAG_00885	cluster157	Without similarity	Cholinesterase (Human)		C	Hexafluronium	approved	inhibitor	96%	6E-172	35%	0.65	-3.53	3A3Y	X-ray, 2.80 Å	33.99%	90%	Receptor1	-0.068719
Lipase 1	PAAG_00885	cluster157	Without similarity	Acetylcholinesterase (Human)		C	Huperzine A	investigational		95%	1E-162	35%	0.65	-3.53	3A3Y	X-ray, 2.80 Å	33.99%	90%	Receptor1	-8.165.504
Lipase 1	PAAG_00885	cluster157	Without similarity	Acetylcholinesterase (Human)		C	Huperzine B	investigational		70%	5E-129	37%	-	-	-	-	-	-	-	-
Lipase 1	PAAG_00885	cluster157	Without similarity	Acetylcholinesterase (Human)		C	Isoflurophate	approved, withdrawn	inhibitor	96%	6E-172	35%	0.65	-3.53	3A3Y	X-ray, 2.80 Å	33.99%	90%	Receptor1	-6.066.512
Lipase 1	PAAG_00885	cluster157	Without similarity	Cholinesterase (Human)		C	Malathion	approved, investigational	inhibitor	95%	1E-162	35%	0.65	-3.53	3A3Y	X-ray, 2.80 Å	33.99%	90%	Receptor1	-8.109.964
Lipase 1	PAAG_00885	cluster157	Without similarity	Acetylcholinesterase (Human)		C	Minaprine	approved	inhibitor	44%	1E-82	45%	-	-	-	-	-	-	-	-
Lipase 1	PAAG_00885	cluster157	Without similarity	Cholinesterase (Human)		C	Mivacurium	approved		96%	6E-172	35%	0.65	-3.53	3A3Y	X-ray, 2.80 Å	33.99%	90%	Receptor1	-5.070.212

Lipase 1	PAAG_00885	cluster157	Without similarity	Cholinesterase (Human)		C	Nizatidine	approved	inhibitor	44%	1E-82	45%	-	-	-	-	-	-	-	-
Lipase 1	PAAG_00885	cluster157	Without similarity	Liver carboxylesterase 1 (Human)		C	Oseltamivir	approved	other	41%	2E-36	31%	-	-	-	-	-	-	-	-
Lipase 1	PAAG_00885	cluster157	Without similarity	Cholinesterase (Human)		C	Pancuronium	approved	inhibitor	97%	6E-129	47%	-	-	-	-	-	-	-	-
Lipase 1	PAAG_00885	cluster157	Without similarity	Acetylcholinesterase (Human)		C	Phenserine	investigational		19%	5E-60	35%	-	-	-	-	-	-	-	-
Lipase 1	PAAG_00885	cluster157	Without similarity	Acetylcholinesterase (Human)		C	Physostigmine	approved	inhibitor	95%	1E-162	35%	0.65	-3.53	3A3Y	X-ray, 2.80 Å	33.99%	90%	No docking	No docking
Lipase 1	PAAG_00885	cluster157	Without similarity	Cholinesterase (Human)		C	Pipecuronium	approved	inhibitor	96%	6E-172	35%	0.65	-3.53	3A3Y	X-ray, 2.80 Å	33.99%	90%	Receptor1	-8.615.794
Lipase 1	PAAG_00885	cluster157	Without similarity	Cholinesterase (Human)		C	Procainamide	approved	inhibitor	41%	2E-36	31%	-	-	-	-	-	-	-	-
Lipase 1	PAAG_00885	cluster157	Without similarity	Cholinesterase (Human)		C	Procaine	approved, investigational, vet_approved	inhibitor	96%	6E-172	35%	0.65	-3.53	3A3Y	X-ray, 2.80 Å	33.99%	90%	Receptor1	-5.298.628
Lipase 1	PAAG_00885	cluster157	Without similarity	Acetylcholinesterase (Human)		C	Pyridostigmine	approved	antagonist, inhibitor	96%	6E-172	35%	0.65	-3.53	3A3Y	X-ray, 2.80 Å	33.99%	90%	Receptor1	-2.570.552
Lipase 1	PAAG_00885	cluster157	Without similarity	Cholinesterase (Human)		C	Ramipril	approved	inhibitor	82%	0.0	65%	-	-	-	-	-	-	-	-
Lipase 1	PAAG_00885	cluster157	Without similarity	Acetylcholinesterase (Human)		C	Rivastigmine	approved, investigational	inhibitor	93%	3E-65	32%	-	-	-	-	-	-	-	-
Lipase 1	PAAG_00885	cluster157	Without similarity	Cholinesterase (Human)		C	Sulpiride	approved	inhibitor	78%	8E-70	43%	-	-	-	-	-	-	-	-
Lipase 1	PAAG_00885	cluster157	Without similarity	Acetylcholinesterase (Human)		C	Tacrine	withdrawn	inhibitor	82%	7E-58	31%	-	-	-	-	-	-	-	-
Lipase 1	PAAG_00885	cluster157	Without similarity	Cholinesterase (Human)		C	Terbutaline	approved	inhibitor	95%	1E-162	35%	0.65	-3.53	3A3Y	X-ray, 2.80 Å	33.99%	90%	Receptor1	-8.783.615
Lipase 1	PAAG_00885	cluster157	Without similarity	Cholinesterase (Human)		C	Triamcinolone	approved, vet_approved	inducer	95%	1E-162	35%	0.65	-3.53	3A3Y	X-ray, 2.80 Å	33.99%	90%	Receptor1	-7.990.050
Lipase 1	PAAG_00885	cluster157	Without similarity	Cholinesterase (Human)		C	Trimethaphan	approved		41%	2E-36	31%	-	-	-	-	-	-	-	-
Lipase 1	PAAG_00885	cluster157	Without similarity	Acetylcholinesterase (Human)		C	Tubocurarine	approved	inhibitor	89%	3E-59	30%	-	-	-	-	-	-	-	-
Lipase 4	PAAG_00885	cluster154	Without similarity	Cholinesterase	C		(-)-Phenserine	Phase 3	Alzheimer's disease	89%	3E-59	30%	-	-	-	-	-	-	-	-
Lipase 4	PAAG_00885	cluster154	Without similarity	Cholinesterase	C		Echothiophate Iodide	Approved	Chronic glaucoma	95%	1E-162	35%	0.65	-3.53	3A3Y	X-ray, 2.80 Å	33.99%	90%	Receptor1	-6.774.782
Lipase 4	PAAG_00885	cluster154	Without similarity	Cholinesterase	C		MEPTAZINOL	Approved	Pain	99%	0.0	73%	-	-	-	-	-	-	-	-
Lovastatin diketide synthase LovF	PAAG_11383	cluster124	Without similarity	Fatty acid synthase	C		PA-824	Phase 3	Mycobacterium tuberculosis infection	95%	1E-162	35%	0.65	-3.53	3A3Y	X-ray, 2.80 Å	33.99%	90%	Receptor1	-7.726.199
L-rhamnose-1-dehydrogenase	PAAG_07794	cluster103	Without similarity	3-beta-hydroxysteroid dehydrogenase	C		Trilostane	Approved	Cushing's syndrome	67%	2E-52	31%	-	-	-	-	-	-	-	-
Malate dehydrogenase, cytoplasmic	PAAG_00053	cluster361	Without similarity	Malate dehydrogenase (Escherichia coli (strain K12))		C	Nitrofural	approved, vet_approved	inhibitor	41%	3E-36	31%	-	-	-	-	-	-	-	-
Mannitol-1-phosphate 5-dehydrogenase	PAAG_06473	cluster602	Without similarity	Mannitol-1-phosphate 5-dehydrogenase		C	Mannitol	Approved	Bronchiectasis	41%	2E-36	31%	-	-	-	-	-	-	-	-
Mannose-6-phosphate isomerase	PAAG_00557	cluster573	DEG20010277	Mannose-6-phosphate isomerase	C	C	Sulfacetamide	Approved	Bacterial infections	96%	6E-172	35%	0.65	-3.53	3A3Y	X-ray, 2.80 Å	33.99%	90%	Receptor1	-5.327.871
Mannose-6-phosphate isomerase	PAAG_00557	cluster573	DEG20010277	Mannose-6-phosphate isomerase	C		Sulfanilamide	Approved	Bacterial infections	92%	5E-121	35%	-	-	-	-	-	-	-	-
Mannose-6-phosphate isomerase	PAAG_00557	cluster573	DEG20010277	Mannose-6-phosphate isomerase	C		Sulfoxone	Approved	Bacterial infections	95%	1E-162	35%	0.65	-3.53	3A3Y	X-ray, 2.80 Å	33.99%	90%	Receptor1	-8.606.586
Meiotic recombination protein dmc1	PAAG_02879	cluster894	Without similarity	DNA repair protein RAD51 homolog 1 (Human)		C	MP470	investigational		88%	2E-25	35%	-	-	-	-	-	-	-	-
Methionine aminopeptidase 2	PAAG_07566	cluster566	Without similarity	Methionine aminopeptidase 2	C		D-Methionine	Phase 3	Discovery agent	30%	8E-35	31%	-	-	-	-	-	-	-	-
Methionine aminopeptidase 2	PAAG_07566	cluster776	Without similarity	Methionine aminopeptidase 2 (Human)		C	Nitroxoline	approved	inhibitor	99%	0.0	73%	-	-	-	-	-	-	-	-
Methionine aminopeptidase 2	PAAG_07566	cluster776	Without similarity	Methionine aminopeptidase 2 (Human)		C	PPI-2458	investigational		56%	2E-33	48%	0.35	-1.85	3AH7	X-ray, 1.90 Å	45.19%	49%	Receptor1	-4.223481
Methionine aminopeptidase 2	PAAG_07566	cluster566	Without similarity	Methionine aminopeptidase 2	C		TNP-470	Discontinued in Phase 2	Solid tumours	99%	0.0	53%	0.49	-4.24	1WKB	X-ray, 2.05 Å	34.22%	70%	No docking	No docking

Methionine--tRNA ligase, mitochondrial	PAAG_00715	cluster929	Without similarity	Methionine--tRNA ligase (Staphylococcus aureus (strain MRSA252))		C	REP8839	investigational		54%	3E-68	40%	0.12	-4.14	5EAK	X-ray, 2.80 Å	45.49%	22%	Receptor1	-6.049.546
Mitogen-activated protein kinase hog1	PAAG_00535	cluster132	Without similarity	MAP kinase p38	C		ARRY-797	Phase 2	Oral Facial Pain	46%	3E-84	36%	-	-	-	-	-	-	-	-
Mitogen-activated protein kinase hog1	PAAG_00535	cluster132	Without similarity	MAP kinase p38	C		BIRB 796	Discontinued in Phase 2	Inflammatory bowel disease	89%	2E-100	50%	-	-	-	-	-	-	-	-
Mitogen-activated protein kinase hog1	PAAG_00535	cluster132	Without similarity	Mitogen-activated protein kinase 14	C		CNI-1493	Phase 2	Inflammatory bowel disease	93%	0.0	38%	-	-	-	-	-	-	-	-
Mitogen-activated protein kinase hog1	PAAG_00535	cluster132	Without similarity	Mitogen-activated protein kinase 14	C		Dilmapimod	Phase 2	Acute lung injury; Acute respiratory distress syndrome	93%	0.0	38%	-	-	-	-	-	-	-	-
Mitogen-activated protein kinase hog1	PAAG_00535	cluster132	Without similarity	MAP kinase p38	C		GSK-681323	Discontinued in Phase 2	Rheumatoid arthritis, Chronic obstructive pulmonary disease	46%	3E-84	36%	-	-	-	-	-	-	-	-
Mitogen-activated protein kinase HOG1	PAAG_00535	cluster92	Without similarity	Mitogen-activated protein kinase 11 (Human)	C	C	KC706	investigational		92%	5E-121	35%	-	-	-	-	-	-	-	-
Mitogen-activated protein kinase Hog1	PAAG_03659	cluster869	Without similarity	Glycogen synthase kinase-3 beta (Human)		C	Lithium	approved	inhibitor	54%	3E-68	40%	0.12	-4.14	5EAK	X-ray, 2.80 Å	45.49%	22%	No docking	No docking
Mitogen-activated protein kinase hog1	PAAG_00535	cluster132	Without similarity	Mitogen-activated protein kinase 14	C		Losmapimod	Phase 3	Acute coronary syndromes	93%	0.0	65%	-	-	-	-	-	-	-	-
Mitogen-activated protein kinase hog1	PAAG_00535	cluster132	Without similarity	Mitogen-activated protein kinase 14	C		PAMAPIMOD	Discontinued in Phase 2	Rheumatold arthritis	70%	3E-151	49%	-	-	-	-	-	-	-	-
Mitogen-activated protein kinase hog1	PAAG_00535	cluster132	Without similarity	Mitogen-activated protein kinase 14	C		R-1487	Discontinued in Phase 1	Rheumatold arthritis	92%	1E-70	60%	-	-	-	-	-	-	-	-
Mitogen-activated protein kinase HOG1	PAAG_00535	cluster92	Without similarity	Mitogen-activated protein kinase 11 (Human)		C	Regorafenib	approved	inhibitor	89%	3E-59	30%	-	-	-	-	-	-	-	-
Mitogen-activated protein kinase hog1	PAAG_00535	cluster132	Without similarity	Mitogen-activated protein kinase 14	C		SB 235699	Discontinued in Phase 1	Psoriasis	92%	5E-121	35%	-	-	-	-	-	-	-	-
Mitogen-activated protein kinase hog1	PAAG_00535	cluster132	Without similarity	Mitogen-activated protein kinase 14	C		SB-242235	Discontinued in Phase 1	Arthritic	61%	3E-136	48%	-	-	-	-	-	-	-	-
Mitogen-activated protein kinase hog1	PAAG_00535	cluster132	Without similarity	MAP kinase p38	C		SB681323	Phase 2	Rheumatoid Arthritis, Coronary Artery Disease	82%	0.0	65%	-	-	-	-	-	-	-	-
Mitogen-activated protein kinase hog1	PAAG_00535	cluster132	Without similarity	MAP kinase p38	C		SCIO-469	Phase 2a	Rheumatoid Arthritis	87%	7E-107	33%	0.60	-2.68	3RBU	X-ray, 1.6Å	37.38%	80%		
Mitogen-activated protein kinase hog1	PAAG_00535	cluster132	Without similarity	MAP kinase p38	C		VX-702	Phase 2	Coronary artery disease	99%	1E-119	80%	0.80	-0.30	1E+96	X-ray, 2.40 Å	80.10%	96%	Receptor	-7.139.526
Mitogen-activated protein kinase hog1	PAAG_00535	cluster132	Without similarity	MAP kinase p38	C		VX-745	Phase 2	Rheumatoid Arthritis	97%	0.0	35%	0.46	-1.67	4FVM	X-ray, 2.30 Å	48.47%	61%	Receptor1	-8.883.558
Mitogen-activated protein kinase HOG2	PAAG_05033	cluster286	Without similarity	Mitogen-activated protein kinase 3 (Human)		C	Sulindac	approved	inhibitor	89%	4E-72	32%	-	-	-	-	-	-	-	-
Myb-like DNA-binding protein myb-1	PAAG_05598	cluster621	Without similarity	mRNA of Myb proto-oncogene protein	C		LR3001	Phase 2	Myeloid Leukemia	71%	4E-56	33%	0.70	-1.28	3IAY	X-ray, 2.00 Å	58.79%	82%	Receptor2	-11.504.438
N/A	PAAG_01563	cluster142	Without similarity	Aromatic-L-amino-acid decarboxylase	C		Carbidopa	Approved	Parkinson's disease	71%	4E-56	33%	0.70	-1.28	3IAY	X-ray, 2.00 Å	58.79%	82%	Receptor2	-7.204.059
N/A	PAAG_00819	cluster29	Without similarity	Type IV phosphodiesterase	C		Oxtriphylline	Approved	Cough	93%	3E-65	32%	-	-	-	-	-	-	-	-
N/A	PAAG_02835	cluster71	Without similarity	Complement C1q subcomponent subunit C (Human)		C	Abciximab	approved		94%	1E-124	40%	-	-	-	-	-	-	-	-
N/A	PAAG_04866	cluster590	Without similarity	Poly [ADP-ribose] polymerase-1	C		ABT-888	Phase 3	Breast cancer	93%	2E-155	58%	0,83	0,36	2D3A	X-ray, 2.63Å	60,96%	97%	Receptor3	-13.394.193
N/A	PAAG_02835	cluster71	Without similarity	Complement C1q subcomponent subunit C (Human)		C	Adalimumab	approved		93%	2E-155	58%	0,83	0,36	2D3A	X-ray, 2.63Å	60,96%	97%	Receptor3	-12.711.921
N/A	PAAG_04866	cluster590	Without similarity	Poly [ADP-ribose] polymerase-1	C		AG-14699	Phase 3	Hypoxia	99%	5E-49	60%	-	-	-	-	-	-	-	-
N/A	PAAG_02835	cluster71	Without similarity	Complement C1q subcomponent subunit C (Human)		C	Alefacept	approved, withdrawn		70%	3E-151	49%	-	-	-	-	-	-	-	-
N/A	PAAG_02835	cluster71	Without similarity	Complement C1q subcomponent subunit C (Human)		C	Alemtuzumab	approved, investigational		88%	2E-25	35%	-	-	-	-	-	-	-	-
N/A	PAAG_00819	cluster29	Without similarity	Phosphodiesterase isozyme 4	C	C	AN2728	Phase 2	Psoriasis	94%	2E-133	50%	-	-	-	-	-	-	-	-
N/A	PAAG_00819	cluster29	Without similarity	CAMP-specific 3',5'-cyclic phosphodiesterase 4A	C		AN-2898	Phase 2	Atopic dermatitis	93%	2E-155	58%	0,83	0,36	2D3A	X-ray, 2.63Å	60,96%	97%	Receptor3	-9.392.894

N/A	PAAG_00819	cluster29	Without similarity	Phosphodiesterase isozyme 4	C	C	Apremilast	Phase 2	Psoriasis	93%	2E-155	58%	0,83	0,36	2D3A	X-ray, 2.63Å	60,96%	97%	Receptor1	-12.641.518
N/A	PAAG_00819	cluster29	Without similarity	Phosphodiesterase isozyme 4		C	Arofylline	Phase 3	Chronic obstructive pulmonary disease	99%	0.0	66%	-	-	-	-	-	-	-	-
N/A	PAAG_01563	cluster142	Without similarity	Aromatic-L-amino-acid decarboxylase	C		AV-201	Phase 2	Parkinson's disease	92%	5E-121	35%	-	-	-	-	-	-	-	-
N/A	PAAG_00819	cluster29	Without similarity	CAMP-specific 3',5'-cyclic phosphodiesterase 4A	C		AWD-12-281	Phase 2	Rhinitis	92%	5E-121	35%	-	-	-	-	-	-	-	-
N/A	PAAG_04866	cluster590	Without similarity	Poly [ADP-ribose] polymerase-1	C		AZD-2281	Phase 2	Discovery agent	46%	3E-84	36%	-	-	-	-	-	-	-	-
N/A	PAAG_02835	cluster71	Without similarity	Complement C1q subcomponent subunit C (Human)		C	Basiliximab	approved, investigational		46%	3E-84	36%	-	-	-	-	-	-	-	-
N/A	PAAG_01563	cluster142	Without similarity	Aromatic-L-amino-acid decarboxylase	C		Benserazide	Phase 3	Discovery agent	97%	5E-152	63%	0.75	0.78	4A5L	X-ray, 1.7 Å	61,22%	87%	No molcharge	No molcharge
N/A	PAAG_02835	cluster71	Without similarity	Complement C1q subcomponent subunit C (Human)		C	Bevacizumab	approved, investigational		41%	2E-36	31%	-	-	-	-	-	-	-	-
N/A	PAAG_04866	cluster590	Without similarity	Poly [ADP-ribose] polymerase-1	C		BMN-673	Phase 3	Psoriatic arthritis	97%	5E-152	63%	0.75	0.78	4A5L	X-ray, 1.7 Å	61,22%	87%	Receptor1	-9.031.322
N/A	PAAG_04866	cluster590	Without similarity	Poly [ADP-ribose] polymerase-1	C		BSI-201	Phase 3	Solid tumours	54%	3E-113	55%	0.19	-3.75	4UAL	X-ray, 1.71 Å	34.81%	37%	Receptor1	-8.294.222
N/A	PAAG_02017	cluster375	Without similarity	Glutamate carboxypeptidase 2 (Human)		C	Capromab	approved	other / unknown	77%	7E-131	35%	0.55	-3.81	1X9N	X-ray, 3.00 Å	37.54%	76%	No molcharge	No molcharge
N/A	PAAG_01563	cluster280	Without similarity	Aromatic-L-amino-acid decarboxylase (Human)		C	Carbidopa	approved	inhibitor	93%	2E-66	34%	0.76	-1.06	4QPF	X-ray, 1.59 Å	44.74%	99%	Receptor1	-17.245.781
N/A	PAAG_00819	cluster29	Without similarity	CAMP-specific 3',5'-cyclic phosphodiesterase 4A	C		CC-1088	Phase 2	Crohn's disease	81%	6E-101	45%	0.76	-1.06	4QPF	X-ray, 1.59 Å	44.74%	99%	Receptor1	-15.799.474
N/A	PAAG_00819	cluster29	Without similarity	CAMP-specific 3',5'-cyclic phosphodiesterase 4A	C		CDP840	Discontinued in Phase 2	Chronic obstructive pulmonary disease	41%	2E-36	31%	-	-	-	-	-	-	-	-
N/A	PAAG_04866	cluster590	Without similarity	Poly [ADP-ribose] polymerase-1	C		CEP-9722	Phase 1/2	Cerebrovascular ischaemia	74%	6E-80	45%	-	-	-	-	-	-	-	-
N/A	PAAG_01563	cluster280	Without similarity	Aromatic-L-amino-acid decarboxylase (Human)		C	CHF-1512	investigational		92%	5E-121	35%	-	-	-	-	-	-	-	-
N/A	PAAG_00819	cluster29	Without similarity	CAMP-specific 3',5'-cyclic phosphodiesterase 4A		C	CI-1018	Discontinued in Phase 2	Asthma	93%	3E-65	32%	-	-	-	-	-	-	-	-
N/A	PAAG_00819	cluster29	Without similarity	Phosphodiesterase isozyme 4	C	C	Cilomilast	Discontinued in Phase 3	Emphysema, Bronchitis, Chronic obstructive pulmonary disease	94%	1E-59	34%	-	-	-	-	-	-	-	-
N/A	PAAG_01563	cluster280	Without similarity	Aromatic-L-amino-acid decarboxylase (Human)		C	Cycloserine	approved	inhibitor	93%	2E-66	34%	0.76	-1.06	4QPF	X-ray, 1.59 Å	44.74%	99%	Receptor1	-20.885.309
N/A	PAAG_00819	cluster29	Without similarity	CAMP-specific 3',5'-cyclic phosphodiesterase 4A	C		D-4418	Discontinued in Phase 1	Cutaneous T-cell lymphoma	70%	3E-151	49%	-	-	-	-	-	-	-	-
N/A	PAAG_02835	cluster71	Without similarity	Complement C1q subcomponent subunit C (Human)		C	Daclizumab	approved, investigational		93%	2E-66	34%	0.76	-1.06	4QPF	X-ray, 1.59 Å	44.74%	99%	Receptor1	-18.478.310
N/A	PAAG_00819	cluster29	Without similarity	CAMP-specific 3',5'-cyclic phosphodiesterase 4A	C		Daxalipram	Discontinued in Phase 2	Multiple sclerosis	93%	2E-66	34%	0.76	-1.06	4QPF	X-ray, 1.59 Å	44.74%	99%	Receptor1	-15.682.286
N/A	PAAG_00819	cluster29	Without similarity	CAMP-specific 3',5'-cyclic phosphodiesterase 4A	C		DENBUFYLLINE	Phase 3	Cognition disorders	87%	5E-126	42%	-	-	-	-	-	-	-	-
N/A	PAAG_00819	cluster21	Without similarity	cAMP-specific 3',5'-cyclic phosphodiesterase 4A (Human)		C	Drotaverine	approved	inhibitor	81%	6E-101	45%	0.76	-1.06	4QPF	X-ray, 1.59 Å	44.74%	99%	Receptor1	-19.165.264

N/A	PAAG_00819	cluster29	Without similarity	CAMP-specific 3',5'-cyclic phosphodiesterase 4A	C	C	Dyphylline	Approved	Asthma	81%	6E-101	45%	0.76	-1.06	4QPF	X-ray, 1.59 Å	44.74%	99%	Receptor1	-17.599.087
N/A	PAAG_00819	cluster29	Without similarity	Phosphodiesterase isozyme 4	C		E6005	Phase 2	Atopic dermatitis	93%	2E-66	34%	0.76	-1.06	4QPF	X-ray, 1.59 Å	44.74%	99%	Receptor1	-15.450.322
N/A	PAAG_04866	cluster590	Without similarity	Poly [ADP-ribose] polymerase-1	C		E7016	Phase 2	Malignant melanoma	92%	5E-121	35%	-	-	-	-	-	-	-	-
N/A	PAAG_02835	cluster71	Without similarity	Complement C1q subcomponent subunit C (Human)		C	Efalizumab	approved, investigational		93%	2E-66	34%	0.76	-1.06	4QPF	X-ray, 1.59 Å	44.74%	99%	Receptor1	-16.386.013
N/A	PAAG_00819	cluster29	Without similarity	CAMP-specific 3',5'-cyclic phosphodiesterase 4A	C	C	Enprofylline	Approved	Asthma	92%	5E-121	35%	-	-	-	-	-	-	-	-
N/A	PAAG_02835	cluster71	Without similarity	Complement C1q subcomponent subunit C (Human)		C	Etanercept	approved, investigational		70%	3E-151	49%	-	-	-	-	-	-	-	-
N/A	PAAG_02835	cluster71	Without similarity	Complement C1q subcomponent subunit C (Human)		C	Gemtuzumab ozogamicin	approved, investigational, withdrawn		41%	2E-36	31%	-	-	-	-	-	-	-	-
N/A	PAAG_00819	cluster29	Without similarity	CAMP-specific 3',5'-cyclic phosphodiesterase 4A	C		GPD-1116	Phase 2	Asthma	86%	3E-180	65%	-	-	-	-	-	-	-	-
N/A	PAAG_03121	cluster753	Without similarity	N-terminal kinase-like protein (Human)		C	Grn163l	investigational		94%	3E-137	51%	-	-	-	-	-	-	-	-
N/A	PAAG_00819	cluster29	Without similarity	CAMP-specific 3',5'-cyclic phosphodiesterase 4A	C		GSK256066	Discontinued in Phase 2	Asthma	83%	0.0	63%	-	-	-	-	-	-	-	-
N/A	PAAG_00819	cluster29	Without similarity	Phosphodiesterase isozyme 4	C		GW842470X	Discontinued in Phase 2	Atopic dermatitis	39%	2E-28	40%	-	-	-	-	-	-	-	-
N/A	PAAG_00819	cluster29	Without similarity	CAMP-specific 3',5'-cyclic phosphodiesterase 4A	C		HT-0712	Phase 2	Cognitive impairment	86%	3E-180	65%	-	-	-	-	-	-	-	-
N/A	PAAG_02835	cluster71	Without similarity	Complement C1q subcomponent subunit C (Human)		C	Ibritumomab tiuxetan	approved		61%	3E-136	48%	-	-	-	-	-	-	-	-
N/A	PAAG_00819	cluster21	Without similarity	cAMP-specific 3',5'-cyclic phosphodiesterase 4C (Human)		C	Ibudilast	approved, investigational	inhibitor	95%	6E-69	32%	-	-	-	-	-	-	-	-
N/A	PAAG_00819	cluster29	Without similarity	Phosphodiesterase isozyme 4	C		IC-485	Phase 2	Chronic obstructive pulmonary disease	95%	6E-69	32%	-	-	-	-	-	-	-	-
N/A	PAAG_00819	cluster21	Without similarity	cAMP-specific 3',5'-cyclic phosphodiesterase 4A (Human)		C	Iloprost	approved, investigational	inhibitor	82%	7E-58	31%	-	-	-	-	-	-	-	-
N/A	PAAG_04866	cluster590	Without similarity	Poly [ADP-ribose] polymerase-1	C		INO-1001	Phase 3	Brain Cancer	97%	9E-105	48%	-	-	-	-	-	-	-	-
N/A	PAAG_04866	cluster590	Without similarity	Poly [ADP-ribose] polymerase-1	C		Intravenous minocycline	Phase 2	Cerebrovascular ischaemia	100%	0.0	69%	-	-	-	-	-	-	-	-
N/A	PAAG_04866	cluster590	Without similarity	Poly [ADP-ribose] polymerase-1	C		KU-0058948	Approved	Ovarian cancer	97%	9E-105	48%	-	-	-	-	-	-	-	-
N/A	PAAG_04866	cluster590	Without similarity	Poly [ADP-ribose] polymerase-1	C		KU-0059436	Discontinued in Phase 2	Gastric cancer; Breast cancer; Ovarian cancer	56%	5E-84	31%	-	-	-	-	-	-	-	-
N/A	PAAG_00819	cluster29	Without similarity	CAMP-specific 3',5'-cyclic phosphodiesterase 4A	C		KW-4490	Discontinued in Phase 2	Asthma	91%	5E-93	31%	-	-	-	-	-	-	-	-
N/A	PAAG_00819	cluster29	Without similarity	CAMP-specific 3',5'-cyclic phosphodiesterase 4A	C		LAS-37779	Discontinued in Phase 2	Psoriasis	92%	5E-121	35%	-	-	-	-	-	-	-	-
N/A	PAAG_01563	cluster280	Without similarity	Aromatic-L-amino-acid decarboxylase (Human)		C	Levodopa	approved		99%	0.0	66%	-	-	-	-	-	-	-	-
N/A	PAAG_00819	cluster29	Without similarity	CAMP-specific 3',5'-cyclic phosphodiesterase 4A	C		LIRIMILAST	Phase 2	Chronic obstructive pulmonary disease	97%	0.0	41%	-	-	-	-	-	-	-	-

N/A	PAAG_01563	cluster280	Without similarity	Aromatic-L-amino-acid decarboxylase (Human)		C	Methyldopa	approved		50%	1E-21	31%	-	-	-	-	-	-	-	-
N/A	PAAG_00819	cluster29	Without similarity	CAMP-specific 3',5'-cyclic phosphodiesterase 4A	C		MK-0873	Phase 2	Psoriasis	82%	7E-58	31%	-	-	-	-	-	-	-	-
N/A	PAAG_04866	cluster590	Without similarity	Poly [ADP-ribose] polymerase-1	C		MK-4827	Phase 2	Ovarian cancer	97%	0.0	59%	-	-	-	-	-	-	-	-
N/A	PAAG_02835	cluster71	Without similarity	Complement C1q subcomponent subunit C (Human)		C	Muromonab	approved, investigational		99%	0.0	66%	-	-	-	-	-	-	-	-
N/A	PAAG_02835	cluster71	Without similarity	Complement C1q subcomponent subunit C (Human)		C	Natalizumab	approved, investigational		62%	2E-81	30%	-	-	-	-	-	-	-	-
N/A	PAAG_04866	cluster590	Without similarity	Poly [ADP-ribose] polymerase-1	C		Nicaraven	Phase 3	Cerebrovascular disorders	87%	5E-126	42%	-	-	-	-	-	-	-	-
N/A	PAAG_00819	cluster29	Without similarity	CAMP-specific 3',5'-cyclic phosphodiesterase 4A	C		Oglemilast	Phase 2	Asthma	82%	0.0	65%	-	-	-	-	-	-	-	-
N/A	PAAG_04866	cluster240	Without similarity	Poly [ADP-ribose] polymerase 2 (Human)	C	C	Olaparib	approved	Inhibitor	68%	2E-29	31%	-	-	-	-	-	-	-	-
N/A	PAAG_04866	cluster590	Without similarity	Poly [ADP-ribose] polymerase-1	C		ONO-2231	Discontinued in Phase 1	Cerebrovascular ischaemia	99%	0.0	79%	-	-	-	-	-	-	-	-
N/A	PAAG_00819	cluster29	Without similarity	Phosphodiesterase isozyme 4	C		ONO-6126	Phase 2	Chronic obstructive pulmonary disease	70%	1E-60	37%	-	-	-	-	-	-	-	-
N/A	PAAG_00819	cluster21	Without similarity	cAMP-specific 3',5'-cyclic phosphodiesterase 4D (Human)	C		OPC-6535	investigational	inhibitor	97%	0.0	42%	-	-	-	-	-	-	-	-
N/A	PAAG_00819	cluster29	Without similarity	CAMP-specific 3',5'-cyclic phosphodiesterase 4A	C		Org-30029	Phase 2	Heart failure	95%	0.0	58%	-	-	-	-	-	-	-	-
N/A	PAAG_00819	cluster29	Without similarity	CAMP-specific 3',5'-cyclic phosphodiesterase 4A	C		Org-9731	Discontinued in Phase 2	Heart failure	96%	2E-92	45%	-	-	-	-	-	-	-	-
N/A	PAAG_00819	cluster29	Without similarity	CAMP-specific 3',5'-cyclic phosphodiesterase 4A	C		OX-914	Phase 2	Asthma	89%	3E-59	30%	-	-	-	-	-	-	-	-
N/A	PAAG_00819	cluster29	Without similarity	Type IV phosphodiesterase	C	C	Oxtriphylline	Approved	Cough	97%	2E-49	63%	-	-	-	-	-	-	-	-
N/A	PAAG_02835	cluster71	Without similarity	Complement C1q subcomponent subunit C (Human)		C	Palivizumab	approved, investigational		82%	7E-58	31%	-	-	-	-	-	-	-	-
N/A	PAAG_01563	cluster142	Without similarity	Aromatic-L-amino-acid decarboxylase	C		Patrome	Phase 3	Parkinson's disease	71%	3E-173	57%	-	-	-	-	-	-	-	-
N/A	PAAG_00819	cluster21	Without similarity	cAMP-specific 3',5'-cyclic phosphodiesterase 4A (Human)		C	Pentoxifylline	approved, investigational	inhibitor	41%	2E-36	31%	-	-	-	-	-	-	-	-
N/A	PAAG_00819	cluster29	Without similarity	CAMP-specific 3',5'-cyclic phosphodiesterase 4A	C		Piclamilast	Phase 2	Rheumatold arthritis	92%	5E-121	35%	-	-	-	-	-	-	-	-
N/A	PAAG_02835	cluster71	Without similarity	Voltage-dependent P/Q-type calcium channel subunit alpha-1A (Human)		C	Pregabalin	approved, illicit, investigational	inhibitor	46%	3E-84	36%	-	-	-	-	-	-	-	-
N/A	PAAG_00819	cluster29	Without similarity	CAMP-specific 3',5'-cyclic phosphodiesterase 4A	C		Pumafentrine	Discontinued in Phase 2	Asthma	91%	5E-93	31%	-	-	-	-	-	-	-	-
N/A	PAAG_00819	cluster29	Without similarity	CAMP-specific 3',5'-cyclic phosphodiesterase 4A	C		Revamilast	Phase 2	Asthma	91%	5E-93	31%	-	-	-	-	-	-	-	-

N/A	PAAG_02835	cluster71	Without similarity	Complement C1q subcomponent subunit C (Human)		C	Rituximab	approved		88%	5E-98	33%	-	-	-	-	-	-	-	-
N/A	PAAG_00819	cluster29	Without similarity	Phosphodiesterase isozyme 4	C	C	Roflumilast	Approved	Asthma	92%	0.0	75%	-	-	-	-	-	-	-	-
N/A	PAAG_00819	cluster29	Without similarity	CAMP-specific 3',5'-cyclic phosphodiesterase 4A	C		ROLIPRAM	Phase 2	Discovery agent	82%	0.0	65%	-	-	-	-	-	-	-	-
N/A	PAAG_00819	cluster29	Without similarity	CAMP-specific 3',5'-cyclic phosphodiesterase 4A	C		RPL-554	Phase 2	Allergic rhinitis	67%	2E-52	31%	-	-	-	-	-	-	-	-
N/A	PAAG_00819	cluster29	Without similarity	CAMP-specific 3',5'-cyclic phosphodiesterase 4A	C		SCH-351591	Discontinued in Phase 1	Chronic obstructive pulmonary disease	97%	0.0	59%	-	-	-	-	-	-	-	-
N/A	PAAG_00819	cluster29	Without similarity	CAMP-specific 3',5'-cyclic phosphodiesterase 4A	C		SOTB07	Phase 3	Asthma	97%	0.0	59%	-	-	-	-	-	-	-	-
N/A	PAAG_00819	cluster29	Without similarity	CAMP-specific 3',5'-cyclic phosphodiesterase 4A	C		TA-7906	Phase 2	Atopic dermatitis	67%	2E-52	31%	-	-	-	-	-	-	-	-
N/A	PAAG_00819	cluster21	Without similarity	cAMP-specific 3',5'-cyclic phosphodiesterase 4A (Human)		C	Theophylline	approved	inhibitor	70%	3E-151	49%	-	-	-	-	-	-	-	-
N/A	PAAG_00819	cluster29	Without similarity	CAMP-specific 3',5'-cyclic phosphodiesterase 4A	C		Tipelukast	Phase 2	Asthma	93%	0.0	65%	-	-	-	-	-	-	-	-
N/A	PAAG_00819	cluster29	Without similarity	CAMP-specific 3',5'-cyclic phosphodiesterase 4A	C		TOFIMILAST	Phase 2	Chronic obstructive pulmonary disease	99%	5E-49	60%	-	-	-	-	-	-	-	-
N/A	PAAG_00819	cluster21	Without similarity	cAMP-specific 3',5'-cyclic phosphodiesterase 4A (Human)		C	Tofisopam	approved	inhibitor	99%	5E-49	60%	-	-	-	-	-	-	-	-
N/A	PAAG_00819	cluster29	Without similarity	CAMP-specific 3',5'-cyclic phosphodiesterase 4A	C		Tolafentrine	Discontinued in Phase 2	Chronic obstructive pulmonary disease	86%	3E-180	65%	-	-	-	-	-	-	-	-
N/A	PAAG_02835	cluster71	Without similarity	Complement C1q subcomponent subunit C (Human)		C	Tositumomab	approved		46%	3E-84	36%	-	-	-	-	-	-	-	-
N/A	PAAG_02835	cluster71	Without similarity	Complement C1q subcomponent subunit C (Human)		C	Trastuzumab	approved, investigational		87%	2E-39	44%	-	-	-	-	-	-	-	-
N/A	PAAG_00819	cluster29	Without similarity	CAMP-specific 3',5'-cyclic phosphodiesterase 4A	C		V-11294A	Discontinued in Phase 2	Asthma	93%	4E-124	37%	-	-	-	-	-	-	-	-
N/A	PAAG_04866	cluster240	Without similarity	Poly [ADP-ribose] polymerase 2 (Human)		C	Veliparib	investigational		92%	3E-145	53%	-	-	-	-	-	-	-	-
Na+/K+-exchanging ATPase alpha chain	PAAG_04243	cluster290	DEG20010344	Sodium/potassium-transporting ATPase subunit alpha-1 (Human)		C	Acetyldigitoxin	approved	inhibitor	96%	0.0	58%	-	-	-	-	-	-	-	-
Na+/K+-exchanging ATPase alpha chain	PAAG_04243	cluster290	DEG20010344	Potassium-transporting ATPase alpha chain 1	C	C	Pantoprazole	approved	inhibitor	99%	2E-99	50%	-	-	-	-	-	-	-	-
Na+/K+-exchanging ATPase alpha chain	PAAG_04243	cluster138	DEG20010344	Potassium-transporting ATPase alpha chain 1	C		AG-SPT201	Phase 3	Ulcerative colitis	78%	5E-177	62%	-	-	-	-	-	-	-	-
Na+/K+-exchanging ATPase alpha chain	PAAG_04243	cluster290	DEG20010344	Sodium/potassium-transporting ATPase subunit alpha-1 (Human)	C	C	Almitrine	approved	binder	82%	7E-58	31%	-	-	-	-	-	-	-	-

Na+/K+-exchanging ATPase alpha chain	PAAG_04243	cluster290	DEG20010344	Sodium/potassium-transporting ATPase subunit alpha-1 (Human)	C	C	Aluminium	approved	binder	71%	3E-173	57%	-	-	-	-	-	-	-	-
Na+/K+-exchanging ATPase alpha chain	PAAG_04243	cluster138	DEG20010344	Sodium/potassium-transporting ATPase alpha-1 chain	C		Artemether	Approved	Plasmodium infection	70%	3E-151	49%	-	-	-	-	-	-	-	-
Na+/K+-exchanging ATPase alpha chain	PAAG_04243	cluster138	DEG20010344	Potassium-transporting ATPase alpha chain 1	C		AZD-0865	Phase 2	Gastrointestinal disease	83%	2E-36	42%	-	-	-	-	-	-	-	-
Na+/K+-exchanging ATPase alpha chain	PAAG_04243	cluster290	DEG20010344	Sodium/potassium-transporting ATPase subunit alpha-1		C	Bretylium	approved	inhibitor	92%	5E-121	35%	-	-	-	-	-	-	-	-
Na+/K+-exchanging ATPase alpha chain	PAAG_04243	cluster138	DEG20010344	Sodium/potassium-transporting ATPase alpha-1 chain	C		Chloroprocaine	Approved	Anesthetic	82%	0.0	65%	-	-	-	-	-	-	-	-
Na+/K+-exchanging ATPase alpha chain	PAAG_04243	cluster290	DEG20010344	Sodium/potassium-transporting ATPase subunit alpha-1 (Human)	C	C	Ciclopirox	approved, investigational	binder	41%	2E-36	31%	-	-	-	-	-	-	-	-
Na+/K+-exchanging ATPase alpha chain	PAAG_04243	cluster290	DEG20010344	Sodium/potassium-transporting ATPase subunit alpha-1 (Human)	C	C	Deslanoside	approved	inhibitor	98%	6E-101	36%	-	-	-	-	-	-	-	-
Na+/K+-exchanging ATPase alpha chain	PAAG_04243	cluster138	DEG20010344	Potassium-transporting ATPase alpha chain 1	C		Dexlansoprazole	Approved	Erosive esophagitis and non-erosive gastro-esophageal reflux disease	46%	3E-84	36%	-	-	-	-	-	-	-	-
Na+/K+-exchanging ATPase alpha chain	PAAG_04243	cluster290	DEG20010344	Sodium/potassium-transporting ATPase subunit alpha-1 (Human)		C	Digitoxin	approved	inhibitor	41%	2E-36	31%	-	-	-	-	-	-	-	-
Na+/K+-exchanging ATPase alpha chain	PAAG_04243	cluster290	DEG20010344	Potassium-transporting ATPase alpha chain 1 (Human)	C	C	Esomeprazole	approved, investigational	inhibitor	88%	2E-25	35%	-	-	-	-	-	-	-	-
Na+/K+-exchanging ATPase alpha chain	PAAG_04243	cluster290	DEG20010344	Sodium/potassium-transporting ATPase subunit alpha-1 (Human)		C	Etacrynic acid	approved	inhibitor	32%	4E-36	31%	-	-	-	-	-	-	-	-
Na+/K+-exchanging ATPase alpha chain	PAAG_04243	cluster290	DEG20010344	Potassium-transporting ATPase alpha chain 1	C	C	Omeprazole	approved, investigational, vet_approved	inhibitor	41%	2E-36	31%	-	-	-	-	-	-	-	-
Na+/K+-exchanging ATPase alpha chain	PAAG_04243	cluster290	DEG20010344	Sodium/potassium-transporting ATPase subunit alpha-1 (Human)	C	C	Hydroflumethiazide	approved	other / unknown	41%	2E-36	31%	-	-	-	-	-	-	-	-
Na+/K+-exchanging ATPase alpha chain	PAAG_04243	cluster138	DEG20010344	Potassium-transporting ATPase alpha chain 1	C		LEMINOPRAZOLE	Discontinued in Preregistration	Ulcerative colitis	65%	1E-69	33%	-	-	-	-	-	-	-	-
Na+/K+-exchanging ATPase alpha chain	PAAG_04243	cluster138	DEG20010344	Sodium/potassium-transporting ATPase alpha-1 chain	C		Lumefantrine	Approved	Malaria	98%	3E-54	30%	-	-	-	-	-	-	-	-
Na+/K+-exchanging ATPase alpha chain	PAAG_04243	cluster138	DEG20010344	Sodium/potassium-transporting ATPase alpha-1 chain	C	C	Ouabain	Approved	Atrial fibrillation and heart failure	41%	2E-36	31%	-	-	-	-	-	-	-	-
Na+/K+-exchanging ATPase alpha chain	PAAG_04243	cluster290	DEG20010344	Sodium/potassium-transporting ATPase subunit alpha-1 (Human)		C	Potassium	approved		88%	5E-98	33%	-	-	-	-	-	-	-	-
Na+/K+-exchanging ATPase alpha chain	PAAG_04243	cluster138	DEG20010344	Potassium-transporting ATPase alpha chain 1	C		PUMAPRAZOLE	Discontinued in Phase 3	Duodenal ulcer	31%	4E-36	31%	-	-	-	-	-	-	-	-
Na+/K+-exchanging ATPase alpha chain	PAAG_04243	cluster290	DEG20010344	Potassium-transporting ATPase alpha chain 1 (Human)	C	C	Rabeprazole	approved, investigational	inhibitor	88%	2E-25	35%	-	-	-	-	-	-	-	-
Na+/K+-exchanging ATPase alpha chain	PAAG_04243	cluster138	DEG20010344	Potassium-transporting ATPase alpha chain 1	C		SORAPRAZAN	Discontinued in Phase 2	Peptic ulcer	98%	0.0	47%	-	-	-	-	-	-	-	-
Na+/K+-exchanging ATPase alpha chain	PAAG_04243	cluster138	DEG20010344	Potassium-transporting ATPase alpha chain 1	C		S-tenatoprazole	Phase 2	Peptic ulcer	92%	5E-121	35%	-	-	-	-	-	-	-	-

Na+/K+-exchanging ATPase alpha chain	PAAG_04243	cluster290	DEG20010344	Sodium/potassium-transporting ATPase subunit alpha-1 (Human)	C	C	Trichlormethiazide	approved, vet_approved	inhibitor	65%	1E-69	33%	-	-	-	-	-	-	-	-
Na+/K+-exchanging ATPase alpha chain	PAAG_04243	cluster138	DEG20010344	Potassium-transporting ATPase alpha chain 1	C		TY-11345	Discontinued in Phase 2	Peptic ulcer	67%	2E-52	31%	-	-	-	-	-	-	-	-
NAD-dependent histone deacetylase SIR2	PAAG_02777	cluster605	Without similarity	NAD-dependent deacetylase sirtuin-1	C		GSK184072	Phase 2	Colorectal cancer	94%	3E-137	51%	-	-	-	-	-	-	-	-
NAD-dependent histone deacetylase SIR2	PAAG_02777	cluster605	Without similarity	NAD-dependent deacetylase sirtuin-1	C		GSK2245840	Phase 2	Chronic obstructive pulmonary disease	88%	2E-25	35%	-	-	-	-	-	-	-	-
NAD-dependent histone deacetylase SIR2	PAAG_02777	cluster605	Without similarity	NAD-dependent deacetylase sirtuin-1	C		SEN-196	Phase 2	Huntington's disease	82%	7E-58	31%	-	-	-	-	-	-	-	-
NAD-dependent protein deacetylase hst2-1	PAAG_01016	cluster617	Without similarity	Sirtuin	C		SRT2104	Phase 2	Psoriasis	82%	0.0	65%	-	-	-	-	-	-	-	-
NAD-dependent protein deacylase	PAAG_02777	cluster739	Without similarity	NAD-dependent protein deacetylase sirtuin-1 (Human)	C		SRT501	investigational		87%	5E-126	42%	-	-	-	-	-	-	-	-
NADPH-cytochrome P450 reductase	PAAG_11783	cluster93	DEG20010460	Nitric-oxide synthase, endothelial	C		ACCLAIM	Phase 2	Angina, Coronary Artery Disease	90%	1E-96	51%	-	-	-	-	-	-	-	-
NAD-specific glutamate dehydrogenase	PAAG_01002	cluster636	Without similarity	Glutamate dehydrogenase	C		Hexachlorophene	Withdrawn from the Market	Bacterial infections	82%	0.0	65%	-	-	-	-	-	-	-	-
Niemann-Pick type C-related protein 1	PAAG_01279	cluster880	Without similarity	Niemann-Pick C1-like protein 1 (Human)	C	C	Ezetimibe	approved	inhibitor	70%	3E-151	49%	-	-	-	-	-	-	-	-
Ornithine decarboxylase	PAAG_03153	cluster206	Without similarity	Ornithine decarboxylase (Human)		C	Eflornithine	approved, withdrawn	antagonist, blocker	88%	2E-25	35%	-	-	-	-	-	-	-	-
PAB1-binding protein 2	PAAG_02643	cluster817	Without similarity	Far upstream element-binding protein 1 (Human)		C	MGI-114	investigational		30%	8E-35	31%	-	-	-	-	-	-	-	-
Palmitoyltransferase AKR1	PAAG_06136	cluster615	Without similarity	Transient receptor potential cation channel subfamily A member 1	C		Menthol	Approved	Throat irritation	98%	6E-85	31%	-	-	-	-	-	-	-	-
Phosphatidylinositol 3-kinase tor2	PAAG_01410	cluster856	DEG20010648	Serine/threonine-protein kinase mTOR (Human)		C	AP1903	investigational		92%	5E-121	35%	-	-	-	-	-	-	-	-
Phosphatidylinositol 3-kinase tor2	PAAG_01410	cluster580	DEG20010648	Serine/threonine-protein kinase mTOR	C		AP23573	Phase 3	Metastatic Soft-Tissue Sarcomas; Metastatic Bone Sarcomas	89%	4E-72	32%	-	-	-	-	-	-	-	-
Phosphatidylinositol 3-kinase tor2	PAAG_01410	cluster580	DEG20010648	Serine/threonine-protein kinase mTOR	C		AZD2014	Phase 2	Cancer	95%	6E-69	32%	-	-	-	-	-	-	-	-
Phosphatidylinositol 3-kinase tor2	PAAG_01410	cluster580	DEG20010648	Serine/threonine-protein kinase mTOR	C		AZD8055	Discontinued in Phase 1/2	Cancer	95%	6E-69	32%	-	-	-	-	-	-	-	-
Phosphatidylinositol 3-kinase tor2	PAAG_01410	cluster580	DEG20010648	Serine/threonine-protein kinase mTOR	C		Dactolisib	Phase 2	Solid Tumours	71%	3E-173	57%	-	-	-	-	-	-	-	-
Phosphatidylinositol 3-kinase tor2	PAAG_01410	cluster580	DEG20010648	Serine/threonine-protein kinase mTOR	C		BGT226	Phase 1/2	Solid Tumours	88%	2E-25	35%	-	-	-	-	-	-	-	-
Phosphatidylinositol 3-kinase tor2	PAAG_01410	cluster580	DEG20010648	Serine/threonine-protein kinase mTOR	C		CC-223	Phase 1/2	Cancer	90%	3E-144	45%	-	-	-	-	-	-	-	-
Phosphatidylinositol 3-kinase tor2	PAAG_01410	cluster856	DEG20010648	Serine/threonine-protein kinase mTOR (Human)	C	C	Everolimus	approved	inhibitor	89%	3E-59	30%	-	-	-	-	-	-	-	-
Phosphatidylinositol 3-kinase tor2	PAAG_01410	cluster580	DEG20010648	Serine/threonine-protein kinase mTOR	C		GDC-0980/RG7422	Phase 2	Non-Hodgkin lymphoma	82%	0.0	65%	-	-	-	-	-	-	-	-
Phosphatidylinositol 3-kinase tor2	PAAG_01410	cluster580	DEG20010648	Serine/threonine-protein kinase mTOR	C		KD032	Discontinued in Phase 2	Non-small-cell lung carcinoma	92%	5E-121	35%	-	-	-	-	-	-	-	-
Phosphatidylinositol 3-kinase tor2	PAAG_01410	cluster580	DEG20010648	Serine/threonine-protein kinase mTOR	C		LY3023414	Phase 2	Cancer	89%	3E-59	30%	-	-	-	-	-	-	-	-
Phosphatidylinositol 3-kinase tor2	PAAG_01410	cluster580	DEG20010648	Serine/threonine-protein kinase mTOR	C		Tacrolimus	Approved	Restenosis	41%	2E-36	31%	-	-	-	-	-	-	-	-
Phosphatidylinositol 3-kinase tor2	PAAG_01410	cluster580	DEG20010648	Serine/threonine-protein kinase mTOR	C		OSI-027	Phase 2	Renal cancer	82%	7E-58	31%	-	-	-	-	-	-	-	-
Phosphatidylinositol 3-kinase tor2	PAAG_01410	cluster580	DEG20010648	Serine/threonine-protein kinase mTOR	C		PF-04691502	Phase 2	Endometrial cancer	71%	3E-173	57%	-	-	-	-	-	-	-	-
Phosphatidylinositol 3-kinase tor2	PAAG_01410	cluster580	DEG20010648	Serine/threonine-protein kinase mTOR	C		PF-05212384	Phase 2	Cancer	71%	3E-173	57%	-	-	-	-	-	-	-	-

Phosphatidylinositol 3-kinase tor2	PAAG_01410	cluster580	DEG20010648	Serine/threonine-protein kinase mTOR	C		Rapamycin	Approved	Multiple myeloma	71%	3E-173	57%	-	-	-	-	-	-	-	-
Phosphatidylinositol 3-kinase tor2	PAAG_01410	cluster580	DEG20010648	Serine/threonine-protein kinase mTOR	C		RG7422	Phase 2	Breast Cancer	78%	5E-177	62%	-	-	-	-	-	-	-	-
Phosphatidylinositol 3-kinase tor2	PAAG_01410	cluster580	DEG20010648	Serine/threonine-protein kinase mTOR	C		Ridaforolimus	Phase 3	Sarcoma	71%	3E-173	57%	-	-	-	-	-	-	-	-
Phosphatidylinositol 3-kinase tor2	PAAG_01410	cluster580	DEG20010648	Serine/threonine-protein kinase mTOR	C		SAR245409	Phase 2	Cancer	71%	3E-173	57%	-	-	-	-	-	-	-	-
Phosphatidylinositol 3-kinase tor2	PAAG_01410	cluster856	DEG20010648	Serine/threonine-protein kinase mTOR (Human)		C	SF1126	investigational		67%	2E-52	31%	-	-	-	-	-	-	-	-
Phosphatidylinositol 3-kinase tor2	PAAG_01410	cluster856	DEG20010648	Serine/threonine-protein kinase mTOR (Human)	C	C	Sirolimus	approved, investigational	inhibitor	71%	3E-173	57%	-	-	-	-	-	-	-	-
Phosphatidylinositol 3-kinase tor2	PAAG_01410	cluster856	DEG20010648	Serine/threonine-protein kinase mTOR (Human)	C	C	Temsirolimus	approved	inhibitor	11%	3E-15	38%	-	-	-	-	-	-	-	-
Phosphatidylinositol 3-kinase tor2	PAAG_01410	cluster856	DEG20010648	Serine/threonine-protein kinase mTOR (Human)	C	C	XL765	investigational		93%	0.0	38%	-	-	-	-	-	-	-	-
Phosphatidylinositol 3-kinase tor2	PAAG_01410	cluster580	DEG20010648	Serine/threonine-protein kinase mTOR	C		Zotarolimus	Approved	Cancer	82%	7E-58	31%	-	-	-	-	-	-	-	-
Phosphatidylinositol 3-kinase vps34	PAAG_04060	cluster52	DEG20010738	Phosphatidylinositol-4,5-bisphosphate 3-kinase catalytic subunit, gamma isoform	C		BAY 80-6946	Phase 3	Cancer	82%	7E-58	31%	-	-	-	-	-	-	-	-
Phosphatidylinositol 3-kinase vps34	PAAG_04060	cluster52	DEG20010738	Phosphatidylinositol-4,5-bisphosphate 3-kinase catalytic subunit, gamma isoform	C		Buparlisib	Phase 3	Breast cancer	98%	0.0	47%	-	-	-	-	-	-	-	-
Phosphatidylinositol 3-kinase vps34	PAAG_04060	cluster52	DEG20010738	Phosphatidylinositol-4,5-bisphosphate 3-kinase catalytic subunit, gamma isoform	C		BYL719	Phase 2	Solid tumors	88%	2E-25	35%	-	-	-	-	-	-	-	-
Phosphatidylinositol 3-kinase vps34	PAAG_04060	cluster52	DEG20010738	Phosphatidylinositol-4,5-bisphosphate 3-kinase catalytic subunit, gamma isoform	C		CHU	Registered	Type 2 diabetes	70%	1E-60	37%	-	-	-	-	-	-	-	-
Phosphatidylinositol 3-kinase vps34	PAAG_04060	cluster52	DEG20010738	Phosphatidylinositol-4,5-bisphosphate 3-kinase catalytic subunit, gamma isoform	C		GDC-0032	Phase 2/3	Solid tumours	96%	0.0	50%	-	-	-	-	-	-	-	-
Phosphatidylinositol 3-kinase vps34	PAAG_04060	cluster52	DEG20010738	Phosphatidylinositol-4,5-bisphosphate 3-kinase catalytic subunit, gamma isoform	C		GDC0941	Phase 2	Advanced solid tumours; non-Hodgkin¡¯s lymphoma	92%	5E-121	35%	-	-	-	-	-	-	-	-
Phosphatidylinositol 3-kinase vps34	PAAG_04060	cluster52	DEG20010738	Phosphatidylinositol-4,5-bisphosphate 3-kinase catalytic subunit, gamma isoform	C		IPI-145	Phase 3	Arthritis	41%	2E-36	31%	-	-	-	-	-	-	-	-
Phosphatidylinositol 3-kinase vps34	PAAG_04060	cluster52	DEG20010738	Phosphatidylinositol-4,5-bisphosphate 3-kinase catalytic subunit, gamma isoform	C		PX-866	Phase 2	Cancer	82%	0.0	65%	-	-	-	-	-	-	-	-
Phosphatidylinositol 3-kinase vps34	PAAG_04060	cluster52	DEG20010738	Phosphatidylinositol-4,5-bisphosphate 3-kinase catalytic subunit, gamma isoform	C		TG100-115	Phase 1/2	Angioedema, Myocardial infarction	70%	3E-151	49%	-	-	-	-	-	-	-	-
Phosphatidylinositol 3-kinase vps34	PAAG_04060	cluster52	DEG20010738	Phosphatidylinositol-4,5-bisphosphate 3-kinase catalytic subunit, gamma isoform	C		XL147	Phase 2	Cancer	89%	3E-59	30%	-	-	-	-	-	-	-	-

Phosphodiesterase	PAAG_00819	cluster29	Without similarity	CAMP-specific 3',5'-cyclic phosphodiesterase 4A	C		YM-976	Discontinued in Phase 1	Asthma	94%	1E-124	40%	-	-	-	-	-	-	-	-
Phospholipase D1	PAAG_08849	cluster205	Without similarity	Phospholipase D1 (Human)		C	LAX-101	investigational		82%	0.0	65%	-	-	-	-	-	-	-	-
Probable 4-hydroxyphenylpyruvate dioxygenase 2	PAAG_08166	cluster200	Without similarity	4-hydroxyphenylpyruvate dioxygenase	C	C	Nitisinone	Approved	Hereditary tyrosinemia type 1	64%	2E-91	31%	-	-	-	-	-	-	-	-
Probable alpha-galactosidase B	PAAG_05254	cluster921	Without similarity	Alpha-galactosidase A (Human)	C	C	Migalastat	investigational		92%	5E-121	35%	-	-	-	-	-	-	-	-
Probable dipeptidyl-aminopeptidase B	PAAG_06844	cluster367	Without similarity	Dipeptidyl peptidase 4 (Human)	C	C	Alogliptin	approved	inhibitor	94%	3E-137	51%	-	-	-	-	-	-	-	-
Probable dipeptidyl-aminopeptidase B	PAAG_06844	cluster367	Without similarity	Dipeptidyl peptidase 4 (Human)	C	C	KRP-104	investigational		97%	0.0	41%	-	-	-	-	-	-	-	-
Probable dipeptidyl-aminopeptidase B	PAAG_06844	cluster367	Without similarity	Dipeptidyl peptidase 4 (Human)		C	PHX1149	investigational		82%	7E-58	31%	-	-	-	-	-	-	-	-
Probable dipeptidyl-aminopeptidase B	PAAG_06844	cluster367	Without similarity	Dipeptidyl peptidase 4 (Human)	C	C	PSN9301	investigational		71%	3E-173	57%	-	-	-	-	-	-	-	-
Probable D-xylulose reductase A	PAAG_11383	cluster189	Without similarity	Fatty acid synthase (Human)		C	Orlistat	approved, investigational	inhibitor	82%	5E-96	44%	-	-	-	-	-	-	-	-
Probable glucose-6-phosphate 1-dehydrogenase C7.13c	PAAG_00633	cluster800	Without similarity	Glucose-6-phosphate 1-dehydrogenase (Human)		C	16-Bromoepiandrosterone	investigational		94%	2E-133	50%	-	-	-	-	-	-	-	-
Probable succinate dehydrogenase [ubiquinone] flavoprotein subunit, mitochondrial	PAAG_04238	cluster210	Without similarity	Fumarate reductase flavoprotein subunit	C		Morantel tartrate	Approved	Mature gastrointestinal nematode infections	88%	2E-25	35%	-	-	-	-	-	-	-	-
Probable succinate dehydrogenase [ubiquinone] flavoprotein subunit, mitochondrial	PAAG_04238	cluster210	Without similarity	Fumarate reductase flavoprotein subunit	C		Oxantel pamoate	Approved	Trichuris trichiura infection	79%	1E-107	36%	-	-	-	-	-	-	-	-
Probable succinate dehydrogenase [ubiquinone] flavoprotein subunit, mitochondrial	PAAG_04238	cluster210	Without similarity	Fumarate reductase flavoprotein subunit	C		Thiabendazole	Approved	Helminth infection	82%	0.0	65%	-	-	-	-	-	-	-	-
Proteasome subunit beta type	PAAG_01150	cluster241	DEG20011080	Proteasome subunit beta type-8 (Human)		C	Carfilzomib	approved	inhibitor	56%	5E-84	31%	-	-	-	-	-	-	-	-
Protein kinase C	PAAG_02441	cluster28	DEG20010032	PKC-Delta	C		4-HYDROXYTAMOXIFEN	Phase 2	Discovery agent	98%	6E-43	40%	-	-	-	-	-	-	-	-
Protein kinase C	PAAG_02441	cluster28	DEG20010032	Protein kinase C, alpha type	C		RUBOXISTAURIN	Phase 3	Lymphoma	41%	2E-36	31%	-	-	-	-	-	-	-	-
Protein kinase C	PAAG_02441	cluster28	DEG20010032	Protein kinase C gamma type	C		Bryostatin-1	Phase 2	Discovery agent	97%	0.0	59%	-	-	-	-	-	-	-	-
Protein kinase C	PAAG_02441	cluster29	DEG20010032	Protein kinase C		C	Tamoxifen	approved		99%	5E-49	60%	-	-	-	-	-	-	-	-
Protein kinase C	PAAG_02441	cluster29	DEG20010032	Protein kinase C alpha type (Human)		C	Ingenol Mebutate	approved	ligand	93%	0.0	65%	-	-	-	-	-	-	-	-
Protein kinase C	PAAG_02441	cluster29	DEG20010032	Protein kinase C epsilon type (Human)		C	KAI-1455	investigational		99%	0.0	66%	-	-	-	-	-	-	-	-
Protein kinase C	PAAG_02441	cluster28	DEG20010032	PKC-Delta	C		KAI-9803/ BMS-875944	Phase 1/2	Prevention of reperfusion injury following acute myocardial infarction (Fast Track)	67%	2E-52	31%	-	-	-	-	-	-	-	-
Protein kinase C	PAAG_02441	cluster28	DEG20010032	Protein kinase C, beta type	C		LY333531	Phase 2	Cancer	89%	3E-59	30%	-	-	-	-	-	-	-	-
Protein kinase C	PAAG_02441	cluster28	DEG20010032	Protein kinase C gamma type	C		Midostaurin	Phase 2	Colon, breast, CLL, AML, GIST, solid tumours & non-Hodgkin's lymphoma	41%	2E-36	31%	-	-	-	-	-	-	-	-
Protein kinase C	PAAG_02441	cluster28	DEG20010032	Protein kinase C, alpha type	C		Sotrastaurin acetate	Phase 2	Renal Transplantation	41%	2E-36	31%	-	-	-	-	-	-	-	-
Protein kinase gsk3	PAAG_03659	cluster624	Without similarity	Glycogen synthase kinase-3 beta	C		CI-1040	Phase 2	Discovery agent	82%	0.0	65%	-	-	-	-	-	-	-	-
Protein kinase gsk3	PAAG_03659	cluster624	Without similarity	Glycogen synthase kinase-3 beta	C		Enzastaurin	Phase 2	Glioblastoma Multiforme	71%	3E-173	57%	-	-	-	-	-	-	-	-
Protein kinase gsk3	PAAG_03659	cluster624	Without similarity	Glycogen synthase kinase-3 beta	C		LY2090314	Phase 2	Cancer	41%	2E-36	31%	-	-	-	-	-	-	-	-
Protein kinase gsk3	PAAG_03659	cluster624	Without similarity	Glycogen synthase kinase-3 beta	C		Neu-120	Phase 1/2	Parkinson's disease	70%	3E-151	49%	-	-	-	-	-	-	-	-
Protein kinase gsk3	PAAG_03659	cluster624	Without similarity	Glycogen synthase kinase-3 beta	C		tideglusib	Phase 2	Osteosarcoma	92%	5E-121	35%	-	-	-	-	-	-	-	-

Putative alanine aminotransferase	PAAG_08207	cluster287	Without similarity	Alanine aminotransferase 2 (Human)		C	Phenelzine	approved	inhibitor	92%	5E-121	35%	-	-	-	-	-	-	-	-
Putative branched-chain-amino-acid aminotransferase TOXF	PAAG_04401	cluster223	Without similarity	Branched-chain-amino-acid aminotransferase, cytosolic (Human)		C	Gabapentin	approved, investigational	inhibitor	92%	5E-121	35%	-	-	-	-	-	-	-	-
Putative dipeptidase UREG_03382	PAAG_02915	cluster907	Without similarity	Dipeptidase 1 (Human)	C	C	Cilastatin	approved	inhibitor	94%	3E-137	51%	-	-	-	-	-	-	-	-
Putative inosine-5'-monophosphate dehydrogenase-like protein YAR075W	PAAG_05803	cluster282	Without similarity	Inosine-5'-monophosphate dehydrogenase (Human)		C	Mercaptopurine	approved	Inhibitor	94%	3E-137	51%	-	-	-	-	-	-	-	-
Putative inosine-5'-monophosphate dehydrogenase-like protein YAR075W	PAAG_05803	cluster282	Without similarity	Inosine-5'-monophosphate dehydrogenase 2 (Human)	C	C	Mycophenolate mofetil	approved, investigational	inhibitor	82%	0.0	65%	-	-	-	-	-	-	-	-
Putative inosine-5'-monophosphate dehydrogenase-like protein YAR075W	PAAG_05803	cluster282	Without similarity	Inosine-5'-monophosphate dehydrogenase 2 (Human)	C	C	Mycophenolic acid	approved	inhibitor	97%	6E-129	47%	-	-	-	-	-	-	-	-
Putative inosine-5'-monophosphate dehydrogenase-like protein YAR075W	PAAG_05803	cluster282	Without similarity	Inosine-5'-monophosphate dehydrogenase 2 (Human)		C	Ribavirin	approved		61%	3E-136	48%	-	-	-	-	-	-	-	-
Putative inosine-5'-monophosphate dehydrogenase-like protein YAR075W	PAAG_05803	cluster282	Without similarity	Inosine-5'-monophosphate dehydrogenase 2 (Human)		C	VX-148	investigational		82%	0.0	65%	-	-	-	-	-	-	-	-
Putative metallocarboxypeptidase ECM14	PAAG_09024	cluster786	Without similarity	Carboxypeptidase B2 (Thermobifida fusca (strain YX))		C	AZD-9684	investigational		94%	1E-59	34%	-	-	-	-	-	-	-	-
Putative purine nucleoside phosphorylase	PAAG_08438	cluster852	Without similarity	Purine nucleoside phosphorylase (Human)		C	Didanosine	approved		41%	2E-36	31%	-	-	-	-	-	-	-	-
Putative purine nucleoside phosphorylase	PAAG_08438	cluster852	Without similarity	Purine nucleoside phosphorylase (Human)		C	Inosine	investigational		97%	6E-129	47%	-	-	-	-	-	-	-	-
Putative succinate-semialdehyde dehydrogenase C1002.12c [NADP(+)]	PAAG_05249	cluster98	Without similarity	Aldehyde dehydrogenase, mitochondrial (Human)		C	Disulfiram	approved	inhibitor	79%	1E-76	30%	-	-	-	-	-	-	-	-
Putative succinate-semialdehyde dehydrogenase C1002.12c [NADP(+)]	PAAG_05249	cluster98	Without similarity	Aldehyde dehydrogenase, mitochondrial (Human)		C	Nitric Oxide	approved	inhibitor	44%	1E-82	45%	-	-	-	-	-	-	-	-
Putative zinc protease mug138	PAAG_04661	cluster932	Without similarity	Insulin-degrading enzyme (Human)	C	C	Bacitracin	approved, vet_approved	inhibitor	71%	3E-173	57%	-	-	-	-	-	-	-	-
Putative zinc protease mug138	PAAG_04661	cluster932	Without similarity	Insulin-degrading enzyme (Human)		C	Insulin Human	approved, investigational		92%	5E-121	35%	-	-	-	-	-	-	-	-
Putative zinc protease mug138	PAAG_04661	cluster932	Without similarity	Insulin-degrading enzyme (Human)		C	Insulin Pork	approved		70%	3E-151	49%	-	-	-	-	-	-	-	-
RAC-alpha serine/threonine-protein kinase	PAAG_05449	cluster614	DEG20010982	MARK3	C		7-hydroxystaurosporine	Discontinued in Phase 2	Renal cell carcinoma; Melanoma and lymphoma; Small cell lung cancer	82%	0.0	65%	-	-	-	-	-	-	-	-
RAC-alpha serine/threonine-protein kinase	PAAG_05449	cluster614	DEG20010982	MARK3	C		CBP-501	Phase 1/2	Mesothelioma	94%	0.0	65%	-	-	-	-	-	-	-	-
Ribonucleoside-diphosphate reductase large chain	PAAG_07682	cluster778	Without similarity	Ribonucleoside-diphosphate reductase large subunit (Human)		C	Cladribine	approved, investigational	inhibitor	82%	0.0	65%	-	-	-	-	-	-	-	-
Ribonucleoside-diphosphate reductase large chain	PAAG_07682	cluster778	Without similarity	Ribonucleoside-diphosphate reductase large subunit (Human)	C	C	Clofarabine	approved, investigational	inhibitor	70%	3E-151	49%	-	-	-	-	-	-	-	-
Ribonucleoside-diphosphate reductase large chain	PAAG_07682	cluster577	Without similarity	Ribonucleoside-diphosphate reductase	C		Didox	Discontinued in Phase 2	Cancer	41%	2E-36	31%	-	-	-	-	-	-	-	-
Ribonucleoside-diphosphate reductase large chain	PAAG_07682	cluster778	Without similarity	Ribonucleoside-diphosphate reductase large subunit (Human)		C	Fludarabine	approved	inhibitor	71%	3E-173	57%	-	-	-	-	-	-	-	-

Ribonucleoside-diphosphate reductase large chain	PAAG_07682	cluster577	Without similarity	Ribonucleoside-diphosphate reductase	C		G-207 virus construct	Phase 1/2	Glioma	99%	5E-49	60%	-	-	-	-	-	-	-	-
Ribonucleoside-diphosphate reductase large chain	PAAG_07682	cluster778	Without similarity	Ribonucleoside-diphosphate reductase large subunit (Human)	C	C	Gallium maltolate	investigational		70%	3E-151	49%	-	-	-	-	-	-	-	-
Ribonucleoside-diphosphate reductase large chain	PAAG_07682	cluster778	Without similarity	Ribonucleoside-diphosphate reductase large subunit (Human)	C	C	Gemcitabine	approved	inhibitor	73%	1E-29	31%	0.59	-3.67	3NRS	X-ray, 1.80 Å	28.00%	88%	Receptor	-9.102.103
Ribonucleoside-diphosphate reductase large chain	PAAG_07682	cluster778	Without similarity	Ribonucleoside-diphosphate reductase large subunit (Human)	C	C	Hydroxyurea	approved	inhibitor	94%	0.0	78%	0.59	1.18	5FPN	X-ray, 2.0Å	93%	75.33%	Receptor1	-9.112.286
Ribonucleoside-diphosphate reductase large chain	PAAG_07682	cluster778	Without similarity	Ribonucleoside-diphosphate reductase large subunit (Human)		C	Imexon	investigational		83%	8E-96	50%	-	-	-	-	-	-	-	-
Ribonucleoside-diphosphate reductase large chain	PAAG_07682	cluster577	Without similarity	Ribonucleoside-diphosphate reductase	C		MDL 101,731	Discontinued in Phase 2	Gastric cancer	44%	1E-82	45%	-	-	-	-	-	-	-	-
Ribonucleoside-diphosphate reductase large chain	PAAG_07682	cluster577	Without similarity	Ribonucleoside-diphosphate reductase	C		Resveratrol	Phase 4	Discovery agent	92%	5E-121	35%	-	-	-	-	-	-	-	-
Ribonucleoside-diphosphate reductase large chain	PAAG_07682	cluster577	Without similarity	Ribonucleoside-diphosphate reductase	C		Triapine	Phase 2	Nerve injury	89%	4E-72	32%	-	-	-	-	-	-	-	-
Ribonucleotide reductase R2 subunit	PAAG_02499	cluster589	DEG20010539	Ribonucleoside-diphosphate reductase subunit M2	C		CO-101	Phase 2	Metastatic pancreatic	93%	0.0	65%	-	-	-	-	-	-	-	-
Serine hydroxymethyltransferase, cytosolic	PAAG_07412	cluster107	Without similarity	Serine hydroxymethyltransferase, cytosolic (Human)		C	Mimosine	approved	inhibitor	71%	3E-173	57%	-	-	-	-	-	-	-	-
Serine/threonine-protein kinase	PAAG_08991	cluster84	DEG20011048	Serine/threonine-protein kinase 6	C		Ilorasertib	Phase 2	Cancer	99%	5E-49	60%	-	-	-	-	-	-	-	-
Serine/threonine-protein kinase	PAAG_08991	cluster257	DEG20011048	Aurora kinase B (Human)	C	C	AT9283	investigational		100%	1E-72	84%	0.96	2.10	1RFJ	X-ray, 2.00 Å	82.30%	100%	Receptor1	-7.095.743
Serine/threonine-protein kinase	PAAG_08991	cluster84	DEG20011048	Serine/threonine protein kinase 12	C		AZD1152	Phase 1/2	Acute Myeloid Leukemia, Haematological malignancies	100%	1E-72	84%	0.96	2.10	1RFJ	X-ray, 2.00 Å	82.30%	100%	Receptor1	-4.571.194
Serine/threonine-protein kinase	PAAG_08991	cluster257	DEG20011048	Aurora kinase A		C	CYC116	investigational		100%	1E-72	84%	0.96	2.10	1RFJ	X-ray, 2.00 Å	82.30%	100%	Receptor2	-6.001.137
Serine/threonine-protein kinase	PAAG_08991	cluster84	DEG20011048	Serine/threonine-protein kinase 6	C		ENMD-2076	Phase 2	Acute myeloid leukemia	100%	1E-72	84%	0.96	2.10	1RFJ	X-ray, 2.00 Å	82.30%	100%	Receptor1	-4.279.902
Serine/threonine-protein kinase	PAAG_08991	cluster84	DEG20011048	Serine/threonine-protein kinase 6	C		MLN8237	Phase 3	Cancer	86%	1E-39	49%	0.96	2.10	1RFJ	X-ray, 2.00 Å	82.30%	100%	No molcharge	No molcharge
Serine/threonine-protein kinase	PAAG_08991	cluster84	DEG20011048	Serine/threonine-protein kinase 6	C		PHA-680632	Phase 2	Chronic myelogenous leukemia	100%	1E-72	84%	0.96	2.10	1RFJ	X-ray, 2.00 Å	82.30%	100%	Receptor2	-4.548.096
Serine/threonine-protein kinase	PAAG_08991	cluster84	DEG20011048	Serine/threonine protein kinase 12	C		PHA-739358	Phase 2	Prostate Cancer	90%	2E-138	58%	-	-	-	-	-	-	-	-
Serine/threonine-protein kinase	PAAG_08991	cluster84	DEG20011048	Serine/threonine protein kinase 12	C		Tozasertib	Phase 2	Solid Tumors	82%	7E-58	31%	-	-	-	-	-	-	-	-
Serine/threonine-protein kinase pef1	PAAG_06020	cluster258	Without similarity	Dual specificity mitogen-activated protein kinase kinase 1 (Human)		C	Cobimetinib	approved	inhibitor	100%	1E-72	84%	0.96	2.10	1RFJ	X-ray, 2.00 Å	82.30%	100%	Receptor1	-6.849.002
Serine/threonine-protein kinase pef1	PAAG_06020	cluster258	Without similarity	Dual specificity mitogen-activated protein kinase kinase 1 (Human)	C	C	Trametinib	approved	inhibitor	100%	1E-72	84%	0.96	2.10	1RFJ	X-ray, 2.00 Å	82.30%	100%	Receptor1	-6.120.092
Serine/threonine-protein kinase SAPK2	PAAG_03141	cluster599	DEG20010785	Serine/threonine-protein kinase PLK1	C		BI 2536	Phase 2	Acute myeloid leukemia	86%	1E-39	49%	0.96	2.10	1RFJ	X-ray, 2.00 Å	82.30%	100%	Receptor1	-6.197.558
Serine/threonine-protein kinase SAPK2	PAAG_03141	cluster599	DEG20010785	Serine/threonine-protein kinase PLK1	C		BI 6727	Phase 3	Acute myeloid leukemia	87%	2E-39	44%	-	-	-	-	-	-	-	-
Serine/threonine-protein kinase SAPK2	PAAG_03141	cluster599	DEG20010785	Serine/threonine-protein kinase PLK1	C		Rigosertib	Phase 3	Solid Tumors	92%	5E-121	35%	-	-	-	-	-	-	-	-
Serine/threonine-protein kinase SAPK2	PAAG_03141	cluster599	DEG20010785	Serine/threonine-protein kinase PLK1	C		Volasertib	Phase 2	Acute myeloid leukemia	100%	1E-72	84%	0.96	2.10	1RFJ	X-ray, 2.00 Å	82.30%	100%	Receptor2	-5.094.836
Squalene monooxygenase	PAAG_08773	cluster210	DEG20010428	Squalene monooxygenase (Human)	C	C	Butenafine	approved	inhibitor	92%	5E-121	35%	-	-	-	-	-	-	-	-

Squalene monooxygenase	PAAG_08773	cluster604	DEG20010428	Squalene monooxygenase	C	C	Naftifine	Approved	Fungal infections	41%	2E-36	31%	-	-	-	-	-	-	-	-
Squalene monooxygenase	PAAG_08773	cluster210	DEG20010428	Squalene monooxygenase (Human)		C	NM100060	investigational		82%	0.0	65%	-	-	-	-	-	-	-	-
Squalene monooxygenase	PAAG_08773	cluster604	DEG20010428	Squalene monooxygenase	C	C	Terbinafine	Approved	Fungal infections	89%	3E-59	30%	-	-	-	-	-	-	-	-
Squalene monooxygenase	PAAG_08773	cluster604	DEG20010428	Squalene monooxygenase	C	C	Tolnaftate	Approved	Jock itch; Athlete's foot	100%	1E-72	84%	0.96	2.10	1RFJ	X-ray, 2.00 Å	82.30%	100%	Receptor1	-3.982.033
Sterol O-acyltransferase 2	PAAG_07527	cluster588	Without similarity	Diglyceride acyltransferase	C		DS-7250	Discontinued in Phase 1	Diabetes	100%	1E-72	84%	0.96	2.10	1RFJ	X-ray, 2.00 Å	82.30%	100%	Receptor2	-4.141.906
Sterol O-acyltransferase 2	PAAG_07527	cluster588	Without similarity	Diglyceride acyltransferase	C	C	Hesperetin	Approved	High Cholesterol level	92%	5E-121	35%	-	-	-	-	-	-	-	-
Sterol O-acyltransferase 2	PAAG_07527	cluster588	Without similarity	Diglyceride acyltransferase	C		JTT-553	Discontinued in Phase 1	Obesity	100%	1E-72	84%	0.96	2.10	1RFJ	X-ray, 2.00 Å	82.30%	100%	Receptor1	-7.156.701
Sterol O-acyltransferase 2	PAAG_07527	cluster588	Without similarity	Diglyceride acyltransferase	C		LCQ908	Phase 3	Familial chylomicronemia syndrome	92%	5E-121	35%	-	-	-	-	-	-	-	-
Superoxide dismutase [Cu-Zn]	PAAG_04164	cluster893	Without similarity	Superoxide dismutase [Cu-Zn] (Human)		C	Arimoclomol	investigational		71%	3E-173	57%	-	-	-	-	-	-	-	-
Superoxide dismutase [Cu-Zn]	PAAG_04164	cluster893	Without similarity	Superoxide dismutase [Cu-Zn] (Human)		C	Carboplatin	approved		100%	1E-72	84%	0.96	2.10	1RFJ	X-ray, 2.00 Å	82.30%	100%	Receptor1	-6.441.166
Thioredoxin reductase	PAAG_07020	cluster572	DEG20010230	Thioredoxin reductase, cytoplasmic	C		Auranofin	Approved	Inflammatory arthritis	93%	0.0	65%	-	-	-	-	-	-	-	-
Thioredoxin reductase	PAAG_07020	cluster572	DEG20010230	Thioredoxin reductase, cytoplasmic	C		Fotemustine	Approved	Cancer	100%	1E-72	84%	0.96	2.10	1RFJ	X-ray, 2.00 Å	82.30%	100%	Receptor1	-6.933.275
Thioredoxin-1	PAAG_02364	cluster630	Without similarity	Thioredoxin	C		PX-12	Phase 2	Cancer	100%	1E-72	84%	0.96	2.10	1RFJ	X-ray, 2.00 Å	82.30%	100%	Receptor1	-7.485.557
Thymidylate synthase	PAAG_08597	cluster600	DEG20010950	Thymidylate synthase	C		Irinotecan	Approved	Colon cancer	70%	3E-151	49%	-	-	-	-	-	-	-	-
Thymidylate synthase	PAAG_08597	cluster600	DEG20010950	Thymidylate synthase	C		Capecitabine	Approved	Colorectal cancer	100%	1E-72	84%	0.96	2.10	1RFJ	X-ray, 2.00 Å	82.30%	100%	Receptor1	-6.386.691
Thymidylate synthase	PAAG_08597	cluster600	DEG20010950	Thymidylate synthase	C		EMITEFUR	Discontinued in Preregistration	Solid tumours	72%	3E-136	52%	-	-	-	-	-	-	-	-
Thymidylate synthase	PAAG_08597	cluster600	DEG20010950	Thymidylate synthase	C		Floxuridine	Approved	Colorectal cancer	100%	1E-72	84%	0.96	2.10	1RFJ	X-ray, 2.00 Å	82.30%	100%	Receptor1	-5.769.975
Thymidylate synthase	PAAG_08597	cluster600	DEG20010950	Thymidylate synthase	C	C	Flucytosine	Approved	Endocarditis	98%	1E-143	61%	0.74	-1.38	2AAZ	X-ray, 2.08 Å	63.82%	84%	Receptor1	-10.837.160
Thymidylate synthase	PAAG_08597	cluster600	DEG20010950	Thymidylate synthase	C		Fluorouracil	Approved	Cancers	98%	1E-143	61%	0.74	-1.38	2AAZ	X-ray, 2.08 Å	63.82%	84%	Receptor1	-10.433.535
Thymidylate synthase	PAAG_08597	cluster600	DEG20010950	Thymidylate synthase	C		FO-152	Discontinued in Phase 2	Cancer	82%	7E-58	31%	-	-	-	-	-	-	-	-
Thymidylate synthase	PAAG_08597	cluster600	DEG20010950	Thymidylate synthase	C		GALOCITABINE	Discontinued in Phase 3	Solid tumours	98%	1E-143	61%	0.74	-1.38	2AAZ	X-ray, 2.08 Å	63.82%	84%	Receptor1	-9.862.947
Thymidylate synthase	PAAG_08597	cluster600	DEG20010950	Thymidylate synthase	C		Leucovorin	Approved	Colon Cancer	94%	1E-59	34%	-	-	-	-	-	-	-	-
Thymidylate synthase	PAAG_08597	cluster600	DEG20010950	Thymidylate synthase	C		LY231514	Phase III	Non-squamous Non-small Cell Lung Cancer	98%	1E-143	61%	0.74	-1.38	2AAZ	X-ray, 2.08 Å	63.82%	84%	Receptor2	-12.402.100
Thymidylate synthase	PAAG_08597	cluster600	DEG20010950	Thymidylate synthase	C		NB1011	Phase 1/2	Breast cancer	98%	1E-143	61%	0.74	-1.38	2AAZ	X-ray, 2.08 Å	63.82%	84%	Receptor2	-8.671.154
Thymidylate synthase	PAAG_08597	cluster600	DEG20010950	Thymidylate synthase	C		Nolatrexed	Phase 3	Solid tumours	98%	1E-143	61%	0.74	-1.38	2AAZ	X-ray, 2.08 Å	63.82%	84%	Receptor2	-7.388.129
Thymidylate synthase	PAAG_08597	cluster600	DEG20010950	Thymidylate synthase	C	C	Pemetrexed	Approved	Pleural mesothelioma	30%	8E-35	31%	-	-	-	-	-	-	-	-
Thymidylate synthase	PAAG_08597	cluster600	DEG20010950	Thymidylate synthase	C		Plevitrexed	Phase 2	Advanced gastric cancer	88%	5E-98	33%	-	-	-	-	-	-	-	-
Thymidylate synthase	PAAG_08597	cluster600	DEG20010950	Thymidylate synthase	C		PREMETREXED	Phase 2	Discovery agent	98%	1E-143	61%	0.74	-1.38	2AAZ	X-ray, 2.08 Å	63.82%	84%	Receptor2	-12.808.945
Thymidylate synthase	PAAG_08597	cluster600	DEG20010950	Thymidylate synthase	C		Raltitrexed	Approved	Colon cancer; Rectal cancer	86%	3E-180	65%	-	-	-	-	-	-	-	-
Thymidylate synthase	PAAG_08597	cluster600	DEG20010950	Thymidylate synthase	C		Trifluridine	Approved	Viral Infection	99%	5E-49	60%	-	-	-	-	-	-	-	-
Thymidylate synthase	PAAG_08597	cluster600	DEG20010950	Thymidylate synthase	C		TT-62	Discontinued in Phase 2	Viral infections	98%	0.0	64%	-	-	-	-	-	-	-	-
Thymidylate synthase	PAAG_08597	cluster600	DEG20010950	Thymidylate synthase	C		ZD9331	Discontinued in Phase 2	Discovery agent	98%	1E-143	61%	0.74	-1.38	2AAZ	X-ray, 2.08 Å	63.82%	84%	Receptor1	-10.605.972

Transcription activator MSS11	PAAG_01233	cluster117	Without similarity	NAD-dependent protein deacylase sirtuin-5, mitochondrial (Human)	C	C	Nicotinamide	approved		41%	2E-36	31%	-	-	-	-	-	-	-	-
Transcription activator MSS11	PAAG_01233	cluster117	Without similarity	NAD-dependent protein deacylase sirtuin-5, mitochondrial (HUman)		C	Suramin	approved	inhibitor	72%	4E-80	44%	-	-	-	-	-	-	-	-
Transcription elongation factor SPT5	PAAG_05679	cluster220	Without similarity	Heat shock protein HSP 90-beta (Human)	C	C	CNF1010	investigational		98%	1E-143	61%	0.74	-1.38	2AAZ	X-ray, 2.08 Å	63.82%	84%	Receptor1	-12.161.037
Transcription elongation factor SPT5	PAAG_05679	cluster220	Without similarity	Heat shock protein HSP 90-alpha (Human)		C	Nedocromil	approved		70%	3E-151	49%	-	-	-	-	-	-	-	-
Transcription elongation factor SPT5	PAAG_05679	cluster220	Without similarity	Heat shock protein HSP 90-alpha (Human)		C	Rifabutin	approved	other / unknown	78%	5E-177	62%	-	-	-	-	-	-	-	-
Transcription elongation factor SPT5	PAAG_05679	cluster220	Without similarity	Heat shock protein HSP 90-beta (Human)	C	C	SNX-5422	investigational		99%	5E-49	60%	-	-	-	-	-	-	-	-
Transcription elongation factor SPT5	PAAG_07037	cluster858	Without similarity	Calnexin (Human)		C	Tenecteplase	approved		71%	3E-173	57%	-	-	-	-	-	-	-	-
Tubulin alpha chain	PAAG_12506	cluster39	DEG20010773	Tubulin alpha-4A chain (Human)		C	Cabazitaxel	approved	binder	41%	2E-36	31%	-	-	-	-	-	-	-	-
Tubulin alpha chain	PAAG_12506	cluster39	DEG20010773	Tubulin alpha-4A chain (Human)		C	Vincristine	approved, investigational	inhibitor	30%	8E-35	31%	-	-	-	-	-	-	-	-
Tubulin beta chain	PAAG_03031	cluster606	DEG20010326	Tubulin beta	C		2-Methoxyestradiol	Phase 2	Pulmonary arterial hypertension	41%	2E-36	31%	-	-	-	-	-	-	-	-
Tubulin beta chain	PAAG_03031	cluster606	DEG20010326	Tubulin beta	C		ABT-751	Phase 2	Solid tumours	98%	1E-143	61%	0.74	-1.38	2AAZ	X-ray, 2.08 Å	63.82%	84%	Receptor1	-13.799.118
Tubulin beta chain	PAAG_03031	cluster32	DEG20010326	Tubulin beta-4B chain (Human)	C	C	Albendazole	approved, vet_approved	inhibitor	98%	1E-143	61%	0.74	-1.38	2AAZ	X-ray, 2.08 Å	63.82%	84%	Receptor1	-8.669.285
Tubulin beta chain	PAAG_03031	cluster606	DEG20010326	Tubulin beta	C		BAL-101553	Phase 1/2	Cancer	98%	1E-143	61%	0.74	-1.38	2AAZ	X-ray, 2.08 Å	63.82%	84%	Receptor2	-12.768.442
Tubulin beta chain	PAAG_03031	cluster606	DEG20010326	Tubulin beta	C		Batabulin	Phase 2/3	Cancer	70%	3E-151	49%	-	-	-	-	-	-	-	-
Tubulin beta chain	PAAG_03031	cluster32	DEG20010326	Tubulin beta chain (Human)		C	CA4P	investigational		98%	0.0	47%	-	-	-	-	-	-	-	-
Tubulin beta chain	PAAG_03031	cluster606	DEG20010326	Tubulin beta	C		CEMADOTIN HYDROCHLORIDE	Discontinued in Phase 2	Cancer	70%	3E-151	49%	-	-	-	-	-	-	-	-
Tubulin beta chain	PAAG_03031	cluster32	DEG20010326	Tubulin beta chain (Human)		C	Colchicine	approved	inhibitor	62%	2E-81	30%	-	-	-	-	-	-	-	-
Tubulin beta chain	PAAG_03031	cluster606	DEG20010326	Tubulin beta	C		DOLASTATIN-10	Phase 2	Cancer	67%	2E-52	31%	-	-	-	-	-	-	-	-
Tubulin beta chain	PAAG_03031	cluster32	DEG20010326	Tubulin beta-4B chain (Human)		C	Epothilone B	experimental, investigational		83%	5E-98	45%	-	-	-	-	-	-	-	-
Tubulin beta chain	PAAG_03031	cluster32	DEG20010326	Tubulin beta-4B chain (Human)		C	Epothilone D	experimental, investigational		67%	2E-52	31%	-	-	-	-	-	-	-	-
Tubulin beta chain	PAAG_03031	cluster32	DEG20010326	Tubulin beta-3 chain (Human)		C	Ixabepilone	approved, investigational	inhibitor	82%	7E-58	31%	-	-	-	-	-	-	-	-
Tubulin beta chain	PAAG_03031	cluster606	DEG20010326	Tubulin beta	C		Lexibulin	Phase 2	Glioblastoma	56%	5E-84	31%	-	-	-	-	-	-	-	-
Tubulin beta chain	PAAG_03031	cluster32	DEG20010326	Tubulin beta-4B chain (Human)	C	C	Mebendazole	approved, vet_approved	inhibitor	98%	1E-143	61%	0.74	-1.38	2AAZ	X-ray, 2.08 Å	63.82%	84%	Receptor1	-12.900.719
Tubulin beta chain	PAAG_03031	cluster32	DEG20010326	Tubulin beta-4B chain (Human)		C	Oxibendazole	investigational, vet_approved		98%	1E-143	61%	0.74	-1.38	2AAZ	X-ray, 2.08 Å	63.82%	84%	Receptor1	-9.840.592
Tubulin beta chain	PAAG_03031	cluster606	DEG20010326	Tubulin beta	C	C	Paclitaxel	Phase 2	Cancers	98%	1E-143	61%	0.74	-1.38	2AAZ	X-ray, 2.08 Å	63.82%	84%	Receptor1	-13.799.118
Tubulin beta chain	PAAG_03031	cluster32	DEG20010326	Tubulin beta chain (Human)		C	Podofilox	approved	inhibitor	98%	4E-30	33%	-	-	-	-	-	-	-	-
Tubulin beta chain	PAAG_03031	cluster606	DEG20010326	Tubulin beta	C		RHIZOXIN	Discontinued in Phase 2	Breast cancer	98%	1E-143	61%	0.74	-1.38	2AAZ	X-ray, 2.08 Å	63.82%	84%	Receptor1	-13.317.190
Tubulin beta chain	PAAG_03031	cluster606	DEG20010326	Tubulin beta	C		S-12363	Discontinued in Phase 2	Cancer	82%	7E-58	31%	-	-	-	-	-	-	-	-
Tubulin beta chain	PAAG_03031	cluster606	DEG20010326	Tubulin beta	C		T-607	Phase 2	Cancer	98%	1E-143	61%	0.74	-1.38	2AAZ	X-ray, 2.08 Å	63.82%	84%	Receptor2	-12.803.749
Tubulin beta chain	PAAG_03031	cluster32	DEG20010326	Tubulin beta chain (Human)		C	Vinblastine	approved	adduct	98%	1E-143	61%	0.74	-1.38	2AAZ	X-ray, 2.08 Å	63.82%	84%	Receptor2	-11.501.788
Tubulin beta chain	PAAG_03031	cluster606	DEG20010326	Tubulin beta	C		Vindesine	Approved	Acute lymphoblastic leukemia	94%	8E-118	51%	-	-	-	-	-	-	-	-

Tubulin beta chain	PAAG_03031	cluster32	DEG20010326	Tubulin beta chain (Human)		C	Vinorelbine	approved, investigational	inhibitor	98%	1E-143	61%	0.74	-1.38	2AAZ	X-ray, 2.08 Å	63.82%	84%	Receptor1	-9.840.592
Tubulin beta chain	PAAG_03031	cluster606	DEG20010326	Tubulin beta	C		ZD-6126	Phase 2	Cancer	96%	1E-103	53%	0.74	-2.85	4C9G	X-ray, 2.49 Å	77.70%	96%	Receptor1	-9.633.862
Tyrosine-protein phosphatase 3	PAAG_02059	cluster51	Without similarity	Receptor-type protein-tyrosine phosphatase S	C		Alendronate	Approved	Osteoporosis and Paget's disease	85%	0.0	48%	0.75	-2.02	5CSK	X-ray, 3.1Å	63.61%	95%	Receptor1	-8.011.677
Tyrosine-protein phosphatase 3	PAAG_02059	cluster51	Without similarity	Receptor-type protein-tyrosine phosphatase S	C		Etidronate	Approved	Hypercalcemia	95%	6E-69	32%	-	-	-	-	-	-	-	-
Uncharacterized aminotransferase C1039.07c	PAAG_00468	cluster838	Without similarity	4-aminobutyrate aminotransferase, mitochondrial (Human)	C	C	Vigabatrin	approved	inhibitor	89%	3E-59	30%	-	-	-	-	-	-	-	-
Uncharacterized membrane protein YBR235W	PAAG_00719	cluster94	Without similarity	Na-K-2Cl cotransporter	C		Aldosterone	Approved	Hypertension	85%	0.0	48%	0.75	-2.02	5CSK	X-ray, 3.1Å	63.61%	95%	Receptor2	-13.658.243
Uncharacterized membrane protein YBR235W	PAAG_00719	cluster94	Without similarity	Solute carrier family 12 member 1	C		Bendroflumethiazide	Approved	High blood pressure	83%	6E-146	54%	0.71	-2.10	4KLR	X-ray, 2.18 Å	55.77%	83%	Receptor1	-7.330.200
Uncharacterized membrane protein YBR235W	PAAG_00719	cluster145	Without similarity	Solute carrier family 12 member 2 (Human)	C	C	Bumetanide	approved	inhibitor	81%	1E-107	42%	-	-	-	-	-	-		
Uncharacterized membrane protein YBR235W	PAAG_00719	cluster94	Without similarity	Solute carrier family 12 member 1	C	C	Chlorthalidone	Approved	Edema	41%	2E-36	31%	-	-	-	-	-	-	-	-
Uncharacterized membrane protein YBR235W	PAAG_00719	cluster94	Without similarity	Solute carrier family 12 member 1	C		Ethacrynic acid	Approved	High blood pressure	81%	1E-107	42%	-	-	-	-	-	-		
Uncharacterized membrane protein YBR235W	PAAG_00719	cluster94	Without similarity	Solute carrier family 12 member 1	C	C	Methyclothiazide	Approved	Hypertension	81%	1E-107	42%	-	-	-	-	-	-		
Uncharacterized membrane protein YBR235W	PAAG_00719	cluster145	Without similarity	Solute carrier family 12 member 2 (Human)		C	Quinethazone	approved	inhibitor	98%	6E-101	36%	-	-	-	-	-	-	-	-
Uncharacterized membrane protein YBR235W	PAAG_00719	cluster145	Without similarity	Solute carrier family 12 member 1 (Human)	C	C	Torasemide	approved	inhibitor	81%	1E-107	42%	-	-	-	-	-	-		
Uncharacterized oxidoreductase C26F1.07	PAAG_02806	cluster145	Without similarity	Alcohol dehydrogenase	C		Fomepizole	Approved	Athylene glycol or methanol poisoning	81%	1E-107	42%	-	-	-	-	-	-		
Uncharacterized oxidoreductase C26F1.07	PAAG_02806	cluster145	Without similarity	Alcohol dehydrogenase	C		MINALRESTAT	Discontinued in Phase 3	Diabetes mellitus	94%	1E-124	40%	-	-	-	-	-	-	-	-
Uncharacterized oxidoreductase C26F1.07	PAAG_02806	cluster145	Without similarity	Alcohol dehydrogenase	C		ZOPOLRESTAT	Discontinued in Phase 2	Diabetic complication	92%	5E-121	35%	-	-	-	-	-	-	-	-
Uncharacterized oxidoreductase C2F3.05c	PAAG_03765	cluster52	Without similarity	Aldo-keto reductase family 1 member C3 (Human)		C	Bimatoprost	approved, investigational		77%	3E-115	52%	0.56	0.15	3D2k	X-ray, 2.50 Å	60.70%	66%	Receptor1	-16.320.869
Uncharacterized oxidoreductase C2F3.05c	PAAG_02806	cluster52	Without similarity	3-oxo-5-beta-steroid 4-dehydrogenase (Human)		C	Finasteride	approved	inhibitor	75%	2E-107	57%	0.56	0.15	3D2k	X-ray, 2.50 Å	60.70%	66%	Receptor1	-10.448.647
Urease	PAAG_00954	cluster638	Without similarity	Urease	C		Acetohydroxamic Acid	Approved	Urinary tract infections	75%	2E-107	57%	0.56	0.15	3D2k	X-ray, 2.50 Å	60.70%	66%	Receptor1	-8.839.811
Urease	PAAG_00954	cluster406	Without similarity	Urease subunit alpha (Enterobacter aerogenes)		C	Acetohydroxamic Acid	approved	inhibitor	77%	3E-115	52%	0.56	0.15	3D2k	X-ray, 2.50 Å	60.70%	66%	Receptor1	-11.125.106
Urease	PAAG_00954	cluster406	Without similarity	Urease subunit alpha(Enterobacter aerogenes)		C	Ecabet	approved, investigational	inhibitor	92%	5E-84	30%	-	-	-	-	-	-	-	-
Vacuolar protein sorting-associated protein 70	PAAG_02017	cluster96	Without similarity	Glutamate carboxypeptidase II	C		ATL101	Phase 2	Influenza virus infections	77%	3E-115	52%	0.56	0.15	3D2k	X-ray, 2.50 Å	60.70%	66%	Receptor1	-14.994.042
Vacuolar protein sorting-associated protein 70	PAAG_02017	cluster96	Without similarity	Glutamate carboxypeptidase II	C		GPI-16072	Phase I	Neuropathic pain	77%	3E-115	52%	0.56	0.15	3D2k	X-ray, 2.50 Å	60.70%	66%	Receptor1	-10.208.675
Vacuolar protein sorting-associated protein 70	PAAG_02017	cluster96	**Without similarity**	Glutamate carboxypeptidase II	C		MDX-070	Discontinued in Phase 2	Prostate cancer	82%	0.0	65%	-	-	-	-	-	-	-	-
Vacuolar protein sorting-associated protein 70	PAAG_02017	cluster96	Without similarity	Glutamate carboxypeptidase II	C		MLN-2704	Phase 1/2	Prostate tumor	97%	0.0	59%	-	-	-	-	-	-	-	-

Vacuolar protein sorting-associated protein 70	PAAG_02017	cluster96	Without similarity	Glutamate carboxypeptidase II	C		MLN-591RL	Phase 2	Prostate tumor	77%	3E-115	52%	0.56	0.15	3D2k	X-ray, 2.50 Å	60.70%	66%	Receptor1	-9.889.464
V-type proton ATPase catalytic subunit A	PAAG_07285	cluster826	Without similarity	V-type proton ATPase catalytic subunit A (Human)		C	Alendronic acid	approved	inhibitor	97%	6E-129	47%	-	-	-	-	-	-	-	-
V-type proton ATPase catalytic subunit A	PAAG_06288	cluster812	Without similarity	V-type proton ATPase subunit B, brain isoform (Human)		C	Gallium nitrate	approved, investigational	inhibitor	97%	6E-129	47%	-	-	-	-	-	-	-	-
V-type proton ATPase catalytic subunit A	PAAG_07285	cluster826	Without similarity	V-type proton ATPase catalytic subunit A (Human)		C	Tiludronate	approved, vet_approved	inhibitor	75%	2E-107	57%	0.56	0.15	3D2k	X-ray, 2.50 Å	60.70%	66%	Receptor1	-10.824.575
Xanthine dehydrogenase	PAAG_02640	cluster88	Without similarity	Xanthine dehydrogenase/oxidase	C		Allopurinol	Approved	Hyperuricemia	75%	2E-107	57%	0.56	0.15	3D2k	X-ray, 2.50 Å	60.70%	66%	Receptor1	-15.114.143
Xanthine dehydrogenase	PAAG_02640	cluster88	Without similarity	Aldehyde oxidase	C		Isovanillin	Approved	Cancer	39%	3E-24	32%	-	-	-	-	-	-	-	-
Xanthine dehydrogenase	PAAG_02640	cluster160	Without similarity	Xanthine dehydrogenase/oxidase (Human)		C	Allopurinol	approved	inhibitor	70%	3E-151	49%	-	-	-	-	-	-	-	-
Xanthine dehydrogenase	PAAG_02640	cluster88	Without similarity	Xanthine dehydrogenase/oxidase	C		BOF-4272	Discontinued in Phase 2	Gout	48%	2E-40	32%	0.67	-2.18	5EMN	X-ray, 2.20 Å	43.27%	85%	Receptor1	-9.658.434
Xanthine dehydrogenase	PAAG_02640	cluster160	Without similarity	Xanthine dehydrogenase/oxidase (Human)		C	Carvedilol	approved, investigational		71%	3E-173	57%	-	-	-	-	-	-	-	-
Xanthine dehydrogenase	PAAG_02640	cluster160	Without similarity	Xanthine dehydrogenase/oxidase (Human)		C	Chlorphenesin	approved, vet_approved, withdrawn	inhibitor	98%	0.0	47%	-	-	-	-	-	-	-	-
Xanthine dehydrogenase	PAAG_02640	cluster88	Without similarity	Xanthine dehydrogenase/oxidase	C		Cyclic pyranopterin monophosphate	Phase 2	Encephalopathy	41%	2E-36	31%	-	-	-	-	-	-	-	-
Xanthine dehydrogenase	PAAG_02640	cluster160	Without similarity	Xanthine dehydrogenase/oxidase (Human)		C	Deferoxamine	approved, investigational	inhibitor	92%	5E-121	35%	-	-	-	-	-	-	-	-
Xanthine dehydrogenase	PAAG_02640	cluster160	Without similarity	Xanthine dehydrogenase/oxidase (Human)		C	Eniluracil	investigational	inhibitor	92%	5E-84	30%	-	-	-	-	-	-	-	-
Xanthine dehydrogenase	PAAG_02640	cluster160	Without similarity	Xanthine dehydrogenase/oxidase (Human)	C	C	Febuxostat	approved	antagonist	89%	3E-59	30%	-	-	-	-	-	-	-	-
Xanthine dehydrogenase	PAAG_02640	cluster88	Without similarity	Aldehyde oxidase	C		Menadione	Approved	Vitamin K deficiency	36%	1E-51	34%	0.10	-2.14	4BF2.2	X-ray, 2.11 Å	40.00%	21%	Receptor1	-9.899.423
Xanthine dehydrogenase	PAAG_02640	cluster160	Without similarity	Xanthine dehydrogenase/oxidase (Human)	C	C	Oxypurinol	investigational		97%	0.0	79%	0.74	-2.22	5KX5	X-ray, 2.50 Å	77.70%	86%	Receptor1	4.073.926
Xanthine dehydrogenase	PAAG_02640	cluster160	Without similarity	Xanthine dehydrogenase/oxidase (Human)		C	Procarbazine	approved		97%	0.0	79%	0.74	-2.22	5KX5	X-ray, 2.50 Å	77.70%	86%	Receptor1	3.547.863
Xanthine dehydrogenase	PAAG_02640	cluster160	Without similarity	Aldehyde oxidase (Human)		C	Raloxifene	approved, investigational	inhibitor	98%	1E-173	34%	0.54	-4.97	1FFY	X-ray, 2.20 Å	36.09%	73%	Receptor1	-7.622.368
Xanthine dehydrogenase	PAAG_02640	cluster88	Without similarity	Xanthine dehydrogenase/oxidase	C		Topiroxostat	Phase 2	Gout	97%	3E-114	51%	-	-	-	-	-	-	-	-
Xanthine dehydrogenase	PAAG_02640	cluster88	Without similarity	Xanthine dehydrogenase/oxidase	C		Y-700	Discontinued in Phase 2	Gout	96%	2E-92	45%	-	-	-	-	-	-	-	-
Zinc metalloprotease mde10	PAAG_02647	cluster815	Without similarity	Disintegrin and metalloproteinase domain-containing protein 10 (Human		C	XL784	investigational		98%	1E-173	34%	0.54	-4.97	1FFY	X-ray, 2.20 Å	36.09%	73%	Receptor1	-9.491.764

Repositioning of drugs aiming the treatment of Paracoccidioidomycosis

OLIVEIRA, A. O.; NEVES, B. J.; SILVA, L.C.; SOARES, C. M. A.; ANDRADE, C. H.; PEREIRA, M.

Abstract:

Paracoccidioidomycosis (PCM) is a systemic mycosis in Latin America caused by thermally dimorphic fungus *Paracoccidioides* spp. PCM treatment is long-term chemotherapeutic approach and causes several side effects, so aiming us was reposition of the drugs more efficient and less harmful to the patients. The *Pb*01 proteins were compared with other two isolates (*Pb*03 and *Pb*18), the orthologous proteins were compared with proteins from compound banks, DrugBank e Therapeutic Target Database, for suggestion composts. After, similarity confirmation by Blast in between the *Pb*01 proteins with suggested proteins by compound banks, and the *Pb*01 proteins were compared with *Saccharomyces cerevisiae* essential genes. As results, 45 *Pb*01 proteins were submitted molecular docking with related compounds.

Introduction

Endemic in Latin America countries, the Paracoccidioidomycosis is systemic mycosis has occurrence in Venezuela, Colombia, Argentina, and Brazil [1], [2]. With high prevalence, in between 1930 to 2012 were more 15000 PCM cases registered, being Brazil the country with bigger number cases [2]. In the Brazilian regions is endemic in the southeast, in the west central, and south (mainly in Paraná and north of Rio Grande do Sul), with registered cases in the states the Pará, Maranhã, Tocantins, Rondônia, and in the region the western Amazônia [2]–[4].

Any organ, apparatus and body system may be harmed by for PCM [5]. The most common route of infection is by inhalation of conidia or fragments of mycelia [6],[7], that becomes in yeast in host tissues [5]. The PCM can be classified, referring to clinical forms, in infection Paracoccidioidomycosis, disease Paracoccidioidomycosis (Acute / subacute: moderate and severe; Chronic form: soft, moderate and severe), and residual form or sequelae [5], [8].

Two thermos-dimorphic fungi species were PCM etiological agents, *Paracoccidioides brasiliensis,* and *Paraciccidioides lutzii*. [5], [9]. These species are composed of different phylogenetic lines, S1, PS2, PS3, PS4, and Pb01, formed like this,

Paracoccidioides genus [10]–[12]. The isolates used this study were: Pb01, Pb01, and Pb18. The Pb01 was endemic in the west center of Brazil and is present in Ecuador [10], [12], [13]. Belonging the PS2 line, Pb03 is found only in Brazil and Venezuela, while the Pb18, belonging the S1 line, is present for all Latin America [10]–[12], [14].

For the PCM treatment, the most used drugs are itraconazole, cotrimoxazole (combination of sulfamethoxazole com trimethoprim), and amphotericin B [5]. However, before starting the medication is required to evaluate the degree of disease, locality of the lesion, if the patient has any special condition that must be taken into account and the contraindications to the use of a particular drug [5], [7]. The treatment time and the side effects depend on the medicine and of disease severity, but the PCM treatment often is long because of the *Paracoccidioides* spp. can't be completely eliminated from the organism, the treatment focus is to reduce the fungal load so that patient immunity controls the fungus[5], [7]. The organs that stay more sequels are lungs, lymphatic system, adrenals and central nervous system [5].

Seeing the PCM severity, the treatment difficulty, and the sequels, this study was goals drugs reposition for PCM treatment that are efficient and have fewer side effects. The drug reposition has been considered an alternative to find alternative medicines for various diseases to need drugs more efficient and less toxic, instead develop new drugs which are a long, expensive and risky process [15], [16]. Thus, the proteins of three *Paracoccidioides* species were compared and for the orthologous proteins were predicted compounds used drugs databases.

Materials and Methods

Compilation of the list *Paracoccidioides* spp. Genes

The FASTA sequences of the Pb01, Pb03 and Pb18 isolates were extracted from *Broad Institute – Paracoccidioides brasiliensis Database* (https://www.broadinstitute.org/fungal-genome-initiative/). The proteins sequences were submitted on the Orthovenn online platform [17] to select orthologous proteins in the three isolates. The Pb01 proteins what presented orthography with the other isolates (*E-value* $\leq 10^{-20}$) were considered next steps.

Identification of drug using publicly database

Aiming to identify drug with therapeutic potential against the PCM, the proteins previously selected were compared with therapeutic targets the drugs approved for human

use and drugs candidates in a clinical study. Based on the concept that proteins sharing enough similarity (orthology) have enhanced the probability of share the same ligands, all therapeutic targets present in the database Drugbank [18]–[20] and Therapeutic Target Database [21]–[24] were compared with Pb01 proteins selected using the OrthoVenn platform (*E-value* $\leq 10^{-20}$). Then, the homology between Pb01 proteins and target therapeutic drug proteins was investigated using BLAST server. Only homologous proteins with sequential identity $\geq 30\%$ were considered for next analyzes.

Comparison with Saccharomyces cerevisiae essential genes

In OrthoVenn platform, the *Pb*01 proteins selected in the previous steps were compared with *S. cerevisiae* essential proteins with the goal of select essential proteins potential for *Pb*01. The essential proteins sequences were downloaded from online platform Database of Essential Genes - DEG (http://tubic.tju.edu.cn/deg/).

Homology modeling

To analyze the structural bases of potential interactions between drug and macromolecule, the three-dimensional structures (3D) of *Pb*01 targets were predicted using homology modeling strategy. First, the amino acids sequences in FASTA of proteins were submitted to the SWISS-MODEL automated server. [25]–[27] This sever basically consisted of four steps: (i) identification and selection of mold protein available in Protein Data Bank, [28] (ii) sequence alignment, (iii) constructions of the 3D coordinates and (iv) validation/selection of the best model using parameters of initials selection as the Global Model Quality Estimation (GMQE) and punctuation function QMEAN. [29] The GMQE represents an estimate of quality what combines alignment properties of mold-protein. Already the punctuation function QMEAN4 estimate the model global quality based on linear combination of four structural descriptors: local geometry, two distance-dependent interaction potentials (based on all atoms or Cβ), and potential for salvation. [29]

Optimization of the initial models

After initial models construction, its structures were submitted separately to structural optimization processes in KoBaMIN server. [30]–[32] The refinement protocol is composed of two steps: (i) minimization of energy using a mean strength potential based on knowledge and (ii) stereo-chemical correction.

Definition of protonation states of cofactors and amino acids

Posteriorly refinement process, the models were submitted separately to Protein Preparation Wizard module, available in the MAESTRO version 9.3 program package.[33] This stage the correction of the interaction orders and hydrogen addition was performed, as well as the definition of states of protonation in pH 7.0 ± 1.0 (for both amino acids, substrate, and cofactors) using the Epik program version 2.7. [34] After this process, the structures were again submitted a one new energy minimization using the force field OPLS-2005. [35]

3D model validação

To evaluating the quality of the *phi* (ϕ) e *psi* (ψ) angles of main chain (Ramachandran analysis) and *chi* (χ) angles of rotamers of the side chain, the 3D structures were submitted the statistical analysis of quality using the MolProbity server. [36] The graphics program PyMOL version 1.3 [33] was used for visualization.

Molecular docking

The compounds structures were imported from Maestro workspace version 9.3 and prepared using LigPrep 2.5 (Schrödinger, LCC, New York, 2012) to pH 7,0 ± 1. Posteriorly, 2000 confirmations were generated using the OMEGA version 2.5.1 (OMEGA versão 2.5.1: *OpenEye Scientific Software*, Santa Fe, NM; http://www.eyesopen.com., no date; Hawkins et al., 2010), while the loads AM1-BCC (Jakalian, Jack, Bayly, 2002) were added using the QUACPAC version 1.6.3 (‘QUACPAC v.1.6.3: OpenEye Scientific Software, Santa Fe, NM. http://www.eyesopen.com.’, no date). Before the docking studies, grids were generated using a molecular probe for detection of pockets around the proteins that could potentially be sites of catalytic links and allosteric sites. Lastly, to molecular docking was used the FRED high-resolution protocol and ChemGauss4 score, both available in OEDocking suite version 3.2.0 (‘OEDocking v.3.2.0: OpenEye Scientific Software, Santa Fe, NM. http://www.eyesopen.com.’, no date; McGann, 2011, 2012).

In vitro tests

Micro-organism and culture conditions

The *Pb*01, *Pb*03 and *Pb*18 isolates were incubated in Fava-Netto liquid medium (0.3% protease peptone, 1% peptone, 0.5% (w/v) meat extract, 0.5% (w/v) Yeast extract, 4% glucose, 0.5% NaCl, pH 7.2) per three days. Then, purposeful of fungal adaptation the chemically defined medium, the cells were transferred to RPMI 1640 medium and incubated for 16 hours.

Minimal inhibitory concentration (MIC)

For MIC determination was fulfilled by microdilution technique, following Clinical and Laboratory Standards Institute (CLSI) and De Paula *et al.* (2013) recommendations. In each microplate orifice, was added 100 µL of dilutions with the addition of 100 µL of *Paracoccidioides* spp. culture, in order to get the last concentration of 1 x 10^4 CFU/mL. The growing medium was RPMI 1640. The plates remained at 36°C in agitation to 150 rpm, after 48 hours the alamar blue reagent (resazurin 0,02%) was added, incubated for more 24 hours in the same conditions that previously. To maximum grown determination (positive control), some microplate orifice with cells received growing medium instead of 100 µL of dilution containing the test compounds.To minimum grown (negative control), some microplate orifice with cells received itraconazole antifungal. The growth was visually measured, by color change the alamar blue reagent and by absorbance reading to 560 nm. The assay was performed in triplicate of sample and duplicate of biological. The selectivity index was calculated from 50% cytotoxicity by 50% MIC value.

Determination of minimum fungicidal concentration (MFC)

Yeast cells from *Paracoccidioides* spp. were incubated with selected compound, diluted serially, keeping the same concentrations and growing conditions used in MIC test. For each microplate orifice was realized a subculture, transferring 10 µL of material from each microplate orifice to plate containing solid Fava-Netto. The plates were incubated in a hothouse at 37ºC for seven days, with posterior visual reading.

Cytotoxicity

The BALB/c 3T3 cells, 1x10^5 cells/ microplate orifice, were distributed in a microplate with 96 orifices, in DMEM medium, supplemented with 10% fetal bovine serum and antibiotic. Per 48h the cells have exposed the concentrations different, obtained during the serial dilution, kept in damp with 5% of CO_2, at 37ºC. After the exhibition, the supernatant was removed, each microplate orifice was washed with PBS and was added 25 µg/mL of neutral red fixative solution (1% acetic acid, 49% deionized water, 50% ethanol). Posteriorly the solubilization, the absorbance was quantified by spectrophotometry in a microplate reader at 560 nm. The absorbance obtained the control

cell was considered 100% of cell viability. Two independent experiments were performed and concentrations six replicates.

Interaction test with antifungals

The combined effect of synthetic antifungals used in Paracoccidioidomycosis treatment with selected compounds was determined through of the dilution technique checkerboard. Initially, 75 µL of each antifungal in combination with 75 µL of MBHA-E1were disposed of in an orderly fashion: in the horizontally, there is a decrease of the compounds tests concentrations, and vertically a decrease of concentrations of synthetic antifungals itraconazole, amphotericin B, Bactrim, and sulfamethoxazole. In addition, were added 50µL of yeast cells of *Paracoccidioides* spp. at the final concentration of $1X10^3$ cells/mL. After two days of incubation at 37ºC, in agitation, the 150 rpm, 20 µL of Alamar blue was added and incubated again for 24 hours.

The fractional inhibitory concentration (FIC) was calculated used following formula (FICs=FICA+FICB), where FICA is the MIC of compound A combined and divided by MIC of compound A alone; FICB is the MIC of compound B combined and divided by MIC of compound B alone. The FICIs were interpreted the following way: sinérgico, FIC ≤ 0,5, additive FIC > 0,5 a ≤ 1, indifference FIC > 1 a ≤ 4, antagônico FIC > 4.

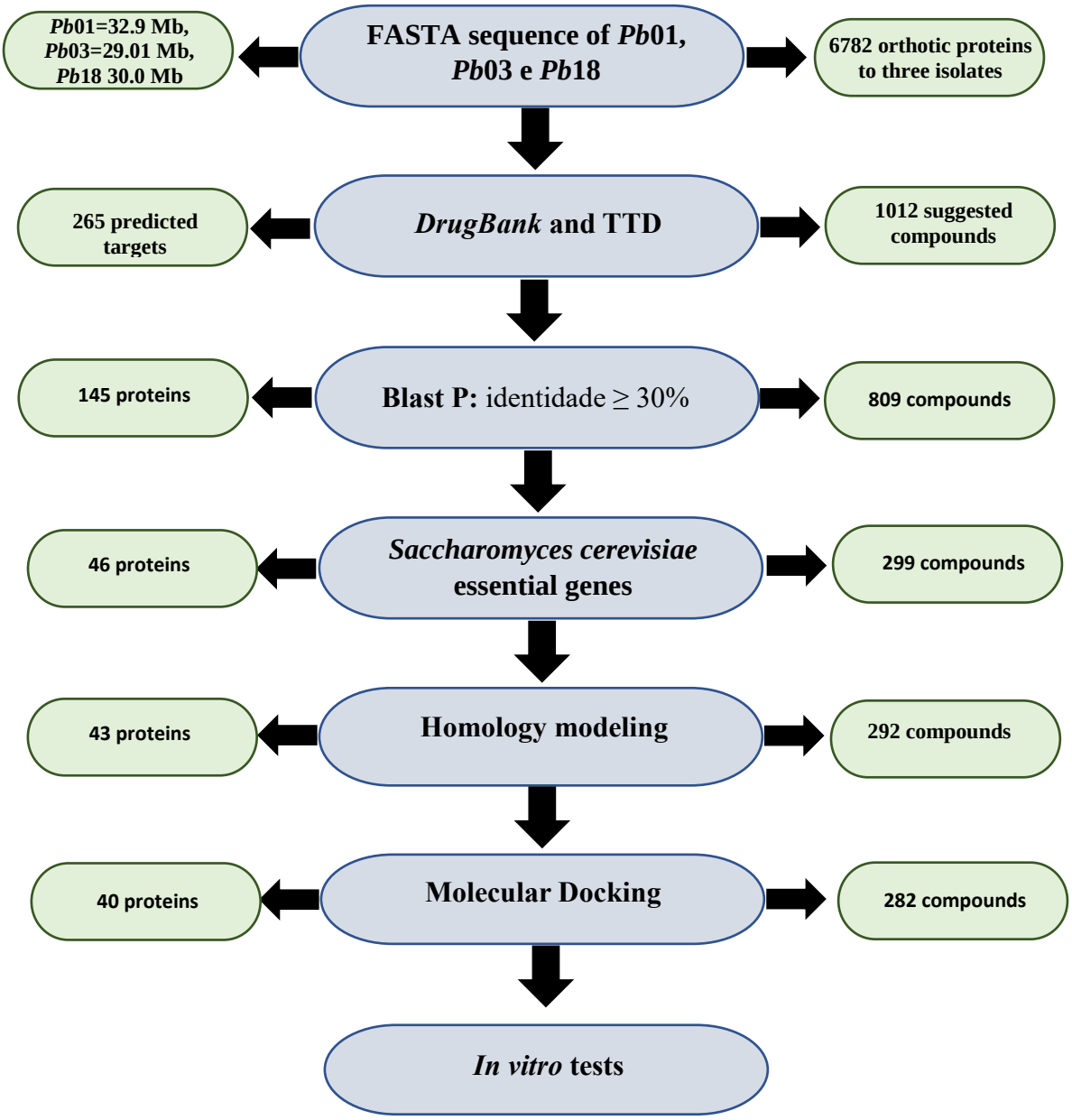

Figure 1: Flowchart summarizing method used and corresponding results. The green boxes represent the summarized results obtained at each stage of the study.

Results

Compilation of the gene list

For chromogenic tracking, it did a comparison of *Pb*01, *Pb*03 and *Pb*18 proteins in order to proceed the studies only with orthologs proteins to the three isolates. The *Pb*03 and *Pb* 18 have the genome of similar size, 29.01 Mb, and 30.0 Mb respectively, and are more similar to each other, sharing 96% similarity [37]. While the genome *Pb*01 is bigger the 32.9 Mb and sharing 90% similarity with other two isolates. When comparing the proteins of the three isolates, it was obtained 6743 clusters containing 6782 *Pb*01 proteins orthologs to the two isolates (figure 2).

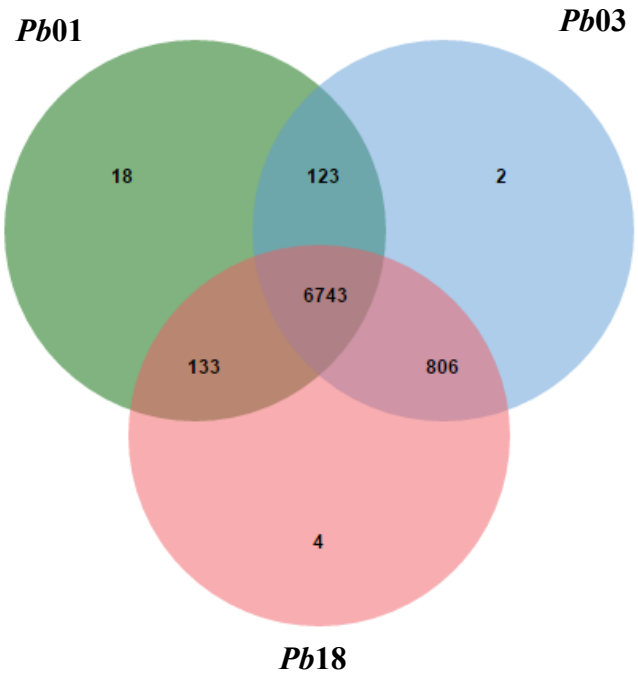

Figure 2: Venn diagram shows the cluster quantity generated after the comparison of isolates in the OrthoVenn platform.

Identification of drug using publicly database

In compounds prediction to PCM combat, the fungus proteins selected in the previous step were compared with proteins of Drugbank and TTD databases. For greater precision, the comparison was done separately, with a show in figure 3, were 318 clusters predicted for *Pb*01 and DrugBank containing 228 proteins, and were 107 clusters predicted for *Pb*01 and TTD containing 120 proteins.

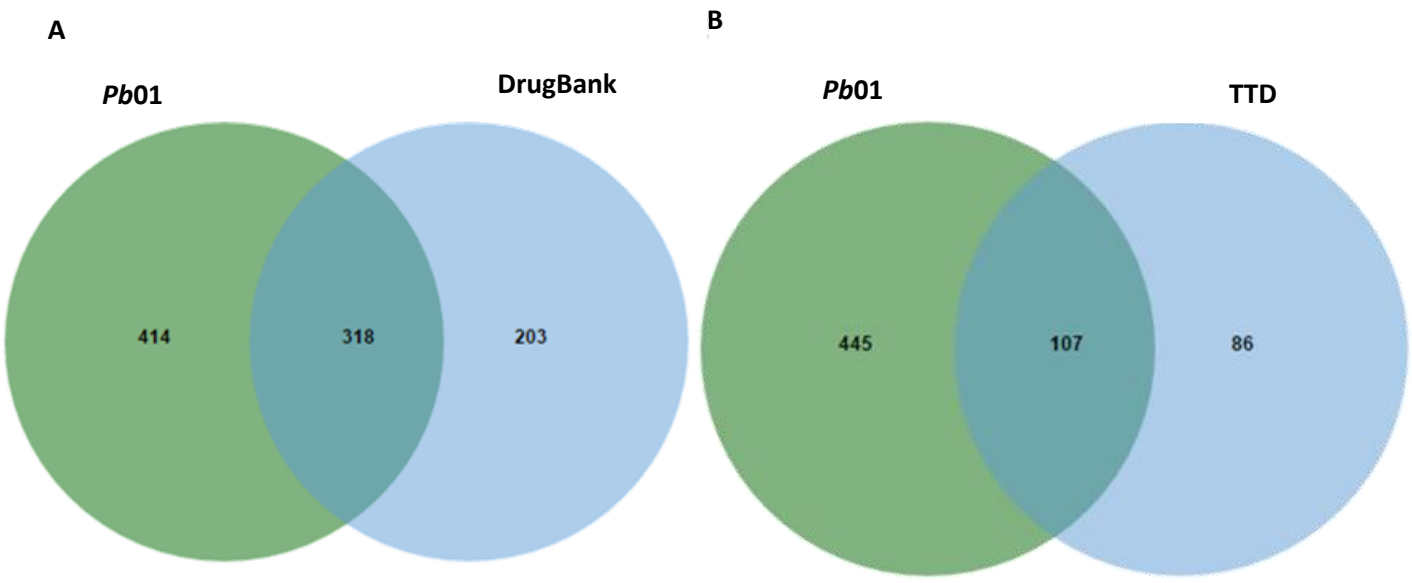

Figure 3: Venn diagram shows the cluster quantity generated in the OrthoVenn platform: **a)** Comparison *Pb*01 proteins with DrugBank proteins; **b)** Comparison *Pb*01 proteins with TTD proteins;

Altogether were 1012 compounds in different stages of development suggested for 265 *Pb*01 proteins by two databases. Of this value, 46% was suggested by DrugBank, 39% by TTD and only 15% was suggested by either.

The Blast was realized by investigating the similarity and identity existing in between *Pb*01 proteins and compounds databases proteins suggested orthologs by OrthoVenn platform. Of 265 proteins, 145 presented identity ≥ 30%.

Comparison with Saccharomyces cerevisiae essential genes

Aiming results curation, the fungus proteins was compared with essential proteins of *S. cerevisiae*, proteins considered important for survival the fungus. [38] The 145 *Pb*01 proteins, 46 were orthologous to essential proteins of *S. cerevisiae*, how to show in figure4.

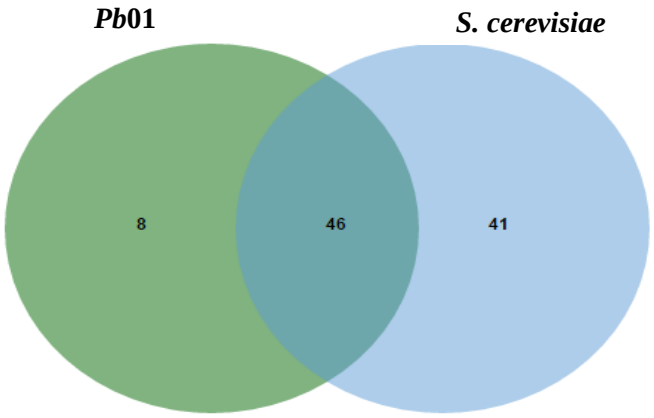

Figure 4: Venn diagram shows the cluster quantity generated by comparison Pb01 with essential proteins of *S. cerevisiae* in the OrthoVenn platform.

Homology modeling and Optimization of the initial models

The sequences of 46 fungus proteins were submitted to SWISS-MODEL server for modeling. The 46 proteins submitted, three don't have a model suggestion. After generation of models, its passed for optimization in KoBaMIN and validated by MolProbity (Table 1). The 46 model proteins, 43 was optimization and for two models proteins, the program did not generate results, even after to be submitted for optimization more than once. Although of not being optimized, those models were used in next steps.

Table 1: Validation of models built by MolProbity of proteins that have selected compounds in vitro tests.

PAAG	Pb01 target proteins	Score MolProbity	Resolution
PAAG_00827	Cytochrome P450 51	1.75	87th percentile
PAAG_07279	Farnesyl pyrophosphate synthetase	1.68	90th percentile
PAAG_04243	Na+/K+ exchanging ATPase alpha chain	2.05	73rd percentile
PAAG_01410	Phosphatidylinositol 3-kinase tor2	1.86	83rd percentile
PAAG_02441	Protein Kinase C	1.83	84th percentile
PAAG_08991	Serine threonine - protein kinase	1.73	88th percentile
PAAG_08597	Thymidylate synthase	1.95	78th percentile
PAAG_03031	Tubulin beta chain	1.60	92nd percentile

Molecular docking

After proteins preparation, grids buildings and generation of conformers, the molecular docking was fulfilled. The 293 compounds subject, the program couldn't analyze the interaction of 11 compounds with proteins for which they were suggested, for being a metal ion, peptides or because they have large structures. The table with all docking results is in the attachment 2.

As selection criterion for compounds that were in vitro test, beyond the molecular docking final results, it was performed bibliographic research in PubMed (HAROON, 1998) and PubChem Bioassay (PUBCHEM, 2017) to exclusion of compounds that

already are using in PCM treatment. Table 2 shows the compounds selected for in vitro tests.

Table 2: Protein geometry analysis for the constructed models.

Targets Pb01	Drug	Development phase	Development phase	Score Docking
PAAG_00827 Lanosterol 14-α demethylase	Luliconazole	Antifungal	Approved	-12.363.360
PAAG_00827 Lanosterol 14-α demethylase	Butoconazole	Antifungal	Approved	-15.730.254
PAAG_00827 Lanosterol 14-α demethylase	Bifonazole	Antifungal	Approved	-18.365.929
PAAG_00827 Lanosterol 14-α demethylase	Sertaconazole	Antifungal	Approved	-14.937.805
PAAG_07279 Farnesyl pyrophosphate synthetase	Pamidronate	Bisphosphonate	Approved	-19.165.264
PAAG_07279 Farnesyl pyrophosphate synthetase	Minodronate	Treatment of osteoporosis	Approved	-18.478.310
PAAG_04243 Na+/K+ exchanging ATPase alpha chain	Dexlansoprazole	Gastroesophageal reflux	Approved	-10.104.547
PAAG_01410 Phosphatidylinositol 3-kinase tor2	Dactolisib	Antineoplastic	Phase 2	-14.269.496
PAAG_01410 Fosfatidilinositol 3-quinase tor2	AZD2014	Antineoplastic	Phase 2	-13.222.617
PAAG_01410 Fosfatidilinositol 3-quinase tor2	BGT226	Antitumoral	Phase 1/2	-13.027.889
PAAG_02441 Protein Kinase C	Midostaurin	Antineoplastic	Phase 2	-14.511.683
PAAG_08991 Serine-threonine protein kinase	ENMD-2076	Acute myeloid leukemia	Phase 2	-14.994.042
PAAG_08991 Serine-threonine protein kinase	Tozasertib	Anticancer	Phase 2	-15.114.143
PAAG_08597 Thymidylate synthase	Raltitrexed	Anticancer	Approved	-13.317.190

PAAG_03031 Tubulin beta chain	ABT-751	Antitumoral	Phase 2	-8.318.228
PAAG_03031 Tubulin beta chain	Mebendazole	Anti-nematodes	Approved	-9.034.729
PAAG_03031 Tubulin beta chain	Albendazole	Antiprotozoal	Approved	-8.118.922

Figure 5 illustrates interaction mode the dexlansoprazole drug in α chain of the (Na^+, K^+)-ATPase. In general, the thionyl, imidazole and pyridine groups of the dexlansoprazole drug make hydrogen interaction with the Gln854, Ser858, and Ser376 residues, respectively. Hydrophobic interactions were observed in between the aromatic rings and trifluoromethyl and Leu174, Ile379, Leu178, Val172, Trp353, Trp364, and Val848.

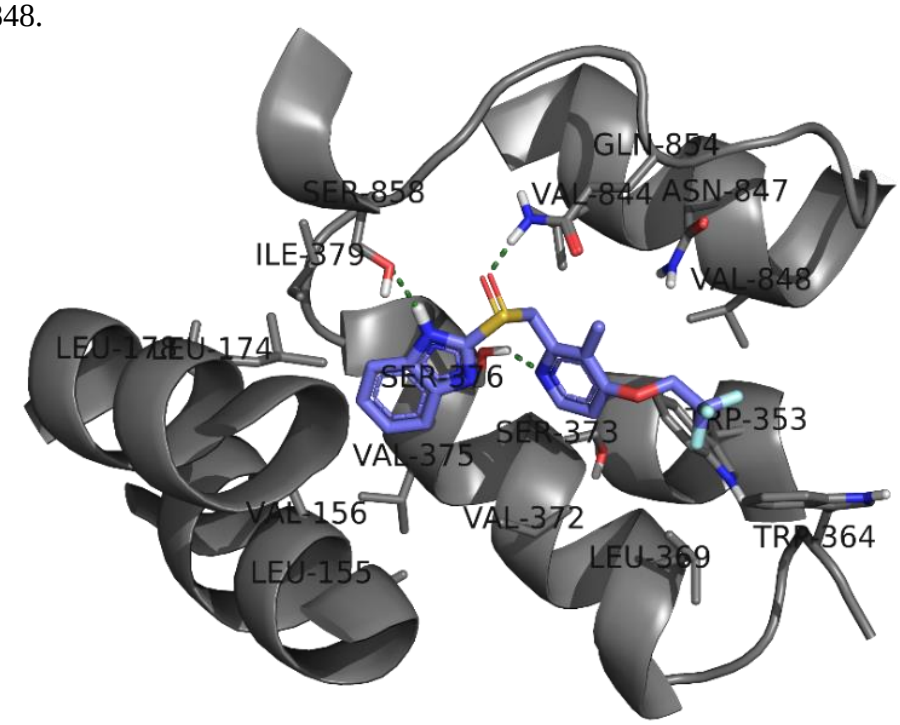

Figure 5: Intermolecular interactions in between the dexlansoprazole drug and residues of amino acids of α chain of the (Na+, K+) ATPase of *Paracoccidioides* spp.

The molecular docking study also shows that some antifungal still doesn't use in PCM treatment have affinity high by the lanosterol 14-α demethylase enzyme of *Paracoccidioides* spp. According to the figure 6, the nitrogen of imidazole ring of bifonazole and sertaconazole drugs coordinate directly with Fe^{2+} heme while the other amino acid residues from the active site (for example, Tyr122, Phe130, Tyr136, Phe130,

etc.) they perform hydrophobic interactions aromatic rings both ligands. The same interaction profile was observed for all inhibitors of lanosterol 14-α demethylase enzyme

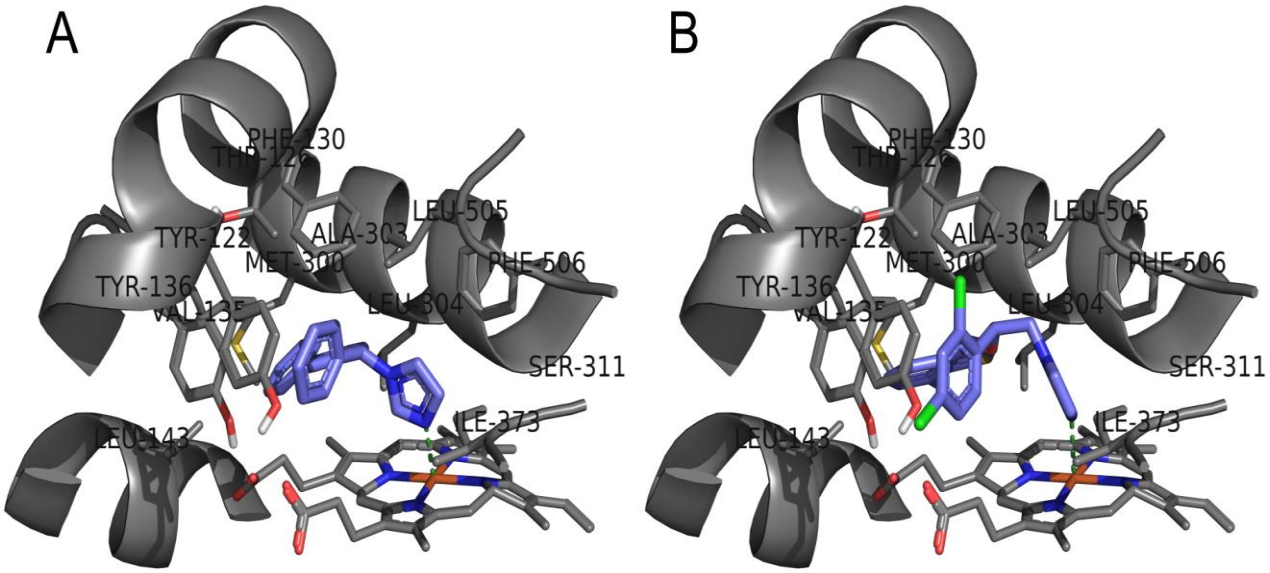

Figure 6: Intermolecular interactions of drugs **(A)** bifonazole and **(B)** sertaconazole with the active site of the lanosterol 14-α demethylase enzyme of *Paracoccidioides* spp.

Figure 7 represents the interaction mode of the midostaurin in ATP binding site of the protein Kinase C. How can it be observed, the nitrogen and oxygen atoms of pyrrolidine ring form hydrogen bonds with the main chain of Ile86 and Glu84 residues, while the carbonyl of the benzamide group forms a hydrogen bond with Lys130. The other chemical groups of the midostaurin form hydrophobic interactions with Phe55, Met86, Phe14, Phe296, Phe292, Leu9, Phe14, Val17 and Met83 residues.

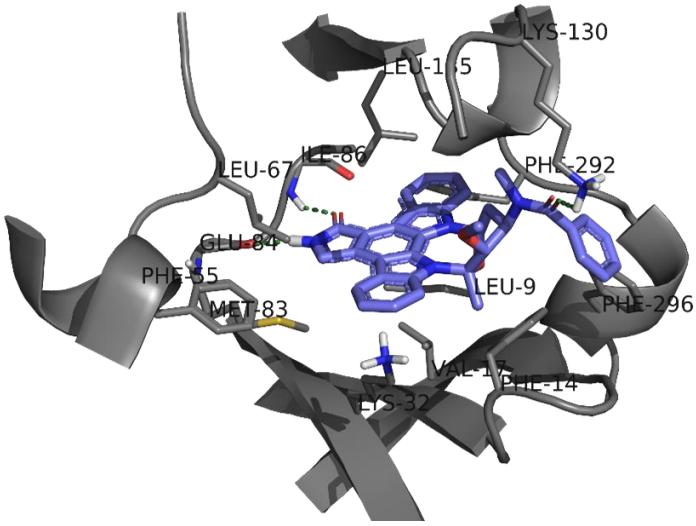

Figure 7: Intermolecular interactions in between midostaurin and amino acid residue of ATP binding site of the protein Kinase C of *Paracoccidioides* spp.

Figure 8 represents the mode of drug biding minodronate (A) and pamidronate (B) with the active site of the farnesyl pyrophosphate synthase enzyme. The interaction profile both drugs is quite similar. In general, the isopentenyl pyrophosphate group is coordinated with the Mg^{2+} atom (ball green) facilitating the formation of the hydrogen bonds with Arg103, Gln231, and Asp234 residues. However, the imidazopyridine ring the minodronato from a hydrogen bond with the Arg53 and hydrophobic interactions with Tyr195, Phe230, and Leu91 residues, while the aliphatic amine of pamidronate forms hydrogen bonds with the Tyr195 and Thr192.

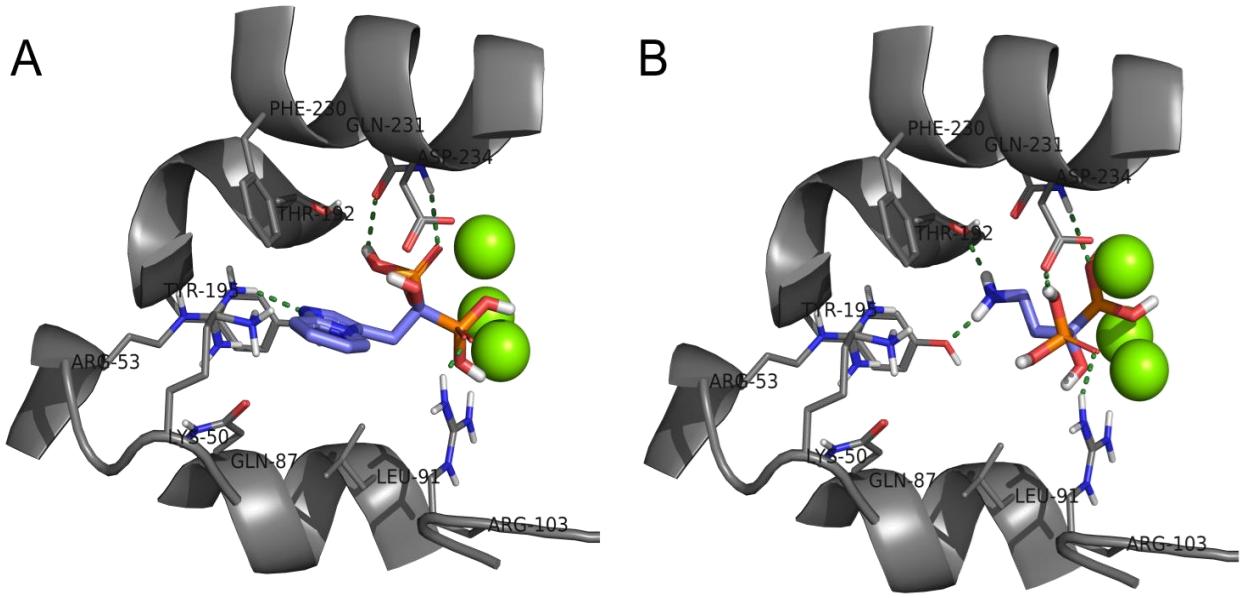

Figure 8: Intermolecular interactions of drugs **(A)** minodronate and **(B)** pamidronate with the active site of the farnesyl pyrophosphate synthase of *Paracoccidioides* spp.

The intermolecular interactions in between raltitrexed drug and amino acid residue of the active site of the thymidylate synthase are represented in figure 9. How can it be observed, the carboxylic acids of the aliphatic chain form a hydrogenic bond with Asn141, Ile360, and His300, while the nitrogen of 1,4-dihydroquinazolin-4-one ring form a hydrogen bond with Asn270. Hydrophobic interactions also are observed in between thiophene ring with Leu265 and Met358, in between the 4-dihydroquinazolin-4-one ring with Trp138 and Tyr164 residues.

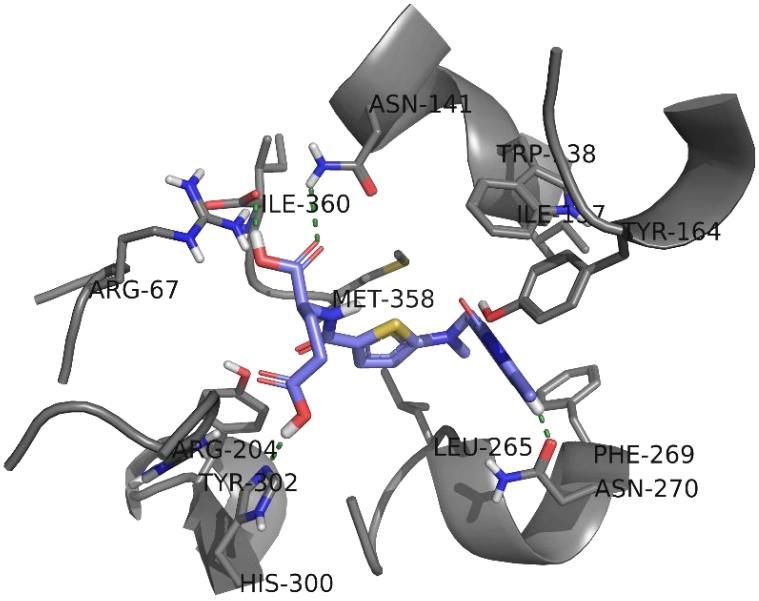

Figure 9*:* Intermolecular interactions in between raltitrexed drug and amino acid residue of the active site of the thymidylate synthase of *Paracoccidioides* spp.

The intermolecular interactions in between mebendazole drug (A) and ABT-751 drug candidate (B) with amino acid residues of the tubulin beta chain are represented in figure 10. When analyzing the interaction mode the mebendazole drug, it is observed the formation of hydrogen bonds in between benzimidazole ring and Gln21, and Arg358 residues, while the acetophenone group forms hydrophobic interactions with His226, Pro357, Leu360 and Phe269 residues. The albendazole drug has similar intermolecular interactions. On the other hand, the nitrogen of the sulfonamide group present in the structure of the drug candidate ABT-751 forms a hydrogen bond with Trp22, while its acetophenone group also form hydrophobic interactions with His226, Pro357, Leu360, and Phe269 residues.

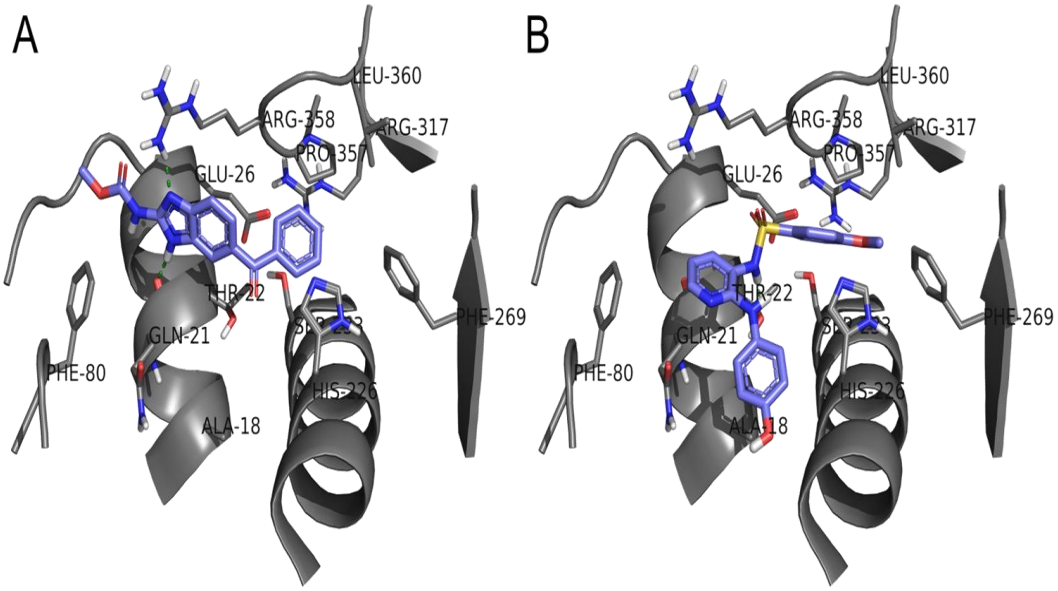

Figure 10: Intermolecular interactions of drugs **(A)** mebendazole and drug candidate **(B)** ABT-751 with amino acid residues of the tubulin beta chain of *Paracoccidioides* spp.

Discussion

This studied has goal identify drugs to combat the PCM, systemic mycosis that is neglected and endemic in Latin America, [39] being Brazil the country with the highest number of cases [6], [39]. With high incidence rate and long treatment [7], [40], the PCM patient can stay with sequels in several organs as lungs, skin and central nervous [5], [7], [41].

The isolates used this studied belong to different species and have different geographic distributions, but the three isolates are present in Brasil [10]–[12]. The comparison among isolates was made to select only common proteins, with goal select compounds with antifungal activity against to three isolates. Although the *Pb*01 is more different, it still has 90% similar sequence with *Pb*03 and *Pb*18 [37], that is why was obtained a bigger number proteins ortholog with two isolates.

The *S. Cerevisiae* has been used to identify possible essential proteins in *Paracoccidioides* spp. The studies using *S. Cerevisiae* to describe functions of genes and proteins in *Paracoccidioides* spp. are common [42], [43]. The use of the *S. Cerevisiae* with model organism was studied and supported by Karathia et al (2011) by proteomics comparison with 704 organisms of different phyla, with representatives of almost all the kingdoms [44].

After the comparison with *S. Cerevisiae* proteins, the selected proteins have their 3D structures constructed by SWISS-MODEL [27], which predicts models for proteins through homology, comparing the sequences submitted with the PDB database. The generated models were optimized using KoBaMIN [45], where structures passed by checks, analyzing if there are atoms absence, lost residues, and mistakes in saved format, being posteriorly refined.

To validate, the models were submitted in MolProbity. The MolProbity score, shown in table 1 and attachment 1, is general quality statistics models which combine parameters, such as clashscore, the percentage of Ramachandran, and percentage of rotamers. The clashscore is the number of serious conflicts by 100 atoms [36]. The percentile value is related to the resolution of Ray-X of the models, the closer to the 100^{th} the better their quality. All the models validated presented a resolution of the MolProbity score above the 50^{th} percentile (attachment 1). The eigh proteins that have the suggested drugs selected for in vitro tests (table 1) presented an equal or higher than 73 percentiles.

The FRED program, used in molecular docking, uses exhaustive search logarithm which analyzes rotations of each drug-generated conformer (ligand) inside of the active site marked by the protein. Filtering was performed, during the exhaustive search, for disregard of irregular positions of conformer and best position score. During the molecular docking the protein is considered rigid and the flexible ligand, for having various conformations evaluated in the interaction with the protein [46].

The FRED score, shown in table 2 and attachment 2, is a set of the various punctuation functions, between them, chemgauss, chemscore, shapegauss [46]. The chemgauss measures the interaction of the ligand on the active site of the protein, analyzing related interactions to the form, hydrogen bond between ligand and protein, hydrogen interactions with implied solvent and metal-chelate interactions [47].

Chemscore is the sum of lipophilic interactions (interaction that occurs between two non-polar atoms, of ligand with the protein), hydrogen bond, metal-chelate (interaction the atoms of ligand with metal atom of the protein), shock (penalty that occurs when atoms of the ligand conflict with the protein), and rotary interaction (penalty term related to ligand bonds that when being docked in the active site of the protein is no longer free to rotate [47].

Shapegauss, score based on the pose more favorable the ligand for to fit in the active site of the protein, without taking into account any chemical interaction existing. This score is calculated adding the potential pairing between protein atoms with ligand atoms, being more favorable when the atoms approach without overlapping [47]. After analyze and calculate all scores generated during molecular docking, the FRED score is generated. The lower its value, the greater the chances to happen off the drug-protein interactions analyzed.

Among the repositioning drugs suggested, were identified drug used for PCM treatment, as itraconazole, ketoconazole, fluconazole and Voriconazole. Although of not being used, miconazole and econazole were used to avoid PCM reactivation [48], and treatment case of disseminated PCM [49], respectively.

The Lanosterol 14-α demethylase protein has four drugs selected for the test *in vitro*. Luliconazole, an efficient antifungal in combat the various mycosis as the caused by *Candida albicans* e *Trichophyton* spp [50]. Butoconazole, bifonazole, and e sertaconazole are used mainly for candidiasis treatment [51]–[53].

Used as a drug target, the farnesyl pyrophosphate synthetase performs crucial functions in the regulation of isoprenoid metabolism [54], and connect to the receptors of

growth factors, participates signal transduction mediated by fibroblast growth factor [55]. Two nitrogen bisphosphonates were repositioned for it: the minodronate indicated for the osteoporosis treatment [56], for which have suggesting studies its use as an alternative to the melanoma treatment [57], and pamidronate used in the treatment of bone-related cancer metastasis [58].

The Na+/K+ exchanging ATPase alpha chain, a transmembrane protein responsible for transport of sodium and potassium against their concentration gradients [59], the dexlansoprazole, an R-enantiomer of lansoprazole used in the treatment of patients with gastroesophageal reflux [60], was suggested for repositioning and selected for in vitro testing.

The compounds selective for phosphatidylinositol 3-kinase tor2, protein related control of cell division [61], are under investigation. The dactolisib an antineoplastic [62], AZD2014 an inhibitor from mTOR (mammalian target of rapamycin) studied for combat of carcinoma of the oral squamous cell [63], and BGT226 studied as antitumoral against head and neck cancer cells [64].

The Protein Kinase C has been related to several vascular changes associated with various diseases, as diabetes, colon cancer [65], stomach cancer [66], prostate cancer [67], and heart diseases [65]. The selected drug with action potential a tyrosine kinase inhibitor was midostaurin which is under investigation for the treatment of acute myeloid leukemia and advanced systemic mastocytosis [68].

The serine-threonine protein kinase is related to bacterial virulence, responsible to identify the medium, realizing various signs and coordinating responses of cellular processes, and for interfering responses of the host immune system [69]. Two compounds in development were suggested to them, ENMD-2076 an inhibitor of small molecules of kinases with action in ways that involve tumor growth and survival is being evaluated in patients with platinum-resistant ovarian cancer [70], and tozasertib a kinase inhibitor with anticancer activity [71].

The thymidylate synthase participates in the formation of thymidylate, essential precursor for DNA biosynthesis [72] considered a good target for drugs [73], the raltitrexed, an anticancer used in the treatment of colorectal tumors [74] was suggested for repositioning in the against PCM.

The tubulin beta chain is important protein for the formation of microtubules, essential elements cytoskeleton of eukaryotic cells [75]. The ABT-751, an antimitotic agent, and vascular disruption agent with anticancer activities, which is under

development [76], Mebendazole and Albendazole, benzimidazole derivatives used in the cystic echinococcosis treatment and other parasites found in the central nervous system [77], [78] were suggested for tubulin beta chain.

All drugs selected are promising candidates for PCM treatment. As a perspective, the in vitro tests minimum inhibitory concentration, determination of the minimum fungicidal concentration, and cytotoxicity will be performed to validate the results obtained in silico.

Conclusion

Using computational strategies, it was possible to compare the proteins of *Pb*01, *Pb*03, and *Pb*18, and predict drug for orthologous proteins to the three isolates. By means of various filtrations steps, 43 proteins and 292 drugs were submitted to molecular docking aiming analyze the probability of interactions between the proteins and their respective drug. With the results obtained, was possible conclude, the method applied was efficient in the repositioning drugs for PCM treatment, listing 17 most promising drug.

Acknowledgment

This work performed at Universidade Federal de Goiás was supported by MCTI/CNPq (Ministério da Ciência e Tecnologia/Conselho Nacional de Desenvolvimento Científico e Tecnológico), FNDCT (Fundo Nacional de Desenvolvimento Científico e Tecnológico), FAPEG (Fundação de Amparo à Pesquisa do Estado de Goiás), CAPES (Coordenação de Aperfeiçoamento de Pessoal de Nível Superior), FINEP (Financiadora de Estudos e Projetos), PRONEX (Programa de Apoio a Núcleos de Excelência) and INCT-IF (Instituto Nacional de Ciência e Tecnologia para Inovação Farmacêutica). Additionally, FSA and BRSN were supported by fellowship from CAPES.

References

[1] a Restrepo, J. G. McEwen, and E. Castañeda, “The habitat of Paracoccidioides brasiliensis: how far from solving the riddle?,” *Med. Mycol.*, vol. 39, no. 3, pp. 233–241, 2001.

[2] R. Martinez, “Epidemiology of Paracoccidioidomycosis.,” *Rev. do Inst. Med.*

Trop. São Paulo, vol. 57 Suppl 1, pp. 11–20, 2015.

[3] W. B. Matos, G. M. Dos Santos, V. E. Silva, E. G. Rosario Goncalves, and a R. Silva, "Paracoccidioidomycosis in the state of Maranhao, Brazil: geographical and clinical aspects," *Rev Soc Bras Med Trop*, vol. 45, no. 3, pp. 385–389, 2012.

[4] G. de D. Vieira, T. da C. Alves, S. M. D. de Lima, L. M. A. Camargo, and C. M. de Sousa, "Paracoccidioidomycosis in a western Brazilian Amazon State: Clinical-epidemiologic profile and spatial distribution of the disease," *Rev. Soc. Bras. Med. Trop.*, vol. 47, no. 1, pp. 63–68, 2014.

[5] M. A. Shikanai-Yasuda *et al.*, "Brazilian guidelines for the clinical management of paracoccidioidomycosis," *Rev. Soc. Bras. Med. Trop.*, no. 0, 2017.

[6] E. Brummer, E. Castaneda, and A. Restrepo, "Paracoccidioidomycosis: An update," *Clin. Microbiol. Rev.*, vol. 6, no. 2, pp. 89–117, 1993.

[7] M. A. Shikanai-Yasuda *et al.*, "Consenso em paracoccidioidomicose," *Rev. Soc. Bras. Med. Trop.*, vol. 39, no. 3, pp. 297–310, 2006.

[8] M. Franco, M. R. Montenegro, R. P. Mendes, S. A. Marques, N. L. Dillon, and N. G. da S. Mota, "Paracoccidioidomycosis: A Recently Proposed Classification of Its Clinical Forms," *Rev. Soc. Bras. Med. Trop.*, vol. 20, no. 2, pp. 129–132, 1987.

[9] M. D. M. Teixeira *et al.*, "Paracoccidioides lutzii sp. nov.: biological and clinical implications," *Med. Mycol.*, vol. 52, no. 1, pp. 1–10, Jun. 2013.

[10] M. M. Teixeira *et al.*, "Phylogenetic analysis reveals a high level of speciation in the Paracoccidioides genus," *Mol. Phylogenet. Evol.*, vol. 52, no. 2, pp. 273–283, 2009.

[11] M. M. Teixeira, R. C. Theodoro, G. Nino-Vega, E. Bagagli, and M. S. S. Felipe, "Paracoccidioides Species Complex: Ecology, Phylogeny, Sexual Reproduction, and Virulence," *PLoS Pathog.*, vol. 10, no. 10, pp. 4–7, 2014.

[12] J. F. Muñoz *et al.*, "Genome Diversity, Recombination, and Virulence across the Major Lineages of Paracoccidioides," *mSphere*, vol. 1, no. 5, pp. e00213-16, Oct. 2016.

[13] V. Koufopanou, A. Burt, and J. W. Taylor, "Concordance of gene genealogies

reveals reproductive isolation in the pathogenic fungus Coccidioides immitis (vol 94, pg 5478, 1997)," *Proc. Natl. Acad. Sci. U. S. A.*, vol. 95, no. 14, p. 8414, 1998.

[14] D. R. Matute *et al.*, "Cryptic Speciation and Recombination in the Fungus Paracoccidioides brasiliensis as Revealed by Gene Genealogies," *Mol. Biol. Evol.*, vol. 23, no. 1, pp. 65–73, Jan. 2005.

[15] T. T. Ashburn and K. B. Thor, "Drug repositioning: identifying and developing new uses for existing drugs.," *Nat. Rev. Drug Discov.*, vol. 3, no. 8, pp. 673–683, 2004.

[16] J. G. Lombardino and J. A. Lowe, "THE ROLE OF THE MEDICINAL CHEMIST IN DRUG DISCOVERY — THEN AND NOW," *Nat. Rev. Drug Discov.*, vol. 3, no. 10, pp. 853–862, Oct. 2004.

[17] Y. Wang, D. Coleman-Derr, G. Chen, and Y. Q. Gu, "OrthoVenn: A web server for genome wide comparison and annotation of orthologous clusters across multiple species," *Nucleic Acids Res.*, vol. 43, no. W1, pp. W78–W84, 2015.

[18] D. S. Wishart *et al.*, "DrugBank: a comprehensive resource for in silico drug discovery and exploration.," *Nucleic Acids Res.*, vol. 34, no. Database issue, pp. D668-72, Jan. 2006.

[19] C. Knox *et al.*, "DrugBank 3.0: a comprehensive resource for 'omics' research on drugs.," *Nucleic Acids Res.*, vol. 39, pp. D1035-41, Jan. 2011.

[20] V. Law *et al.*, "DrugBank 4.0: Shedding new light on drug metabolism," *Nucleic Acids Res.*, vol. 42, no. D1, pp. 1091–1097, 2014.

[21] X. Chen, Z. L. Ji, and Y. Z. Chen, "TTD: Therapeutic Target Database.," *Nucleic Acids Res.*, vol. 30, no. 1, pp. 412–415, Jan. 2002.

[22] F. Zhu *et al.*, "Update of TTD: Therapeutic Target Database.," *Nucleic Acids Res.*, vol. 38, no. Database issue, pp. D787–D791, Jan. 2010.

[23] F. Zhu *et al.*, "Therapeutic target database update 2012: A resource for facilitating target-oriented drug discovery," *Nucleic Acids Res.*, vol. 40, no. D1, pp. 1128–1136, 2012.

[24] H. Yang *et al.*, "Therapeutic target database update 2016: Enriched resource for

bench to clinical drug target and targeted pathway information," *Nucleic Acids Res.*, vol. 44, no. D1, pp. D1069–D1074, 2016.

[25] L. Bordoli, F. Kiefer, K. Arnold, P. Benkert, J. Battey, and T. Schwede, "Protein structure homology modeling using SWISS-MODEL workspace.," *Nat. Protoc.*, vol. 4, no. 1, pp. 1–13, 2009.

[26] M. Biasini *et al.*, "SWISS-MODEL: Modelling protein tertiary and quaternary structure using evolutionary information," *Nucleic Acids Res.*, vol. 42, no. W1, pp. 252–258, 2014.

[27] S. Bienert *et al.*, "The SWISS-MODEL Repository-new features and functionality," *Nucleic Acids Res.*, vol. 45, no. D1, pp. D313–D319, 2017.

[28] H. M. Berman *et al.*, "The Protein Data Bank.," *Nucleic Acids Res.*, vol. 28, no. 1, pp. 235–242, 2000.

[29] P. Benkert, M. Kunzli, and T. Schwede, "QMEAN server for protein model quality estimation," *Nucleic Acids Res.*, vol. 37, no. Web Server, pp. W510–W514, Jul. 2009.

[30] G. Chopra, C. M. Summa, and M. Levitt, "Solvent dramatically affects protein structure refinement," *Proc. Natl. Acad. Sci.*, vol. 105, no. 51, pp. 20239–20244, Dec. 2008.

[31] G. Chopra, N. Kalisman, and M. Levitt, "Consistent refinement of submitted models at CASP using a knowledge-based potential," *Proteins Struct. Funct. Bioinforma.*, vol. 109, no. 10, p. n/a-n/a, Jun. 2010.

[32] J. P. G. L. M. Rodrigues, M. Levitt, and G. Chopra, "KoBaMIN: a knowledge-based minimization web server for protein structure refinement," *Nucleic Acids Res.*, vol. 40, no. W1, pp. W323–W328, Jul. 2012.

[33] "QikProp, version 3.4; Schrödinger Inc.: New York, 2011; http://www.schrodinger.com/." .

[34] J. C. Shelley, A. Cholleti, L. L. Frye, J. R. Greenwood, M. R. Timlin, and M. Uchimaya, "Epik: A software program for pKa prediction and protonation state generation for drug-like molecules," *J. Comput. Aided. Mol. Des.*, vol. 21, no. 12, pp. 681–691, 2007.

[35] J. L. Banks *et al.*, “Integrated Modeling Program, Applied Chemical Theory (IMPACT),” *J. Comput. Chem.*, vol. 26, no. 16, pp. 1752–1780, 2005.

[36] V. B. Chen *et al.*, “MolProbity: All-atom structure validation for macromolecular crystallography,” *Acta Crystallogr. Sect. D Biol. Crystallogr.*, vol. 66, no. 1, pp. 12–21, 2010.

[37] C. A. Desjardins *et al.*, “Comparative genomic analysis of human fungal pathogens causing paracoccidioidomycosis,” *PLoS Genet.*, vol. 7, no. 10, 2011.

[38] M. Seringhaus, A. Paccanaro, A. Borneman, M. Snyder, and M. Gerstein, “Predicting essential genes in fungal genomes,” *Genome Res.*, vol. 16, no. 9, pp. 1126–1135, 2006.

[39] J. F. Muñoz *et al.*, “Genome Update of the Dimorphic Human Pathogenic Fungi Causing Paracoccidioidomycosis,” *PLoS Negl. Trop. Dis.*, vol. 8, no. 12, 2014.

[40] F. Bellissimo-Rodrigues, A. A. Machado, and R. Martinez, “Paracoccidioidomycosis epidemiological features of a 1,000-cases series from a hyperendemic area on the southeast of Brazil,” *Am. J. Trop. Med. Hyg.*, vol. 85, no. 3, pp. 546–550, 2011.

[41] a M. Tobón *et al.*, “Residual pulmonary abnormalities in adult patients with chronic paracoccidioidomycosis: prolonged follow-up after itraconazole therapy.,” *Clin. Infect. Dis.*, vol. 37, no. 7, pp. 898–904, 2003.

[42] L. Fernandes, M. A. M. Araújo, A. Amaral, V. C. B. Reis, N. F. Martins, and M. S. Felipe, “Cell signaling pathways in Paracoccidioides brasiliensis--inferred from comparisons with other fungi.,” *Genet. Mol. Res.*, vol. 4, no. 2, pp. 216–231, 2005.

[43] M. de M. Teixeira, R. C. Theodoro, L. da S. Derengowski, A. M. Nicola, E. Bagagli, and M. S. Felipe, “Molecular and morphological data support the existence of a sexual cycle in species of the genus Paracoccidioides,” *Eukaryot. Cell*, vol. 12, no. 3, pp. 380–389, 2013.

[44] H. Karathia, E. Vilaprinyo, A. Sorribas, and R. Alves, “Saccharomyces cerevisiae as a Model Organism: A Comparative Study,” *PLoS One*, vol. 6, no. 2, p. e16015, Feb. 2011.

[45] J. P. G. L. M. Rodrigues, M. Levitt, and G. Chopra, “KoBaMIN: a knowledge-

based minimization web server for protein structure refinement," *Nucleic Acids Res.*, vol. 40, no. W1, pp. W323–W328, Jul. 2012.

[46] M. McGann, "FRED Pose Prediction and Virtual Screening Accuracy," *J. Chem. Inf. Model.*, vol. 51, no. 3, pp. 578–596, Mar. 2011.

[47] "OEDocking v.3.2.0: OpenEye Scientific Software, Santa Fe, NM. http://www.eyesopen.com."

[48] R. Negroni, P. Rubinstein, A. Herrmann, and A. Gimenez, "Results of miconazole therapy in twenty-eight patients with paracoccidioidomycosis (South American blastomycosis)," *Proc. R. Soc. Med.*, vol. 70, p. 24, 1977.

[49] Carmen Marcano, "Iv encuentro internacional sobre paracoccidioidomicosis," vol. 28, pp. 37–39, 1990.

[50] D. Khanna and S. Bharti, "Luliconazole for the treatment of fungal infections: an evidence-based review," *Core Evid.*, vol. 9, p. 113, Sep. 2014.

[51] B. Wächtler, D. Wilson, and B. Hube, "Candida albicans adhesion to and invasion and damage of vaginal epithelial cells: Stage-specific inhibition by clotrimazole and bifonazole," *Antimicrob. Agents Chemother.*, vol. 55, no. 9, pp. 4436–4439, 2011.

[52] L. Z. Heng, Y. Chen, and T. C. Tan, "Treatment of recurrent vulvo-vaginal candidiasis with sustained-release butoconazole pessary," *Singapore Med. J.*, vol. 53, no. 12, pp. 269–271, 2012.

[53] C. Borelli, G. Klövekorn, T.-M. Ernst, R.-H. Bödeker, H. C. Korting, and C. Neumeister, "Comparative study of 2% sertaconazole solution and cream formulations in patients with tinea corporis, tinea pedis interdigitalis, or a corresponding candidosis.," *Am. J. Clin. Dermatol.*, vol. 8, no. 6, pp. 371–8, 2007.

[54] M. K. Dhar, A. Koul, and S. Kaul, "Farnesyl pyrophosphate synthase: A key enzyme in isoprenoid biosynthetic pathway and potential molecular target for drug development," *N. Biotechnol.*, vol. 30, no. 2, pp. 114–123, 2013.

[55] J. F. REILLY, S. D. MARTINEZ, G. MICKEY, and P. A. MAHER, "A novel role for farnesyl pyrophosphate synthase in fibroblast growth factor-mediated signal transduction," *Biochem. J.*, vol. 366, no. 2, pp. 501–510, Sep. 2002.

[56] R. Okazaki *et al.*, “Efficacy and safety of monthly oral minodronate in patients with involutional osteoporosis,” *Osteoporos. Int.*, vol. 23, no. 6, pp. 1737–1745, 2012.

[57] S. Yamagishi *et al.*, “Minodronate, a newly developed nitrogen-containing bisphosphonate, suppresses melanoma growth and improves survival in nude mice by blocking vascular endothelial growth factor signaling.,” *Am. J. Pathol.*, vol. 165, no. 6, pp. 1865–74, 2004.

[58] D. Stefanik, J. Sarin, T. Lam, L. Levin, P. Leboy, and S. Akintoye, “Disparate osteogenic response of mandible and iliac crest bone marrow stromal cells to pamidronate,” *Oral Dis.*, vol. 14, no. 5, pp. 465–471, Jul. 2008.

[59] G. Tejral, B. Sopko, A. Necas, W. Schoner, and E. Amler, “Computer modelling reveals new conformers of the ATP binding loop of Na^{+}/K^{+}-ATPase involved in the transphosphorylation process of the sodium pump,” *PeerJ*, vol. 5, p. e3087, 2017.

[60] D.-C. Wu, C.-H. Kuo, F.-W. Tsay, W.-H. Hsu, A. Chen, and P.-I. Hsu, “A Pilot Randomized Controlled Study of Dexlansoprazole MR-Based Triple Therapy for Helicobacter Pylori Infection.,” *Medicine (Baltimore).*, vol. 95, no. 11, p. e2698, 2016.

[61] M. A. Krasilnikov, “Phosphatidylinositol-3 kinase dependent pathways: the role in control of cell growth, survival, and malignant transformation.,” *Biochem. Biokhimiiâ*, vol. 65, no. 1, pp. 59–67, 2000.

[62] I. A. Netland *et al.*, “Dactolisib (NVP-BEZ235) toxicity in murine brain tumour models,” *BMC Cancer*, pp. 1–12, 2016.

[63] C. C. Yu *et al.*, “AZD2014 Radiosensitizes Oral Squamous Cell Carcinoma by Inhibiting AKT/mTOR Axis and Inducing G1/G2/M Cell Cycle Arrest,” *PLoS One*, vol. 11, no. 3, p. e0151942, 2016.

[64] K. Y. Chang, S. Y. Tsai, C. M. Wu, C. J. Yen, B. F. Chuang, and J. Y. Chang, “Novel phosphoinositide 3-kinase/mTOR dual inhibitor, NVP-BGT226, displays potent growth-inhibitory activity against human head and neck cancer cells in vitro and in vivo,” *Clin. Cancer Res.*, vol. 17, no. 22, pp. 7116–7126, 2011.

[65] J. C. B. Ferreira, P. C. Brum, and D. Mochly-Rosen, "βIIPKC and εPKC isozymes as potential pharmacological targets in cardiac hypertrophy and heart failure," *J. Mol. Cell. Cardiol.*, vol. 51, no. 4, pp. 479–484, Oct. 2011.

[66] M. S. Song, Y. K. Park, J. H. Lee, and K. Park, "Induction of glucose-regulated protein 78 by chronic hypoxia in human gastric tumor cells through a protein kinase C-epsilon/ERK/AP-1 signaling cascade.," *Cancer Res.*, vol. 61, no. 22, pp. 8322–8330, 2001.

[67] D. Wu *et al.*, "Protein kinase cepsilon has the potential to advance the recurrence of human prostate cancer," *Cancer Res*, vol. 62, no. 8, pp. 2423–2429, 2002.

[68] B. Peter *et al.*, "Target interaction profiling of midostaurin and its metabolites in neoplastic mast cells predicts distinct effects on activation and growth.," *Leukemia*, vol. 30, no. 2, pp. 464–72, 2016.

[69] M. J. Canova and V. Molle, "Bacterial serine/threonine protein kinases in host-pathogen interactions," *J. Biol. Chem.*, vol. 289, no. 14, pp. 9473–9479, 2014.

[70] G. C. Fletcher *et al.*, *ENMD-2076 is an orally active kinase inhibitor with antiangiogenic and antiproliferative mechanisms of action.*, vol. 10, no. 1. 2011.

[71] M. Michaelis, F. Selt, F. Rothweiler, M. Wiese, and J. Cinatl, "ABCG2 impairs the activity of the aurora kinase inhibitor tozasertib but not of alisertib," *BMC Res. Notes*, vol. 8, no. 1, p. 484, 2015.

[72] C. W. Carreras and D. V. Santi, "The Catalytic Mechanism and Structure of Thymidylate Synthase," *Annu. Rev. Biochem.*, vol. 64, no. 1, pp. 721–762, Jun. 1995.

[73] A. Chernyshev, T. Fleischmann, and A. Kohen, "Thymidyl biosynthesis enzymes as antibiotic targets," *Appl. Microbiol. Biotechnol.*, vol. 74, no. 2, pp. 282–289, 2007.

[74] D. Cunningham *et al.*, "Final results of a randomised trial comparing Tomudex'® (raltitrexed) with 5-fluorouracil plus leucovorin in advanced colorectal cancer," *Ann. Oncol.*, vol. 7, pp. 961–965, 1996.

[75] C. Janke, "The tubulin code: Molecular components, readout mechanisms, functions," *J. Cell Biol.*, vol. 206, no. 4, pp. 461–472, 2014.

[76] C. M. Rudin *et al.*, "Phase I/II study of pemetrexed with or without ABT-751 in advanced or metastatic non-small-cell lung cancer," *J. Clin. Oncol.*, vol. 29, no. 8, pp. 1075–1082, 2011.

[77] D. Press, "Study of Albendazole-Encapsulated Nanosize Liposomes," *Int. J.*, vol. 5, pp. 101–108, 2010.

[78] P. Pantziarka, G. Bouche, L. Meheus, V. Sukhatme, and V. P. Sukhatme, "Repurposing Drugs in Oncology (ReDO)-mebendazole as an anti-cancer agent.," *Ecancermedicalscience*, vol. 8, p. 443, 2014.

Attachments

Attachment 1: Validation of models built by MolProbity of proteins that have selected compounds in vitro tests.

PAAG	Pb01 target proteins	Score MolProbity	Resolution
PAAG_04259	2Fe 2s iron-sulfur cluster binding domain-containing protein	1.93	79th percentile
PAAG_01387	3 ketoacyl CoA thiolase B	1.70	89th percentile
PAAG_02414	26S proteasome regulatory subunit RPN1	2.15	68th percentile
PAAG_03447	Acetyl-CoA acetyltransferase	Not optimized	
PAAG_08731	Acetyl-CoA carboxylase	1.93	79th percentile
PAAG_08620	ADP, ATP carrier protein	1.65	91th percentile
PAAG_00826	Calcium-calmodulin-dependent protein kinase type IV	2.02	75th percentile
PAAG_08247	Calmodulin	1.38	97th percentile
PAAG_01186	Cell division control protein 1	1.91	80th percentile
PAAG_05894	Cell division control protein 2	1.77	87th percentile
PAAG_00827	Lanosterol 14-α demethylase	1.75	87th percentile
PAAG_04743	Casein kinase II subunit alpha	1.60	92nd percentile
PAAG_00299	Delta-aminolevulinic acid dehydratase	1.74	88th percentile
PAAG_07676	Dihydrofolate synthetase	2.20	65th percentile
PAAG_07212	DNA ligase	2.21	64th percentile
PAAG_06486	DNA polymerase 1	1.87	82th percentile

PAAG	Pb01 target proteins	Score MolProbity	Resolution
PAAG_06601	DNA polymerase 2	1.88	82th percentile
PAAG_03486	DNA topoisomerase 2	1.79	86th percentile
PAAG_07279	Farnesyl pyrophosphate synthetase	1.68	90th percentile
PAAG_01524	Fatty acid synthase subunit beta dehydratase	Not optimized	
PAAG_08770	Ferrochelatase	1.92	80th percentile
PAAG_05758	Glutamate carboxypeptidase	2.23	62nd percentile
PAAG_07003	Glutamine synthetase	1.78	86th percentile
PAAG_08003	Heat shock 70 kDa protein 2	1.57	93rd percentile
PAAG_12584	Isoleucine-tRNA ligase	2.35	56th percentile
PAAG_05015	Leucyl-tRNA synthetase	2.27	60th percentile
PAAG_00557	Mannose-6-phosphate isomerase	1.99	76th percentile
PAAG_04243	Na+/K+ exchanging ATPase alpha chain	2.05	73rd percentile
PAAG_11783	NADPH-cytochrome P450 reductase	2.01	75th percentile
PAAG_01410	Phosphatidylinositol 3-kinase tor2	1.86	83rd percentile
PAAG_04060	Phosphatidylinositol 3-kinase vps34	1.64	91st percentile
PAAG_01150	Proteasome subunit beta type	1.87	82nd percentile
PAAG_02441	Protein Kinase C	1.83	84th percentile
PAAG_05449	RAC-alpha serine threonine protein kinase	2.09	71st percentile
PAAG_02499	Ribonucleotide reductase R2 subunit	2.15	67th percentile
PAAG_08991	Serine threonine - protein kinase	1.73	88th percentile
PAAG_07148	Serine threonine - protein kinase ksg1	2.28	60th percentile
PAAG_03141	Serine threonine-protein kinase SAPK2	1.79	86th percentile
PAAG_12360	STE-STE11-BCK1 protein kinase	1.92	80th percentile
PAAG_07020	Thioredoxin reductase	1.90	81st percentile
PAAG_08597	Thymidylate synthase	1.95	78th percentile
PAAG_12506	Tubulin alpha chain	1.73	88th percentile
PAAG_03031	Tubulin beta chain	1.60	92nd percentile